

**High-throughput screening for
novel regulators of Beta-catenin in
Wnt signalling**

Bethan Lloyd-Lewis

**A thesis submitted to Cardiff University for the degree of Doctor of
Philosophy.**

School of Biosciences

Submission date: September 2011

ACKNOWLEDGEMENTS

I would like to thank everybody on third floor east, past and present, for 4 years of help and support. In particular, I would like to thank Jamie Freeman, Perihan Nalbant, Katja Seipel and Lorraine Tyas for assistance and advice with regards to the project, in addition to Pete Watson who deserves all the beer in the world for his continuing support and enthusiasm. I would also like to thank Gui Jie Feng and Thierry Jarde; both have been inspiring post docs to work alongside and made E3.19 a pleasant working environment.

I would also like to thank my collaborators, Dr. Frank Buchholz and Dr Mirko Theis, for helping with the esiRNA libraries, in addition to several people at GE Healthcare for their invaluable input into the project. I am especially grateful to Val Miller, Albie Santos, Christopher Norey, Ian Davies and Mike Looker for all their help. I was also very lucky to have two talented undergraduate students to supervise, namely James Platt and Rosalind Roberts, who were a pleasure to teach and ably contributed to the hnRNP A1 story.

I am incredibly grateful to my supervisor, Professor Trevor Dale, for his invaluable guidance and input into the work, in addition to his unwavering encouragement and faith over the years.

Finally, I would like to thank my family and friends for all their support, encouragement and for putting up with my science talk (and images...and movies....). Yn arbennig, diolch o galon i fy rhieni am ddangos diddordeb yn fy ngwaith ac am yr holl help a chymorth dros y flynyddoedd diwethaf.

Diolch yn fawr.

ABSTRACT

Beta-catenin is a crucial component of the Wnt signalling pathway, which is imperative in many developmental processes and aberrantly regulated in several different cancers. The standard model of Wnt/Beta-catenin signalling states that, upon stimulation by Wnt ligand, Beta-catenin accumulates and subsequently translocates to the nucleus to activate TCF-dependent transcription of a variety of target genes, including oncogenes. However, the mechanisms regulating the nuclear localisation of Beta-catenin and its correlation with TCF-dependent transcription are poorly understood.

In order to identify novel regulators of Beta-catenin levels and localisation in Wnt signalling imaging-based high-throughput knockout screens were developed in a Wnt inducible cell line, in addition to a cancer cell line in the presence of normal and downregulated APC. Results from the screens show that, in addition to known Wnt signalling components, genes not previously ascribed to the pathway appeared to modulate Beta-catenin. The study has provided sources of possible mechanistic insights into a number of areas of biology that may be involved in β -catenin regulation. Furthermore, it reveals an unprecedented degree of cross talk between Wnt and many other major signalling pathways. Moreover, the data indicated a degree of cell-type specificity in the regulators identified and, significantly, a lack of correlation between β -catenin levels and transcriptional activity.

The study also identified heterogeneous nuclear ribonucleoprotein A1 (hnRNP A1) as a negative regulator of β -catenin. Investigations into its mechanistic role implied that hnRNP A1 modulates β -catenin post-transcriptionally, revealing an unanticipated level of β -catenin regulation at the mRNA level. Further work is required to decipher its precise mechanism of action, with the gene lists identified in this study providing a useful entry point into the future analysis of regulators of β -catenin and how they relate to Wnt signalling.

Table of Contents

ACKNOWLEDGEMENTS	2
ABSTRACT	3
Table of Contents	4
1. INTRODUCTION	8
1.1 Wnt signalling	9
1.1.1 The Canonical Wnt/Beta-catenin signalling pathway.....	12
1.1.1.1 Mechanism of canonical Wnt signal transduction	13
1.1.1.1.1. Wnt/ β -catenin signalling at the cell surface – the receptor complex.....	14
1.1.1.1.2 The β -catenin destruction complex.....	16
1.1.1.1.3 β -catenin nuclear/cytoplasmic shuttling and retention.....	18
1.1.1.1.3.1 Alternative mechanisms of β -catenin nucleocytoplasmic transport.....	20
1.1.1.1.4 The nuclear transcription complex.....	21
1.1.2 Wnt / β -catenin signalling in development and disease.	22
1.1.2.1 Wnt signalling in intestinal homeostasis and colon cancer.....	24
1.1.3 Beta-catenin.....	26
1.1.3.1 Transcriptional and translational regulation of β -catenin.....	26
1.1.3.2 β -catenin and activated TCF-dependent transcription.....	27
1.1.3.3 The role of phosphorylation in the regulation of β -catenin transcriptional activity.	29
1.2 RNA Interference	33
1.2.1 Using RNAi in High Throughput Screens	33
1.2.2 endoribonuclease-derived siRNA (esiRNA).	34
1.2.3 Genome-wide high-throughput RNAi screens.....	35
1.2.3.1 High-throughput functional genetic screens for novel regulators of the β -catenin dependent Wnt signalling pathway.	36
1.3 Aims of the project	40
Chapter 2. Materials and Methods	42
2.1 The 7df3 TCF-luciferase reporter cell line	43
2.2 Cell culture	44
2.2.1 7df3 reporter cell line.....	44
2.2.2 U2OS cell lines	45
2.2.2.1 eGFP- β -catenin U2OS cells	45
2.2.2.2 U2OS cells	46
2.3 esiRNA	46
2.3.1 Genome-wide esiRNA Library and secondary esiRNA sublibrary.....	46
2.3.2 Control esiRNA production.....	47
2.4 Transfection procedures	47
2.4.1 Reverse transfections.....	47
2.4.2 DNA and esi/siRNA forward transfections – Rescue experiments.....	48
2.5 Primary Screens	48
2.5.1 7df3 Reporter cell line (H) screen.....	49
2.5.2 eGFP- β -catenin U2OS cell line – UA and UB screens.....	50
2.5.2.1 eGFP- β -catenin U2OS screen (UB screen).....	50
2.5.2.2 eGFP- β -catenin U2OS APC (UA) screen	50
2.6 Fixation and immunocytochemistry	50
2.7 Imaging and Analysis	51
2.7.1 7DF3 H screen.....	51
2.7.2 eGFP- β -catenin U2OS UA and UB screens	52

2.8 Statistical Methods.....	53
2.8.1 Z-factor analysis.....	53
2.8.2 Non-controls based normalisation	54
2.8.3 Z scores	55
2.8.4 Other statistical procedures.....	56
2.9 Luminescence assays	56
2.10 Cell Extraction.....	56
2.10.1 Whole cell extractions	56
2.10.2 Crude cytoplasmic and nuclear extractions.....	57
2.11 Immunoprecipitation.....	57
2.12 SDS/PAGE and Western Blotting.....	Error! Bookmark not defined.
2.13 Pulse-Chase (Metabolic Assay)	58
2.14 RNA Extraction and RT-PCR.....	59
2.15 qRT-PCR.....	60
2.16 RNP-IP Assays	61
2.17 Time-lapse microscopy.....	62
2.18 Plasmids and siRNA	62
2.18.1 siRNA.....	62
2.18.2 Plasmids.....	62
CHAPTER 3. DEVELOPMENT OF HIGH-THROUGHPUT RNAI SCREENS FOR IDENTIFYING REGULATORS OF β-CATENIN LEVELS AND LOCALISATION	63
3.1 High-throughput, high content imaging RNAi screens for novel β-catenin regulators.	64
3.1.1 IN Cell Analyzer 1000 – A semi automated, high-throughput fluorescence imaging system.....	64
3.1.2 Z-factor analysis for an image-based high-throughput assay.....	66
3.2 Development of a HTS esiRNA imaging screen in the 7df3 reporter cell line	67
3.2.1 The 7df3 Cell line.....	68
3.2.2. Induction of β -catenin levels with Estradiol treatment	68
3.2.3 Optimisation of 7df3 reporter cell line transfection conditions for an imaging-based, RNAi high-throughput screen.	69
3.2.3.1 Z-factor analysis for an image-based HTS assay in the 7df3 cell line.....	74
3.2.3.2 Effect of plate edge location on esiRNA.	75
3.3 Development of two HTS esiRNA imaging screens in an eGFP-β-catenin-U2OS cell line.	78
3.3.1 Image based high-throughput screen in the U2OS eGFP-Beta-catenin cell line.	79
3.3.1.1 Z-factor analysis for an image-based HTS assay.....	84
3.3.2 Image based high-throughput screen in the U2OS eGFP-Beta-catenin cell line with APC downregulation.....	86
3.3.2.1 Z-factor analysis for an image-based HTS assay.....	88
3.4 Summary	91
CHAPTER 4. GLOBAL SCALE INSIGHTS INTO β-CATENIN REGULATION AND ITS ROLE IN WNT SIGNALLING.....	92
4.1 esiRNA screens for novel regulators of β-catenin accumulation and localisation in Wnt signalling.....	93
4.1.1 7df3 (H) primary screen.....	94
4.1.1.1 Z-factor analysis of the H primary screen.	94
4.1.1.2 Z-score analysis of β -catenin stabilisation and localisation data from the H primary screen.	95
4.1.2 eGFP- β -catenin U2OS primary screens.....	102
4.1.2.1 Z-factor analysis of the U2OS primary screens.	102

4.1.2.2 Z-score analysis of β -catenin stabilisation and localisation data from both U2OS primary screens.....	102
4.2 In silico analysis of the esiRNA regulators identified in the primary screens.....	109
4.2.1 Enrichment analysis of the 7df3 (H) primary screen.....	110
4.2.2 Enrichment Analysis of the U2OS primary (UA and UB) screens.....	115
4.2.2.1 U2OS UB screen enrichment analysis.....	116
4.2.2.2 U2OS APC (UA) screen enrichment analysis.....	122
4.2.3 Overlaps and enrichment analysis summary of the 3 screens.....	127
4.2.3.1 Signalling crosstalk.....	127
4.2.3.2 Adhesion and cytoskeletal organisation.....	128
4.2.3.3 mRNA processing and translation.....	128
4.3 Comparative analysis of the β-catenin esiRNA screens.....	129
4.4 Reconfirmation assays.....	135
4.4.1 Reconfirmation of the selected H screen hits.....	136
4.4.2 Reconfirmation of UB screen primary hits.....	141
4.4.3. Reconfirmation of UA primary screen hits.....	146
4.4.4 Reconfirmation Summary.....	151
4.5 The relationship between β-catenin accumulation, nuclear localisation and TCF-dependent transcription.....	156
4.6 Comparative analysis of Wnt/β-catenin siRNA screens in different cell lines to identify modulators of β-catenin and TCF-dependent transcription.....	161
4.6.1 Integration of functional genomic data.....	169
4.7 Potential cell type specificity of the identified regulators of β-catenin.....	174
4.8 Summary.....	177
CHAPTER 5. HNRNP A1 – A NOVEL REGULATOR OF β-CATENIN.....	178
5.1 Background.....	180
5.1.1 Heterogeneous nuclear ribonucleoproteins (hnRNPs).....	180
5.1.2 hnRNP A1.....	183
5.1.2.1 hnRNP A1 and KSRP.....	184
5.2 hnRNP A1 identified as a novel repressor of β-catenin – primary screening data.....	186
5.3 hnRNP A1 identified as a novel repressor of TCF-dependent transcription.....	190
5.4 Reconfirmation of hnRNP A1 as a novel repressor of β-catenin and subsequent TCF-dependent transcription.....	190
5.4 Reconfirmation of hnRNP A1 as a novel repressor of β-catenin and subsequent TCF-dependent transcription.....	192
5.4.1 Secondary hnRNP A1 esiRNA reagents result in β -catenin accumulation in both eGFP- β -catenin and parent U2OS cell lines.....	192
5.4.2 Rescue of hnRNP A1 depletion.....	194
5.5 hnRNP A1 interacts with β-catenin.....	196
5.6 hnRNPA1 negatively regulates β-catenin levels independently of its protein turnover.....	196
5.6.1 Dynamic regulation of β -catenin.....	199
5.7 hnRNPA1 negatively regulates β-catenin levels independently of its mRNA synthesis and stabilisation.....	201
5.7.1 β -catenin mRNA half-life appears unaffected by hnRNP A1 downregulation.....	201
5.7.1.1 hnRNP A1 and KSRP do not associate in eGFP- β -Catenin U2OS cells.....	202
5.7.2 β -catenin mRNA synthesis is unaltered upon hnRNP A1 downregulation....	205
5.7.3 hnRNP A1 may bind β -catenin mRNA.....	205
5.8 Summary.....	207

CHAPTER 6. DISCUSSION.....	208
6.1 Cell type specificity of β-catenin and TCF-dependent transcription regulation.....	209
6.2 β-catenin and TCF-dependent transcription.....	212
6.2.1 β -catenin phosphor-isoforms and transcriptional activity.....	213
6.2.2 Fine tuning the Wnt signalling output	215
6.2.2.1 Switching between β -catenin's roles in adhesion and activated TCF-dependent transcription.	216
6.3 Mechanistic insights from the primary screen data.....	219
6.3.1 Ephrin-mediated signalling	220
6.3.2 Integrin mediated signalling.	222
6.3.3 Non-canonical Wnt pathways in β -catenin regulation	224
6.3.3.1. Wnt/Calcium signalling.....	224
6.3.4 Transcriptional and Translation regulation of β -catenin	225
6.4 Dynamic regulation of β-catenin	226
6.5 hnRNP A1's regulation of β-catenin and TCF-dependent transcription.....	228
6.5.1 hnRNP A1 and β -catenin protein regulation	229
6.5.2 hnRNP A1 and β -catenin mRNA synthesis and stability	230
6.5.3 hnRNP A1 and β -catenin mRNA transport and translation.....	230
6.5.4 hnRNP A1 in sequestering β -catenin mRNA?	231
6.5.5 Alternative roles for hnRNPA1 in β -catenin regulation	233
6.6 Conclusions	234
Bibliography.....	237
Appendices	268
Appendix A - Chapter 3	268
Appendix B - Chapter 4	268
Tables folder:.....	268
PNG folder.....	269
Cytoscape Folder	270
Appendix C - Chapter 5	270

1. INTRODUCTION

Cell fate is highly influenced by environmental cues or ‘signals’ secreted from neighbouring cells. Dynamic research over two decades resulted in the identification of a plethora of signalling molecules and a greater understanding of the intracellular transduction pathways and interacting networks they instigate to drive the development of complex multicellular organisms [1]. Seven major signalling pathways appear in several developmental contexts and are sufficient for the majority of metazoan development [2]. These are the wingless related (Wnt) [3, 4], Hedgehog (Hh) [5], transforming growth factor β (TGF- β) [6], receptor tyrosine kinase (RTK) [7], Janus kinase (JAK)/signal transducer and activator of transcription (STAT) [8], Notch [9] and nuclear receptor pathways [10]. From the direct transcriptional control by the nuclear receptor proteins to sequential protein phosphorylation cascades of RTK pathways, these seven are highly diverse pathways, whilst sharing the same principal outcome of the signal-regulated transcription of specific target genes required in response to a myriad of stimuli at any given time [2].

The development of complex multicellular organisms relies on the tightly regulated, coordinated and dynamic equilibrium between migration and adhesion [11, 12]. Adherens junctions (AJs) are especially important as they connect the adhesive function of cadherin-catenin protein complexes to the dynamics of the actin cytoskeleton and are vital for sustaining tissue plasticity during development [12]. Moreover, members of cadherin-catenin protein complexes are inextricably linked to many of the important aforementioned developmental signalling pathways [12]. An interesting protein involved in both adhesion and a major developmental signalling pathway is Beta-catenin (β -catenin), a key mediator of the Wnt signalling pathway.

1.1 Wnt signalling

The Wnts are a large family of conserved growth factors that, upon binding to extracellular receptors, initiate a cascade of signalling events that regulate a variety of cellular processes. Wnt signalling is fundamentally important during the development and maintenance of multicellular differentiated organisms. Studies in *Drosophila melanogaster*, *Caenorhabditis elegans*, *Xenopus laevis* and mice have demonstrated the involvement of Wnt signalling in developmental processes as diverse as

asymmetric cell division, CNS patterning, segmentation and axis formation in vertebrates, in addition to controlling cell growth and fate [3, 13, 14]. Furthermore, Wnt signalling has also been linked with stem cell differentiation and regulation in various systems [15]. The crucial role of Wnt signalling in such diverse processes highlights the importance of its precise regulation, with its aberrant signalling implicated in a wide variety of developmental disorders and disease [13].

To date, 19 Wnt proteins have been described. So called ‘canonical’ Wnts include Wnt-1, Wnt-3a and Wnt-8, which were first observed to cause duplication of the embryonic axis when overexpressed in ventral blastomeres of *Xenopus laevis* embryos [16, 17], with many others demonstrated to promote transformation of mammary epithelial cells [18, 19]. So called ‘non-canonical’ Wnts, including Wnt-5a and Wnt-4, were unable to replicate these effects [18, 19] and were able to antagonise the effects of ‘canonical’ Wnts in *Xenopus laevis* axis duplication assays [20, 21].

A variety of extracellular receptors, such as Frizzled family of receptors [22], LRP5/6 (low-density lipoprotein receptor-related protein 5/6) co-receptors [23-25], or the tyrosine kinases Ryk [26, 27] or Ror2 [28] mediate the activation of intracellular signalling pathways upon binding of Wnt ligands. Different Wnt ligands can stimulate distinct Wnt pathways, even upon recruiting shared intracellular components, through binding different combinations of unrelated receptors [29, 30]. Currently, there are five Wnt pathways identified that are activated by various combinations of Wnt ligands and receptors (Figure 1.1).

The Wnt/ β -catenin (often referred to as the canonical) pathway is the best described and was the main focus of this study. The mechanism and consequences of its activation will be described in further detail within this chapter, with schematic representations of this pathway displayed in Figures 1.1 and 1.2.

Other Wnt induced pathways include the ‘Planar cell polarity’ (also referred to as the Wnt/JNK pathway) where Wnt-5a or Wnt-11 activate mediators such as JNK or Rho kinase (ROK) downstream of Dishevelled activated Rho GTPases [31, 32]. In vertebrates this pathway has been shown to regulate convergent extension movement

during gastrulation and the migration of neural crest cells [33, 34], in addition to epithelial polarity in *Drosophila melanogaster* [31, 32].

Binding of Wnt-4/Wnt-5a/Wnt-11 induces the Wnt/calcium pathway to release intracellular calcium, and subsequently activate enzymes such as PKC, CamKII, and the calcium sensitive phosphatase calcineurin that can activate the transcription factor NFAT [35, 36]. This pathway, through the activation of Nemo-Like Kinase (NLK), can also lead to inhibition of Wnt/ β -catenin signalling by phosphorylation of TCF transcription factors [37].

Ryks are conserved tyrosine kinase-related Wnt receptors which play key roles during neurogenesis, axon guidance and synaptogenesis [38]. The Wnt/Ryk pathway has been demonstrated to both activate TCF-dependent transcription, through Dishevelled dependent inhibition of the β -catenin destruction complex, in addition to also being able to inhibit transcription [26].

The Wnt5A/Ror2 pathway has been shown to inhibit TCF-dependent transcription induced by Wnt/ β -catenin pathway activation [39]. This complexity is further exemplified by observations where non-canonical Wnts can inhibit or activate canonical Wnt/ β -catenin signalling depending on receptor context, such as Wnt5a, which was demonstrated to activate canonical signalling when co-expressed with Fz4 and LRP5 in Human Embryonic Kidney 293 (HEK293) cells [39]. In addition, the Wnt5A/Ror2 pathway has been shown to activate the JNK signalling cascade by signalling through cdc42 and PI3Kinase [40].

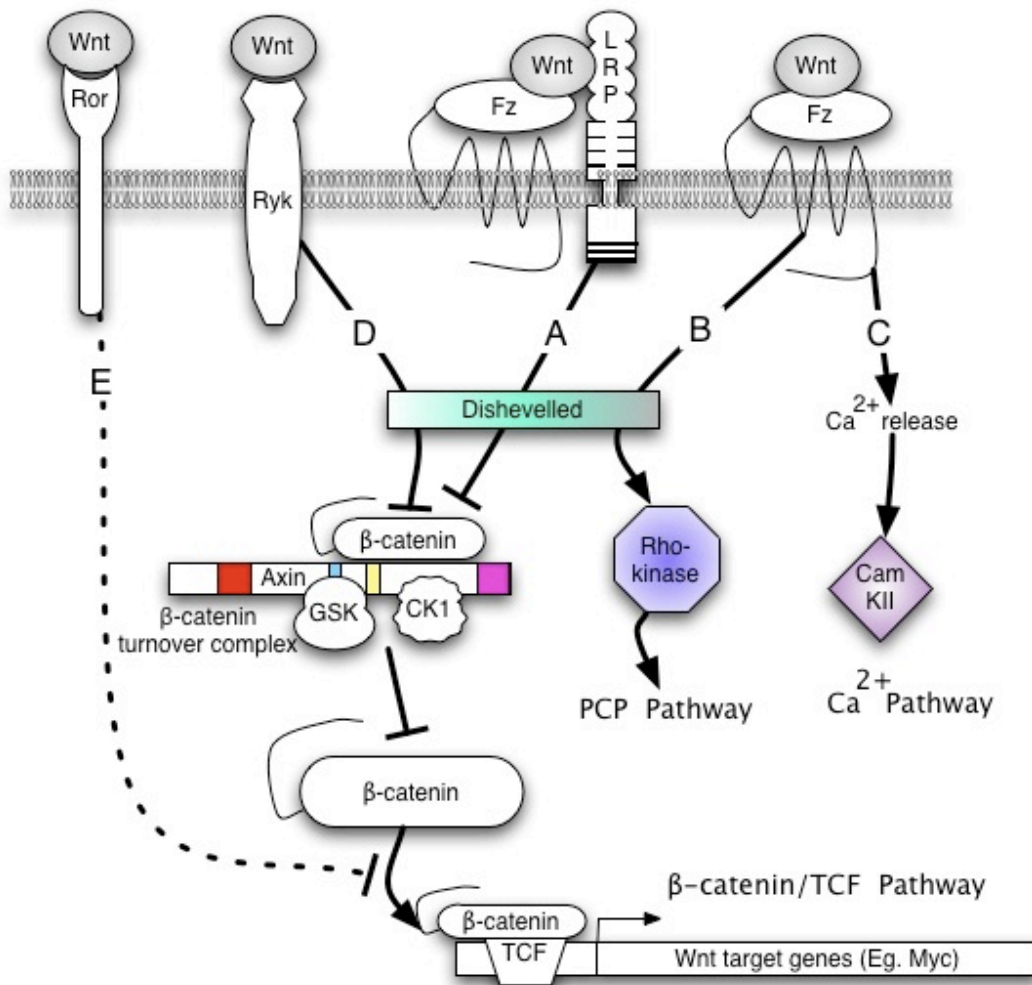


Figure 1.1 Wnt ligands at the cell surface activate at least 5 different pathways. The best characterised is the 'canonical' β -catenin/TCF pathway (A) where Wnt binding to a receptor complex involving Frizzled and LRP5/6 leads to the inhibition of β -catenin turnover. Downstream of Frizzled receptors two other pathways have been described, the PCP and the Ca²⁺ pathway (B, C). Two tyrosine kinase receptors appear to mediate Wnt signalling. Ryk binds Wnts through an extracellular Wnt Inhibitor protein domain (WIF; D) with Ror binding Wnts through an extracellular Frizzled-like domain (E). Figure kindly provided by Dr J.Freeman.

1.1.1 The Canonical Wnt/Beta-catenin signalling pathway

β -catenin is a 90 kDa vertebrate homologue of Armadillo; a *Drosophila melanogaster* protein involved in inducing segment polarity during embryogenesis and the first characterised member of the armadillo protein family. Armadillo proteins share a central "arm repeat" domain consisting of a repeating 42 amino acid motif that acts as a versatile interface to mediate protein binding [41]. The central armadillo domain of

β -catenin possesses 12 arm repeats that form a superhelix of helices that creates a long positively charged groove. This can act as a binding surface for many of its negatively charged interactors such as lymphoid enhancer factor (LEF)/T-cell factor (TCF) transcription factors, the Axin/APC degradation complex and the cadherin adhesion receptor [42, 43]. Different binding partners interact with β -catenin's arm domain in a mutually exclusive fashion and will often dictate its localisation within the cell and subsequently its function [42, 44].

In addition to its key role in canonical Wnt signalling, β -catenin acts as a central structural component of adherens junctions (AJs). β -catenin mediates the association of plasma membrane cadherins with other catenins, such as α -catenin, which dynamically links AJs with the actin cytoskeleton [45]. Furthermore, β -catenin protects the cytoplasmic domain of cadherins from degradation; in addition to recruiting α -catenin to cell-cell contact sites and is therefore a prerequisite for adhesion [42, 45, 46]. Disruption of β -catenin/cadherin interactions has significant consequences for cell-cell adhesion, with abnormal adherens junctions implicated in many disease states, such as cancer [47, 48].

The events that dictate β -catenin's binding partners and function is especially complex, which will be discussed after an introduction into β -catenin's role in the Wnt/ β -catenin signalling pathway, the most widely characterised Wnt pathway.

1.1.1.1 Mechanism of canonical Wnt signal transduction

In the standard text-book model of the Wnt/ β -catenin pathway (Figure 1.2), binding of Wnt ligands to an extracellular receptor induces a signalling cascade that results in the accumulation of β -catenin and subsequently its translocation to the nucleus, where it acts as a co-transcriptional activator by interacting with the transcription factors T-Cell Factors (TCFs) or Lymphoid EnHancing Factors (LEFs). This in turn activates the transcription of Wnt target genes, which include oncogenes, developmental and proliferation regulators from c-myc [49] to BMP4 [50] and cyclinD1 [51].

Briefly, in the absence of a Wnt ligand the signalling pathway remains inactive with cytoplasmic levels of β -catenin kept at low levels by continuous proteasomal degradation thus preventing unnecessary activation of Wnt target genes [52]. In the inactive state β -catenin is held in a ‘destruction complex’ with several other proteins, including Axin, Adenomatous Polyposis Coli (APC), Casein Kinase 1α (CK1 α) and Glycogen Synthase Kinase 3β (GSK3 β) amongst many other undefined players [15, 53-55]. Within this complex, β -catenin is sequentially phosphorylated by CK1 α and GSK3 β [55], which targets β -catenin for ubiquitination and subsequent degradation by the proteasome [56]. Meanwhile in the nucleus the TCFs/LEFs are bound to transcriptional repressors [57] (Figure 1.2 [58]).

Binding of Wnt ligand to its extracellular receptors, low-density lipoprotein receptor-related protein (LRP)5/6 and Frizzled, activates the protein Dishevelled leading to the apparent relocation of Axin to the cytoplasmic domains of the LRP receptors [59, 60]. This leads to the dissociation of the destruction complex, which prevents β -catenin from being phosphorylated and results in its accumulation and subsequent translocation to the nucleus where it binds TCFs/LEFs to activate TCF-dependent transcription of Wnt target genes [61].

The Wnt/ β -catenin signalling pathway can be broken down to four key stages that employ specific complexes of proteins at the cell surface, in the cytosol and in the nucleus. These will be described in further detail in the following sub-sections before describing β -catenin’s roles and regulation in further detail.

1.1.1.1.1. Wnt/ β -catenin signalling at the cell surface – the receptor complex.

Various ligand/receptor complexes at the cell surface tightly regulate Wnt signalling. With 19 Wnt proteins, 10 Frizzled (Fz) receptor proteins and 2 LRP co-receptor proteins, a vast variety of different ligand:receptor combinations can be formed. Frizzled (Fz) receptors bind to different Wnt ligands with varying efficiencies [62] through their extracellular Cysteine Rich Domains (CRDs) [63]. Proteoglycans, such as Dally [64] or Syndecan 1 [65], concentrate Wnt ligands at cell surfaces where they can bind to LRP5/6 and Fz receptors to mediate their interaction. Various antagonists

can inhibit Wnt signalling, including Wnt inhibitory factor 1 (WIF 1), secreted Frizzled related proteins (sFRPs), Dickkopf (Dkk) proteins and the Wise/SOST family, with Norrins and R-spondin (Rspo) proteins acting as agonists for Wnt/ β -catenin [66]. Dkk family members bind with high affinity the LRP6 receptor, at domains distinct from those mediating Wnt/Fz interaction and are considered specific inhibitors of the Wnt/ β -catenin signalling pathway [66, 67]. Dkk1's inhibitory action has been suggested to be either due to disruption of the Wnt-induced Fz-LRP6 complex [68] or by inducing LRP6 internalisation/degradation through transmembrane Kremen (Krm) proteins [69]. Secreted Frizzled related proteins (sFRPs) sequester Wnt ligands with their CRDs, which are similar to Fz CRD domains but are incapable of activating signalling [70]. [66].

Upon Wnt ligand binding, the LRP co-receptor undergoes phosphorylation of highly conserved motifs on its intracellular domain, which contain CK1 consensus sites and PPPSPxS motifs (P, proline; S, serine or threonine; x, a variable residue) [71, 72]. The PPPSPxS sites are phosphorylated by GSK3 in response to Wnt signalling (Zeng et al, 2005), enabling the subsequent phosphorylation of the CK1 sites by CK1 γ or CK1 ϵ isoforms [72, 73]. In turn this results in the plasma membrane recruitment of Axin for inactivation/degradation [60, 71], in addition to the inhibition of β -catenin phosphorylation by GSK3 β by phosphorylated PPPSPxS in a sequence and phosphorylation dependent manner [74, 75]. How these processes result in elevated β -catenin levels are discussed in the following sub-section. Fz co-receptors are believed to mediate Dvl membrane recruitment and activation, although the precise mechanisms of Dvl activation are still unclear [66]. Both Dvl and Axin harbour homologous DIX domains that demonstrate dynamic polymerisation that allows them both to form large aggregates that facilitate dynamic protein interactions [66, 76, 77] with Wnt-induced receptor clustering requiring an intact DVL DIX domain [77]. Dvl recruitment following Wnt binding to the Fz-LRP6 receptor complex induces the production of phosphatidylinositol 4,5-bisphosphate [PtdIns (4,5) P2 or PIP2] by binding (via its DIX domain) and activating the phosphatidylinositol kinases PI4KII and PIP5KI [78]. The resulting PIP2 generated in regions of activated receptors serves to promote LRP6 clustering and phosphorylation through the recruitment of adenomatous polyposis coli membrane recruitment 1 (Amp1, also called WTX),

which in turn recruits Axin/GSK3 β and CK1 γ to LRP6 [79]. These LRP6 protein complexes (often called signalsomes [80]) are presumed to represent endocytic vesicles with many reports implicating Wnt in the internalisation of the ligand/receptor complexes, possibly by caveolin-mediated endocytosis [81, 82].

1.1.1.1.2 The β -catenin destruction complex

In the absence of Wnt signalling, a multi-protein complex mediates the phosphorylation of β -catenin within the cytosol, which targets it for degradation. This so called destruction complex consists primarily of the scaffold proteins Axin and APC and the kinases CK1 α and GSK3 β [15, 53-55], although many more components are envisaged with its complexity yet to be fully revealed [83].

Within the destruction complex, Axin scaffolds CK1 α , GSK β and β -catenin to coordinate the sequential phosphorylation of β -catenin at serine45 by CK1 α [55], which primes it for subsequent phosphorylation at threonine 41, serine 37 and serine 33 by GSK3 β [55, 84]. This targets β -catenin for ubiquitination by the Skp1-Cul1-Fbox β -Trcp ubiquitin conjugation complex and subsequent degradation by the proteasome [85]. GSK3 β and CK1 α also phosphorylate Axin and APC, leading to their increased association, and therefore phosphorylation/degradation of β -catenin [86].

The role of APC in β -catenin regulation appears multi-functional. It recruits β -catenin to the ubiquitination complex and protects it from dephosphorylation by Protein Phosphatase 2A [87]. Interestingly, phosphorylated APC (by GSK3 β /CK1 α) and Axin compete for the same β -catenin interaction surface, suggesting that APC may act to remove phosphorylated β -catenin from Axin for ubiquitination thus enabling Axin to be free to participate in further rounds of β -catenin phosphorylation events [86, 88]. APC has also been demonstrated to act as a chromatin-associated suppressor for β -catenin target genes (discussed below) and is implicated in promoting β -catenin nuclear export, which will be discussed in the subsequent sub-section.

As mentioned above, binding of Wnt ligands to Fz-LRP6 receptors induces LRP6 phosphorylation, providing docking sites for Axin and subsequent disruption of the destruction complex, although the exact nature of Wnt induced inhibition of the complex and of β -catenin phosphorylation is unclear [60, 71, 73, 89]. Postulated mechanisms include Wnt induced and Dvl-dependent Axin-GSK3 (or β -catenin) dissociation [90, 91], Axin degradation [60, 92, 93] and inhibition of GSK3 β by the phospho-PPPSPxS sites in the cytoplasmic domain of LRP6 [74, 75]. Activation of Wnt/ β -catenin signalling upon ligand binding results in the inhibition of the destruction complex and β -catenin phosphorylation, resulting in its stabilisation and translocation to the nucleus. Further details regarding the role of β -catenin's phospho/dephospho status in dictating its localisation and function will be discussed in more detail later in the chapter.

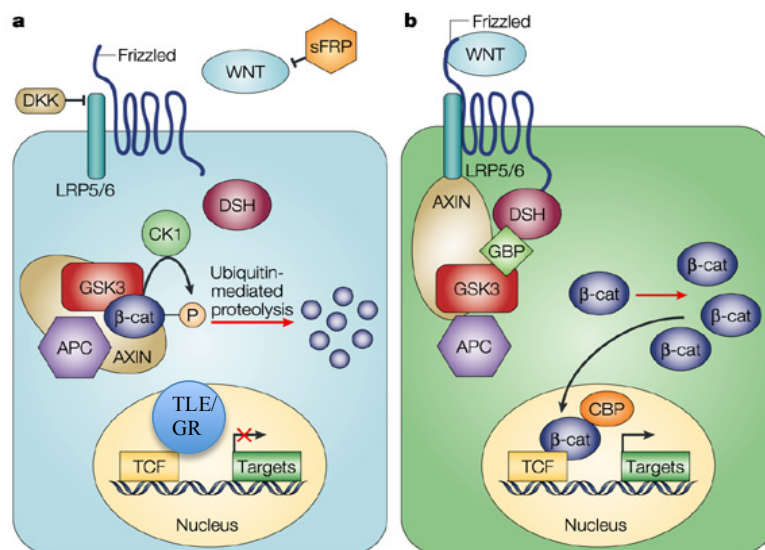


Figure 1.2 The mechanism of Wnt/ β -catenin signalling (Reproduced from [58] with permission from Nature Publishing Group).

A. 'OFF' state - β -catenin is held in the destruction complex where it is phosphorylated and targeted for degradation by the proteasome in the absence of Wnt ligand. TCF transcription factors are complexed with transcriptional inhibitors such as TLE/Groucho (GR), and target genes are not transcribed. **B.** 'ON' state - Wnt binding causes disassembly of the complex in a Dishevelled dependent manner, allowing the nuclear translocation of beta-catenin to activate transcription of target genes/ APC, adenomatous polyposis coli; β -cat, β -catenin; CBP, CREB-binding protein; CK, casein kinase; DKK, Dickkopf; DSH, Dishevelled; GBP, GSK3-binding protein; GSK, glycogen synthase kinase; LRP, LDLreceptor-related protein; P, phosphorylation; sFRP, secreted Frizzled-related protein; TCF, T-cell factor.

1.1.1.1.3 β -catenin nuclear/cytoplasmic shuttling and retention

The standard model of Wnt/ β -catenin signalling presented above states that upon Wnt induced stabilisation, β -catenin translocates to the nucleus to activate TCF-dependent transcription of Wnt target genes [66, 91]. While this view has become increasingly challenged of late, which will be discussed in detail later, this part of the chapter will describe current knowledge with regards to the shuttling of β -catenin between the nucleus and cytosol.

Selective and active nucleocytoplasmic transport of proteins through the nuclear pore complex (NPC) is mediated by carriers called Karyopherins, that either facilitate the RanGTPase dependent nuclear import (importins) or export (exportins/CRM) of their cargoes [94]. These transport receptors recognise specific basic nuclear localisation signals (NLS) or nuclear export signals (NES) on their cargoes to mediate their transport. NLS signals typically consist of one, or more, short sequences of positively charged arginines/lysines exposed on the protein surface, while NES's normally comprise of a short amino acid sequence of 4 hydrophobic residues within a protein [95].

Earlier studies implied that β -catenin's nuclear translocation was independent of classical NLS and importin mediated mechanisms and that, due to structural similarities with importin- β HEAT repeats, it could bind directly with nucleoporins in the NPC thus facilitate its own transport [96]. However, this was challenged by observations that β -catenin was unable to interact with nucleoporins [97].

β -catenin is reported to shuttle between compartments via its binding partners that possess the required motifs for the importin/exportin mediated transport pathway [98, 99]. APC has been suggested to bind β -catenin in the nucleus and transport it back to the cytoplasm for degradation [100], in addition to Axin [101, 102]. RanBP3 (Ran binding protein 3), a cofactor of CRM1 mediated nuclear export that binds β -catenin in a Ran-GTP dependent manner [103], has also been implicated in its nucleocytoplasmic shuttling. Pegylated-Interferon- α 2a was demonstrated to inhibit β -catenin signalling through the up-regulation of RanBP3 and subsequent decreased β -

catenin nuclear accumulation in human hepatoma cell lines [104]. However, β -catenin has been shown to shuttle between the cellular compartments independently of APC, importin- β and Ran, suggesting the existence of a carrier-independent import pathway in cells [96, 105-107].

Other β -catenin interacting proteins proposed to play a role in directly and actively transporting it across the nuclear envelope include its co-activator of transcription, B-cell lymphoma 9 (BCL9 – a homologue of *Drosophila* Legless), and its nuclear binding partner Pygopus, with their roles in relation to the nuclear transcription complex discussed in the following section [108, 109].

Live-cell imaging and fluorescence recovery after photobleaching (FRAP) assays revealed that APC, Axin, TCF and BCL/Pygo modulated β -catenin subcellular distribution by retention, rather than by active nucleocytoplasmic transport [109]. More recently, it was demonstrated that β -catenin accumulation in the nucleus in response to GSK-3 β inhibition was mediated by increased LEF-1 levels in response to Wnt signalling [110]. Figure 1.3 summarises the above theories on β -catenin nucleocytoplasmic shuttling. Taken together, the data suggests that β -catenin nuclear and cytoplasmic partitioning results from both dynamic shuttling and retention between compartments and that this is mediated by several mechanisms [66].

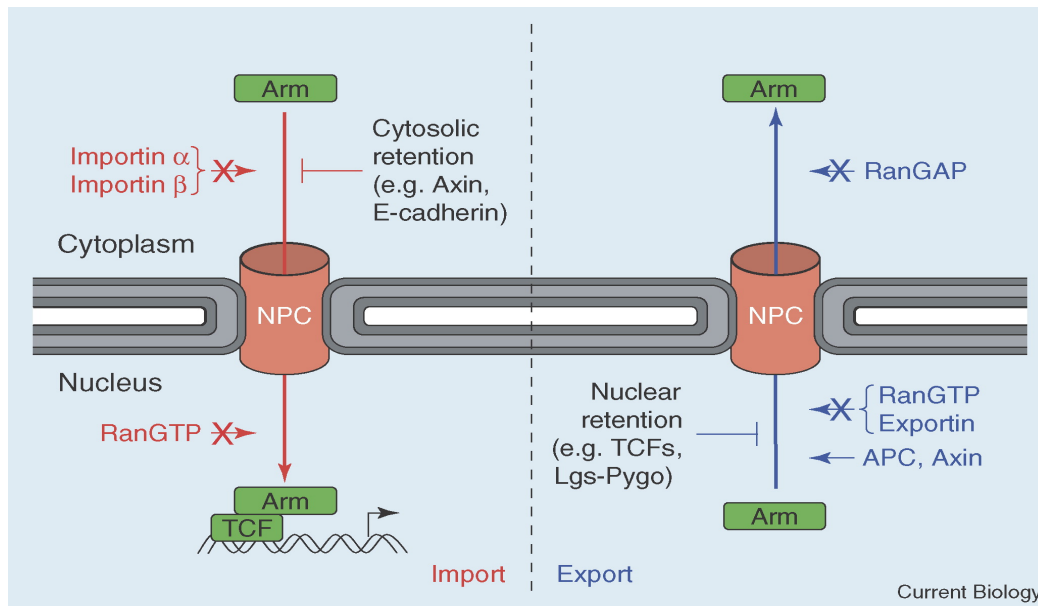


Figure 1.3. Nucleo-cytoplasmic shuttling of β -catenin (reproduced from [111] with permission from Elsevier).

Summary of the various theories regarding the transport of beta-catenin (Arm) through the NPC. β -catenin itself is not directly dependent on import by the carrier proteins importin α/β and the cycling of Ran, although it may be imported in by its binding partners that do utilise this pathway. Export can also be Exportin/RanGTP independent or by interaction partners that are Ran dependent. More likely β -catenin is retained in specific compartments by its interaction partners rather than actively transported across the nuclear envelope.

1.1.1.1.3.1 Alternative mechanisms of β -catenin nucleocytoplasmic transport

In addition to the above models of β -catenin nuclear localisation, other alternative mechanisms have been recently suggested, with many revolving around β -catenin's post-translational modifications. HDAC6 deacetylation of β -catenin at lysine 49 in response to EGF stimulation was observed to inhibit β -catenin phosphorylation at serine 45, resulting in its nuclear localisation and increased c-myc gene expression [112]. Leucine zipper tumour suppressor 2 (LZTS2) was identified as a novel β -catenin interacting protein that could regulate its export from the nucleus [113], in addition to Chibby, which has been shown to interact with 14-3-3 proteins to also facilitate its nuclear export and cytoplasm sequestration [114]. O-GlcNAc glycosylation (O-GlcNAcylation) of β -catenin was shown to negatively regulates its levels in the nucleus [115], while another study demonstrated that β -catenin's nuclear accumulation may be dependent on Rac1 activation and its phosphorylation on

specific serine residues by JNK2 kinase [116]. The regulation of β -catenin's levels, localisation and transcriptional activity by phosphorylation will be discussed in further detail in a specific subsection within this chapter.

1.1.1.1.4 The nuclear transcription complex

In the absence of activated Wnt signalling and nuclear β -catenin, members of the TCF or LEF family of DNA-bound transcription factors reside in complexes with transcriptional repressors, such as CtBP and Groucho/TLE, which promote histone deacetylation and chromatin compaction. Following Wnt induction, active β -catenin translocates into the nucleus and displaces these repressors to associate with TCFs/LEFs and recruit further co-activators to form a transcriptionally active complex, leading to the expression of target genes such as c-myc and cyclin D1 [49, 51, 57, 117-119]. Dominant negative forms of TCF-1 and LEF-1, lacking the amino-terminal β -catenin binding domain, are generated through alternative promoter usage in TCF-1 and LEF-1 genes [120]. TCFs have also been shown to bind to alternative sequences, leading to Wnt dependent gene repression [121].

Associated co-activators of β -catenin include BCL-9/Legless, which interacts with β -catenin's N-terminal region and recruits Pygopus (Pygo) and Parafibromin with TCF/LEF [122, 123]. As mentioned, Pygo was demonstrated to play a role in recruiting/retaining BCL-9/ β -catenin in the nucleus upon activated Wnt signalling [124, 125]. Upon interaction with BCL-9, Pygo's PHD (plant homology domain) appears to bind preferentially to dimethylated H2K4, suggesting a role for Pygo/BCL-9 in participating in histone methylation changes during activation of Wnt-induced transcription [126], although its precise mechanism of action is far from clear [66].

β -catenin also recruits the histone acetyltransferase CREB Binding Protein CBP/p300, both an inhibitor and an activator of TCF-dependent transcription depending upon cellular context [127-129] and various other chromatin remodelling complexes through its C-terminal region, such as TRRAP/TIP60 histone acetyltransferases (HATs), MLL1/2 histone methyltransferases (HMTs) and the SWI/SNF family of ATPases for chromatin remodelling [66, 130]. Post-translational

modifications of TCF/LEFs such as phosphorylation and sumoylation provide an additional level of control over gene expression activation by Wnt/ β -catenin signalling [66]. For example, TCFs can be inhibited by phosphorylation by kinases such as NLK (Nemo-like kinase) as a target of ‘non-canonical’ Wnt signalling [131], while PIASy mediated sumoylation of TCF-4 and LEF-1 enhances and represses transcription respectively [66, 132].

To summarise, Wnt/ β -catenin signal transduction is mediated by a variety of protein complexes at various cellular locations, which heavily relies on the coordinated interactions between these complexes for the strict regulation of transcriptional output [66].

The remainder of this section of the chapter will mostly focus on β -catenin’s regulation and the relationship between its levels, localisation and transcriptional activity within Wnt signalling. Firstly, the role of Wnt/ β -catenin signalling in development and disease will be briefly discussed.

1.1.2 Wnt / β -catenin signalling in development and disease.

The Wnt/ β -catenin signalling pathway is fundamentally important in most aspects of embryonic development across many species, from regulating asymmetric cell division in *Caenorhabditis elegans* [133], segmentation in *Drosophila* [134] and axis formation in vertebrates [16, 135]. *Wingless (wg)*, which regulates segment polarity during larval development in *Drosophila*, was demonstrated to be a fly homolog of Wnt1 [136]. In *wg* mutant fly embryos, epidermal segmentation is impaired with the overlying ventral cuticle covered with denticles compared to the alternative denticle and naked belts exhibited in wild-type cuticle [136]. Mutations in *armadillo*, *porcupine* and *dishevelled* genes result in similar cuticle abnormalities to mutant embryos, while naked cuticles are observed in mutant *shaggy/ zeste-white 3* embryos [14]. Duplication of the body axis in *Xenopus* was observed following the injection of mouse Wnt1 mRNA into ventral blastomers of 4-cell embryos with Wnt11 subsequently identified as the specific Wnt signal that triggered axis induction in *Xenopus* [137]. Axis duplication was also induced by β -catenin (the vertebrate

homolog of *armadillo*), Dishevelled (Dsh) and dominant-negative glycogen synthase kinase 3 (GSK3, the vertebrate homolog of *shaggy/zeste-white 3*) [138-140]. These combined observations in *Drosophila* and *Xenopus* delineated a highly conserved signalling pathway activated by secreted Wnt proteins. In turn, this supported the notion that Wnt signalling was shared between vertebrates and invertebrates [14]. Independently, the *adenomatous polyposis coli* (*APC*) gene was discovered in familial adenomatous polyposis (FAP), a hereditary cancer syndrome [141, 142]. The discovery that the large cytoplasmic APC protein interacted with β -catenin provided the first connection between human cancer and the Wnt signalling pathway [143].

In adult tissues, Wnt/ β -catenin signalling has been implicated with regulating diverse processes from cell fate decisions [144], cell morphology [145], motility [146] and proliferation [147]. Furthermore, it has also been linked with stem cell differentiation and regulation in various systems [15, 148]. Thus, Wnt signals can co-ordinately regulate both proliferative responses, and subsequent tissue expansion, along with cell fate determination or terminal differentiation of postmitotic cells [14]. Moreover, the Wnt pathway is able to activate these disparate events in different cell types within the same structure, such as the intestinal crypt or the hair follicle [15].

Wnt signalling is widely recognised as a crucial regulator of intestinal homeostasis, having a vital role in maintaining a pool of undifferentiated cells in the colon [149]. Additionally, Wnt/ β -catenin regulates stemness, proliferation and differentiation in other adult stem niches from the haematopoietic systems [150] and mammary gland [151] to the skin and hair follicle in a dosage and context-dependent manner [152, 153]. Consequently, the key roles Wnt signalling plays in self-renewing adult tissues intimately links it to disease development upon its deregulation, from defects in kidney formation [154] and the production of nervous system progenitors [155] to the progression of a plethora of cancers, including colorectal, breast, skin and bone marrow [14, 156, 157]. Furthermore, given β -catenin's key role in cell-cell adhesion, the integration between this and its role Wnt driven gene expression must be tightly and co-ordinately regulated for the correct development and maintenance of multicellular, differentiated organisms [158]. Mutated β -catenin has been implicated

in a myriad of developmental defects in various organs, such as the CNS, limb, kidney and heart [12].

While many studies have demonstrated Wnt pathway activation in different cancers often the mechanisms of action are unknown [159-164], (reviewed in [13, 15, 156]). In certain malignancies epigenetic inactivation of secreted Wnt inhibitors have been implicated in disease progression, such as the inactivation of Dkk in colorectal [165] and breast [166] cancers or sFRPs in lung cancer[167]. Abnormal β -catenin levels and localisation has been implicated in the progression of oncogenesis, through inactivating mutations of negative regulatory Wnt components, such as Axin and APC, in addition to activating mutations of β -catenin itself observed in various cancers from colorectal cancers to hepatocellular carcinomas [61, 168]. Consequently, the Wnt signalling pathway is a prime target for therapeutic intervention in the treatment of cancer. The role of Wnt signalling in the development and tumourigenesis of one particular tissue, the colon, is discussed in detail below to further explore the implications of Wnt pathway activation in key biological processes.

1.1.2.1 Wnt signalling in intestinal homeostasis and colon cancer.

A single layer of absorptive epithelium, ordered into luminal protrusions (villi) surrounded by sub-mucosal invaginations (crypts), lines the rapidly self-renewing small intestine (Figure 1.4) [14]. Crypts consist of undifferentiated multipotent stem or progenitor cells anchored at the base, which give rise to transit amplifying (TA) cells. TA cells rapidly proliferate and expand into non-proliferating daughter cells upon reaching the crypt-villus junction, which are capable of differentiating toward all epithelial lineages that make up the villi, (enterocytes, enteroendocrine cells and goblet cells) [169], in addition to paneth cells [170]. While the paneth cells migrate to the crypt bottom the other differentiated cell types migrate upwards to the apex of the villus where they undergo apoptosis (Figure 1.4) [171, 172].

Current evidence demonstrates the importance of Wnt signalling in the regulation of cell fate along the crypt-villus axis of the intestine. Nuclear β -catenin is observed throughout crypts [173], with neonatal TCF4 knockout mice completely lacking the

crypt progenitor compartment, implying the requirement of physiological Wnt signalling for the establishment of this compartment [174]. Furthermore, transgenic expression of DKK-1 and resulting Wnt signalling inhibition in adult mice induces the complete loss of crypts, with overexpression of the Wnt agonist R-spondin resulting in crypt hyperproliferation [175]. Similarly, APC inactivation results in the repopulation of the villi by crypt-like cells, which are unable to migrate and differentiate and have nuclear β -catenin [176]. In addition, a decreasing gradient of β -catenin nuclear accumulation was observed from the crypt base towards the crypt-villus axis [149, 173]. Wnt target genes were revealed by microarray analysis to be repressed in the differentiated villus cells but highly expressed in proliferative crypt cells [149]. As a result, the Wnt/ β -catenin pathway is widely recognised as being a crucial regulator of intestinal homeostasis through the maintenance of cells in an undifferentiated state [149]. The recent identification of the Wnt target gene Lgr5 as a specific marker for the stem cell in colonic crypts further supports this [177], with neoplastic transformation of the intestine being driven by abnormal activation of Wnt signalling specifically in these stem cells [178].

This image has been removed by the author for copyright reasons

Figure 1.4 Adult Intestinal homeostasis (Reproduced from [172] with permission from CSH Press).

(A) Tissue section of mature small intestine. Black arrowheads indicate Ki67 positive transit-amplifying cells, while white arrowheads indicate the Paneth cell compartment. (B) Schematic representation of the crypt-villus unit. While differentiated cells occupy the villus, cells residing in crypts are highly proliferative. Crypt progenitors migrate up (red arrow) the crypt-villus axis before undergoing apoptosis and shedding into the lumen. Asymmetrically dividing stem cells at the bottom of the crypts ensure epithelial renewal in approximately 3-6 days. The proliferation of progenitor or transit-amplifying (TA) cells is regulated by a Wnt signalling gradient, which also regulates commitment toward secretory lineages.

Deregulation of intestinal homeostasis results in hyperproliferation and a loss of differentiation, which in turn drives tumourigenesis. Germline loss of function mutations in the tumour suppressor gene APC results in FAP (Familial Adenomatous Polyposis) (124) with 1% of these resulting in colorectal cancers [142]. 80% of sporadic colon cancers have been observed to also contain loss of function mutations in APC, with the majority of the remaining tumours resulting from activation mutations in β -catenin [179]. Whilst sufficient for neoplastic transformation other mutations, such as k-Ras activation or loss of p53, are required to drive a tumour into an adenoma [180]. Mouse models of colon cancer with bi-allelic truncation and inactivation of APC in the colorectal epithelium develop colorectal tumours that are lethal within 4 weeks, thus demonstrating that APC is sufficient for tumour progression [181]. Knockdown of c-Myc, a known Wnt target gene in the intestine, was demonstrated to rescue the colorectal tumorigenic phenotype induced by APC loss, even in the presence of high nuclear β -catenin levels [182]. The majority of target genes activated as a result of APC loss were demonstrated by microarray analysis to be dependent on Myc expression [182]. Therefore, the Wnt/ β -catenin signalling pathway is not only a vital regulator of intestinal homeostasis but leads to tumour formation upon abnormal β -catenin stabilisation in a manner dependent on the expression of a Wnt target gene.

Wnt signalling's similar role in other mammalian self-renewing adult tissues, such as bone, hair follicle and the haematopoietic system, intimately links it to disruption in the homeostatic balance in such tissues upon its deregulation, resulting in profound pathological conditions ranging from cancer to disturbances in bone mass [14].

1.1.3 Beta-catenin

1.1.3.1 Transcriptional and translational regulation of β -catenin.

Given β -catenin's vital function in mediating Wnt activation of TCF-dependent transcription its regulation at the protein level has been subject to dynamic research. Its regulation at the transcriptional and translational level however has, for the most part, been largely ignored due to an overwhelming assumption that it plays no part

during Wnt signalling itself. However, more recent work suggests otherwise and point to an unanticipated level of β -catenin regulation in Wnt signalling [183, 184]. β -catenin mRNA was observed to be stabilised upon the activation of both PI3K-AKT and Wnt signalling through the inhibition of KSRP, an RNA-binding protein involved in mRNA degradation [185]. KSRP was later demonstrated to bind Dishevelled with Wnt stimulation mediating the release of β -catenin mRNA from this complex, resulting in its translation [183]. In addition, another apparent Dishevelled-associated protein, G3BP1, was postulated to regulate β -catenin mRNA in response to Wnt signalling [184]. While these examples could be cell type specific, it may also be a general level of Wnt regulation that has been, thus far, overlooked.

1.1.3.2 β -catenin and activated TCF-dependent transcription

A widely held belief, extensively advocated in major reviews of the field, is that increased total levels of β -catenin correlates with increased nuclear localisation and subsequently with activation of transcription [66, 91]. Recently, this philosophy has been increasingly challenged with evidence emerging that the relationship between β -catenin levels, localisation and activation of TCF-dependent transcription is far more intricate than envisioned, with many reports demonstrating a lack of increased transcriptional activity with increased levels of wild-type β -catenin [92, 186-188]. Indeed, correlations between stabilised β -catenin (from mutations in the GSK3 phosphorylation sites for example) and increased TCF-dependent transcription have been demonstrated to be as a result of the stabilised mutant form titrating negative regulators such as APC, thus allowing for wild-type β -catenin to mediate signalling [102, 189, 190]. Additionally, research in the colorectal cell line HCT116 that harbours both an oncogenic and wild type β -catenin allele demonstrated that the transcriptional activity of the two resulting proteins were equivalent [191]. Furthermore, studies suggest that other pathways may regulate transcriptionally active β -catenin independently of its overall cellular levels, such as Notch [192-194].

While nuclear β -catenin accumulation is a more reliable indicator of Wnt activation than simply increased levels, this 'hallmark of Wnt signalling' does not always hold

true, with Wnt driven transcriptional activity reported even in the absence of detectable nuclear β -catenin [195-197]. For example, conflicting observations are reported in colon carcinoma cells, where mutations in APC (leading to hyperactivation of Wnt/ β -catenin signalling) is believed to be one of the earliest events in the sequence of genetic changes that result in intestinal tumourigenesis, with increased transcription of Wnt target genes such as c-myc and cyclin D1 observed [49, 51, 198-200]. According to the standard model for Wnt/ β -catenin (as represented in Figure 1.2), one would predict that within colon tumours initiated by APC (or activating β -catenin mutations) each tumour cell should possess elevated β -catenin intracellular levels and/or nuclear accumulation, associated with increased TCF-dependent transcription of Wnt target genes. Yet, highly heterogeneous β -catenin distributions are observed upon immuno-histochemical analysis of colorectal cancers, with membranous β -catenin, akin to normal colon epithelium, observed in well-differentiated cells in the tumour centre and only invasive tumour cells at the invasion front observed to possess nuclear β -catenin accumulation [153, 201]. This indicates that APC loss, which was shared by all tumour cells, does not consistently result in detectable nuclear β -catenin, with this ' β -catenin paradox' observed in both human and mouse intestinal adenomas and carcinomas [153, 197, 202]. The non-random distribution of tumour cells with β -catenin accumulation and nuclear localisation at the invasive front has been suggested to be due to differential levels of Wnt signalling activation, in response to both intrinsic (autocrine) and extrinsic (paracrine) factors, which can differentially modulate β -catenin levels, localisation and active TCF-dependent transcription [153, 203, 204].

Interestingly, recent theoretical and functional assays suggested that fold changes in β -catenin and not absolute levels dictated the output of Wnt signalling and is a more precise reporter of Wnt stimulation in a heterogeneous cell population [205]. This signalling system may act to compensate for natural biological (both environmental and genetic) noise so that, despite large variations in basal nuclear levels of β -catenin, the actual fold change is equivalent between all cells [205].

Furthermore, it has been demonstrated that distinct molecular forms of β -catenin, with different binding properties to TCF and cadherins, dictate its functions within the cell

[158, 206]. The non-Wnt-stimulated form of β -catenin forms a dimer with α -catenin, while Wnt induces a monomeric form selective for TCF-binding, with β -catenin's C-terminus regulating the availability of the ARM repeat region for other binding partners [206-208]. Overall, it is becoming increasingly appreciated that β -catenin levels does not always couple with transcriptional activity.

Ascertaining the roles of elevated β -catenin in circumstances of inactive or low basal transcriptional activation has proven to be challenging. Albeit controversial, with contradictory studies published, β -catenin has been increasingly linked with maintenance of the pluripotency of Embryonic Stem (ES) cells [209-214], in a role that appears to be intriguingly independent of its transcriptional activity, with its overall levels seemingly imperative to this process [215, 216]. It is postulated that in this role β -catenin titrates TCF3 thus preventing its repressive function [216] and given's β -catenin ability to bind a plethora of proteins this may hint at an important function of β -catenin as an 'interactor'; where it dictates its binding partners functions through the regulation of their amounts and localisations in response to specific signals at any given time. More recently, β -catenin has been implicated as a component of the centrosome involved in its function and activity [217], suggesting that it may be involved in many more biological processes other than in adhesion and Wnt signalling.

1.1.3.3 The role of phosphorylation in the regulation of β -catenin transcriptional activity.

As described above, while accumulation and especially nuclear localisation of β -catenin are often regarded as hallmarks of Wnt activation, this has been increasingly disputed [92, 186-188]. For example, in *Xenopus* embryos, β -catenin's signalling ability was demonstrated to be dependent on its N-terminal GSK3- β phosphorylation sites (S33, S37, T41), irrespective of its total levels [186]. This was corroborated in mammalian cells whereby a β -catenin Ser37 and Thr41 de-phospho specific antibody was utilised to demonstrate that transcriptional activity was mediated by molecular forms of β -catenin that remained unphosphorylated at these sites [187]. Levels and

nuclear localisation of this N-terminally de-phosphorylated form of β -catenin (often called ABC –Active β -catenin) correlated well with TCF-dependent transcriptional activation [187]. This pool represents a very small percentage of total β -catenin and intriguingly is normally localised in cadherin complexes at the plasma membrane but with decreasing prevalence upon increasing TCF-dependent transcription [188, 218]. Another isoform, termed PS45 (phospho-serine 45), has also been implicated with enhanced correlation with TCF-dependent transcriptional activity, but is less well-characterised than ABC [219]. As mentioned, β -catenin was demonstrated to be exported from the nucleus independently of CRM1 but in a RanGTPase dependent manner by interacting with Ran binding protein 3 (RanBP3) (Hendriksen et al, 2005). Interestingly it was demonstrated that RanBP3's antagonism of nuclear accumulation was specific to the de-phospho ABC form of β -catenin involved in transcriptional activation, although how it distinguished phosphorylated and unphosphorylated forms was unknown [103, 220].

Other notable phospho-serine residues for β -catenin include phospho-S552 and S675 mediated by AKT [221] and PKA[222], which have been reported to promote interactions with its transcriptional co-activators, such as CBP, to enhance TCF-dependent transcription [42]. Furthermore, Rac1 and JNK have been implicated in regulating β -catenin nuclear localisation by phosphorylation on S191 and S605, downstream of PI3-kinase [116]. Tyrosine kinases and phosphatases are associated in the shift between cadherin-mediated adhesion and activated TCF-dependent transcription [42, 158]. Phosphorylation of β -catenin at the C-terminal Y654 by src kinase lowers its affinity for E-cadherin, thus increasing its availability for interactions with TCF proteins to activate transcription [223]. Phosphorylation at Y142 by the tyrosine kinases Fer, Fyn or Met also disrupts β -catenin's interactions with α -catenins in adherens junctions [224] and promotes its interaction with BCL9-2 to sequester it in the nucleus [124]. β -catenin phosphorylation at Y489 by Abl kinase (Rhee et al, 2007) has also been suggested to modulate β -catenin's interaction with cadherin and enhance Wnt activity [124, 225]. Given the key role for phosphorylation in β -catenin regulation, it and its regulatory components are subject to fine tuning by a myriad of kinases involved in diverse signalling pathways, from src kinases [224]

and PKC[226] to AKT[221] and CDKs [227]. Figure 1.5 and Table 1.1 summarises key phosphorylation sites on β -catenin and their associated effects.

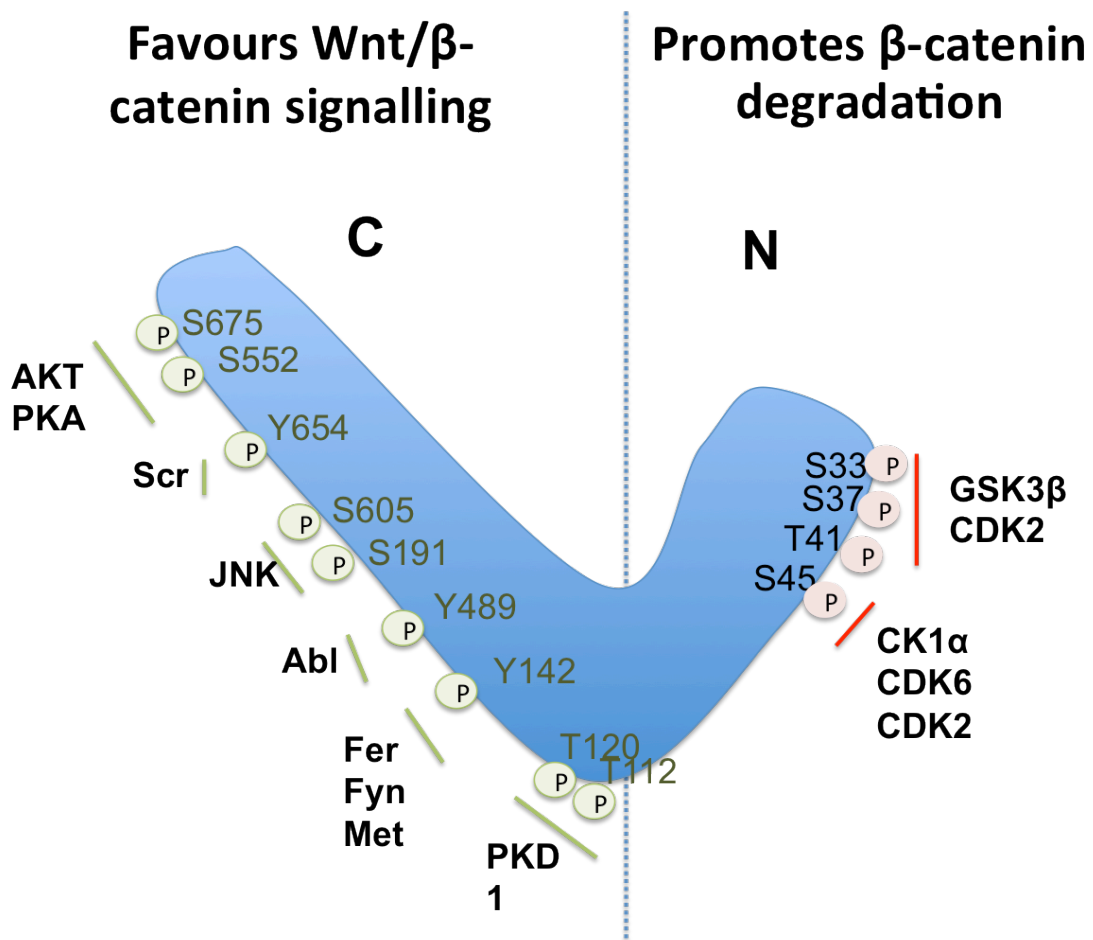


Figure 1.5 β -catenin phosphorylation sites

Phosphorylation of β -catenin can promote its degradation or its signalling activity in Wnt signalling. Phosphorylation in the armadillo domain alters its affinity to cadherins thus promoting nuclear localisation, while phosphorylation at the amino terminus promotes β -catenin degradation. Adapted from [158].

Kinase	Sites	Effects	References
CK1 α	S45	Favours degradation	[84]
GSK3 β	S33	Favours degradation	[228]
	S37 T41		
Fyn		Reduce cadherin binding and adhesive functions	[229]
Fer Met	Y142	Favours Nuclear translocation and transcriptional activation	
Abl	Y489	Favours Nuclear translocation and transcriptional activation	[225]
Scr	Y654	Favours Nuclear translocation and transcriptional activation - reduce cadherin binding and adhesive functions	[223]
AKT / PKA	S552	Favours Nuclear translocation and transcriptional activation	[221]
	S675		[222]
JNK	S191 S605	Favours Nuclear translocation and transcriptional activation	[116]
PKC α	S33/S37/S45	Non canonical mediated inhibition of canonical signalling	[226]
PKD1	T112	Favours Nuclear translocation and transcriptional activation (overexpression inhibits transcriptional activation)	[230]
	T120		
CDK2	S33/S37/ T41/S45	Favours degradation	[227]
CDK6	S45	Favours degradation	[231]

Table 1.1. β -catenin phosphorylation sites and effects.

To summarise, post-translational modifications can dictate β -catenin's binding partners and therefore its subcellular localisation and subsequent function within a cell [232-234]. The levels and localisation of specific transcriptionally competent forms of β -catenin, especially ABC, are increasingly considered as the hallmark of β -catenin transcriptional activity rather than simply changes to total levels. Depending on the cell and environmental contexts at the time, both Wnt-dependent and -independent β -catenin modifications are likely to co-operate, or compete, in modulating its localisation and function, in order to regulate the required adhesion and signalling responses [42, 235].

Several aspects of Wnt signalling are currently ill defined from early events leading to the dissociation of the destruction complex to the precise mechanisms regulating the nuclear transport of β -catenin. Although many core components of the Wnt/ β -catenin pathway required for β -catenin mediated signal transduction have been identified, discrepancies are clearly prevalent with regards to the current model. In particular the relationship between β -catenin levels and localisation and activated TCF-dependent

transcription is poorly understood, with this aspect especially important as a better understanding would aid interpretation, diagnosis and prognosis of various tumours. Due to the importance of Wnt/ β -catenin signalling in development and disease, it has been the subject of several high-throughput RNAi screens to identify novel regulators of the pathway.

1.2 RNA Interference

RNA interference (RNAi) is a naturally occurring biological phenomenon that has been manipulated to become a powerful tool for targeted gene silencing in research.

In brief, long dsRNA molecules triggers the RNAi process and these are cleaved intracellularly by a ribonuclease III-type protein called DICER to generate small interfering (si)RNA double stranded duplexes. These siRNA duplexes are ~21-23 nucleotides and possess a 3' hydroxy termini with 2nt overhangs and a 5'-phosphate termini. The siRNAs then become incorporated into a multimeric nuclease-containing complex called RNA-induced silencing complex (RISC), which gets activated following the loss of one siRNA strand. This siRNA (now single stranded) can bind to a complementary mRNA molecule thus guiding the RISC complex for its endonucleolytic cleavage and subsequent decreased expression of that target sequence [236].

1.2.1 Using RNAi in High Throughput Screens

RNAi has become a powerful tool for targeted gene silencing in research and it is often used for the assessment of gene functions. Whilst the introduction of long dsRNAs into mammalian cells triggers a cytotoxic non-specific interferon response this is not observed with shorter dsRNAs (which are the active mediators of RNAi processed from long dsRNA). Since the genome sequences of many model organisms such as human, mouse and rat, are now known, in addition to the availability of sophisticated algorithms to design efficient RNAi sequences, it has become possible to use siRNAs against the entire genome in a high-throughput format.

1.2.2 endoribonuclease-derived siRNA (esiRNA).

Whilst siRNA has clear potential in high-throughput knock out screens the use of synthetic siRNA is hampered, not only by its cost, but also by its variation in its inhibitory ability to different sequences within a gene [237]. However, upon enzymatic processing into shorter dsRNAs, different siRNA capable of interacting with various sites on target mRNA are generated and this in turn enhances the likelihood that at least one of them will pair with its target sequences [237]. This highlighted the possibility of generating multiple siRNA for a target from long dsRNA *in vitro* using DICER or RNaseIII, which led to the development of endoribonuclease-derived siRNA (esiRNA) [238-240]. Endoribonuclease digestion of long dsRNA transcribed from DNA *in vitro* results in a heterogeneous pool of several overlapping esiRNAs, capable of interacting with different sites on target mRNA. This in turn recapitulates the enhanced potency and specificity of gene knockdown conferred by long dsRNA utilised in *C.elegans* and *D.melanogaster* [238] (Figure 1.6). This is a major advantage over siRNA in large scale studies as siRNA often possess variable inhibitory abilities, often requiring more than one siRNA per gene for efficient gene targeting [238]. Furthermore, esiRNA not only have the advantage of being relatively cheap to generate a full genome-wide library (when compared to synthetic siRNA), it is also less likely to cause off target effects because each individual siRNA present in the pool is at a very low concentration [237-239, 241].

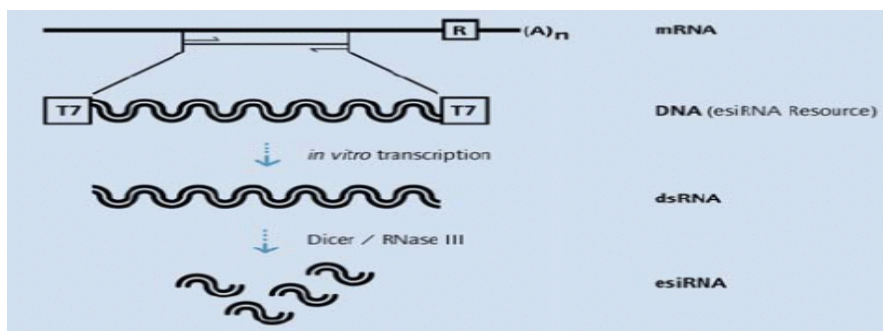


Figure 1.6. Production of esiRNA (Reproduced and adapted from).

Further details can be found in Chapter 2.

1.2.3 Genome-wide high-throughput RNAi screens

As mentioned, since the advent of genomic sequencing, RNAi technology has been utilised in high-throughput formats to define the functional influence of nearly every gene to specific cellular processes and signalling pathways [242]. A range of high-throughput genome wide screens have been undertaken, from a full genome analysis of the immune deficiency pathway using a reporter gene system in *D. melanogaster* [243] to a genome-wide analysis of fat storage and mobilisation in living *C. elegans* using imaging based methods [244].

Due to the inherent simplicity of their workflows and generally strong robustness and high reproducibility, plate reader based assays, such as those that rely on the use of luminescent reporters for example, are widely used as read-outs for high throughput cell-based screens [245]. Despite these obvious advantages, limited information and insights into cellular physiology are gained from such assays that average the biological response of entire cell populations. This, in turn, has driven the development of automated high-throughput imaging platforms to capture functional and morphometric information from single cells, with this so-called high content analysis (HCA) defined as the ‘extracting and understanding of multi-parametric data from high-throughput, sub-cellular imaging’ [245, 246]. This is highly relevant in assays with heterogeneous populations or when subtle ‘shifts’ in responses may be expected in different subpopulations of cells, which would be lost by taking single measurements of cell populations [246]. The power of HCA as a tool in compound and genetic screening lies in the use of various imaging filters that enables the acquisition of multiple fluorophores, and subsequently the simultaneous measurement of multiple features, in addition to the capability for both fixed and live cell imaging [247-249].

The combination of HCA and RNAi screening has been especially powerful in ascertaining potential gene function from cellular phenotypes, with a wide variety of HCA assays utilised in genome-wide RNAi screens in various systems, from screening for novel components regulating mitotic spindle integrity in human cells [250] and cell division [240] to the genome-wide analysis of the role of kinases in

endocytosis [251]. Moreover, this technology is becoming increasingly applied to studying more complex systems such as stem cell biology [252, 253] and organotypic human cell co-culture system [254].

HCA has been extensively applied to the analysis of transcription factor activity, from single-cell kinetic studies of intracellular localisation of transcription factors to screening large compound libraries to identify novel selective inhibitors of transcription factor nuclear translocation for example [255].

Transcription factors that have been successfully studied by HCA include members of the AP-1 complex [256], HSF-1 [257], p53 [258], Stat3 [259], NF- κ B [260] and forkhead transcription factor (FOXO) family [255, 261]. For example, the first potent and selective inhibitor of phosphoinositide 3-kinase (PI3K) was discovered and developed through employing a high content imaging screen of nearly 34,000 compounds that monitored the nuclear translocation of the Akt effector, Forkhead box O (FOXO [261]. Activation of the PI3-kinase/Akt pathway results in FOXO phosphorylation and cytoplasmic retention with decreased phosphorylation and subsequent nuclear translocation of FOXO members observed upon PI3K inhibition. Therefore, nuclear translocation can be used as a marker of the activation status of the whole pathway in this case, with HCAs generally providing an excellent means of studying intracellular pathways and the subsequent characterisation of the hits identified [255]. Table 1.2 summarises the differences between high content image based assays and transcriptional reporter gene assays.

1.2.3.1 High-throughput functional genetic screens for novel regulators of the β -catenin dependent Wnt signalling pathway.

Although the major players within the β -catenin dependent Wnt pathway are fairly well characterised, it is believed that a great number of core and cell-specific components are still to be identified [242]. With improving RNAi technology, several genome-wide and smaller select RNAi screens for additional components of the Wnt signalling pathway have been undertaken [262-267]. These screens mainly utilised a TCF-dependent reporter as their assay readouts, thus identifying regulators of TCF

dependent transcription. The first whole-genome RNAi screen to identify modulators of the Wnt signalling pathway was performed in *Drosophila* where Wg overexpression was used as a means of activating the pathway alongside an RNAi library [268]. A more recent screen in DLD-1 cells used a luciferase reporter gene to identify regulators of TCF-dependent transcription in the context of elevated endogenous transcriptional activation in a colon cancer cell background [242].

Within this laboratory, a human embryonic kidney (HEK293) cell line, based on the TOPflash reporter [269], was derived, which can be activated in response to Wnt signalling. The cell line contains a Dishevelled2-estrogen receptor ligand-binding site (DVL-ER) construct, which allows the activation of the fused protein, and subsequently TCF-dependent transcription, upon addition of β -estradiol to cells [270]. In addition, the cell line also contains a construct consisting of multimerised TCF binding sites driving the transcription of a Luciferase-IRES-GFP sequence (IRES=Internal Ribosomal Entry Sequence) allowing the monitoring of TCF-dependent transcription via a luciferase assay [271] (Figure 2.1 in Chapter 2). This gives a system that is easily inducible by Wnt signalling activation, with the ability to measure the response given by quantifiable levels of reporter activation. This reporter cell line has already been used in a luciferase based, genome-wide esiRNA screen to identify novel regulators of TCF-dependent transcription in the context of Wnt-signalling (manuscript under preparation). However, whilst this screen was able to identify components that played a role in the activity of the Wnt signalling on a transcriptional level, no information could be obtained in relation to β -catenin levels and subcellular localisation and how this would then correlate to transcriptional activity.

Image-based high-content assays (HCA)	Transcriptional reporter gene assays (RGA)
Target specificity in compound screening - specific hits can be identified if the assay uses a substrate of the target as the assay endpoint	No target specificity in compound screening - transcriptional reporters respond to compounds that affect any step in the pathway
Pathways specificity - transcription factors and other proteins that respond to the activation of a pathway can be used as assay endpoint	Pathway specific
Early identification of false positives in compound or genetic screens (e.g. toxic compounds)	Toxic effects or false positives not easy to observe
Non-destructive approach	Lysis of cells required
Images can be re-analysed to address other questions	No opportunities for re-assay
Ability to directly and quantitatively monitor transcription factor activation events in cells (phosphorylation, stabilization, protein-protein interactions, nuclear relocalisation);	Limited information and narrow insight into cellular biology
Possibility to perform multiplexed, kinetic, single-cell analyses	Secondary reporters can be developed into a cell line but not as straightforward for multiplexing
The primary readout can be integrated with morphometric and cytotoxicity data – multiparametric data can be obtained. Data rich Information gained on assays with heterogeneous populations or different subpopulations of cells	No morphometric data can be obtained. Cytotoxicity not as straightforward and may involve splitting lysis samples into two batches (laborious) Average measurements of cell populations, therefore loss of information
Readout signal magnitude is independent of the total number of cells in the sample	Readout signal magnitude is dependent of the total number of cells in the sample
Laborious sample preparation, particularly for immunofluorescence assays	Generally fast sample preparation
Specific reagents may not be available or robust enough for screening	Specific reagents may not be available or robust enough for screening
Low throughput of some HCA readers. Requirement for fast automated microscopes	Good for high-throughput assays Plate readers cheaper than advanced screening microscopes
In some cases, HCAs have lower signal-to-noise ratio and dynamic range with respect to corresponding RGAs	Often sensitive with high signal-to-noise ratios and large dynamic ranges
Higher degree of assay 'noise' due to heterogeneous cell responses	Robust, often reproducible data
Cost of reagents (i.e. antibodies) or cell lines stably expressing fluorescent protein constructs (a license agreement is usually needed for commercial cell lines)	No antibody costs but assay reagents still potentially expensive
More complex data management and analysis	Relatively straightforward data management and analysis

Table 1.2 Comparison of high content and gene reporter assays in high-throughput screening

Adapted from [255] and [272].

Inherent differences in screen experimental set up, be it different cell types, pathway activation status (either exogenously or endogenously), and whether an overexpression or knockdown system is utilised, can not only provide novel information on Wnt signalling regulation but also an improved global insight into the organisation of the pathway. However, none of the screens for Wnt pathway regulators indicated above investigated β -catenin levels, with TCF-dependent transcriptional activation as the primary readout. The relationship between β -catenin and TCF-dependent appears to be far more complex and intricate than what the standard textbook model of the Wnt/ β -catenin signalling pathway (Figure 1.2) portrays, therefore screening for regulators of β -catenin would potentially be very powerful.

A brief report described the development of a fluorescent imaging screening assay in primary human preosteoblasts capable of identifying compounds that modulated β -catenin nuclear translocation, but only presented experiments using Wnt3a and GSK3- β inhibitors to validate the method, with no new biological insights revealed [273, 274]. More recently, studies applied enzyme fragment complementation to measure β -catenin nuclear localisation to identify novel compounds that activated β -catenin [275], whereby complementation occurs between a peptide fragment of β -galactosidase tagged to β -catenin and a nuclear-resident complementary enzyme [276] [275].

Notably, comparative or parallel studies using both traditional gene reporter assays and image based assays have been undertaken for certain proteins, such as the FOXO3a transcription factor, whereby the transcriptional activity of endogenous FOXO3a was measured using both a high-content FOXO3a-GFP nuclear translocation assay in parallel with a luciferase reporter assay [255, 277]. Whilst not in parallel, high throughput functional screens have been undertaken for regulators of both TGF β -driven gene expression and the nuclear localisation of SMADs that activate downstream TGF- β gene transcription, thus allowing for potential integration and correlation between these data sets [278-281]. The ability to correlate β -catenin levels and nuclear accumulation data with TCF-dependent transcription, in addition to utilising similar integrative screening approaches employed in another recent Wnt

screen [242] would hold immense power in furthering our understanding of β -catenin regulation within Wnt signalling. As mentioned, a refinement of the current textbook model of Wnt/ β -catenin is required for the better interpretation of not only bench-side biological data but, more significantly, for improved diagnosis and treatment of patient tumours. Furthermore, given the increasing awareness of the complexity of Wnt/ β -catenin signalling, it is widely believed that there are many components, both core and cell specific, yet to be identified [242]. Moreover, the presence of extensive cross-talk between different signalling pathways further complicates our understanding of this important pathway and this aspect should also be a major focus of future signal transduction studies [282]. Determining the core components involved in Wnt/ β -catenin signalling and cell-type specific differences is crucial for the improved understanding of the development of specific tissues, in determining how signalling becomes perturbed in different cancers and importantly in the generation of new target therapeutics [58, 242].

1.3 Aims of the project

The primary aim of the project was to develop image-based high-throughput genome-wide esiRNA knockout screens to identify novel regulators of β -catenin levels and nuclear localisation in the context of Wnt-signalling. Furthermore, this project aimed to investigate the correlation between β -catenin accumulation and nuclear targeting with subsequent transcriptional activation through comparative analysis with the previously undertaken screen for regulators of TCF-dependent transcription. The following chapters describes the development of three screening assays for regulators of β -catenin levels and localisation; one in the aforementioned HEK293 derived TCF-dependent reporter cell line in an active Wnt signalling context, the other two in a U2OS derived cancer cell line of differential Wnt activation levels. The results from the screens were integrated with screening data for regulators of TCF-dependent transcription in the reporter cell line in addition to other published work. Furthermore, a selection of hits were reconfirmed, in addition to initial characterisation of one promising potential novel regulator of β -catenin and subsequent TCF-dependent transcription. Results from the study hold great potential in shedding light on how β -

catenin modulation is linked to Wnt induced initiation, continuation and termination of gene expression.

Chapter 2. Materials and Methods

2.1 The 7df3 TCF-luciferase reporter cell line

The 7df3 luciferase reporter cell line was constructed by Dr. Helen Wildish using a cell line originally generated by Dr. Matthew Smalley [283] and is described in Ewan et al, 2010 [271].

Briefly, HEK293 cells expressing a Dishevelled-estrogen receptor (Dvl2-ER) fusion protein that allowed estrogen-dependent induction of the Wnt signalling pathway were engineered to express a Wnt-responsive bicistronic reporter.

A cDNA encoding a mouse Dvl2-ER fusion protein was integrated into the FRT site of 'Flp-In' HEK293 cells (Invitrogen) using Flp recombinase (Invitrogen), and selected with 200 µg/ml hygromycin (Invitrogen) to isolate stably transfected clones [283]. Similar to the rationale used to create inducible activation of Raf-1 [283, 284], this enabled inducible activation of TCF-dependent transcription in all cells by the addition of Estradiol [283, 284].

A fragment of the Xnr3 enhancer [285] (-180 to -60) was fused to four TCF consensus-binding sites and a c-Fos minimal promoter [286]. This promoter construct was inserted into the pUB-bsd blasticidin resistance plasmid (Invitrogen). The luciferase gene from pGL3-basic (Clontech) and the IRES-GFP-SV40 polyA sequences from pIRES-hrGFP-2a (Stratagene) were inserted downstream of the promoter (Figure 2.1). The reporter vector was transfected into a stable HA-Dvl2-ER (estrogen receptor) expressing cell line [283]. Stably transfected cells were selected using 3µg/ml Blasticidin (Invitrogen) and 200µg/ml hygromycin (Invitrogen) with resistant clones were exposed to the GSK-3 inhibitor lithium (9 mM concentration for 16 hours) to induce the Wnt-dependent expression of GFP. FACS was used to enrich for responsive cells that had high levels of GFP. A second round of lithium induction and FACS was used to isolate highly inducible clones, which were confirmed with luciferase assays. The clone 7df3 was selected based on its low background luciferase expression and high induction in response to Lithium and estradiol (Figure 2.2).

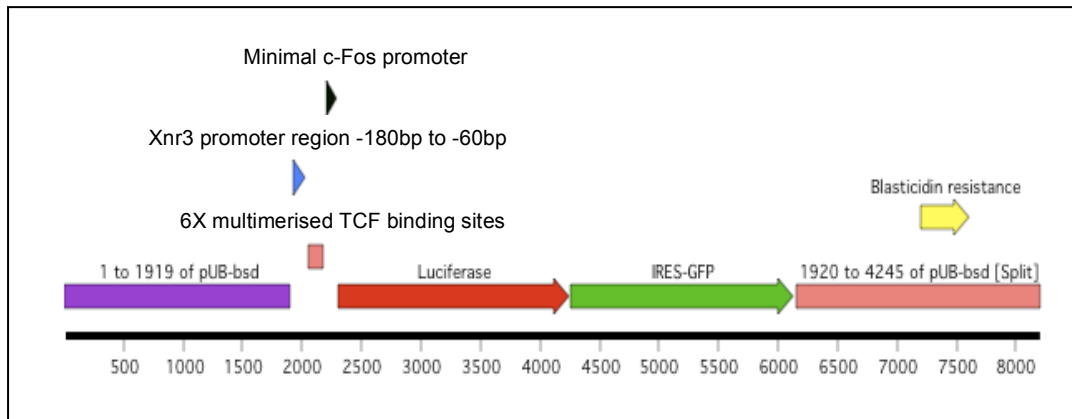


Figure 2.1 Schematic representation of the reporter plasmid

The plasmid was stably transfected into HEK293 cells to create a sensitive reporter cell line for assaying the level of activity of the Wnt signalling pathway. The plasmid contains 4 multimerised TCF binding sites driving the transcription of luciferase and GFP reporter genes. Figure kindly provided by Dr Jamie Freeman.

2.2 Cell culture

2.2.1 7df3 reporter cell line

The 7df3 TCF-luciferase reporter cells were cultured at 37°C and 5% CO₂ in DMEM (Invitrogen) supplemented with 10% heat inactivated Fetal Calf Serum (Invitrogen), 50units/ml Penicillin (Invitrogen), 50µg/ml Streptomycin (Invitrogen) and 0.5% L-Glutamine 50mg/ml (Invitrogen). They were maintained under constant antibiotic selection using 200µg/ml hygromycin (Invitrogen) and 3µg/ml blasticidin (Invitrogen). β-estradiol (Sigma) was added to the luciferase reporter cells 24 hours prior to analysis at a final concentration of 4µM to induce Wnt signalling.

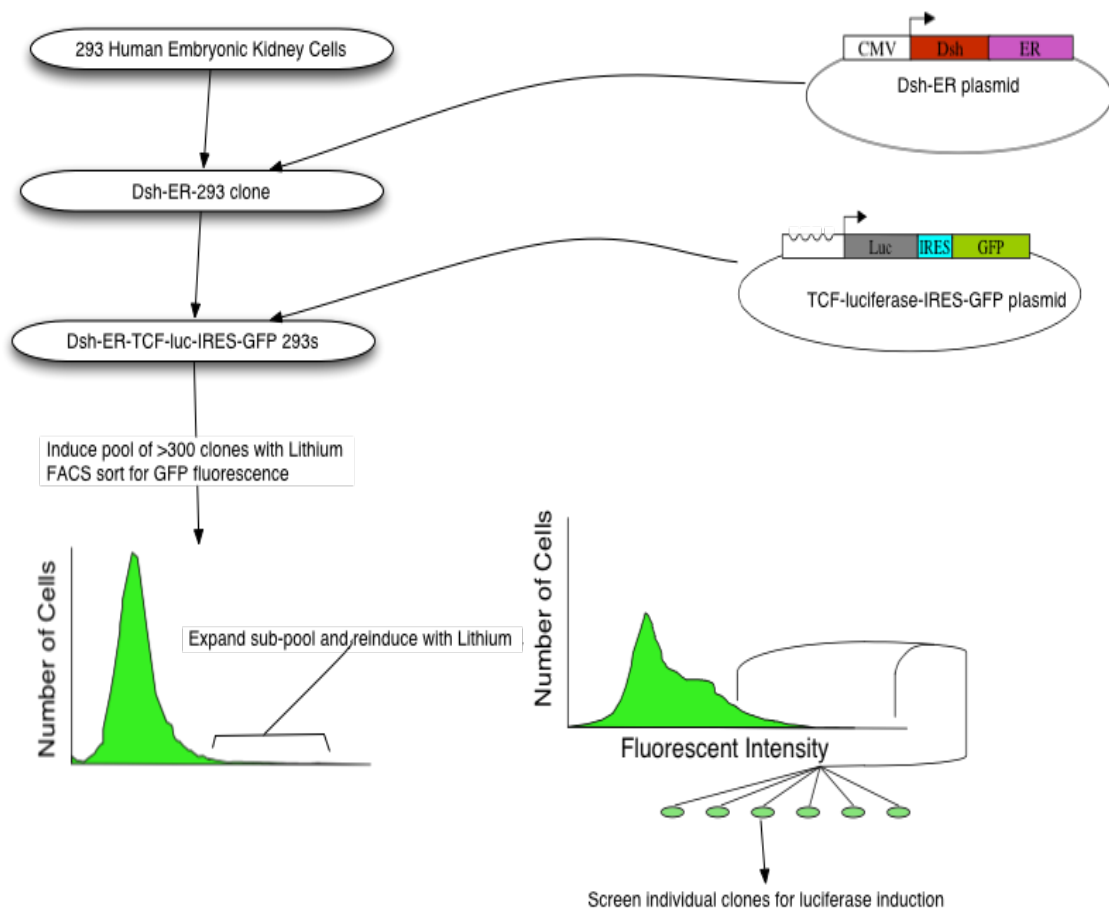


Figure 2.2 Schematic representation of the selection process used to produce the reporter cell line.

HEK293 cells were sequentially stably transfected with a Dsh-ER fusion, and the TCF reporter construct. The clones were selected for responsiveness to Lithium induction, before individual clones were screened for the highest induction:lowest background ratio. Figure kindly provided by Dr K.Ewan and Dr J. Freeman.

2.2.2 U2OS cell lines

2.2.2.1 eGFP- β -catenin U2OS cells

The U2OS Osteocarcinoma cell line stably expressing GFP-tagged β -catenin was purchased from BioImage (Fisher BioImage, Denmark, data sheet displaying construct provided in Appendix A).

These cells were cultured at 37°C and 5% CO₂ in DMEM-GlutaMAX (Invitrogen), supplemented with 10% heat inactivated Fetal Calf Serum (Biochrom), 50units/ml

Penicillin (Invitrogen), 50µg/ml Streptomycin (Invitrogen) and 0.5% L-Glutamine 50mg/ml (Invitrogen). They were maintained under constant antibiotic selection using 0.5mg/ml geneticin G418 (Invitrogen). A GSK3β inhibitor, (2'Z,3'E)-6-Bromoindirubin-3'-oxime (BIO; Sigma) was added to the U2OS cells 16 hours prior to analysis at the concentrations indicated in figure legends.

2.2.2.2 U2OS cells

The U2OS Osteocarcinoma cell line (ATCC) was cultured at 37°C and 5% CO₂ in DMEM-GlutaMAX (Invitrogen), supplemented with 10% heat inactivated Fetal Calf Serum (Biochrom), 50units/ml Penicillin (Invitrogen), 50µg/ml Streptomycin (Invitrogen) and 0.5% L-Glutamine 50mg/ml (Invitrogen).

2.3 esiRNA

2.3.1 Genome-wide esiRNA Library and secondary esiRNA sublibrary.

A genome-wide esiRNA library was obtained from Professor Frank Buchholz at the Max-Planck-Institute for Molecular and Cell Biology and Genetics in Dresden (Germany) and represents 17,188 human genes [239, 240]. The library was diluted and plated onto test plates using the JobiWell robotic micropipetting system (CyBio) at GE Healthcare, Maynard Centre, Cardiff. The library was used at a final concentration of 20ng per well in the primary and secondary screening experiments. Table 1, Appendix B (on the DVD) provides information regarding well IDs and sequences of the primary library.

A secondary sub-library of 164 esiRNAs (representing 161 different genes) was used for the reconfirmation assays of a subset of genes identified in the primary screens. These esiRNAs were generated from non-overlapping sequences designed and produced by Dr Mirko Theis and Professor Frank Buchholz from the MPI-CBG at

Dresden. Gene IDs and esiRNA sequences for the sublibrary can be found in Appendix B, Table 27.

2.3.2 Control esiRNA production.

Control esiRNA (APC, R-luciferase, and β -catenin esiRNA) were made from purchased PCR templates containing T7 sites at both ends (ImaGenes; previously RZPD) and from the MPI (Dresden). In vitro transcription of the templates by T7 RNA polymerase (RNAmass High yield transcription kit, Stratagene) was undertaken to yield dsRNA, which was digested by RNaseIII for 4 hours at 28°C, followed by 2 hours at 37°C, resulting in a pool of short siRNA duplexes. These were run on 4% agarose gel to check that the duplexes were between 18-21 nucleotides long before being spun through siRNA purification columns (Ambion), which removed impurities and undigested/partially digested duplexes.

2.4 Transfection procedures

2.4.1 Reverse transfections

Cells were cultured to ~80% confluency prior to transfection. Reverse transfection is an alternative method of transfecting multi-well plates (96-well and above) where cells are transfected while still in suspension (i.e. after trypsinisation and prior to plating). Briefly, esi or siRNA are plated at the desired concentration followed by addition of transfection reagent in optimem (serum free) media (Invitrogen). After 20 minutes incubation, cells are seeded onto the transfection complex at the desired densities. During optimisation experiments, various reagents at different concentrations were used in addition to various cell counts as indicated in figure legends where appropriate. Screening conditions per screen are described in section 2.5 below.

For follow up studies in 384 well format, 3000 7df3 cells/well were reverse transfected with 20ng esiRNA/siRNA and 5ul of Interferin (Polyplus):Optimem complex, diluted at 1:100 according to manufacturers guidelines. 1500 eGFP- β -catenin U2OS cells/well were reverse transfected with 20ng esiRNA/siRNA and

0.12µl Lipofectamine 2000 (Invitrogen) in 5ul Optimem according to manufacturers guidelines.

2.4.2 DNA and esi/siRNA forward transfections – Rescue experiments.

7df3 cells were cultured to ~80% confluency then seeded into 96 well plates at a density of 3×10^5 cells/ml in 100 µl antibiotic free DMEM 24hrs prior to transfecting. Each well of a black-walled 96 well plate (Nunc) were transfected using Lipofectamine 2000 (Invitrogen). Briefly, cells were co-transfected with 50ng esiRNA (hnRNPA1 or control), 10ng CMV-LacZ and 90ng empty vector control or mouse hnRNPA1 cDNA per well using 0.3 µl/well of Lipofectamine 2000 diluted in 10 µl optimem (Invitrogen) following manufacturers guidelines. 24 hours after transfection β-estradiol was added to 4uM. 48 hours after transfection cells were lysed in Glo lysis buffer and incubated with luciferase substrate (Promega Bright-Glo) and β-galactosidase substrate as detailed in 2.9. TCF-luciferase activity was normalised to β-galactosidase expression levels since esiRNAs had been co-transfected with the CMV-LacZ plasmid to allow assessment of relative transfection efficiencies.

2.5 Primary Screens

As mentioned, the library was seeded at a concentration of 20ng per well in a volume of 5ul, in 384-well format and stored at -80°C until assay. On the day of screening 20ng of controls were added to the following wells. In the 7df3 H screen however, β-catenin esiRNA were only added to wells M 18 and N18.

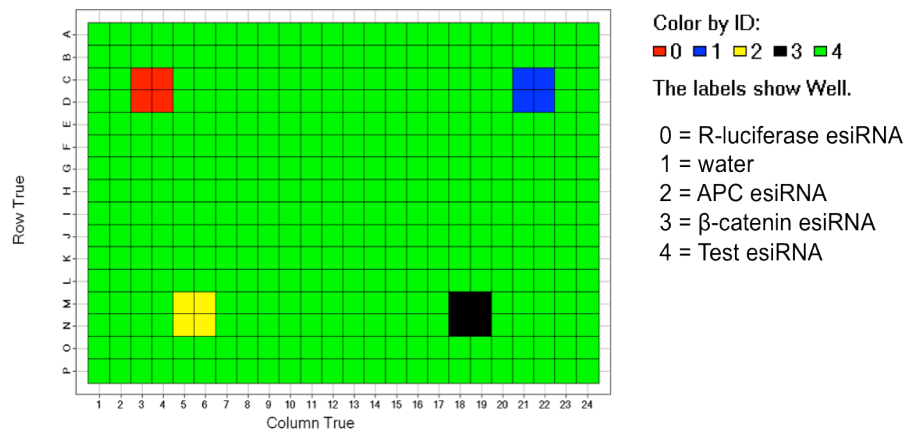


Figure 2.3 384-well plate plans indicating control well locations

In small-scale optimising experiments of screening conditions all liquid handling steps were undertaken manually. In the full screen of the entire esiRNA library, all liquid-handling procedures were performed using a WellMate liquid dispenser (Matrix Technologies). Screens were undertaken as a single experiment with all 47 384-welled plates corresponding to the whole screen transfected using the same passage cells grown from the same original vial, during the same day and processed together as one during latter stages to minimise day-to-day experimental variability.

2.5.1 7df3 Reporter cell line (H) screen

The 7df3 cell line was reverse-transfected with the esiRNA library using Interferin (Polyplus) according to manufacturers instructions. In brief, 20ng of esiRNA was pre-plated onto 384-well plates with 20ng of control esiRNA (or water) spotted onto each plate on the day of the screen as indicated in Figure 2.3 above. Only 2 wells of control β -catenin esiRNA, however, were added in this particular screen. The transfection reagent Interferin (Polyplys) was diluted 1:100 in Optimem and after a 5 minute incubation added to the esiRNA in the plates (5 μ l per well) and incubated for 20 minutes. The 7df3 cells were subsequently seeded onto the esiRNA/Transfection complex in antibiotic free media, with approximately 3000 cells per well deemed to be a suitable number following optimisation. 24 hours post-transfection cells were treated with 4 μ M β -estradiol for a further 24hrs prior to fixation and

immunocytochemistry for β -catenin (48hrs hours post transfection) as detailed in section 2.6.

2.5.2 eGFP- β -catenin U2OS cell line – UA and UB screens.

2.5.2.1 eGFP- β -catenin U2OS screen (UB screen)

The U2OS cell line was reverse-transfected with the esiRNA library using Lipofectamine2000 (L2K; Invitrogen) according to manufacturers instructions. In brief, 20ng of esiRNA was pre-plated onto 384-well plates with 20ng of control esiRNA (or water) spotted onto each plate on the day of the screen as indicated in Figure 2.3. The desired concentration of L2K (optimised at 0.12nl/well L2K) was added to optimum, incubated for 5 minutes at room temperature, prior to addition of 5ul of L2K/optimum mix onto the esiRNA plates. Following a 20 minute incubation, the U2OS cells were subsequently seeded onto the esiRNA/transfection complex in antibiotic free media, with approximately 1500 cells per well deemed to be a suitable number following optimisation.

2.5.2.2 eGFP- β -catenin U2OS APC (UA) screen

20ng/well of APC esiRNA (produced by myself as detailed in section 2.3.2) was added to each well of the entire esiRNA library on the day of the screen. Otherwise, experimental procedures for the UA screen were identical to the UB screen, unless otherwise mentioned (section 2.5.2.1).

2.6 Fixation and immunocytochemistry

Cells were reverse transfected and treated as described above. 48hrs post transfection the luciferase reporter cells were fixed in 4% Paraformaldehyde for 20mins, permeabilised in 0.2% Triton X-100 for 5 minutes and blocked with 10% horse serum (Invitrogen) for 40 minutes, all made up in phosphate-buffered saline (PBS) and at room temperature. Cellular β -catenin was immunostained by incubating the cells for 1

hour at room temp and then 4⁰C overnight with primary monoclonal β -catenin antibody (Becton-Dickinson), used at 1:500 in 10% Horse serum/PBS. Next day, cells were incubated for 1 hour with Alexa fluor.488 goat anti-mouse secondary antibody (Invitrogen), used at a 1:500 dilution in 10% Horse Serum/PBS. Cells were then incubated for 20 minutes with 3 μ g/ml DAPI (4',6'-diamidino-2-phenylindole; Sigma) in PBS to stain for nuclei. Cells were thoroughly washed in PBS following all antibody incubation steps at room temperature and left in PBS following completion, with plates sealed and stored at 4⁰C prior to imaging.

U2OS cells stably expressing eGFP-tagged β -catenin were fixed as above and subsequently incubated with 3 μ g/ml DAPI and 0.2% TritonX-100 in PBS for 20 minutes. Between steps cells were washed with PBS and treated at room temperature and left in PBS following completion, with plates sealed and stored at 4⁰C prior to imaging.

2.7 Imaging and Analysis

Following fixation and staining image acquisition was performed using the IN Cell Analyzer 1000 system (GE Healthcare, Maynard Centre, Cardiff). Acquisition and analysis parameters for each screen are indicated in their specific subsections below.

2.7.1 7DF3 H screen

One field of view was acquired per well using a x10 objective, with a 1 second exposure time for DAPI and 2 seconds for Alexa 488 secondary antibody labelling β -catenin. Image analysis was carried out using the Multi Target Analysis assay in the IN Cell Analyzer1000 Workstation software version 3.4 (GE Healthcare). Algorithms for data analysis were established and optimised according to assay conditions and manufacture instructions. In brief, the final segmentation protocol used was as follows:

‘Top-hat’ algorithm applied to both DAPI and β -catenin channels

DAPI channel : minimum area $60\mu\text{m}^2$ / sensitivity setting 60

β -catenin channel : minimum area $100\mu\text{m}^2$ / sensitivity setting 60

The ‘Top-hat’ algorithm is a relatively rapid transformation used to accentuate objects of a specified size, thus increasing the efficiency of their detection. Furthermore, it is also useful for distinguishing objects from a surrounding uneven background. This algorithm is optimal for objects that are fairly uniform in size and shape, for example nuclei and cells that are generally similar sizes/shapes such as the 7df3 cells utilised in this particular screen. The sensitivity setting determines which pixel clusters qualify as objects based on their intensity relative to local background. Increasing the percent sensitivity increases the detection of dimmer objects. Conversely, the lower the sensitivity setting the brighter a cluster of pixels is required to be in order to be differentiated from the background.

2.7.2 eGFP- β -catenin U2OS UA and UB screens

Two fields of view were acquired per well using a x10 objective, with a 1 second exposure time for DAPI and 3 seconds for eGFP- β -catenin. Image analysis was carried out using the Multi Target Analysis assay in the IN Cell Analyzer1000 Workstation software version 3.4 (GE Healthcare). Algorithms for data analysis were established and optimised according to assay conditions and manufacture instructions. In brief, final segmentation protocol used was as follows

‘Top-hat’ algorithm was applied to the DAPI channel, collar algorithm applied for β -catenin channel

DAPI channel : minimum area $60\mu\text{m}^2$ / sensitivity 80

β -catenin channel : collar $2\mu\text{m}$

The collar algorithm defines a ring-shaped cytoplasmic sampling region by dilating outwards a set distance (e.g. $2\mu\text{m}$ in this case) from the established nuclear region as defined by the DAPI channel. This has the advantage of being able to sample the cytoplasmic intensity rapidly. The same analysis protocol was applied to both U2OS

screens.

2.8 Statistical Methods.

2.8.1 Z-factor analysis

The Z-factor is a dimensionless screening window coefficient that reflects the quality and suitability of a screen in identifying true hits by assessing the signal dynamic range and its associated variation. It is defined as the ratio of the separation band to the dynamic range of the assay, based on the positive and negative control data, and is given by the formula:

$$\mathbf{Z\ factor = 1 - 3 \times SSD/R}$$

whereby SSD is the sum of the standard deviations of the positive and negative controls with R representing the range between the means of the positive and negative controls (Figure 2.4) [287].

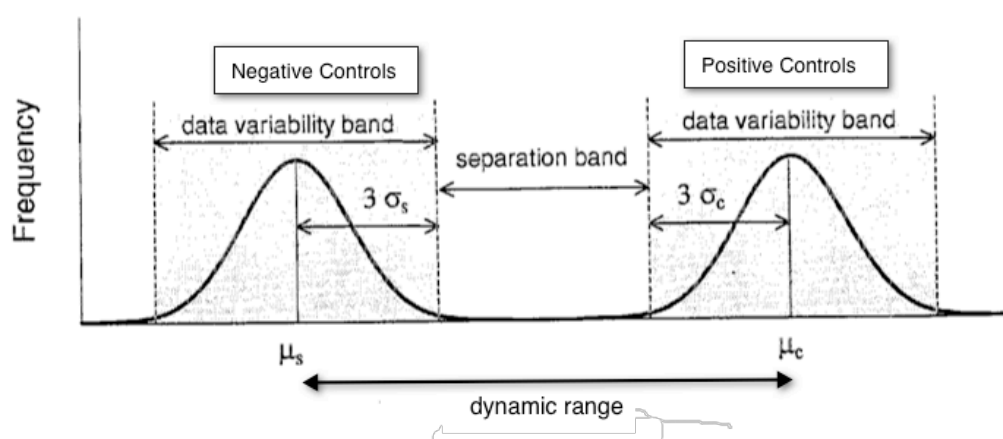


Figure 2.4 Schematic adapted from [288] with permission from SAGE publications. See text below for details.

Figure 2.4 displays data for both negative and positive controls and defines the separation band between the two. The horizontal axis displays the value determined by the assay while the vertical axis illustrates the prevalence of each value. The

dynamic range of the assay is defined as the difference between the means of the negative and positive controls. As defined by the arbitrary equation above, all background values will be less than a threshold defined as the mean of the background, plus three times the standard deviation of those values. With normally distributed data (a Gaussian distribution) 99.86% of the values would be expected to be less than that threshold, with 0.14% of the values expected to be greater. Similarly, true hits in the assays would be expected to have values greater than a threshold set by the mean of the positive controls minus three times the standard deviation of those values. The difference between these two thresholds (difference between the mean signal of the positive and negative controls) defines the separation band (Figure 2.4).

A robust HTS will have a large dynamic range between positive and negative controls, with small standard deviations, resulting in high Z factors. A Z-factor between 0 and 0.5 indicates that an assay is workable, with Z-factors greater than 0.5 indicative of an ‘excellent screening assay’[288].

Z-factor analysis was used in preliminary tests to assess the quality of the assay to predict its suitability for use in a high-throughput screen. Subsequently it was used in optimisation assays as a means of comparing the effects of different conditions on the positive and negative controls, thus allowing the assay to be fine-tuned to obtain the most optimal conditions for use in the full screen. Furthermore, each screen plate possessed control wells allowing the Z-factor for each plate to be worked out after screening, thus giving an indication of the success of the transfection for that particular plate.

2.8.2 Non-controls based normalisation

Normalisation (also termed standardisation) of screening raw data is beneficial as it allows measurements to be comparable across plates by removing systemic plate-to-plate variation. The nature of screening means that the overwhelming majority of samples screened are assumed to be inactive and can serve as their own controls. Therefore, it is possible to remove the control data from each plate and normalise the raw data to plate means and select as ‘hits’ those that deviate significantly from this

sample average. If from plate to plate the sample average shifts by a significant amount then this is likely to be due to a shift in the measurement process and not in the samples being measured themselves [289].

2.8.3 Z scores

Each esiRNA was expressed as fold over plate means in both β -catenin parameters under investigation, followed by conversion into their equivalent z-scores. This statistical measure represents the number of standard deviations a sample is from its plate mean. This allows the esiRNAs from across the whole screen to be rank-ordered as it provides clear information on the strength of each esiRNA relative to the distribution of the rest of the plate [289]

It is calculated by subtracting the plate mean from each data point sample value, with this difference then divided by the plate standard deviation.

$$Z = \frac{x_i - X}{S_x}$$

Z is the Z-score for the raw value x_i as defined by the formula above with X being the mean of all the raw values (minus controls) on a plate and S the standard deviation of these values (plate standard deviations). A positive Z-score means that the data point was greater than the mean while negative Z-scores reveal that the data point was below the mean.

Different thresholds were set for generating lists of primary hits as indicated in the text. These included selecting genes with Z-score of >2 and <-1.5 with cell numbers greater than 30% of the mean cell number/well of associated plates. For less stringent analysis cut offs of Z-scores >1.75 and <-1.3 were set.

Following analysis in Excel, the database program FilemakerPro (version 10) was used to store and sort the screening data.

2.8.4 Other statistical procedures.

All other statistical procedures (as indicated in figure legends) were carried out in GraphPad Prism software, version 4.0a.

2.9 Luminescence assays

48 hours post-transfection, cells were lysed in 50 μ l/well of a 96 well plate of Glo-lysis buffer (Promega) and incubated with agitation at room temperature for 30 minutes. 20 μ l was set aside for β -Galactosidase activity, with 30 μ l Bright-Glo reagent added to the remaining 30 μ l lysates, and assayed immediately for luciferase activity by luminescence using a FluoStar Optima plate reader (BMG Labtech). 20 μ l of β -Glo (Promega) reagent was added to the 20 μ l lysates set aside, incubated with agitation at room temperature for 30 minutes prior to assaying luminescence using a FluoStar Optima plate reader (BMG Labtech).

To control for transfection efficiencies and potential toxic effects, luciferase values were normalised to β -Galactosidase activity.

2.10 Cell Extraction

Cells were seeded in 6 well plates at a density of 2×10^5 cells per well and transfected (if required) 24hrs later using Lipofectamine 2000, according to manufacturers guidelines. 48 hours post-transfection cells were placed on ice, washed in ice-cold PBS before scraping in the required lysis buffer (as described below).

2.10.1 Whole cell extractions

Cells were lysed in a 1% Triton X, 150mM NaCl, 50mM Tris HCl pH8 buffer supplemented with Roche Complete protease inhibitor cocktail, stored on ice for 10

minutes prior to centrifugation at 13,000g, 4°C, for 10 minutes with the supernatant kept for use in downstream assays.

2.10.2 Crude cytoplasmic and nuclear extractions

To extract crude cytoplasmic extracts, cells were lysed in a 50mM TrisCl (pH 8.0), 100mM NaCl, 5mM MgCl₂, 0.5% NP-40 buffer supplemented with Roche Complete protease inhibitor cocktail, stored on ice for 5 minutes prior to centrifugation at 500g, 4°C, for 5 minutes with the supernatant kept for use in downstream assays (cytoplasmic fraction).

To extract crude nuclear extracts, pellets obtained from above were lysed in a 50mM TrisCl (pH 8.0), 150mM NaCl, 0.1% SDS buffer supplemented with Roche Complete protease inhibitor cocktail, stored on ice for 20 minutes prior to centrifugation at 500g, 4°C, for 5 minutes with the supernatant kept for use in downstream assays (nuclear fraction).

2.11 Immunoprecipitation

Glutathione-sepharose 4B beads were pre-equilibrated by washing 3 times in lysis buffer (1% Triton X, 150mM NaCl, 50mM Tris HCl pH8). 20ul of a 2x bead slurry (packed bead volume of 10ul) was used per sample and incubated with the cell lysates (cell fractions or whole cell lysates as indicated in legends) and 2ul β -catenin (BD Transduction laboratories), hnRNP A1 (Sigma) or KSRP (provided by Dr. Douglas L. Black (Howard Hughes Medical Institute at UCLA, Los Angeles, USA)) antibodies with agitation for 2 hours at 4°C. Beads were then washed in lysis buffer 3 times before eluting the protein in 2x NuPage Sample Buffer (containing 5% β -mercaptoethanol) to undergo gel electrophoresis and western blotting as described below.

2.12 SDS/PAGE and Western Blotting.

Proteins were separated on 4-12% linear gradient SDS-PAGE gels and transferred to nitrocellulose using the Iblot Module (Invitrogen), according to manufacturers guidelines. Membranes were blocked in 5% milk in Tris-buffered saline with 0.1% Tween (TBS-T; 20mM Tris pH7.6, 137mM NaCl, 0.1% Tween) for 1hr at room temperature then incubated overnight with primary antibody at 4 ° C. Mouse monoclonal anti- β -catenin (BD Biosciences) and mouse monoclonal anti-hnRNPA1 (Sigma) were used 1:1000 except where stated. Anti-tubulin and Anti- β -Actin antibodies (Thermo scientific, Loughborough, UK and Sigma respectively) were used at 1:5000 with Ab5 anti-KSRP (provided by Dr. Douglas L. Black [Howard Hughes Medical Institute at UCLA, Los Angeles, USA]) used at 1:500. All primary antibodies were used in TBS-T+ 5% BSA. Membranes were washed in TBS-T 5 times over 30min before incubating for an hour at room temperature with an HRP-conjugated secondary anti-mouse or anti-rabbit antibody (GE Healthcare) diluted at 1:5,000 in TBS-T. Membranes were again washed in TBS-T 5 times over 30min before being developed using SuperSignal West Pico chemiluminescent substrate (Thermo scientific, Loughborough, UK) followed by exposure to film (Kodak, Hemel Hempstead, UK).

2.13 Pulse-Chase (Metabolic Assay)

48 hours prior to transfection cells were seeded in 25cm² flasks (five flasks per treatment: hnRNP A1, APC esiRNA and water control) so that they were 30-50% confluent on the day of transfection. 2 μ g of esiRNA (R-luc control, APC and hnRNP A1) was transfected into cells using Interferin (Bio-Rad, 15 μ l) at 1:100 dilution, for the 7df3 cell line, and Lipofectamine 2000 for the eGFP- β -catenin cell line following manufacturers guidelines. 24 hours post transfection, 7df3 cells were treated with estradiol (4 μ M) to stimulate Wnt signalling for a further 24 hours before pre-starving of methionine and cysteine for 1 hour (48 hours post transfection in total). Media was then replaced with Pro-mix medium (GE Healthcare) containing 3.2MBq/ml (1.6MBq per flask) ³⁵S methionine and cysteine and incubated for a further hour to label newly

synthesised proteins. Media was subsequently replaced with normal medium (indicating the start of the chase) with cells harvested and extracted in lysis buffer (1% Triton X, 150mM NaCl, 50mM Tris HCl pH8 supplemented with Roche complete protease inhibitor cocktail) at the time points indicated in the figures after the removal of ³⁵S medium for each esiRNA treated condition. β -catenin was immunoprecipitated (as above) and proteins re-suspended in NuPage Sample Buffer (containing 5% β -mercaptoethanol), denatured and run on pre-cast 4-12% NuPAGE gels (Invitrogen) as described in 2.12. The gel was fixed in acetic acid (10%)-methanol (30%), dried and exposed to film (Kodak) to detect radioactive bands.

2.14 RNA Extraction and RT-PCR

RNA was extracted from transfected reporter cells using High Pure RNA Extraction Kit (Roche) according to manufacturers guidelines and quantified using the Nanodrop small volume spectrophotometer (Thermo scientific). Reverse transcription was performed using 1 μ g RNA and 1 μ g primers (random or OligodT) using M-MLV Reverse Transcriptase, RNase H minus (Promega, Southampton, UK). PCR of exons 13 and 16B of β -catenin and 18S rRNA (as a control) was undertaken with primer sequences displayed below. PCR on 0.2 μ g template DNA was undertaken using the GoTaq[®] Flexi DNA polymerase (Promega), 0.5 μ M primers with 30 cycles of denaturing at 95°C, annealing at 55°C and extension at 72°C with products subsequently separated on a 1% agarose gel.

Primers for RT-PCR were as follows:

18S rRNA (control)

Forward TCA AGA ACG AAA GTC GGA GGT

Reverse GGA CAT CTA AGG GCA TCA CA

β -catenin (exon 13)

Forward GAC CAG CTC TCT CTT CAG AAC A

β -catenin (exon 16B)

Reverse TTC TTG TGC ATT CTT CAC T

2.15 qRT-PCR

Cells were treated with 5µg/ml Actinomycin D (Sigma) 48hrs post transfection with total RNA isolated using High Pure RNA Extraction Kit (Roche), at the indicated time points in figure legends, and quantified using the Nanodrop small volume spectrophotometer (Thermo scientific). Relative levels of β-catenin, hnRNP A1 and housekeeping gene mRNA at each time point following Actinomycin D treatment were assessed by qRT-PCR.

1µg of total RNA was reverse transcribed using random primers from the Quantitect Reverse Transcription kit (Qiagen, Crawley, UK) and the cDNA produced diluted 1:100 with 5 µl of the diluted material used in qPCR assays. iQ SYBR green supermix (BioRad, Hemel Hempstead, UK) was used alongside the primers indicated below (Sigma). Opticon Monitor software (MJ Research, Waltham, USA) was used to analyse the course of the reaction and calculate C_T values.

Relative amounts of mRNA at each time point were derived using the $2^{(-\Delta C_T)}$ formula [290], where ΔC_T is $(C_{T, \text{Time X}} - C_{T, \text{Time 0}})$. The amount of mRNA at time zero was set at 100%. As Actinomycin D treatment inhibits all general transcription this formula was used instead of the $2^{(-\Delta\Delta C_T)}$ formula, where relative mRNA values are normalised to a housekeeping gene as, in this particular assay, it was deemed inappropriate to normalise to housekeeping genes as each would possess different mRNA decay rates.

In untreated cells (i.e. no Actinomycin D treatment), the $2^{(-\Delta\Delta C_T)}$ formula was used, where $\Delta\Delta C_T$ is $(C_{T, \text{Target gene}} - C_{T, \text{Housekeeping gene}})_{\text{hnRNP A1 knockdown cells}} - (C_{T, \text{Target gene}} - C_{T, \text{Housekeeping gene}})_{\text{Control cells}}$. Several housekeeping genes were tested, with GAPDH or RPL32 used as housekeeping genes in the data displayed within Chapter 5, with the amount of mRNA in cells treated with R-luciferase (control) esiRNA set to 100%.

qPCR primers were as follows:

β-catenin

Forward CCATTCCATTGTTTGTGCAG

Reverse GGTCAGCTCAACTGAAAGCC

HnRNP A1

Forward AAAGCCCTGTCAAAGCAAGA

Reverse ACGACCGAAGTTGTCATTCC

GAPDH

Forward TGCACCACCAACTGCTTAGC

Reverse GGCATGGACTGTGGTCATGAG

RPL32

Forward TTAAGCGTAACTGGCGGAAAC

Reverse GAGCGATCTCGGCACAGTAA

 β -actin

Forward CTGGAACGGTGAAGGTGACA

Reverse AAGGGACTTCCTGTAACAATGCA

 β 2M

Forward TGCTGTCTCCATGTTTGATGTATC

Reverse TCTCTGCTCCCCACCTCTAAG

HPRT1

Forward TGACACTGGCAAAAACAATGCA

Reverse GGTCCTTTTACCCAGCAAGCT

2.16 RNP-IP Assays

Nuclear and cytosolic extracts were prepared from U2OS and eGFP- β -catenin U2OS cells as described in 2.10 followed by hnRNP A1 immunoprecipitation (and bead only control) as described in 2.11. After the third IP wash, STAT60 reagent (500 μ l/IP) was added directly to the beads to extract RNA, vortexed and incubated at room temperature for 5 minutes. 100 μ l of chloroform was added, followed by vortexing and incubating at room temperature for 2 minutes, prior to a high speed spin at 14,000 RPM for 15 min. 250 μ l isopropanol was then added to the supernatant, followed by spinning at 14,000 RPM for 10 minutes. The resulting pellet was washed once with 70% ethanol (500 μ l) prior to another spin at 14,000 for 5 minutes. Ethanol was then removed with the pellet dissolved in 10 μ l water with qRT-PCR carried out as above on the resulting RNA.

2.17 Time-lapse microscopy

48hrs after transfection eGFP- β -catenin cells were treated with 100 μ g/ml cycloheximide with time lapse images taken every 10minutes for 15 hours using an Olympus IX71 inverted microscope with a x40 objective. The rate of eGFP fluorescence decay was quantified using ImageJ, and displayed as a % of the fluorescence at Time 0, which was set at 100%. esiRNA treated cells and Wnt3a treated (400ng/ml) that weren't treated with cycloheximide were imaged every 10minutes for approximately 29 hours (Movies provided in Appendix C on the associated DVD).

2.18 Plasmids and siRNA

2.18.1 siRNA

Chemically synthesised hnRNP A1 siRNA were obtained from Ambion with product siRNA ID and sequences provided below:

hnRNP A1 siRNA ID: s6711

Sense sequence AAUUAUAGAUGGGAAUGAAtt

Antisense sequence UUCAUCCCAUCUAUAAUUtt

hnRNP A1 siRNA ID: s6710

Sense sequence GAAUAAUGGUACCAGAUAAtt

Antisense sequence UUAUCUGGUACCAUUAUUCaa

2.18.2 Plasmids

CMV-Lac Z plasmid (Invitrogen)

CytoMegalovirus driven constitutively active LacZ expression plasmid. Used as a transfection control.

Mouse hnRNP A1

Purchased from Open Biosystems (Thermo Scientific) used in rescue experiments in Chapter 5. Catalogue number MMM1013-98477917.

**CHAPTER 3. DEVELOPMENT OF HIGH-
THROUGHPUT RNAI SCREENS FOR
IDENTIFYING REGULATORS OF β -
CATENIN LEVELS AND LOCALISATION**

The primary objective of this project was to identify novel regulators of β -catenin accumulation and nuclear localisation in a Wnt signalling context. To facilitate this aim, genome-wide screens utilising esiRNA technology, in combination with high-throughput, high content fluorescence imaging, were employed to investigate β -catenin levels and localisation in fixed cells. An esiRNA library targeting over 17,000 human genes was used in two different cell lines with differing Wnt signalling activities. This enabled the development of screens that were able to identify both positive and negative regulators of β -catenin. The current chapter will describe the work involved in developing the high-throughput screening experiments. High false positive and negative rates are prevalent in high-throughput screens, with the setting up phase of establishing and optimising parameters essential for preventing screen failure and for controlling this issue, as rescreening thousands of genes in secondary assays is unfeasible [291]. Later chapters will present the primary data obtained and subsequent follow up studies that were initiated as a result of their successful completion.

3.1 High-throughput, high content imaging RNAi screens for novel β -catenin regulators.

In order to identify novel regulators of β -catenin in a Wnt signalling context three high content image based, high-throughput RNAi screens were developed in two cell lines. The rationale for the use of these cells in addition to the specifics of their assay development is discussed in their respective sections of this chapter. Before describing these in further detail, a brief introduction to the cell based assays is provided.

3.1.1 IN Cell Analyzer 1000 – A semi automated, high-throughput fluorescence imaging system

As part of an on-going collaboration with GE Healthcare (Maynard Centre, Cardiff), the IN Cell Analyzer 1000 platform was to be used in the high content, high-throughput fluorescence imaging of the screens.

To screen for regulators of β -catenin accumulation and nuclear localisation, two main parameters were to be assessed during image analysis; β -catenin nuclear to cytosolic ratio (nuc/cyt ratio) and whole cell (WC) fluorescence intensities. WC fluorescence intensity represented β -catenin's accumulation in the cell as a whole. The nuclear to cytosolic ratio on the other hand represents its localisation, with increased β -catenin nuclear to cytosolic ratios indicative of enhanced translocation/targeting to the nucleus for example. Comparing β -catenin WC intensities with the ratio parameter allows for the correlation between β -catenin accumulation and its subsequent nuclear localisation to be assessed.

A dual channel approach enabled the analysis of the aforementioned β -catenin parameters. In addition to β -catenin fluorescence (be it by immunocytochemistry or by GFP), nuclei were stained with DAPI, allowing for the creation of a nuclear mask (Figure 3.1, blue) thus enabling the accumulation of β -catenin fluorescence intensity specifically within this mask to be quantified in another channel (green; Figure 3.1). A second outer 'cellular' mask in the region outside the nucleus was generated based on the β -catenin fluorescence channel (green), with fluorescence intensity in this region also quantified. This process of distinguishing defined objects within images, such as the nucleus and the cell boundary, from the background is referred to as segmentation. The degree of nuclear accumulation is then represented by the ratio of the average β -catenin nuclear intensity over the average β -catenin cytosolic intensity. Two examples of segmentation parameters are displayed in Figure 3.1, one where the 'cytosolic' mask extends to the cell edge (A) and one where a 'collar' is drawn around the nuclear mask defined by DAPI (B). For each screen, various algorithms for image analysis were tested and optimised prior to analysing the primary screen data; details of which are given in Chapter 2. A further advantage of staining nuclei with DAPI was the ability to extract information regarding cell numbers from the images, thus enabling the degree of cytotoxicity caused by any individual esiRNA to be assessed.

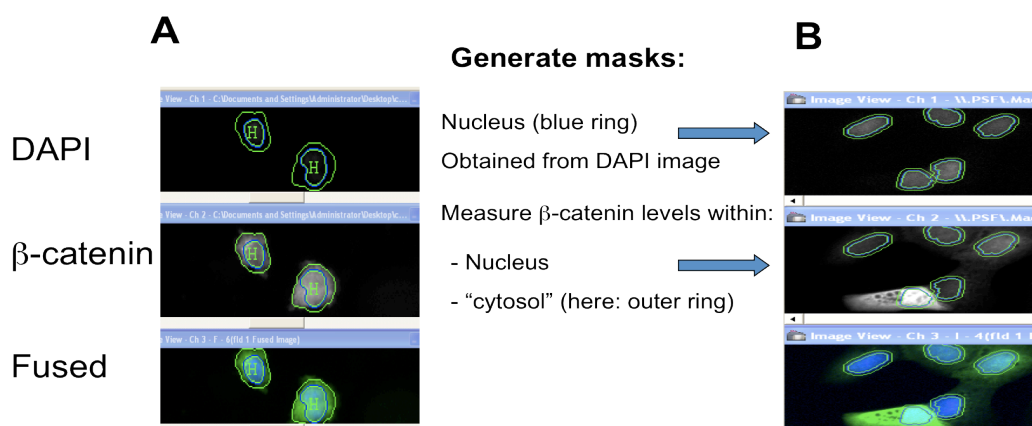


Figure 3.1 Screen shots of image analysis using two different segmentation parameters.

Nuclear masks are obtained using the DAPI image (blue channel, top panels) with a secondary 'cytosolic' mask applied in β -catenin image (green channel, middle panels). β -catenin levels can be then measured within both of the segmentation masks. (A) 7df3 cells stained for β -catenin and DAPI, x10 objective. (B) eGFP- β -catenin U2OS cells, DAPI stained. x10 objective.

3.1.2 Z-factor analysis for an image-based high-throughput assay

High-throughput screens (HTS) require sufficient robustness and sensitivity in order to identify true 'hits' in large compound or siRNA/cDNA libraries, especially given each reagent are often only tested once in a primary screen. Theoretically based, interpretable quality control (QC) metrics are utilised to ascertain the quality and power of a screen in identifying, with a high degree of confidence, true hits with significant biological activity in a given assay [292]. Z-factor [288] and Strictly Standardised Mean Difference (SSMD) [292, 293] are commonly employed QC metrics developed to evaluate data quality in HTS assays. Both are able to assess dynamic ranges between signals in addition to capturing variability within a data set, which is of added benefit in assays with narrow, but highly significant, dynamic ranges [288, 292, 293]. SSMD was proposed more recently as a method of assessing HTS data quality so the extensively cited and widely used Z-factor [288] was favoured in the present study.

The Z-factor is a dimensionless screening window coefficient that reflects the quality and suitability of a screen in identifying true hits by assessing the signal dynamic range and associated variation (see Chapter 2 for formula). A robust HTS will have a

large dynamic range between positive and negative controls, with small standard deviations, resulting in high Z factors. A Z-factor between 0 and 0.5 indicates that an assay is workable, with Z-factors greater than 0.5 indicative of an ‘excellent screening assay’[288].

To assess whether both the experimental and imaging approach were suitable for identifying novel regulators of β -catenin accumulation and nuclear localisation on a high-throughput scale, a Z-factor for each potential screen was obtained. During optimisation of screening conditions, Z-factor analysis was performed throughout to refine the assay to maximise its potential for identifying esiRNAs that had real significant biological effects on β -catenin levels and nuclear localisation.

In order to assess the dynamic range of the proposed screening assay, APC and β -catenin esiRNA were employed as controls with esiRNA against R-luciferase serving as a control for non-specific effects of esiRNA transfection per se. Along with water, these esiRNAs were also to be used as positive and negative controls on each plate in the primary screens to enable the screening performance of each individual plate to be assessed (see Chapter 2 for details).

3.2 Development of a HTS esiRNA imaging screen in the 7df3 reporter cell line

As mentioned in Chapter 1, an RNAi screen for regulators of TCF-dependent transcription was successfully undertaken in a human embryonic kidney (HEK293) derived reporter cell line by Dr Katja Seipel (unpublished). This cell line was named the 7df3 cells and will hence be referred to as such from now on [271]. Undertaking a concurrent screen for regulators of β -catenin accumulation and nuclear localisation in the same cell line would allow for the correlation between the two data sets to be investigated. This in turn could provide valuable information towards deciphering the relationship between Wnt regulated β -catenin and TCF-dependent transcription of target genes. Before describing the development of the β -catenin imaging screen a brief introduction into this particular cell line is first provided.

3.2.1 The 7df3 Cell line

The 7df3 cell line is a HEK293 derived cell line that possesses two stably integrated constructs; a luciferase reporter gene under the control of a promoter containing multimerised TCF binding sites and a Dishevelled2-Estrogen receptor ligand-binding site fusion (DVL-ER). β -estradiol treatment of the cell line results in the activation of this fused protein and subsequent induction of TCF-dependent transcription that is quantifiable using luciferase-based assays [271, 283]. The 7df3 clone was selected as it possessed a large dynamic range and very low background luminescence, leading to the development of a cell line that was easily inducible and gave a quantifiable level of reporter activation upon induction of the Wnt signalling pathway [271]. The inducible nature of the cell line allows for identification of both positive and negative modulators of the pathway in a more physiologically relevant context than using cancer cell lines possessing long-term constitutively active Wnt signalling for example.

The previous esiRNA screen for regulators of TCF-dependent transcription in this cell line identified potential novel Wnt pathway components, which will be further discussed in Chapter 4. The approach taken in developing a screen for regulators of β -catenin accumulation and nuclear localisation in this particular cell line is described in the subsequent section of this chapter. Dr Perihan Nalbant, a visiting research fellow, contributed to the early stages of the project and in the undertaking of the primary screen and is acknowledged where appropriate.

3.2.2. Induction of β -catenin levels with Estradiol treatment

In the previous esiRNA screen for modulators of TCF-dependent transcription, it was ascertained that the optimal β -estradiol concentration to induce Wnt signalling and increase reporter activity to a significant and quantifiable level was $4\mu\text{M}$ for 24hrs prior to assay. It was deemed appropriate to retain these treatment parameters to enable any non-specific estradiol-induced effects to be consistent between the two screens. β -catenin levels in 7df3 cells could be induced with β -estradiol at concentrations of $2\mu\text{M}$ and $4\mu\text{M}$ but with no further increase apparent at a

concentration of 6 μ M (Figure 3.2A). 4 μ m β -estradiol treatment for 24hrs results in approximately a two-fold increase in cellular β -catenin levels, which was observed to be robust and reproducible both by immunofluorescence and western blotting (Figure 3.2B and C). β -estradiol treatment also resulted in significantly increased TCF-dependent transcription (Figure 3.3A) that could be further induced or downregulated by esiRNA against APC and β -catenin itself respectively (Figure 3.3B).

3.2.3 Optimisation of 7df3 reporter cell line transfection conditions for an imaging-based, RNAi high-throughput screen.

Dr Seipel previously established that the lipid-based transfection reagent Interferin was highly efficient at introducing esiRNA into 7df3 cells by reverse transfection. Reverse transfection is an alternative transfection method where cells are transfected while still in suspension rather than having been pre-plated. This method has been shown to be highly efficient at transfecting cells with low siRNA concentrations on a high-throughput scale and is less time consuming than standard pre-plated ‘forward’ transfections, having no need to pre-plate the cells in advance [294-296].

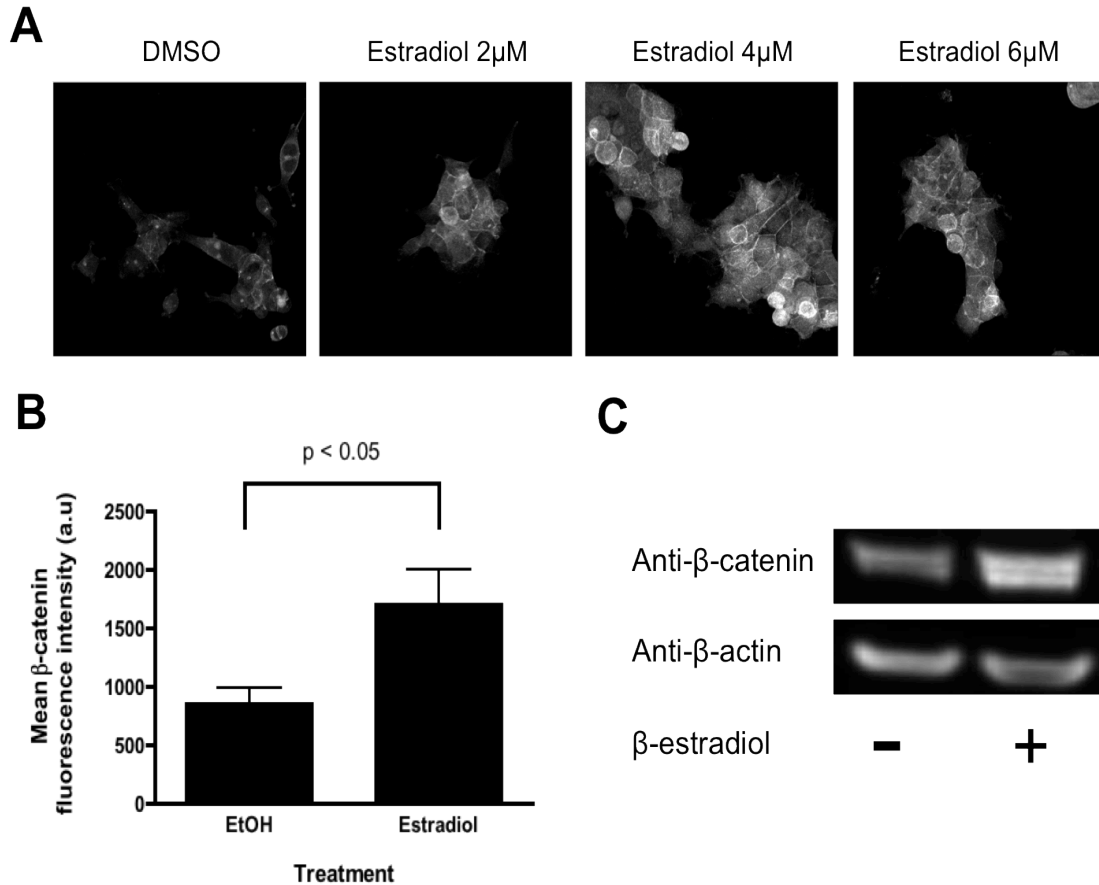


Figure 3.2 β -estradiol treatment induces β -catenin levels in 7df3 cells.

(A) 7df3 cells were seeded on glass coverslips and treated with the indicated β -estradiol concentrations for 24hours before fixation and immunostaining for β -catenin. Confocal imaging (x60 objective) undertaken and images provided by Dr Perihan Nalbant.

(B) 7df3 cells were treated with ethanol (control) or 4 μ M β -estradiol for 24hrs prior to fixation and immunostaining for β -catenin. Mean whole cell fluorescence intensities \pm s.e.m of 4 replicate wells per condition (n=4) are displayed. P-value <0.05 (two-tailed independent samples t-test).

(C) 7df3 cells were treated with ethanol (control) or 4 μ M β -estradiol for 24hrs prior to extracting cytoplasmic lysates for western blot analysis of β -catenin protein levels.

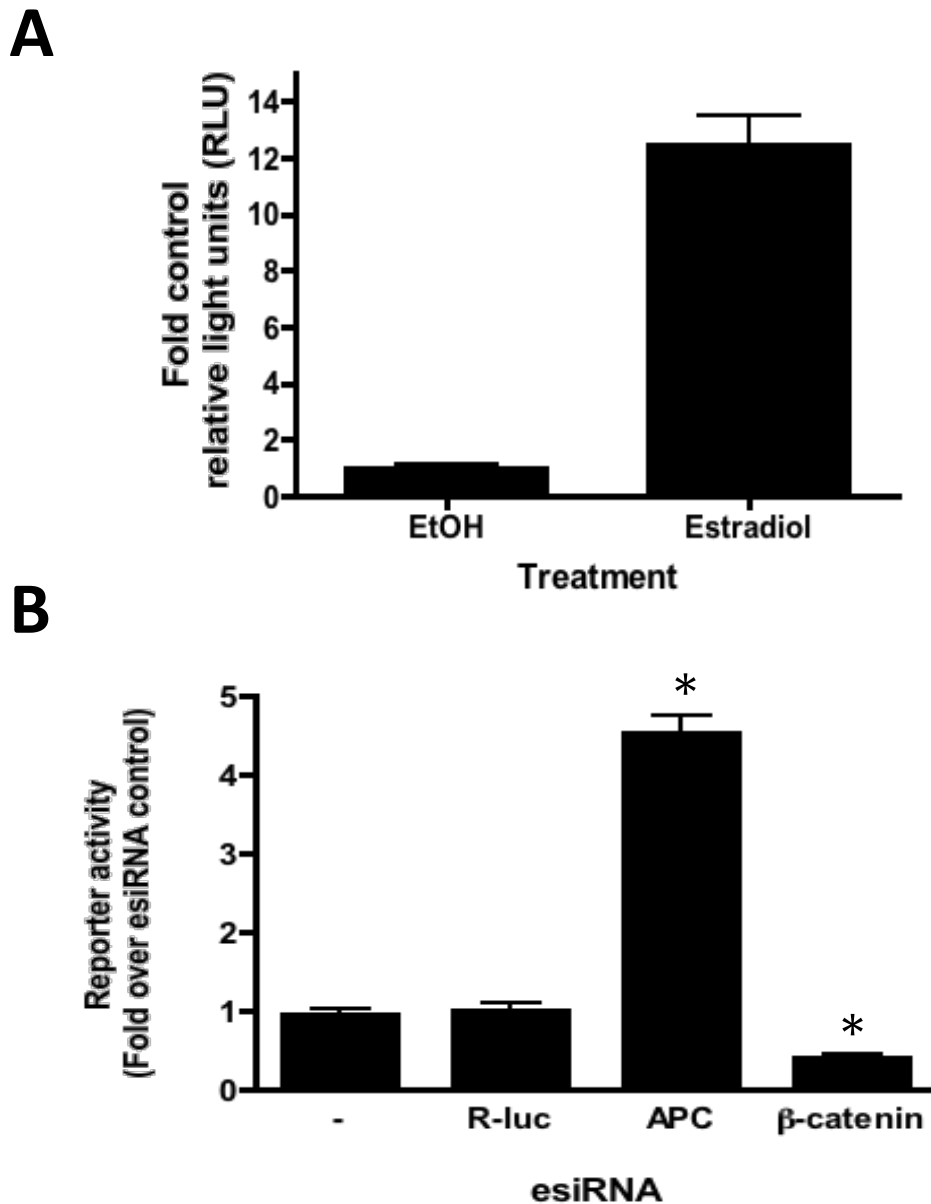


Figure 3.3 β -estradiol treatment results in activated TCF reporter activity that can be modulated by downregulating key Wnt pathway components.

(A) 7df3 cells were treated with ethanol (control) or 4 μ M β -estradiol for 24hrs prior to luminescence assays for TCF-dependent reporter activity. Mean values \pm s.e.m of three independent experiments (n=3; multiple replicate wells per condition) are displayed, p = 0.0015 versus EtOH control. (Two-tailed independent samples t-test). (B) 7df3 cells were transfected with esiRNA (or water '-') and treated with 4 μ M β -estradiol after 24hrs with luminescence assays undertaken 48hrs post transfection. Mean luciferase values \pm s.e.m of two independent experiments (n=2, multiple replicate wells per condition) are displayed as fold over control esiRNA (R-luciferase) * p = <0.0001 versus control esiRNA (two-tailed independent samples t-test).

Two main β -catenin parameters were to be analysed during the imaging screens; the nuc/cyt ratio and WC fluorescence intensity. For an imaging readout, optimal cell numbers are paramount for obtaining high quality images that can be accurately segmented by image analysis software. Therefore, cell density during the reverse transfection procedure was extensively optimised due to the tendency of these HEK293 derived cells to grow in large 3-dimensional colonies (Figure 3.2). At lower cell concentrations, increased cytotoxicity was often observed with consequently decreased cell numbers per field of view. Higher cell seeding densities on the other hand resulted in healthier but often overcrowded cells by fixation 48 hours later, with accurate segmentation of images challenging (Figure 3.4). Importantly, published observations suggest that β -catenin nuclear localisation is lower in confluent contact-inhibited cells [297, 298], which in turn may indirectly affect the cells response to estradiol and esiRNA treatment. In support of this, it was observed that the abilities of control esiRNAs to modulate β -catenin levels and localisation were attenuated with increasing cell densities, resulting in decreased dynamic ranges between these controls (Figure 3.4). Nonetheless, it should be noted that it was unclear at this point if this was due to increased cell-cell junctions or simply due to lower transfection efficiencies at higher seeding densities.

Optimal seeding densities (approximately 3000 cells per well), in addition to longer trypsinisation times to improve single cell re-suspension, resulted in 7df3 cells that displayed more appropriate spreading behaviour to aid image analysis. Despite their small size and characteristic 'clonal' growth properties, the 7df3s yielded good quality images with high signal:noise ratios. Furthermore, this seeding density resulted in sufficient numbers within one field of view to achieve a statistically relevant population without being to the detriment of the dynamic range of the assay window, with significant alterations in β -catenin levels and localisation observed in response to APC and β -catenin downregulation (Figure 3.5).

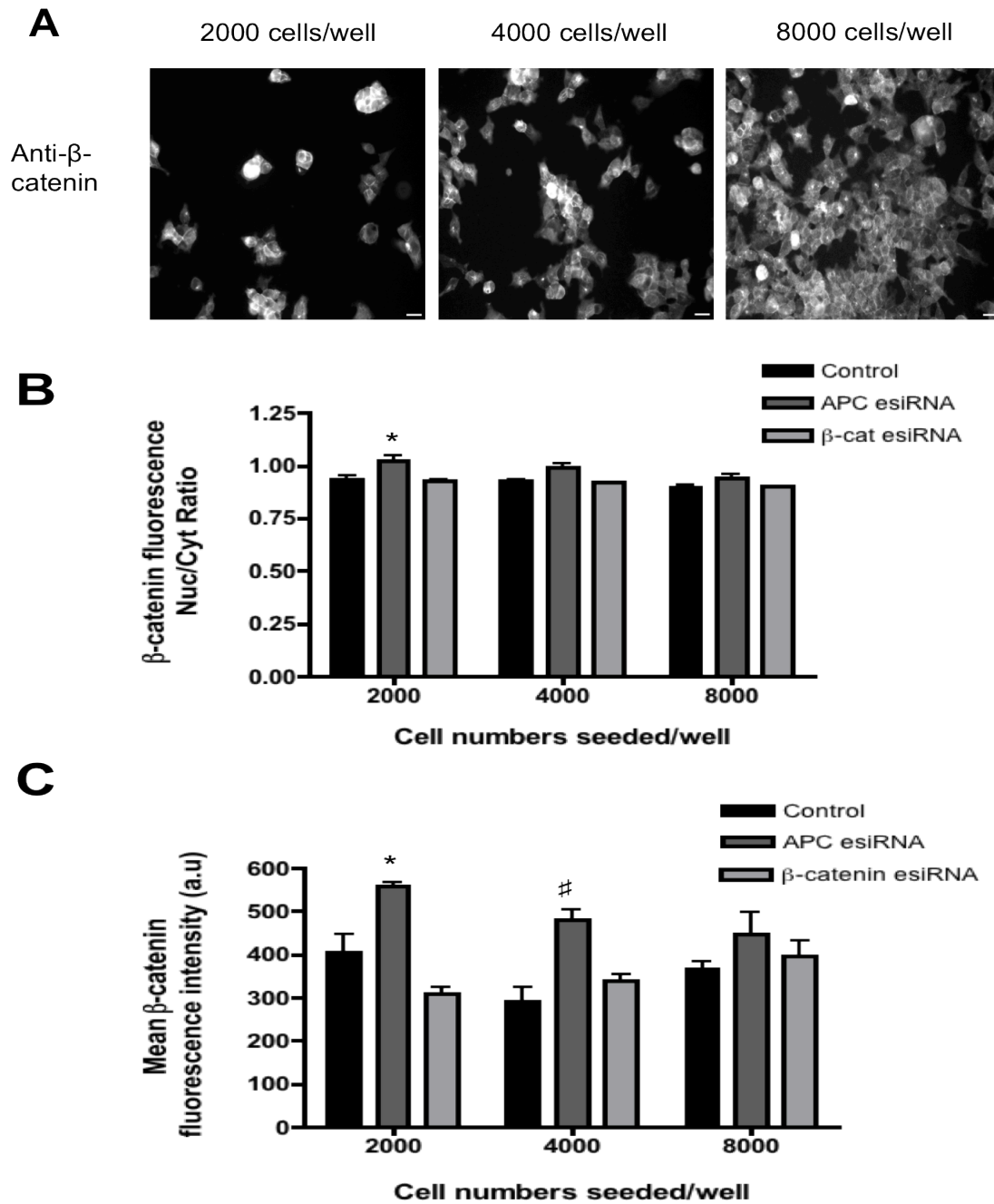


Figure 3.4 esiRNA effects on β -catenin levels and localisation are reduced in densely packed cells

7df3 cells were reverse transfected with esiRNA at different cell densities, treated with $4\mu\text{M}$ β -estradiol after 24hrs, followed by β -catenin immunocytochemistry and DAPI staining at 48hrs post transfection. Images were acquired using the IN Cell Analyzer 1000. (A) Representative images from control esiRNA. Bars, $25\mu\text{m}$. Images were analysed using IN Cell Analyzer Workstation software with β -catenin Nuclear/Cytosolic ratio (B) and whole cell intensities (C) quantified. Mean values \pm s.e.m of 3 replicate wells per condition are displayed. * $p = 0.06$, # $p = 0.02$ compared to corresponding esiRNA controls (two-tailed independent samples t-test).

3.2.3.1 Z-factor analysis for an image-based HTS assay in the 7df3 cell line

To assess whether both the experimental and imaging approach were suitable for identifying novel regulators of β -catenin accumulation and nuclear transport in a high-throughput system, a Z-factor for the assay was required [288].

During assay development, Z-factor analysis of the data was undertaken to assess the optimisation of esiRNA reverse transfection in order to obtain the greatest dynamic range possible between the controls, with minimal associated variation. Whilst depletion of APC could significantly enhance β -catenin nuclear localisation (as displayed by the nuclear to cytosolic ratio), in addition to overall levels, the dynamic range between controls was low with approximately a 15-20% increase in β -catenin nuc/cyt ratio observed upon APC knockdown compared to control. However, this small effect was observed to be highly reproducible and robust, resulting in a Z-factor of 0.44 for β -catenin nuc/cyt ratio, therefore a workable assay just slightly below the ideal Z-factor of 0.5 and above. Upon assessing the single cell data it was clear that there many cells displayed far higher β -catenin Nuc/Cyt ratios in the APC treated sample but variable responses from cell-to-cell resulted in a lower effect upon taking the mean of the cell population. Imaging at higher resolutions gave similar results, and it was noticed that whilst the degree of β -catenin nuclear accumulation was indeed marginal, the percentage of cells displaying such accumulation had increased dramatically compared to control cells. When displayed as a histogram, the percentage of cells above a certain β -catenin nuc/cyt threshold were far greater with APC esiRNA treated cells compared to control and provided an additional method for analysing an esiRNA effect (Appendix A, Figure 1). These relatively small changes in β -catenin nuclear to cytosolic ratio, despite subtle, was in line with published work on the nuclear translocation of other similar proteins such as STAT3 [259] and ERK1/2 ([http://www.gelifesciences.com/aptrix/upp00919.nsf/Content/A1F48F519178F8BAC1257628001D1617/\\$file/ERK-AN.pdf](http://www.gelifesciences.com/aptrix/upp00919.nsf/Content/A1F48F519178F8BAC1257628001D1617/$file/ERK-AN.pdf)). Whilst APC downregulation often resulted in small but nevertheless significant increases in β -catenin accumulation in β -estradiol treated 7df3 cells (which already possessed only a partially activated β -catenin destruction complex due to DVL2 activation), β -catenin esiRNA markedly reduced β -catenin levels as expected. Z-factor analysis

demonstrated that this β -catenin accumulation parameter possessed a Z-factor 0.6, again comfortably within the acceptable range for a HTS (Figure 3.5). Intriguingly, in the 7df3 cells, small increases in β -catenin fluorescent intensity levels led to significant increases in transcriptional activity (Figure 3.3B).

3.2.3.2 Effect of plate edge location on esiRNA.

Systematic errors are common in HTS assays, with those linked to well position within a multi-well plate often dictating the subsequent analysis procedures required to minimise the impact of such effects [293]. Briefly, the effect of APC control esiRNA on various edges were compared to those in mid plate wells, with results suggesting that, in the case of APC esiRNA, well location had minimal effects on the degree of β -catenin accumulation and localisation compared to water control (Figure 3.6).

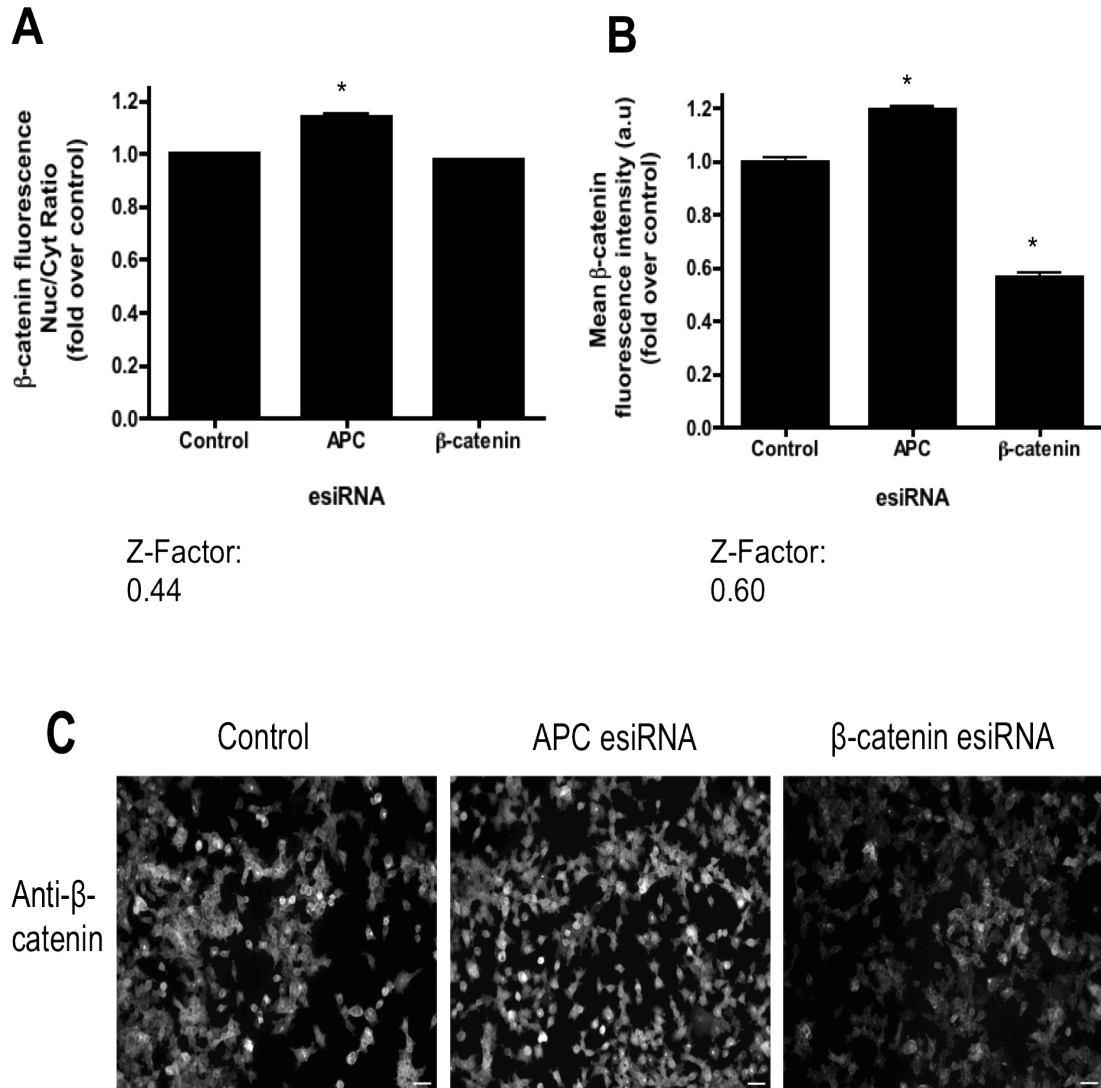


Figure 3.5 Z-factor analysis of screening conditions.

Following refinement of transfection conditions, 7df3 cells were reverse transfected with esiRNA, treated with β -estradiol after 24hrs, followed by β -catenin immunocytochemistry and DAPI staining at 48hrs post transfection. Images were acquired using the IN Cell Analyzer 1000. Images were analysed using IN Cell Analyzer Workstation software with β -catenin Nuclear: Cytosolic ratio (A) and whole cell intensities (B) quantified. Mean values \pm s.e.m of 2 independent experiments displayed as fold over control. * $p = 0.001$ (One-way ANOVA, Bonferroni's multiple comparison correction post test). (C) Representative images of cells treated with the indicated esiRNA. Bar, 25 μ m.

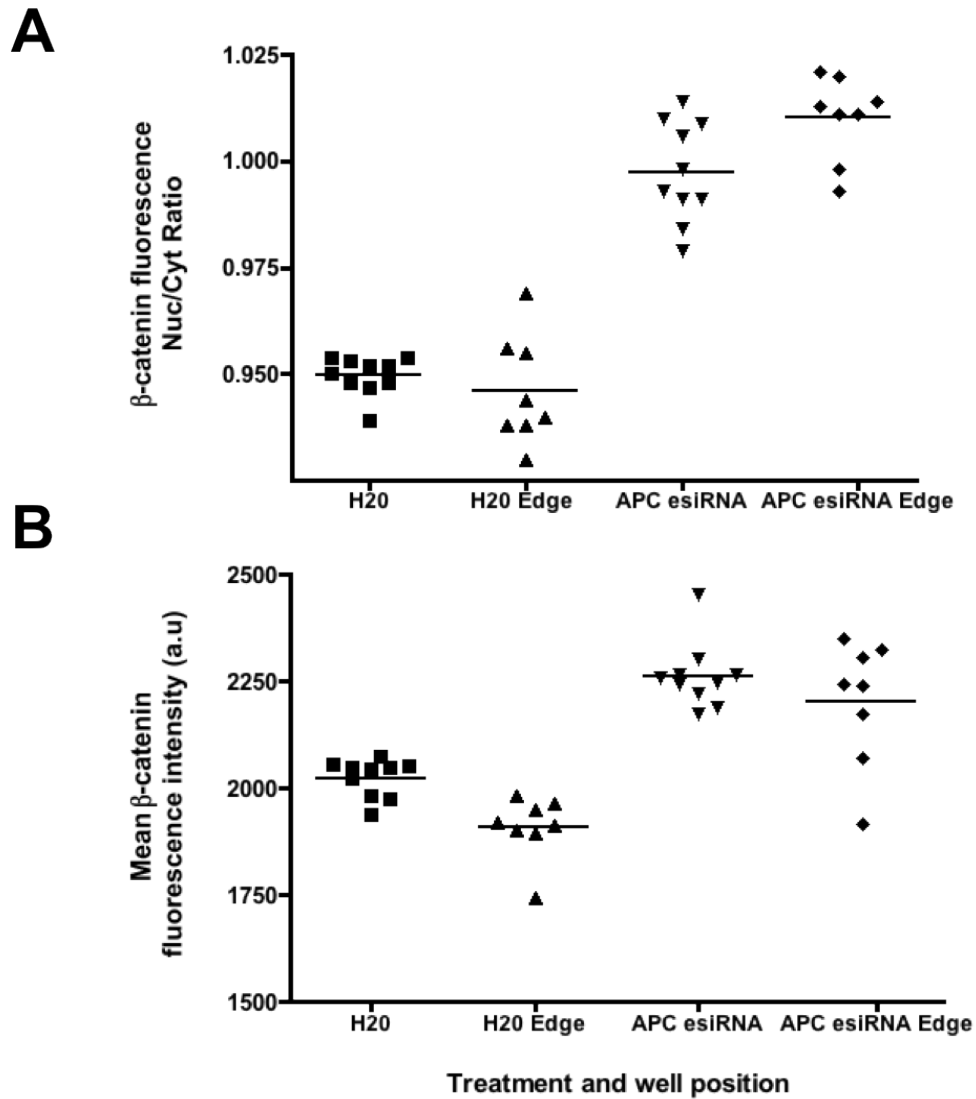


Figure 3.6 esiRNA on plate edges behave similarly to those in the middle of the plate.

esiRNA against APC and water were plated in the middle of the plate in addition to various edges with 7df3 cells reverse transfected, treated with β -estradiol after 24hrs, followed by β -catenin immunocytochemistry and DAPI staining at 48hrs post transfection. Images were acquired using the IN Cell Analyzer 1000. Images were analysed using IN Cell Analyzer Workstation software with β -catenin Nuclear:Cytosolic ratio (A) and whole cell intensities (B) quantified. Mean values of at least 8 replicate wells per condition are displayed with individual well values as points around the mean. APC esiRNA significantly increased both β -catenin parameters to a similar degree regardless of plate location (p -value <0.001) with no significant effect observed between locations of the same treatment (One-way ANOVA, Bonferroni's multiple comparison correction post test).

3.3 Development of two HTS esiRNA imaging screens in an eGFP- β -catenin-U2OS cell line.

The aforementioned screen was undertaken in the reporter cell line to enable the correlation of the data with a corresponding TCF-dependent transcriptional screen undertaken previously. The screen was successfully completed with the primary data discussed further in Chapter 4.

In addition, an approach to use a human osteocarcinoma cell line stably expressing an enhanced green fluorescent protein- β -catenin fusion (eGFP- β -catenin) was initiated. For high-throughput, high content screening purposes these cells were good candidates for several reasons. Firstly, the intensity and redistribution of the eGFP- β -catenin could be easily followed and quantified without the need for expensive and laborious antibody based immunocytochemistry procedures. Additionally, the large, flat nature of these epithelial-like cancer cells were ideal for image segmentation and could provide a more robust system for assessing β -catenin nuclear localisation; a parameter that was challenging to analyse in the small, 'clumpy' 7df3 cell line. U2OS cells possess normal Wnt/ β -catenin signalling with no reported mutations in known key components of this pathway. Moreover, upon treatment with the GSK3- β inhibitor, (2'Z,3'E)-6-Bromindirubin-3'-oxime (BIO), robust β -catenin accumulation and subsequent nuclear translocation was observed (Figure 3.7A). Increasing BIO concentration resulted in β -catenin accumulation with approximately a two-fold increase observed at a concentration of 10 μ M (Figure 3.7), with drug-induced cytotoxicity becoming apparent past this concentration. Z-factors for individual experiments ranged between 0.4-0.7 for both β -catenin nuc/cyt ratio and whole cell intensity parameters (data not shown). Intriguingly, the effect of BIO treatment on β -catenin accumulation and nuclear localisation was observed to be attenuated in more confluent cells (data not shown) suggesting that increased cell-cell junctions may be functioning to sequester β -catenin at the membrane. Overall, these cells were deemed excellent candidates for two esiRNA screens for β -catenin to not only corroborate data from the 7df3 screen but also highlight other potential novel regulators of β -catenin accumulation and nuclear localisation in different contexts.

The first screen in the eGFP- β -catenin U2OS cells was to be undertaken in unstimulated cells with negligible amounts of detectable cytosolic and nuclear β -catenin levels (Figure 3.7A, DMSO panel). The subsequent follow up screen was to be undertaken in an active Wnt-signalling context, with β -catenin accumulation induced by APC depletion alongside the transfection of the esiRNA library.

3.3.1 Image based high-throughput screen in the U2OS eGFP-Beta-catenin cell line.

Undertaking an esiRNA screen in cells with very low basal levels of cytosolic and nuclear β -catenin levels would allow for the identification of esiRNAs that resulted in elevated β -catenin levels and nuclear localisation. Similarly to the 7df3 primary screen, the same esiRNA controls were used in this particular cell line at the same concentration, with an incubation time of 48hrs also selected to maintain consistency with the previous screen.

Reverse transfection was again to be utilised for high-throughput transfection of this particular cell line. Extensive optimisation showed that the transfection reagent Lipofectamine 2000 was superior to other reagents tested (Figure 3.8) and that a concentration of 120nl (Figure 3.9) alongside 1500 cells/well was optimal for significant APC and β -catenin esiRNA effects (Figure 3.10). This seeding density resulted in sufficient numbers within one field of view without being to the detriment of the dynamic range of the assay window, with significant alterations in β -catenin levels and localisation observed in response to APC and β -catenin downregulation.

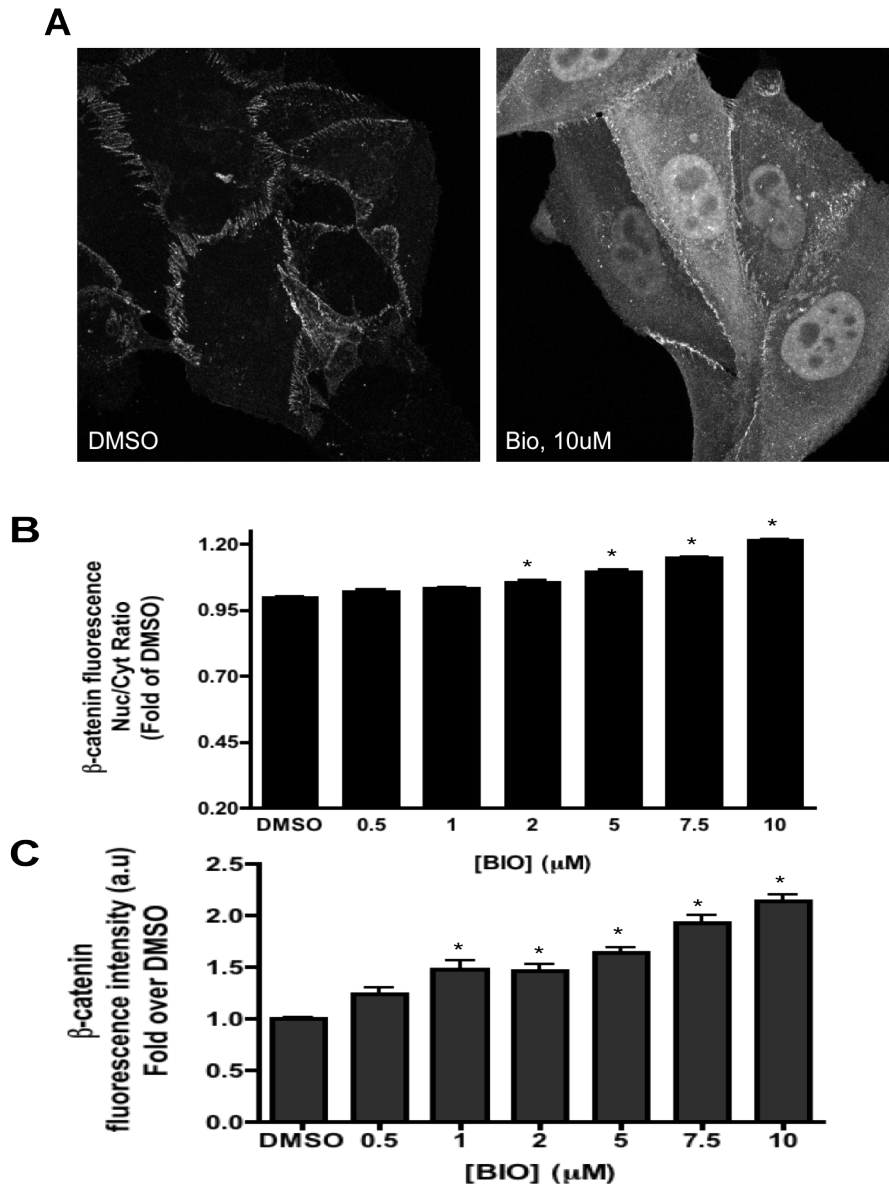


Figure 3.7 Inhibition of GSK- β results in increased β -catenin levels and nuclear localisation in U2OS-eGFP- β -catenin cells.

(A) eGFP- β -catenin cells were seeded on glass coverslips prior to 10 μ M BIO treatment for 16hrs before fixation. Confocal images (x60 objective) kindly provided by Dr P. Nalbant. U2OS-eGFP- β -catenin cells treated with increasing concentrations of BIO for 16 hrs prior to fixation and DAPI staining were imaged and analysed using the IN Cell Analyzer 1000 platform. β -catenin Nuclear:Cytosolic ratio (B) and whole cell intensities (C) were quantified. Mean values \pm s.e.m of 3 independent experiments (of multiple replicate wells per concentration) are displayed as fold over DMSO control. * $p = 0.001$ (One-way ANOVA, Bonferroni's multiple comparison post test).

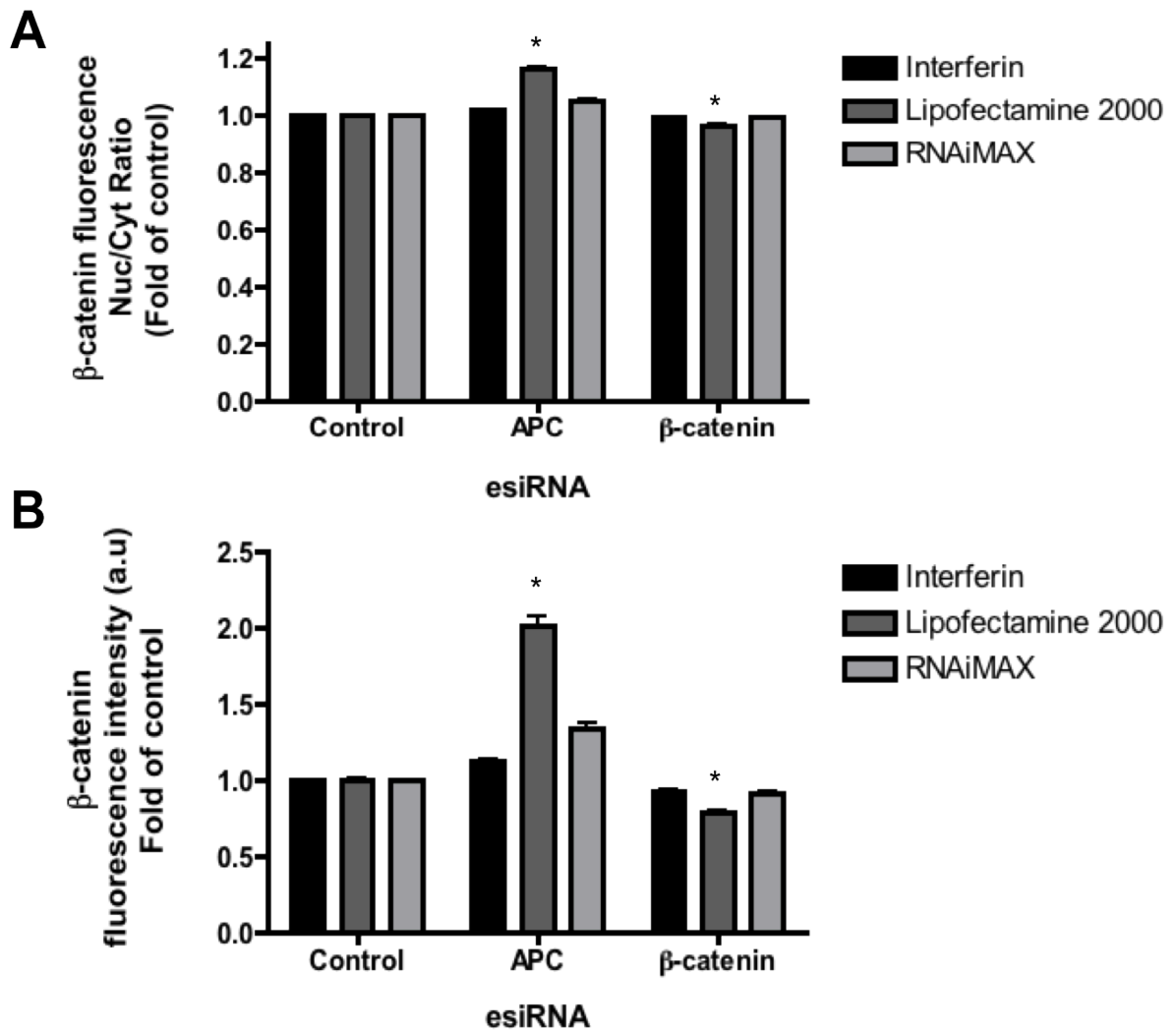


Figure 3.8 Lipofectamine 2000 appears superior to Interferin and RNAiMAX for esiRNA transfection in U2OS-eGFP-β-catenin cells.

U2OS-eGFP-β-catenin cells were reverse transfected with esiRNA using different reagents and fixed after 48hrs. Images were acquired and analysed using IN Cell Analyzer 1000 platform with eGFP-β-catenin Nuclear:Cytosolic ratio (A) and whole cell intensities (B) quantified. Mean values ± s.e.m of 3 independent experiments (of multiple replicate wells per condition) displayed as fold over esiRNA control. * p = 0.001 (One-way Anova, Bonferroni's multiple comparison post test).

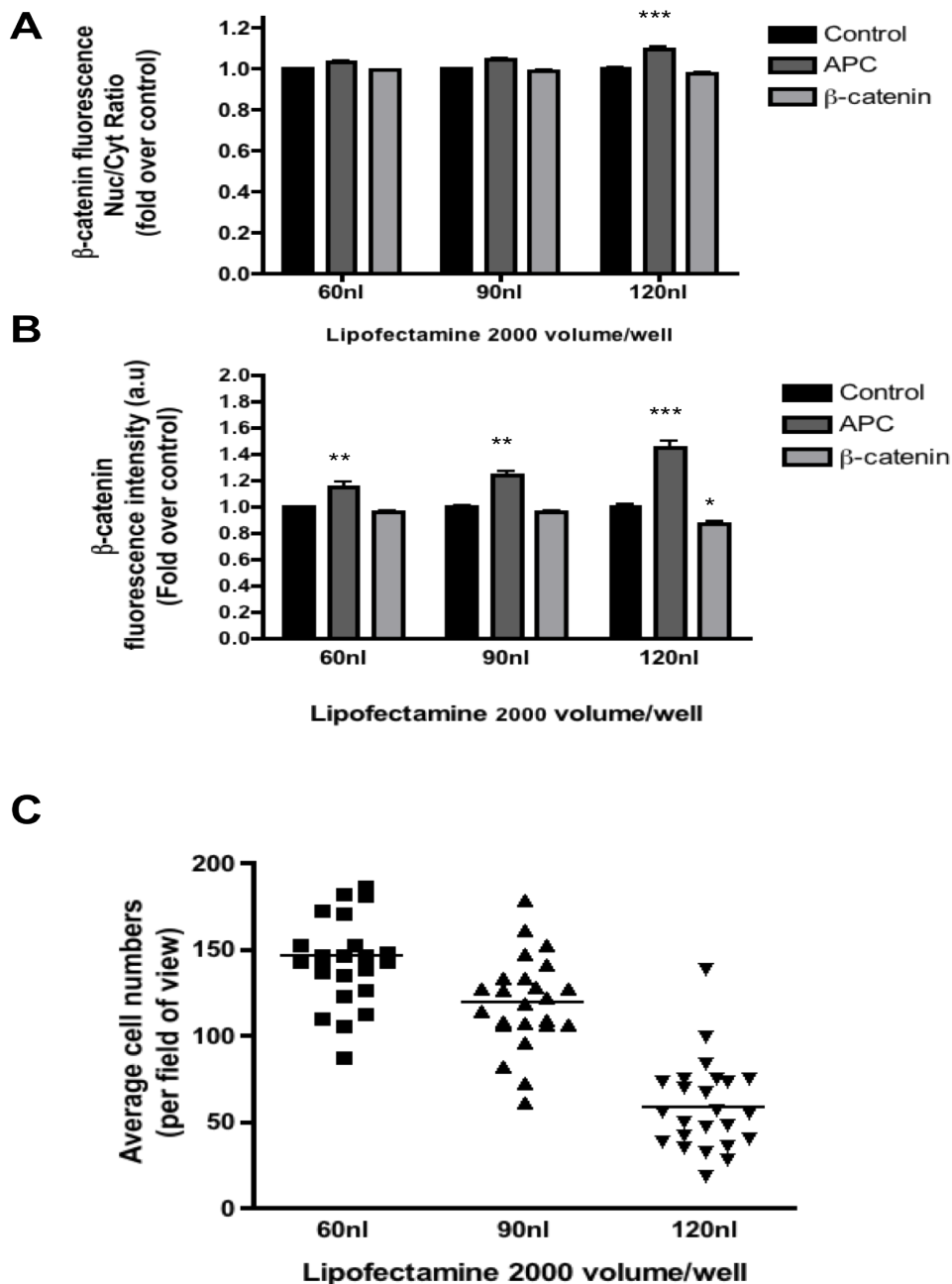


Figure 3.9 APC esiRNA results in increased β -catenin stabilisation and nuclear localisation in eGFP- β -catenin U2OS cells with increasing concentrations of Lipofectamine 2000 but to the detriment of cell numbers.

U2OS-eGFP- β -catenin cells were reverse transfected with varying concentrations of Lipofectamine 2000 and fixed after 48hrs. Images were acquired and analysed using the IN Cell Analyzer 1000 platform with eGFP- β -catenin Nuclear:Cytosolic ratio (A) and whole cell intensities (B) quantified. Mean values \pm s.e.m of 2 independent experiments (of multiple replicate wells per condition) displayed as fold over esiRNA control. *** $p < 0.001$, ** $p < 0.01$ * $p < 0.05$ (One-way Anova with Bonferroni's multiple comparison post test). (C) Mean cell numbers per condition are displayed along with their associated scatter. Data points from 2 independent experiments of multiple replicate wells per condition, with changes significant to at least $p < 0.01$ (One-way Anova with Bonferroni's multiple comparison post test).

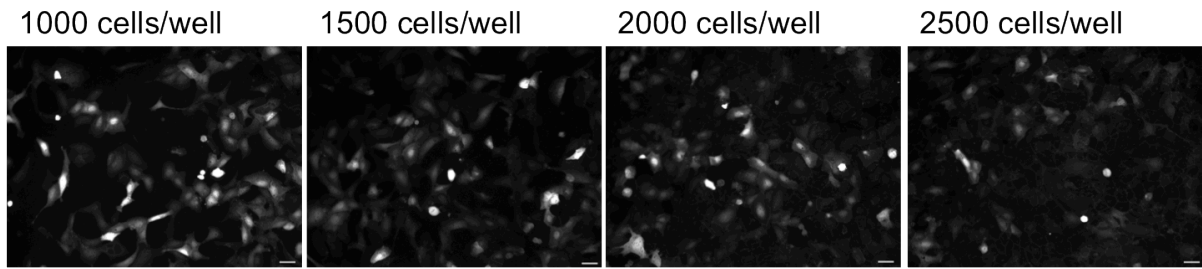
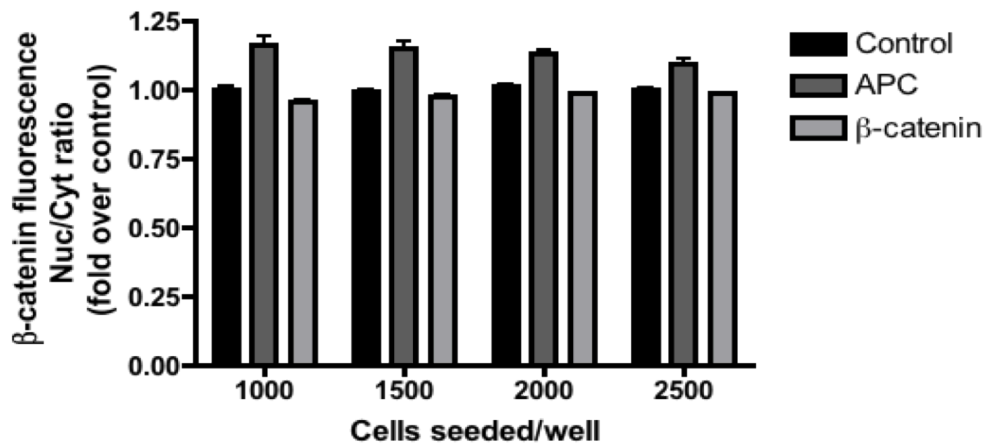
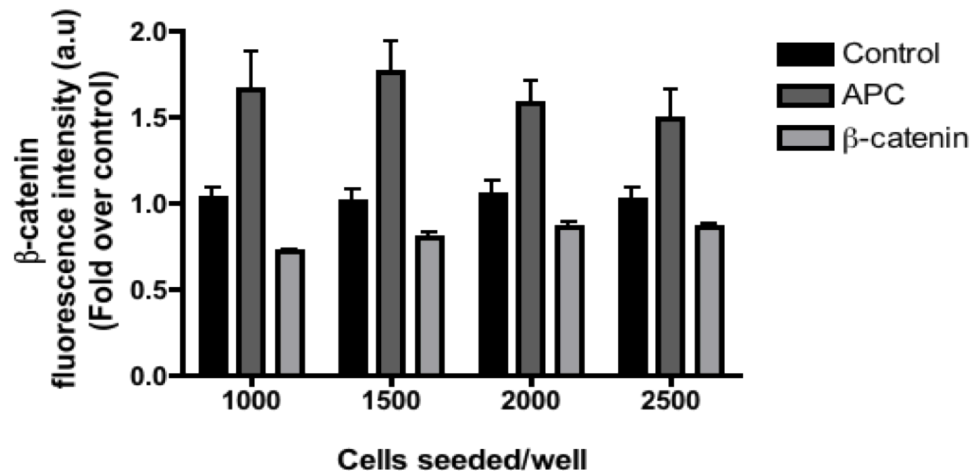
A**B****C**

Figure 3.10 Increasing cell densities reduces the dynamic range between esiRNA controls in eGFP-β-catenin U2OS cells

U2OS-eGFP-β-catenin cells were reverse transfected with the indicated esiRNA at varying cell densities and fixed after 48hrs. Images were acquired and analysed using IN Cell Analyzer 1000 platform with representative images from APC esiRNA treated cells displayed (A). Bar; 50µm. Images were analysed for eGFP-β-catenin Nuclear:Cytosolic ratio (B) and whole cell intensities (C). Mean values ± s.e.m of 2 independent experiments (of multiple replicate wells per condition) displayed as fold over esiRNA control.

3.3.1.1 Z-factor analysis for an image-based HTS assay

During assay development, Z-factor analysis of the data was undertaken to assess the optimisation of esiRNA reverse transfection. Depletion of APC enhanced the nuclear localisation of β -catenin as displayed by the nuclear to cytosolic ratio and, whilst the dynamic range between the controls was once again narrow at approximately 15-20%, it was shown to be highly robust and reproducible (Figure 3.11). This robustness resulted in an average Z-factor of 0.42 for this β -catenin localisation parameter, indicative of a good screening assay. Contrary to the 7df3s, APC downregulation resulted in much greater β -catenin accumulation due to there being low basal levels of β -catenin in the cells. β -catenin esiRNA markedly reduced β -catenin levels as expected, although the more stable membrane associated β -catenin pool was still observable 48hrs post transfection. Z-factor analysis demonstrated that the β -catenin accumulation parameter also possessed a Z-factor 0.42, again comfortably within the acceptable range for a HTS (Figure 3.11).

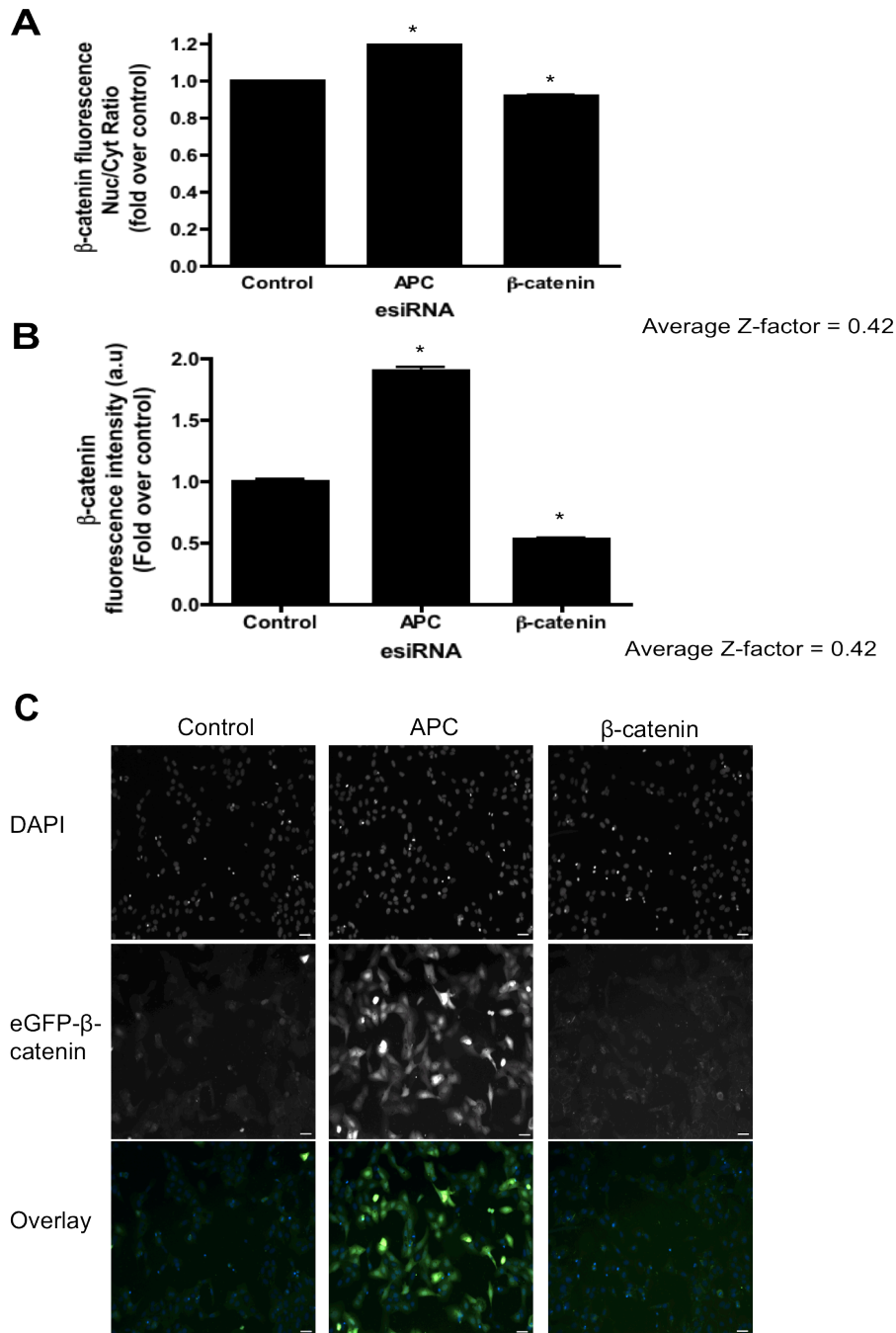


Figure 3.11 APC and β -catenin downregulation can robustly and reproducibly modulate β -catenin levels and nuclear accumulation in eGFP-B-catenin U2OS cells, resulting in good Z-factors for a potential screen.

U2OS-eGFP- β -catenin cells were reverse transfected at a density of 1500 cells per well with esiRNA using 120nl/well Lipofectamine 2000 and fixed after 48hrs. Images were acquired and analysed using IN Cell Analyzer 1000 platform with eGFP- β -catenin Nuclear:Cytosolic ratio (A) and whole cell intensities (B) quantified. Mean values \pm s.e.m of 3 independent experiments (of multiple replicate wells per condition) displayed as fold over esiRNA control. * $p = <0.001$ (Kruskal-wallis test with Dunn multiple comparison test/correction). (C) Representative images displayed. Bar; 50 μ m.

3.3.2 Image based high-throughput screen in the U2OS eGFP-Beta-catenin cell line with APC downregulation

In the screen undertaken above, genes that led to increased β -catenin levels and nuclear accumulation upon knockdown were clearly identifiable compared to those that decreased amounts, due to the low basal levels of β -catenin within these cells. Therefore, the feasibility of undertaking a screen in the presence of enhanced β -catenin levels to identify both up-regulators and downregulators within an active Wnt signalling context was investigated. Downregulating APC as a means of enhancing β -catenin was proposed due to the prohibitive cost of purified Wnt3a ligand, with Wnt conditioned media treatment deemed inappropriate due to inherent variation between different batches, which could potentially hinder re-confirmation of the primary screen data. APC downregulation consistently produced robust and reproducible β -catenin accumulation and nuclear translocation within this cell line (Figure 3.11) and would also be synonymous to several cancers where APC mutations contribute to tumourigenesis. In turn, the potential of identifying downregulators of APC esiRNA induced β -catenin within this screen was deemed highly attractive.

The ability to knockdown elevated levels of β -catenin by co-transfecting more than one esiRNA was investigated. Co-transfecting increasing concentrations of APC esiRNA with control esiRNA resulted in increased β -catenin accumulation and nuclear localisation compared to control on its own, with the highest concentration displaying the most robust induction of β -catenin nuclear localisation and accumulation (Figure 3.12). Importantly, co-transfecting β -catenin esiRNA was able to reverse the effect of APC esiRNA, even at the highest concentration, returning β -catenin levels and nuclear localisation to control levels (Figure 3.12).

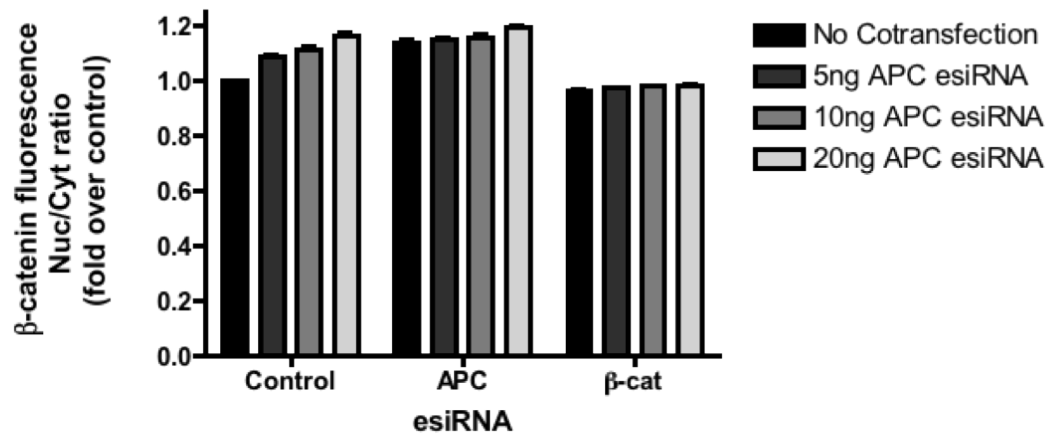
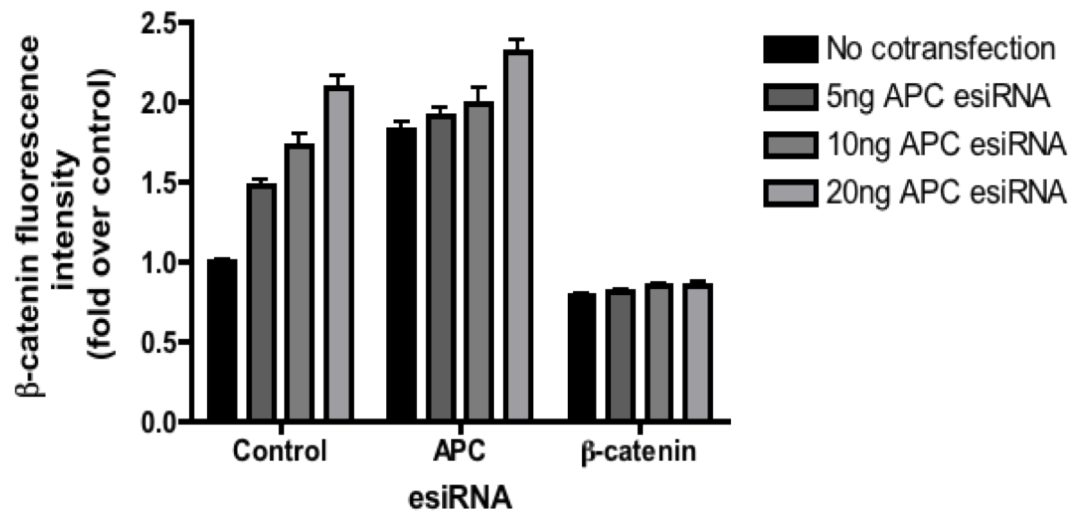
A**B**

Figure 3.12 Co-transfecting varying concentrations of APC esiRNA with controls result in enhanced β -catenin nuclear accumulation and levels, which is reversible in the presence of β -catenin esiRNA.

U2OS-eGFP- β -catenin cells were reverse transfected with the indicated esiRNA in addition to increasing concentrations of APC esiRNA. 48 hours post transfection, cells were fixed, imaged and analysed using IN Cell Analyzer 1000 platform for eGFP- β -catenin Nuclear:Cytosolic ratio (A) and whole cell intensities (B). Mean values \pm s.e.m of 3 independent experiments (of multiple wells per condition) displayed as fold over esiRNA control.

3.3.2.1 Z-factor analysis for an image-based HTS assay

Co-transfecting APC esiRNA along with control R-luciferase and APC esiRNA resulted in increased β -catenin nuc/cyt ratios and whole cell intensity, which could be abrogated when co-transfected with β -catenin esiRNA. A representative experiment displayed Z-factors of 0.68 and 0.61 for β -catenin nuclear localisation (Nuc/Cyt ratio) and β -catenin whole cell intensity respectively upon comparing APC/ β -catenin esiRNA with APC/control esiRNA transfected cells. These Z-factors are indicative of an ‘excellent’ screening assay and gave confidence in the assay’s suitability for the high-throughput screening of the esiRNA library for regulators that are able to modulate APC esiRNA induced β -catenin levels and localisation in the eGFP- β -catenin U2OS cells (Figure 3.13). Representative images demonstrate the induction of β -catenin levels in the control wells following APC esiRNA co-transfection and its downregulation in the presence of β -catenin esiRNA.

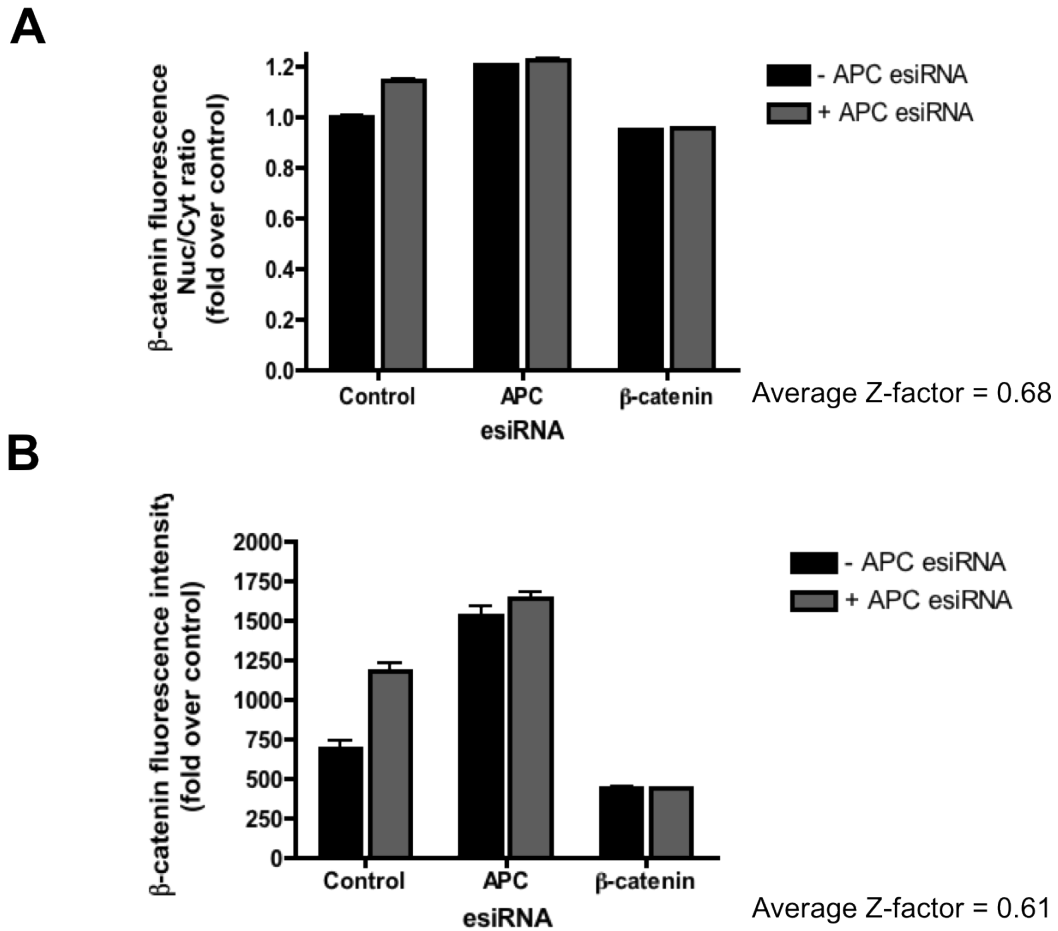


Figure 3.13 Co-transfecting APC esiRNA with controls result in robust accumulation and nuclear translocation of β -catenin, which can be downregulated by β -catenin esiRNA.

U2OS-eGFP- β -catenin cells were reverse transfected at a density of 1500 cells/well with esiRNA using 120nl/well Lipofectamine 2000 and fixed after 48hrs. Images were acquired and analysed using IN Cell Analyzer 1000 platform with eGFP- β -catenin Nuclear:Cytosolic ratio (A) and whole cell intensities (B) quantified. Mean values \pm s.e.m of 4 wells in a representative experiment displayed as fold over esiRNA control. Average Z-factors of 3 independent experiments displayed.

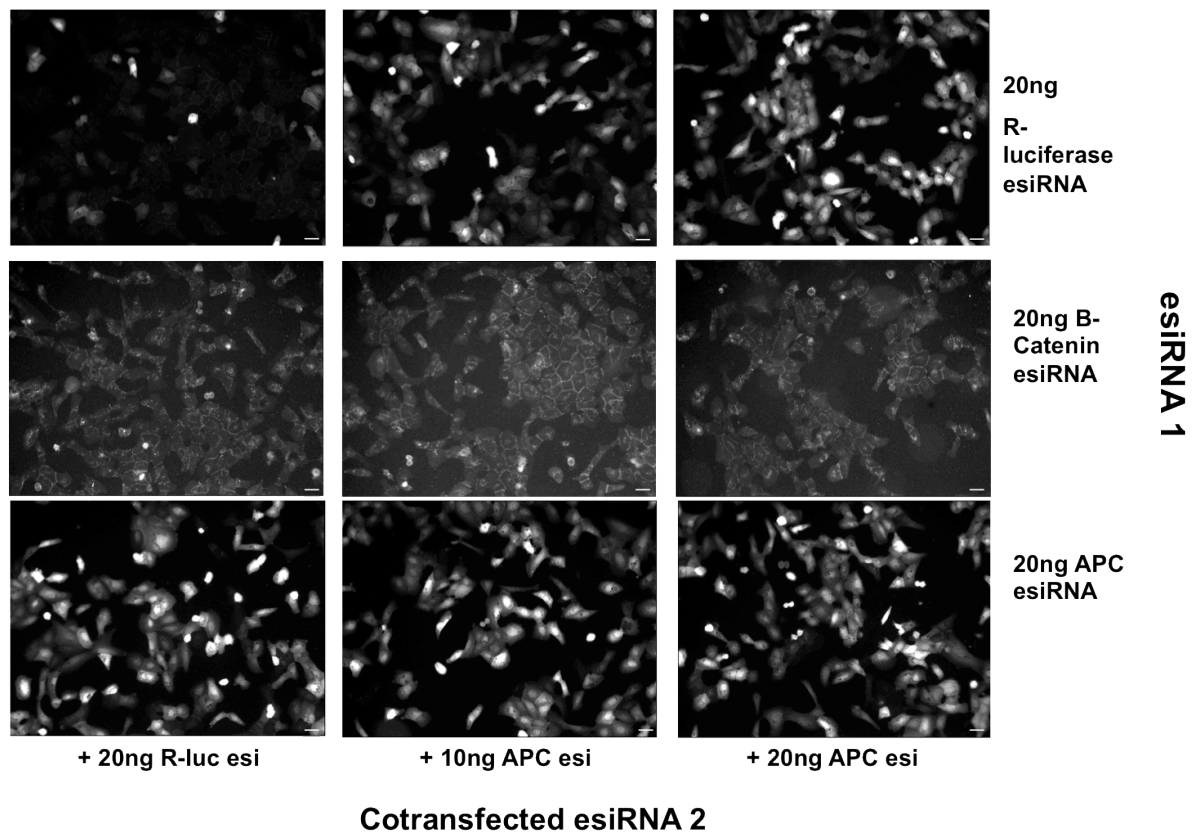


Figure 3.13 continued. Co-transfecting APC esiRNA with controls result in robust accumulation and nuclear translocation of β -catenin, which can be downregulated by β -catenin esiRNA.

(C) U2OS cells were reverse transfected with 20ng esiRNA or water control along with varying concentrations of APC esiRNA for 48hrs before fixation and DAPI staining. Images were acquired and analysed using IN Cell Analyzer 1000 platform. Representative images displayed. Bar; 50 μ m.

3.4 Summary

The primary aim of the project was to develop and employ high content imaging based high-throughput esiRNA screens to identify novel regulators of β -catenin levels and localisation in Wnt signalling. Additionally, a particularly important objective was to correlate the results from the imaging screens with the previous screen for regulators of TCF-dependent transcription. Three screens were developed as described, with Z-factors of approximately 0.5 for each screen, suggestive of robust screening assays for detecting potential novel regulators or β -catenin accumulation and nuclear localisation. High Z-factors imply low false positive and false negative rates, a potential major issue in downstream assays as thousands of genes cannot feasibly be re-assessed. The first screen in the HEK293-derived reporter cell line with activated Wnt signalling, utilised in the aforementioned transcriptional screen, possessed good signal to noise ratio although an assessment of β -catenin nuclear to cytosolic ratio was challenging due to their morphology. In contrast, the U2OS cell line possessed superior imaging qualities although in the endogenous state, intracellular levels of β -catenin were very low, suggesting it would be difficult to identify downregulators of β -catenin in the screen. Undertaking the same screen in an active Wnt signalling context upon APC downregulation resulted in an assay capable of identifying both up- and down-regulators of β -catenin levels and localisation. Initial experiments in the 7df3 reporter cell line suggested a non-linear relationship between TCF-dependent luciferase activity and β -catenin levels, in contrast to the textbook model of Wnt/ β -catenin signalling.

**CHAPTER 4. GLOBAL SCALE
INSIGHTS INTO β -CATENIN
REGULATION AND ITS ROLE IN
WNT SIGNALLING.**

In this chapter, the primary screening data will be presented in addition to extensive pathway analysis and cross comparisons between the three screens undertaken. These were as follow:

1. **H** - 7df3 screen - HEK293 derived (7df3) reporter cell line
2. **UB** - U2OS screen - eGFP- β -catenin U2OS screen, esiRNA library only
3. **UA** - U2OS APC screen - eGFP- β -catenin U2OS APC screen, esiRNA library +APC esiRNA

For simplicity, the three screens will be referred to by their codes in bold above in the text when comparing screens.

Comparative analysis of the primary data with RNAi screens for regulators of TCF-dependent transcription will also be presented, with the regulators and biological processes that couple β -catenin to transcriptional activity highlighted. Additionally, validation of a subset of hits identified from each screen will be described.

4.1 esiRNA screens for novel regulators of β -catenin accumulation and localisation in Wnt signalling

An esiRNA library targeting 17,188 human genes [238-240], plated in 384-well format, was screened in each of the three assays developed in Chapter 3. Specific details regarding the library and production of test plates are provided in Chapter 2 with esiRNA sequences, ENSEMBL IDs and associated plate/well locations provided in Table 1, Appendix B (on disc provided). Images taken using the IN Cell Analyzer 1000 were analysed using the associated IN Cell Investigator image analysis software to quantify both β -catenin whole cell fluorescence intensity, in addition to β -catenin nuclear:cytosolic ratio. Detailed experimental and image analysis parameters for each screen is provided in Chapter 2.

4.1.1 7df3 (H) primary screen

Having established screening conditions, the library of 17,188 esiRNAs was screened in the reporter cell line as described in Chapter 2. All raw and normalised data of β -catenin nuclear/cytosolic ratio and whole cell intensities, along with cell numbers from this screen, are provided in Table 2 in Appendix B on the disc provided.

4.1.1.1 Z-factor analysis of the H primary screen.

To assess the screening performance of the 47 plates, individual plate Z-factors were calculated using the replicate control wells within each plate (Figure 4.1). Plate Z-factors for β -catenin whole cell fluorescence intensity were highly robust, resulting in an average Z-factor of 0.61; indicative of an excellent screening assay [288]. However, plate Z-factors for β -catenin fluorescence nuclear to cytosolic (nuc/cyt) ratio were unfortunately variable, resulting in an average Z-factor of 0.21 for this parameter, which is towards the lower end of a 'workable' screening assay (Figure 4.1). Given the small size and colony-like growth patterns of the HEK293 derived 7df3 reporter cells, accurate segmentation of the cells during image analysis proved challenging, which in turn could have affected the data. However, on further inspection, low Z-factors could be attributed to a failure in one well of four within a control set, which resulted in increased standard deviations. All other positive control wells displayed the expected response, indicating that transfection of the overall plate had not failed. Therefore, whilst potential issues must be noted, the potential for extracting useful information from this dataset was still highly promising.

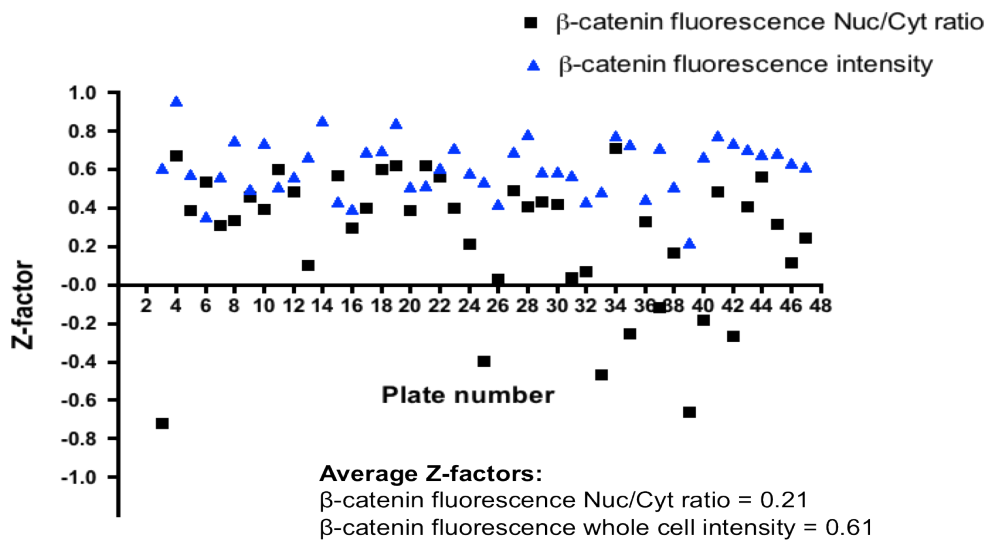


Figure 4.1 Plate Z-factors for the H esiRNA screen

Plate Z-factors for β -catenin Nuclear to Cytosolic (nuc/cyt) Ratio (black squares) and β -catenin whole cell intensity (blue triangles) parameters. Z-factors assess the dynamic range and associated variability between controls on each plate, with Z-factors between 0-0.5 indicative of a workable assay and >0.5 deemed an 'excellent' screening assay. Low or negative Z-factors could be attributed to failed transfection in 1 of 4 positive control wells resulting in greater variability (see text).

4.1.1.2 Z-score analysis of β -catenin stabilisation and localisation data from the H primary screen.

To allow for data integration and to enable all the esiRNAs to be compared to each other, raw data were normalised to remove systematic plate-to-plate variation, thus make the measurements comparable across all plates. Histogram visualisation of the raw screening data for both the β -catenin nuc/cyt ratio parameter as well as β -catenin whole cell (WC) intensities suggested that the data was normally distributed, hence standard statistical measures (such as means and standard deviations) could be used for normalisation and analysis (data not shown).

It was assumed that the majority of esiRNAs would not influence β -catenin levels and localisation, with the average β -catenin nuc/cyt ratios and whole cell intensities across a plate equivalent to the level caused by β -estradiol activation of the Wnt pathway. This is especially valid in libraries such as this where esiRNAs targeting functionally or structurally related genes are not grouped but are randomly distributed across all

plates. Therefore, within the two parameters investigated, each well was normalised to their corresponding plate mean values, excluding control wells, with the samples themselves acting as *de facto* negative controls (so-called “non-controls-based” normalisation [289, 299]). Each esiRNA was therefore expressed as fold over plate means in both β -catenin parameters under investigation, followed by conversion into their equivalent z-scores, which represents the number of standard deviations a sample is from its plate mean (See Chapter 2 for z-score formula). This allows the esiRNAs from across the whole screen to be rank-ordered as it provides clear information on the strength of each esiRNA relative to the distribution to the rest of the plate [289].

Figures 4.2 A and B display the spread of the screen Z-scores for β -catenin nuclear: cytosolic ratio and whole cell intensities respectively. Cell numbers for the most part were relatively stable across the entire screen although, given they were transfected in batches (but within the same experiment using cells from the same passage), some variability was observed across certain plates (Figure 4.2 C). To control for this when assessing for cytotoxic effects, cell numbers were expressed as a percentage of the mean number of cells per well of their corresponding plates. Wells with less than 30% of the average cell number of the plate were considered toxic.

esiRNAs with Z-scores greater than 2 and less than -1.5 in each parameter (coloured red in Figure 4.2) that passed the cell toxicity filter were considered as primary ‘hits’. 432 and 745 esiRNAs resulted in increased and decreased β -catenin nuclear localisation (as denoted by the nuc/cyt ratio) respectively, resulting in a list of 1177 esiRNAs (Table 3 in Appendix B). 453 and 737 esiRNAs resulted in increased and decreased β -catenin whole cell levels respectively, resulting in a list of 1190 esiRNAs (Table 4 in Appendix B). Known Wnt components were enriched in these lists of primary hits, including CTNNB1, AXIN1, DVL2, DKK2, LRP5, SKP1, CUL1, CTNNBIP1, CSNK1A1 and TCF7L1, providing confidence in the validity of the screen’s ability to identify both positive and negative regulators of β -catenin mediated by Wnt signalling. Other notable hits included many proteasomal components, especially in the list of modulators of β -catenin whole cell levels, in addition to those involved in regulating translation, such as multiple elongation initiation factors. Table

4.1 summarises the number of hits extracted that passed the set thresholds, along with examples of known β -catenin regulators identified.

Intriguingly, the overlap between the esiRNAs that modulated β -catenin nuclear localisation and those that modulated β -catenin whole cell levels was small, with only 143 genes present in both data sets (Figure 4.3, Appendix B Table 5), which included known components as indicated in Table 4.1. One could argue that this may be due to poor screen performance with regards to extracting β -catenin fluorescence nuclear to cytosolic ratios as indicated by the lower than expected average Z-factor for this parameter. However, as introduced in Chapter 1, it has become increasingly apparent that stabilisation of β -catenin in the cytoplasm does not always result in its increased nuclear localisation, with the current data supporting this notion.

Having extracted lists of genes that appear to modulate β -catenin levels and nuclear localisation, detailed reconfirmation assays were carried out on a subset of select esiRNAs, which is described later. Furthermore, extensive *in silico* analysis was undertaken on the primary data so that genome-scale observations could be made, although individual genes within the data sets may not be reconfirmed. The screening process and threshold criteria for selecting esiRNAs for further investigation is summarised in Figure 4.4. Results from the *in silico* analysis will be displayed alongside the primary data obtained from both U2OS screens, which will first be presented in the subsequent section.

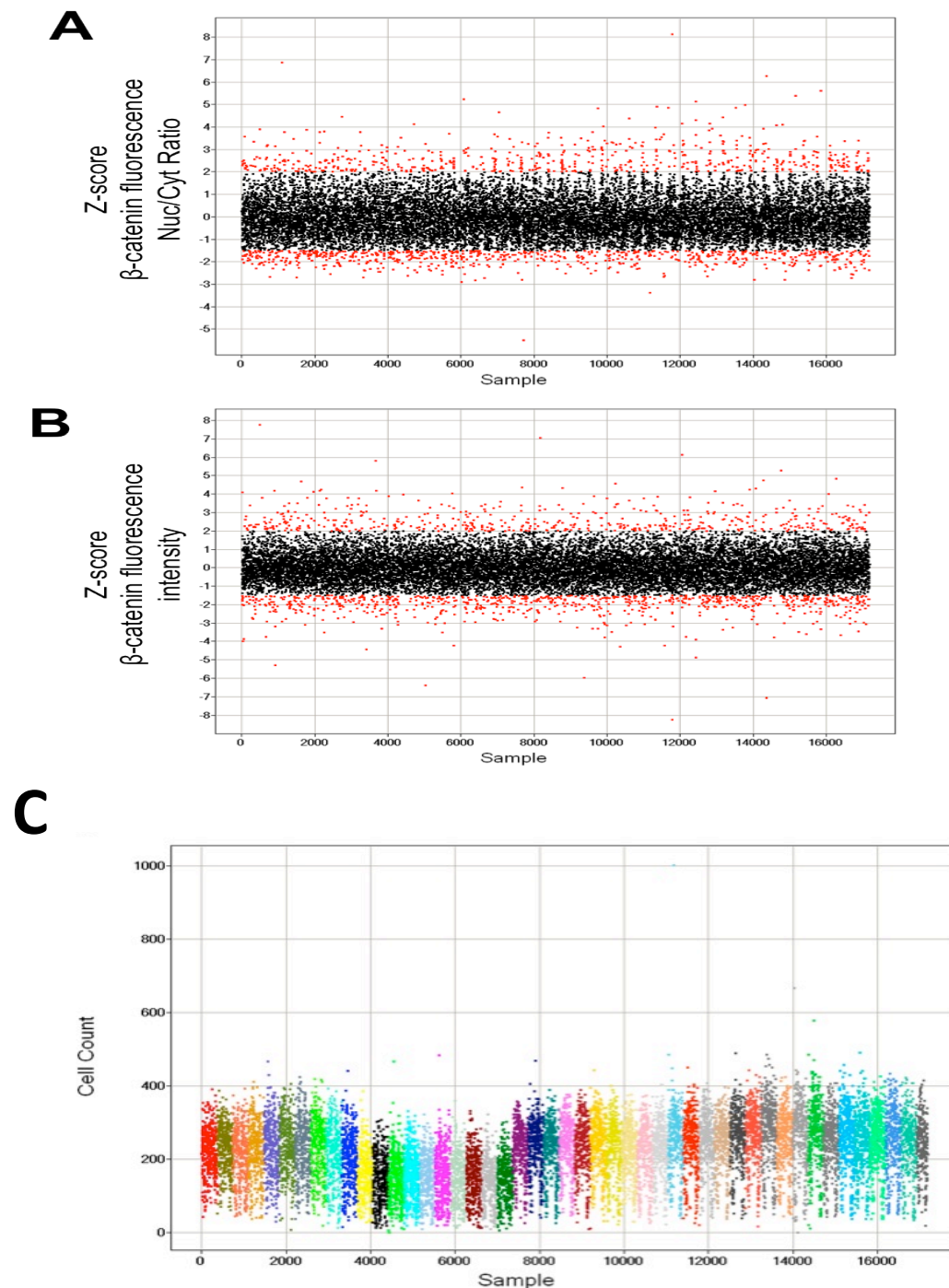
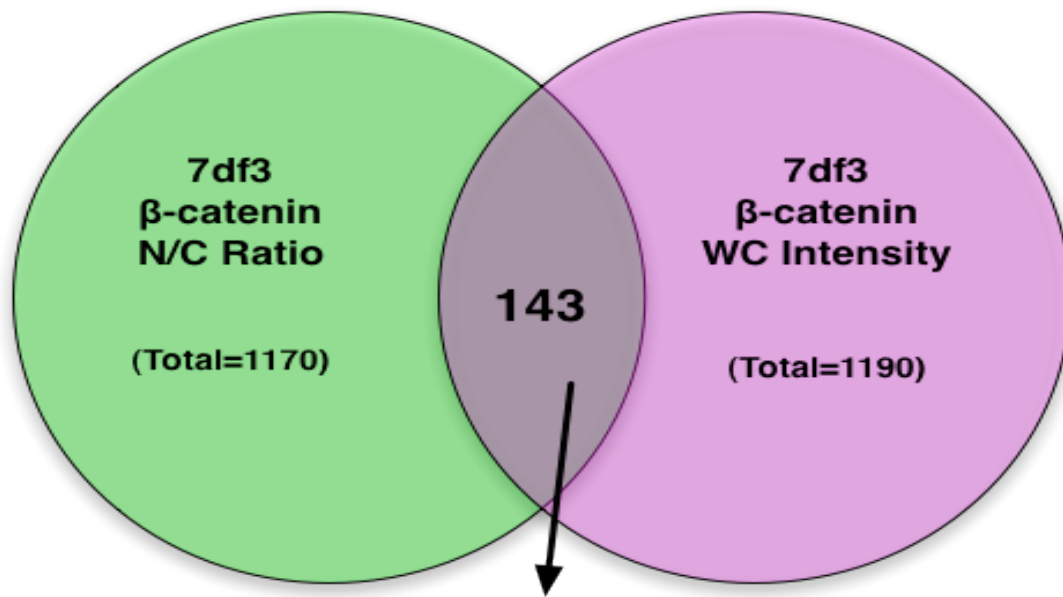


Figure 4.2 Over 1000 esiRNAs appear to affect β -catenin nuclear localisation and accumulation in 7df3 reporter cells

After transfection and subsequent β -catenin immunostaining, cells were imaged and analysed using the IN Cell Analyzer 1000 platform. Raw data from the entire screen were analysed for their respective Z-scores for the parameters β -catenin Nuc/Cyt Ratio (A) and β -catenin whole cell accumulation (B). The graphs indicate the spread of data obtained from the primary screen with each point representing a single esiRNA. A subset of genes of Z-scores greater than 2 and less than -1.5 are coloured red and were considered for further analysis alongside other criteria. (C) Raw cell numbers per well. Each point corresponds to an esiRNA and is colour-coded by plate number with 384 spots per plate. The graphs indicate the spread of cell numbers obtained across each plate and the entire screen.



ADORA2A	FAM120A	NAPA	SAV1	ZBTB24
ANKRD53	FAM125A	NIP30	SCN2B	ZFYVE19
ARHGAP21	FANCA	NKG7	SLC35C1	ZNF271
ATP1B2	FBXO17	NKIRAS1	SLC4A8	ZNF276
BMP2	FLJ39822	ODAM	SMAD3	ZNF335
C16orf44	FPGS	OR52H1	SNRPD2	ZNF552
C17orf45	FXYD6	OR6B3	SOCS6	ZNF83
C1orf35	GAL3ST1	OTC	SPG3A	
C3orf10	GATA6	PCP4	STK38	
C6orf65	GFM1	PFKP	STRN	
C8orf34	HBP1	POP7	TAAR1	
CACNB3	HMGCL	PPP2R5D	TIMM44	
CCDC135	HSPBP1	PSMC3	TMEM135	
CCL18	IBSP	PSMC6	TMEM69	
CCNL1	IFIT1	QTRTD1	TOMM7	
CDH2	KIAA0494	RAB7L1	TP53TG3	
CDK5RAP1	KIAA1727	RAD21	TP73L	
CENPJ	KRTCAP2	RFPL3	TRAPPC2L	
CNOT2	LAD1	RPL15	TSPAN18	
CRY1	LOC390667	RPL18A	TSPAN4	
CTAGE5	LPPR4	RPL23	UBP1	
CTNNB1	LRRC8C	RPL38	UPF1	
CTNNBIP1	LYPLAL1	RPL6	USP18	
CUL1	MAFA	RPL9	USP28	
CUTA	MGC33657	RPLP2	VCP	
DHRS13	MID2	RPS3A		
DKK2	MMP12	RRBP1		
EIF2B5	MMP28			
EIF3S10	MSLN			
	MSR1			

Figure 4.3 Venn diagram of overlapping modulators of β-catenin nuclear localisation and whole cell accumulation from the 7df3 primary screen.

Raw data from the primary screen were analysed for their respective Z-scores for β-catenin nuc/cyt ratios and whole cell (WC) accumulation. Numbers of esiRNAs with z-scores >2 or <-1.5 in each β-catenin parameter that passed toxicity thresholds are indicated, in addition to the degree of overlap between screens. Gene symbols of a subset of the overlapping esiRNAs are indicated, with the full list provided in Appendix B, Table 5.

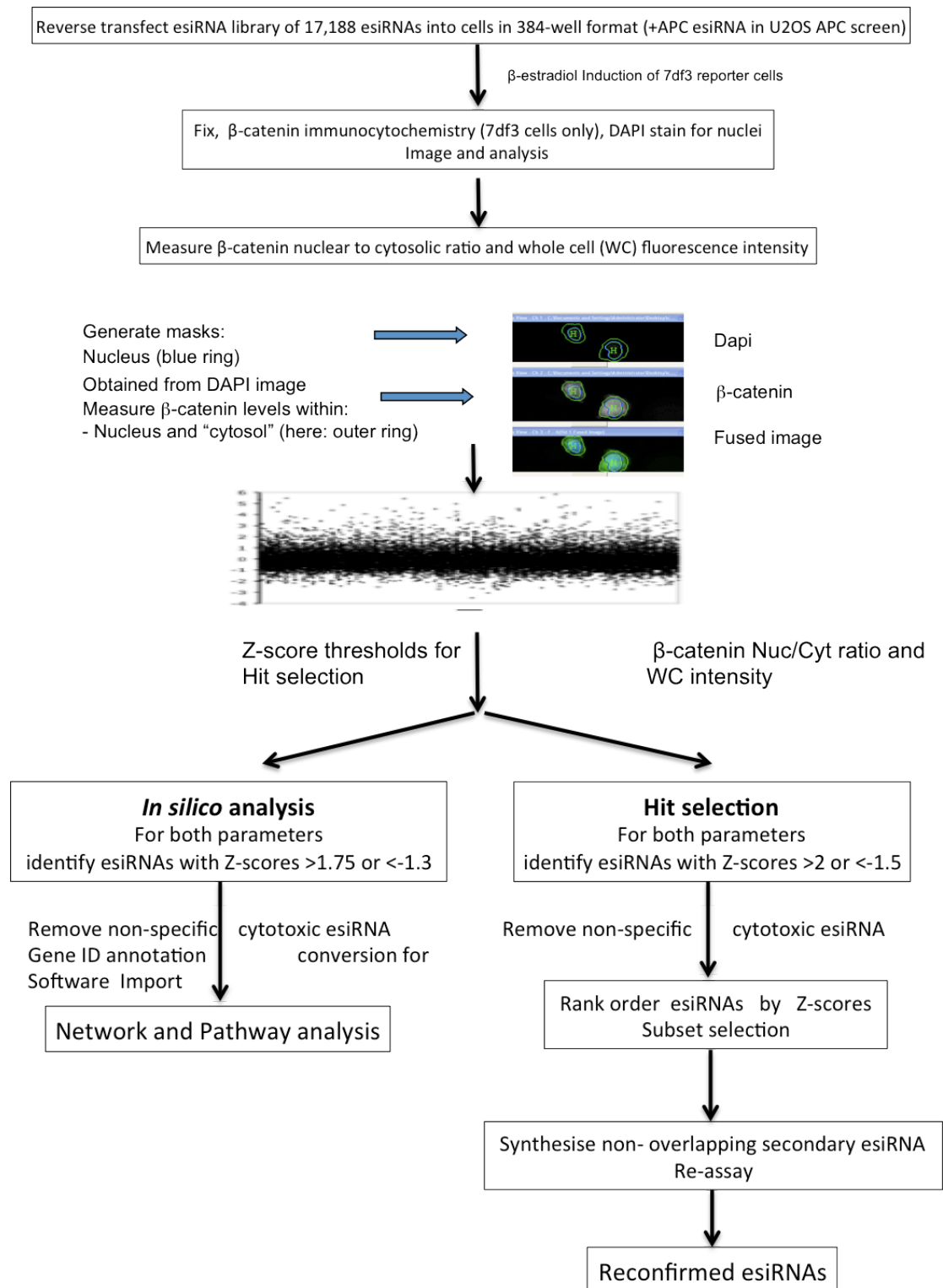


Figure 4.4 Schematic representation of the screening workflow

Screen	For hit selection (Z score > 2 or <-1.5)								For <i>in silico</i> analysis(Z score > 1.75 or <-1.3)					
	β-catenin nuc/cyt ratio				β-catenin WC levels				β-catenin nuc/cyt ratio			β-catenin WC levels		
	↑	↓	Total	Examples	↑	↓	Total	Examples	↑	↓	Total	↑	↓	Total
1. 7df3 Screen	432	745	1177	CTNNB1, CTNNB1IP, DKK2, RYK, WNT2, TCF7L, LEF-1, FBXW11, PYGO2, CUL1	453	737	1190	CTNNB1, CTNNB1IP, DKK2, AXIN1, DVL2	642	1217	1859	688	1140	1828
2. U2OS Screen	543	114	657	CTNNB1, APC, AXIN1, WNT5B, p300, SIAHBP1, RYK, FBXW11	605	73	678	CTNNB1, FBXW11, WNT5B, RBX1, TNK2, TWIST1, WNT2, SIAHBP1, APC, RYK	817	435	1253	846	315	1161
3. U2OS APC Screen	481	597	1078	CTNNB1, APC, P300, RBX1, FBXW11, SKP1, DKK, WNT2/7B	610	136	746	CTNNB1, APC, RBX1, FBXW11, SKP1, WNT2/7B	758	1244	2002	898	540	1438

Table 4.1 Summary of primary screen assays

Numbers of esiRNA's that led to increased (↑) or decreased (↓) β-catenin accumulation (WC levels) and nuclear localisation (nuc/cyt ratio) above set thresholds in the three primary screens are displayed. Thresholds were set at z-scores of >2 and <-1.5 for genes considered for reconfirmation while less stringent cut offs were set at z-scores >1.75 and <-1.5 for selecting genes for *in silico* analysis in addition to passing the cell toxicity filter (set at 30% of plate mean cell numbers). Examples of known β-catenin regulators that passed the stringent thresholds are provided for each parameter. Full lists of ENSEMBL IDs and associated z-scores are provided in Appendix B with table numbers indicated by the associated contents page.

4.1.2 eGFP- β -catenin U2OS primary screens

Two screens were developed in the eGFP- β -catenin U2OS cell line; the first in a background of unstimulated β -catenin, synonymous of inactive Wnt signalling (referred to as the UB screen) with the second undertaken in a backdrop of elevated β -catenin induced by APC downregulation (referred to as the UA screen); a setting synonymous to active Wnt signalling found in certain tumours.

Following the establishment of screening conditions, the library of 17,188 esiRNAs was again employed in this cell line with imaging and analysis undertaken once more using the IN Cell Analyzer 1000 platform to quantify β -catenin whole cell fluorescence intensity and nuclear:cytosolic ratio. All the raw and normalised UB and UA screen data of β -catenin nuclear to cytosolic ratio and whole cell intensities along with cell numbers are provided in Tables 6 and 7 respectively in Appendix B on the disc provided.

4.1.2.1 Z-factor analysis of the U2OS primary screens.

Unless otherwise mentioned, experimental and analysis approaches were identical to the H screen. In the UB screen, the β -catenin nuc/cyt ratio and whole cell intensity parameters possessed good Z-factors, averaging at 0.51 and 0.4 respectively (Figure 4.5A). Similarly, the UA screen possessed excellent Z-factors of 0.57 and 0.52 for β -catenin ratio and whole cell intensity parameters respectively (Figure 4.5 B). Similarly to the H screen, low or even negative Z-factors could be attributed to an error in one specific control well which increased the variability between the 4 control wells that resulted in the lower than expected Z-factors. However, this did not indicate a failure in transfection across the plate as other control wells displayed the expected phenotypes.

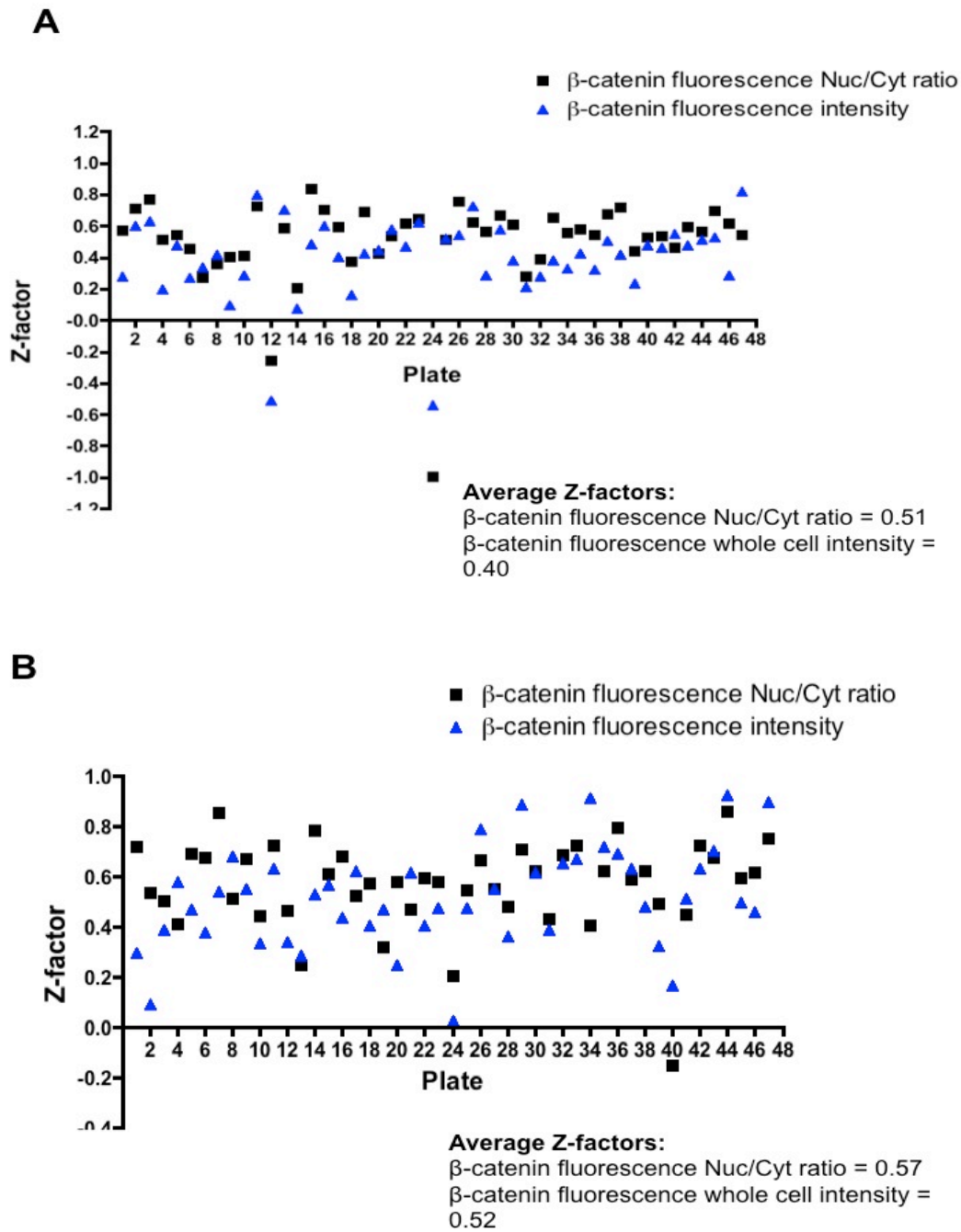


Figure 4.5 Z-factor analysis of eGFP- β -catenin U2OS esiRNA primary screens

Plate Z-factors for β -catenin Nuc/Cyt Ratio (black squares) and β -catenin whole cell intensity (blue triangles) parameters in eGFP- β -catenin U2OS cells transfected with the library only (A – UB screen) and when co-transfected with APC esiRNA (B, UA screen). Z-factors assess the dynamic range and associated variability between controls on each plate with Z-factors between 0-0.5 indicative of a workable assay and >0.5 deemed an ‘excellent’ screening assay.

4.1.2.2 Z-score analysis of β -catenin stabilisation and localisation data from both U2OS primary screens.

Raw data from both screens were normalised and analysed similarly to the H screen. For both β -catenin measurements under investigation, each well was expressed as fold over their corresponding plate mean values (excluding controls), which were then converted into z-scores (number of standard deviations away from plate mean, see chapter 2 for formula) thus enabling the data to be compared across the entire screen as one data set. Figures 4.6 and 4.7 display the spread of the screen Z-scores for β -catenin nuclear to cytosolic ratio and whole cell intensities in the UB and UA screens respectively. Cell numbers were slightly variable across plates (Figures 4.6 C and 4.7 C), especially in the UA screen given they were transfected in batches (but within the same experiment using cells from same passage). As before, to control for this, cell numbers for each esiRNA were expressed as a percentage of the mean number of cells per well of their corresponding plates. Wells with less than 30% of the average cell number of the plate were considered toxic.

esiRNAs with Z-scores greater than 2 and less than -1.5 in each parameter (coloured red in Figures 4.6 and 4.7) that passed the cell toxicity filter were considered as primary 'hits'. In the UB screen, 657 (543 up, 114 down) and 678 (605 up, 73 down) esiRNAs modulated β -catenin nuclear localisation and whole cell levels respectively, with full lists provided in Appendix B, Tables 8 and 9. In the UA screen 1078 (481 up, 597 down) and 746 (610 up, 136 down) esiRNAs modulated β -catenin nuclear localisation and whole cell levels respectively, with full lists provided in Appendix B, Tables 10 and 11. Table 4.1 summarises the number of hits extracted that passed the set thresholds for both β -catenin parameters in the two U2OS screens. Known Wnt components were enriched in the datasets from both U2OS screens, including AXIN1, APC, CTNNB1, WNT7A, WNT2, WNT5B, FBXW11, CTBP1, RBX1, DKK, and SKP1 (Appendix B, Tables 8-11) therefore giving credibility to both screens in terms of their abilities to identify both positive and negative regulators of β -catenin mediated by Wnt signalling. As expected, proteasomal components were also picked up in addition to several RhoGTPases and components involved in focal adhesion,

such as ITGA5, ITGB8, TLN1/2, RHOA, CDC42, RAC1, RAP1GAP and RAP2A (Appendix B, Tables 8-11).

In both U2OS screens the degree of overlaps between regulators of β -catenin nuclear localisation and β -catenin levels, whilst still relatively low, were far more significant compared to that observed in the H screen, with over 300 genes overlapping between the sets in both primary screens (Figure 4.8). Selected components known to regulate β -catenin are indicated with full lists of overlapping esiRNAs provided in Appendix B, Tables 12 and 13.

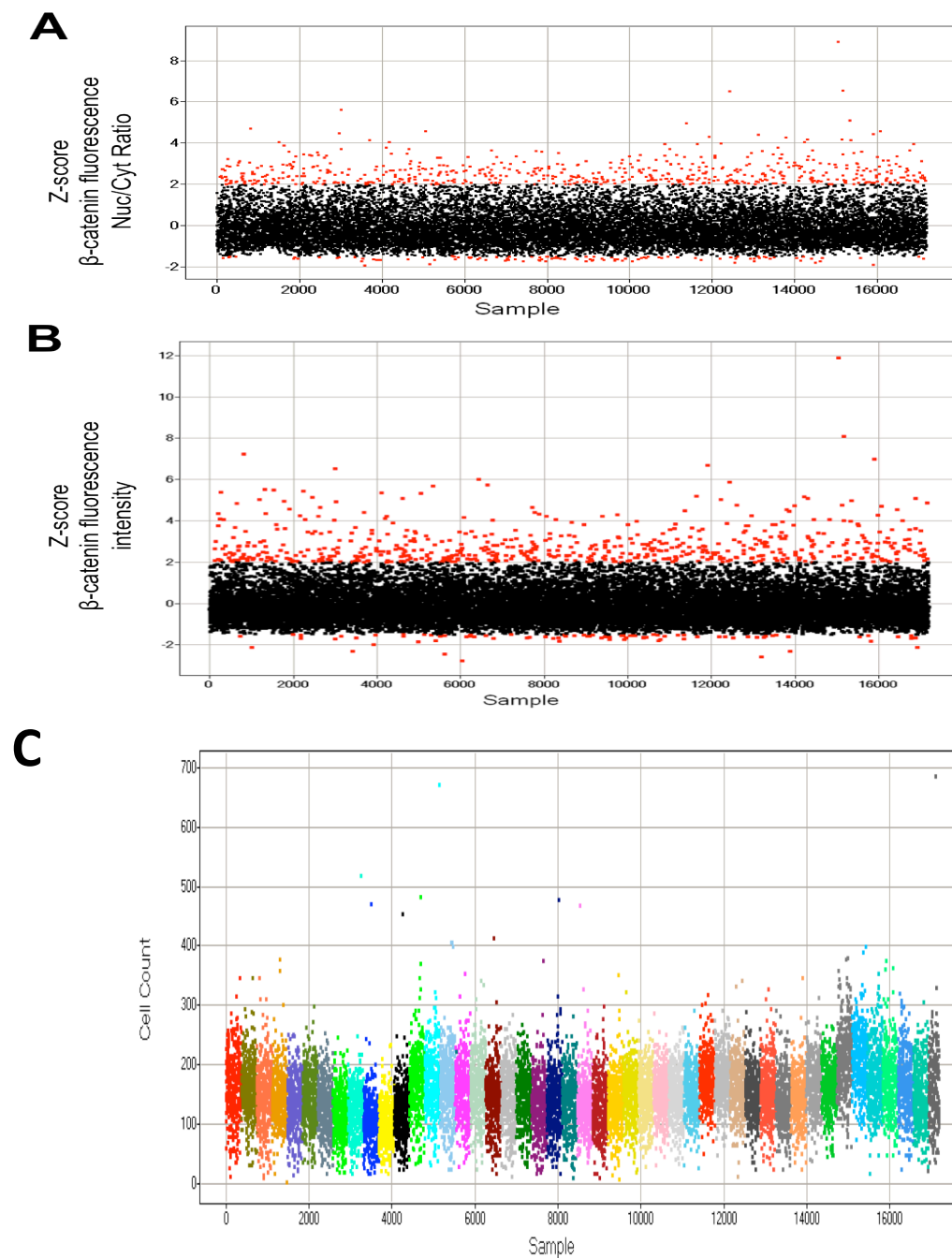


Figure 4.6 Over 600 esiRNAs appear to affect β -catenin nuclear localisation and accumulation in the UB screen.

After transfection and subsequent fixation and DAPI staining, cells were imaged and eGFP- β -catenin intensity in both nucleus and cytoplasmic compartments quantified. Raw data from the entire screen were analysed for their respective Z-scores for the parameters β -catenin Nuc/Cyt Ratio (A) and β -catenin whole cell accumulation (B). The graphs indicate the spread of data obtained from the primary screen with each point representing a single esiRNA. A subset of genes of Z-scores greater than 2 and less than -1.5 are coloured red and were considered for further analysis alongside other criteria. (C) Raw cell numbers per well - each point corresponds to an esiRNA (17,188) and is colour-coded by plate number with 384 spots per plate. The graphs indicate the spread of cell numbers obtained across each plate and the entire screen in the UB screen.

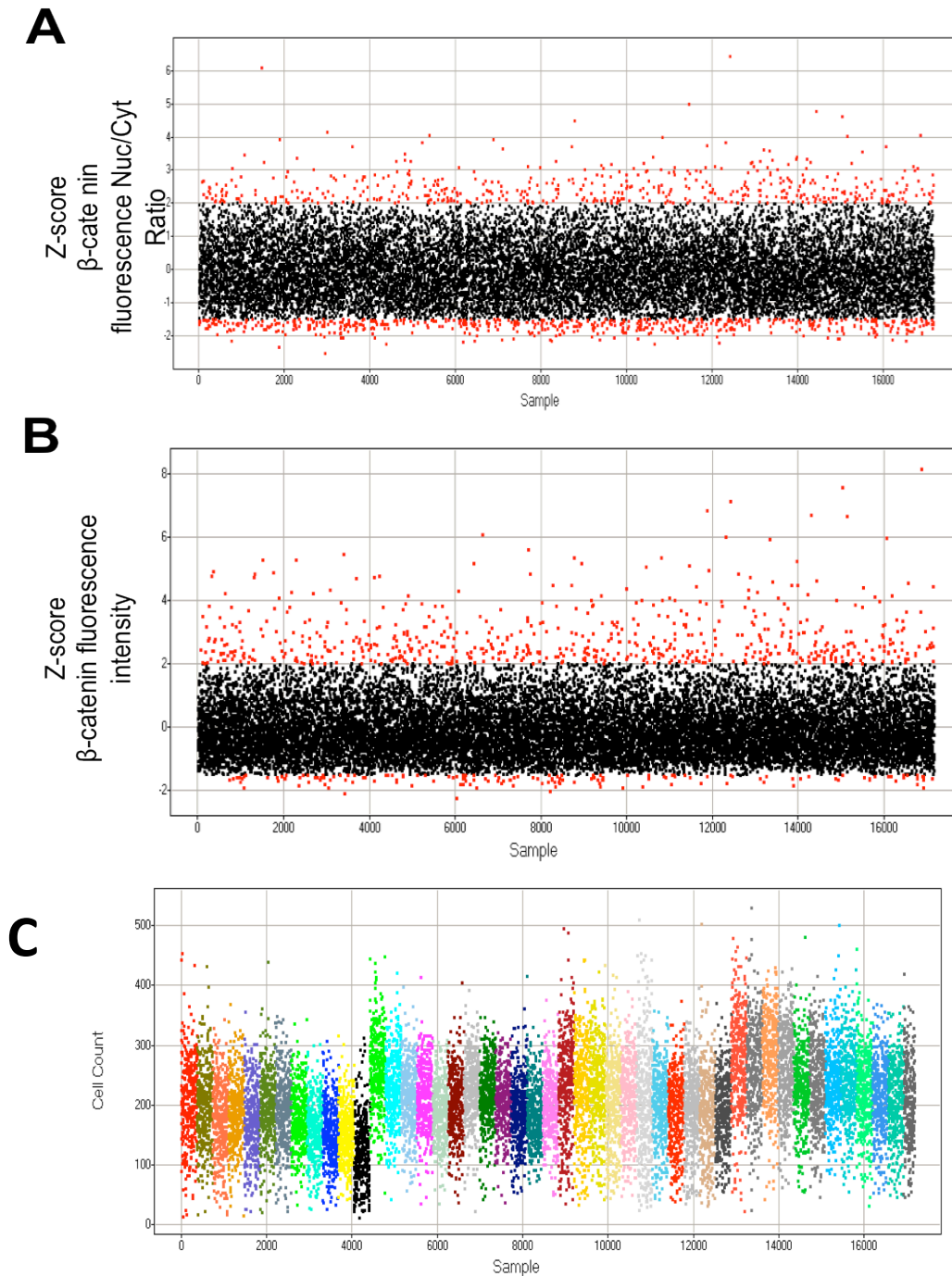


Figure 4.7 Over 10000 esiRNAs appear to affect β -catenin nuclear localisation and accumulation in the UA screen

After co-transfection of the esiRNA library and APC esiRNA, subsequent fixation and DAPI staining, cells were imaged with eGFP- β -catenin intensity in both nucleus and cytoplasmic compartments quantified. Raw data from the entire screen were analysed for their respective Z-scores for the parameters β -catenin Nuc/Cyt Ratio (A) and β -catenin whole cell accumulation (B). The graphs indicate the spread of data obtained from the primary screen with each point representing a single esiRNA. A subset of genes of Z-scores greater than 2 and less than -1.5 are coloured red and were considered for further analysis alongside other criteria. (C) Raw cell numbers per well - each point corresponds to an esiRNA (17,188) and is colour-coded by plate number with 384 spots per plate. The graphs indicate the spread of cell numbers obtained across each plate and the entire screen in the UA screen.

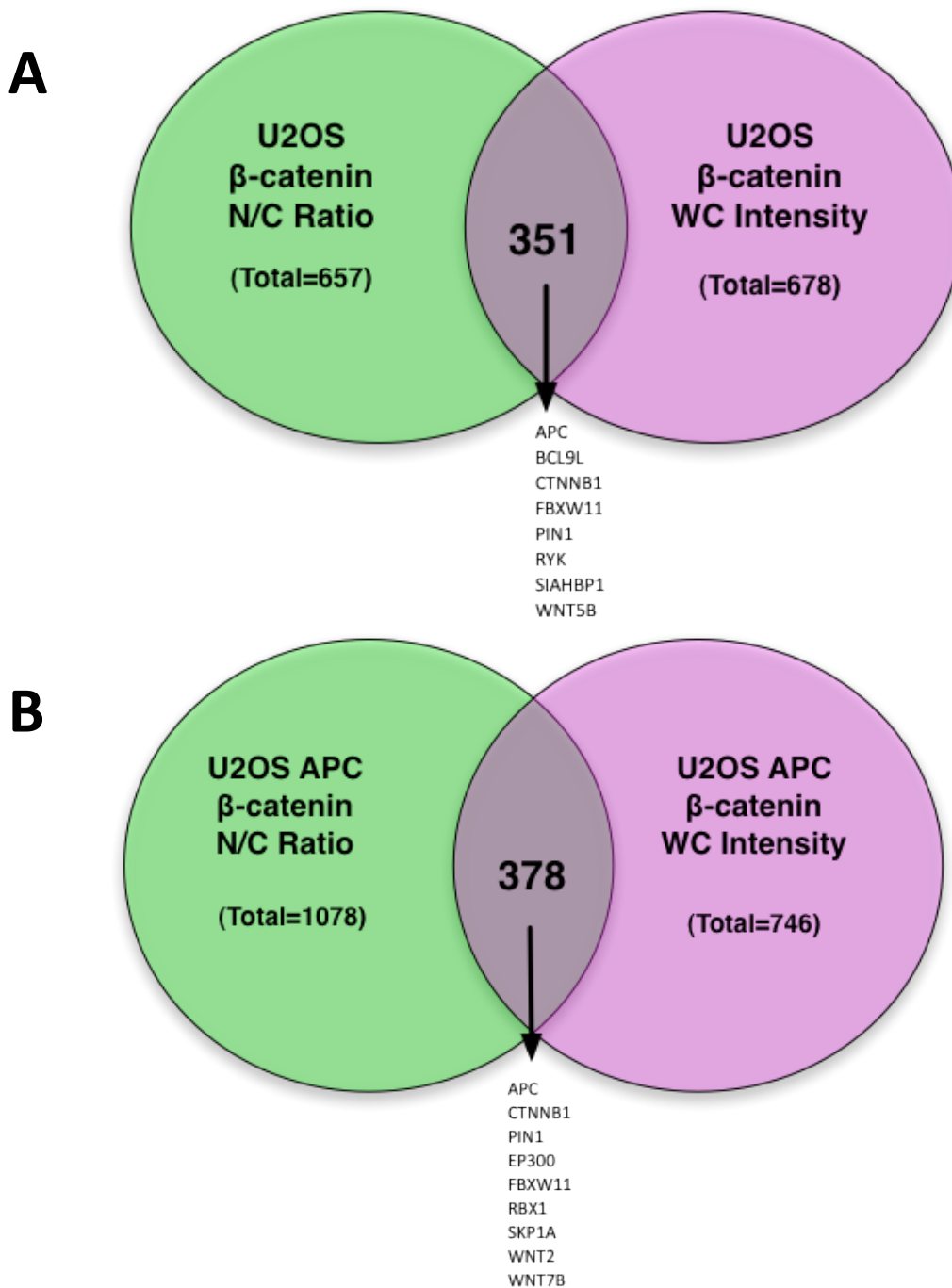


Figure 4.8 Venn diagrams of overlapping modulators of β -catenin nuclear localisation and whole cell accumulation from the U2OS primary screens.

Raw data from the UB (A) and UA (B) screens were analysed for their respective Z-scores for β -catenin nuc/cyt ratios and whole cell (WC) accumulation. Numbers of esiRNAs with z-scores >2 or <-1.5 in each screen that passed toxicity thresholds are indicated, in addition to the degree of overlap between the β -catenin parameters. Gene symbols of a subset of the overlapping esiRNAs are indicated, full lists are provided in Appendix B Tables 12 and 13 for (A) and (B) respectively.

4.2 In silico analysis of the esiRNA regulators identified in the primary screens

While RNAi-based screens can identify new components that functionally contribute to the phenotype under investigation, they are unable to establish physical relationships between identified ‘hits’ and hence provide little mechanistic insights [242]. Data integration from various sources in addition to taking a global analysis of the data in the context of pathways and networks can be particularly useful in understanding how genes work together in different contexts, as well as highlighting un-anticipated processes within a system [242, 262, 300]. For instance, by investigating whether pathways, processes or functionally related groups of genes are enriched in the primary screening data, the process of elucidating and extracting biological meaning to the dataset can be vastly improved [300, 301]. A vast majority of genes are annotated with a Gene Ontology (GO) identifier that represents information on three ontologies or ‘terms’; namely biological process, cellular component and molecular function. Genes are annotated to the most detailed GO term possible but can be associated with broader ‘GOSlim’ terms (such as transport, signal transduction etc) to provide a higher-level view of the ontologies. Additionally, KEGG (Kyoto Encyclopaedia of Gene and Genomes) is a collection of manually curated pathway maps that represent up to date knowledge on the molecular interaction and reaction networks for various processes [302].

The esiRNAs identified in the aforementioned screens as potential modulators of both β -catenin levels and nuclear localisation were subject to analysis for over-representation of features such as cellular localisation, biological processes and pathways in Genecodis, an open source online program (<http://genecodis.dacya.ucm.es/>) [301]. A similar program, MetaCore [303], was also used, but to a limited degree due to licence requirements. This integrated knowledge database for pathway and network analysis is based on a proprietary, manually curated database of human protein-protein, protein-DNA and protein compound interactions, metabolic and signalling pathway. A slightly less stringent list was used for this purpose, whereby esiRNAs with Z-scores >1.75 and <-1.3 , which passed the toxicity filter, were selected to try and capture esiRNAs that may have weaker, but

still significant, effects on β -catenin levels and nuclear localisation, in order to provide a better global picture of the processes involved in its regulation. The numbers of esiRNAs extracted in each list is provided in Table 4.1 with these extended subset lists provided in Tables 14-19, Appendix B. Converting ENSEMBL IDs to gene symbols for *in silico* analysis resulted in slightly smaller lists than indicated in Table 4.1 due to the gene ID conversion software failing to associate a gene symbol for every single ENSEMBL ID.

Firstly, a brief overview of the results obtained from each of the three screens will be presented individually in their associated screen specific sections. Subsequently, a summary of the over-represented processes and pathways common to more than one screen is provided at the end of this particular section.

4.2.1 Enrichment analysis of the 7df3 (H) primary screen

Analysis of the primary esiRNA datasets identified in the H screen (Tables 14 and 15, Appendix B) revealed that the majority of the putative regulators of both β -catenin accumulation and nuclear translocation are localised to the cytoplasm, with the remainder mainly split between localisation at the plasma membrane and nucleus (Figure 4.9). Both datasets were also analysed for enrichment in their occurrence in GeneGo pathway maps in Metacore (GeneGo's equivalent to KEGG). Within both datasets, pathways that were significantly over-represented included Wnt and TGF signalling, especially with regards to their role in cytoskeletal remodelling (Tables 4.2 and 4.3). The TGF- β components that modulated β -catenin included BMP2/4, TGF β 1 and SMAD 3, with this pathway possessing extensive links to Wnt/ β -catenin signalling, which will be discussed further in the summary subsection of this part of the chapter [304, 305].

Notable differences between the data sets are the enrichment of genes involved in cell adhesion and E-cadherin signalling within the esiRNAs that modulated β -catenin nuclear localisation (Table 4.2) compared to the over-representation of regulators of β -catenin accumulation in cell cycle pathways (Table 4.3). These included CKS,

CDKN1A, CDKN1B, CDKN3, CDC6, CINP, CDC5L and CCND3. CDKN3 is an inhibitor of CDK2, which, along with CDK6, has been shown to phosphorylate β -catenin, leading to its degradation [227, 231]. This may in turn explain the modulation of β -catenin levels upon CDKN3 knockdown. As a regulator of cell cycle progression at G1, CDKN1A (p21) inhibits the activity of cyclin D-CDK2/4 complexes and is reported to be a Wnt target gene [306]. Its identification as a potential regulator of β -catenin accumulation is intriguing as it may imply the existence of an alternative feedback mechanism in certain contexts.

Direct links between Wnt signalling and the cell cycle are emerging, with the mitotic CDK14/cyclin Y complex recently demonstrated to promote Wnt signalling through phosphorylation of the LRP6 co-receptor [307, 308]. Additionally, β -catenin has also been demonstrated to possess a non-transcriptional function in mitosis as an important component of centrosomes, where, as a Nek2 substrate, it is essential for centrosomal separation at the onset of spindle formation [217]. Interestingly, centromere proteins such as CENPH, CENPJ and CEP63 were among the genes identified as regulating β -catenin accumulation and may function to localise β -catenin to centrosomes for example. Additional experiments, such as further microscopic analysis at higher resolutions than undertaken in the current study, could be used to assess β -catenin's distribution to subcellular structures, such as centromeres, upon knockdown of the components identified in this screen.

Adhesion processes were highly over-represented within the modulators of β -catenin levels and localisation identified in the H screen. Many reports describe links between cell adhesion and Wnt signalling, with β -catenin's crucial function in adherens junctions delicately balanced with its transcriptional role [158, 309]. This is highlighted by the enrichment of both E-cadherin and Wnt signalling regulators associated with gastric cancer within the esiRNAs that modulated β -catenin nuclear localisation, in addition to genes that regulate gastric cell motility upon *H.pylori* infection (Table 4.2) [310, 311]. A link between *H.pylori* -induced activation of β -catenin via inhibition of GSK3- β [312] or phosphorylated LRP6 and Dvl [313] has been described, with this particular screen dataset potentially able to provide further insight into this process. The role of adhesion and cytoskeletal modulators in β -

catenin regulators will be broached again in the summary section of 4.2, in addition to Chapter 6.

Within the esiRNAs that modulated β -catenin nuclear localisation there was an over-representation of genes involved in proteolysis, specifically ubiquitin-proteasomal proteolysis, in addition to Wnt signalling and cell adhesion processes (Table 4.4). The esiRNAs that regulated β -catenin accumulation however were enriched in mRNA processing and translational processes (Table 4.5), implying an unanticipated level of regulation at β -catenin synthesis. These included a plethora of ribosomal components, EIF4A1/G3/B5, EXOSC4/C8, HNRNPA1, MAGOH, DCPS, SNRPB, XPO1, SNRPD2/3 and UPF1. This interesting result will be addressed in further detail in the summary of this particular section (4.2.3).

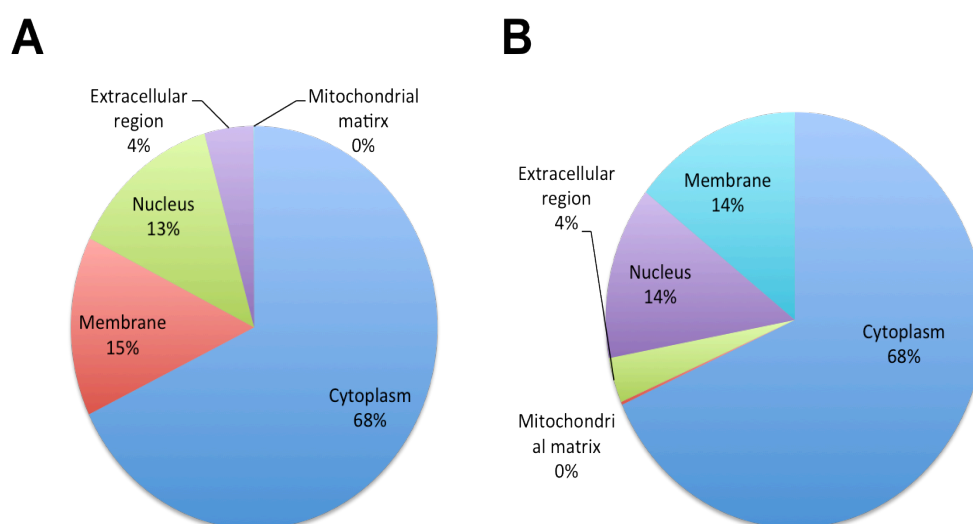


Figure 4.9 The majority of the identified genes in the primary H screen are localised to the cytoplasm.

The datasets were analysed for enrichment in cellular compartments by their GeneGO annotations in Metacore, with modulators of β -catenin localisation (defined by their effect on β -catenin Nuc/Cyt ratio) and β -catenin accumulation (defined by β -catenin whole cell fluorescence intensity) represented in (A) and (B) respectively. Of the genes linked to cellular compartments that were over-represented, 68% reside in the cytoplasm, which was similar across both data sets.

GeneGo Pathway Maps	min(pValue)
Cytoskeleton remodeling_TGF, WNT and cytoskeletal remodelling	2.19168E-06
Effect of H. pylori infection on gastric epithelial cells motility	5.92672E-06
E-cadherin signalling and its regulation in gastric cancer	7.07663E-06
Cell adhesion_Cadherin-mediated cell adhesion	2.62274E-05
WNT signalling in gastric cancer	5.153E-05
Cell cycle progression in Prostate Cancer	0.000101432
LKB1 signalling pathway in lung cancer cells	0.00015336
Cell adhesion_Endothelial cell contacts by junctional mechanisms	0.000216736
Immune response_IL-7 signalling in B lymphocytes	0.00022578

Table 4.2 Wnt pathway genes are significantly enriched within the dataset of esiRNAs that modulated β -catenin nuclear localisation in the H screen.

The dataset of esiRNA regulators of β -catenin nucleus:cytoplasmic ratio was analysed for enrichment in their occurrence in GeneGo pathway maps in Metacore. Pathways that were significantly over-represented included Wnt, TGF and adhesion. Min(pValue); Hypergeometric pValue.

GeneGo Pathway Maps	min(pValue)
Development_WNT signalling pathway. Part 1. Degradation of beta-catenin in the absence WNT signalling	2.11757E-07
Cytoskeleton remodeling_TGF, WNT and cytoskeletal remodelling	6.8437E-06
Cytoskeleton remodeling_Cytoskeleton remodelling	7.67822E-06
Signal transduction_AKT signalling	1.24455E-05
DNA damage_Brca1 as a transcription regulator	1.9182E-05
Cell cycle_Regulation of G1/S transition (part 1)	2.37034E-05
Transport_RAN regulation pathway	2.47221E-05
Cell cycle_Role of Nek in cell cycle regulation	3.41226E-05
Cell cycle_Start of DNA replication in early S phase	3.41226E-05

Table 4.3 Wnt pathway genes are significantly enriched within the dataset of esiRNAs that modulated β -catenin accumulation in the H screen.

The dataset of esiRNA regulators of β -catenin whole cell intensity was analysed for enrichment in their occurrence in GeneGo pathway maps in Metacore. Pathways that were significantly over-represented included Wnt, TGF and cell cycle. Min(pValue); Hypergeometric pValue.

GeneGO Biological Processes	min(pValue)
Proteolysis_Ubiquitin-proteasomal proteolysis	5.14875E-05
Signal transduction_WNT signalling	0.000411066
Cell adhesion_Synaptic contact	0.000813642
Cytoskeleton_Actin filaments	0.001690293
Immune response_Phagosome in antigen presentation	0.003651981
Cell adhesion_Cell junctions	0.004146235
Cell adhesion_Cadherins	0.004701852
Cardiac development_BMP_TGF_beta_signaling	0.005531568
Apoptosis_Apoptotic nucleus	0.006385719
Signal transduction_NOTCH signalling	0.006764402

Table 4.4 A large proportion of the esiRNA dataset that modulated β -catenin nuclear localisation in the H screen are associated with Ubiquitin-proteasomal proteolysis and Wnt signalling

esiRNAs were analysed for enrichment in biological processes in Metacore. Processes that were significantly over-represented included proteolysis, signal transduction and cell adhesion. Min(pValue); Hypergeometric pValue.

GeneGo Biological Processes	min(pValue)
Translation_Translation initiation	2.0585E-09
Cell cycle_G1-S	0.000359049
Cell cycle_Mitosis	0.000397643
Transcription_mRNA processing	0.000581988
Translation_Elongation-Termination	0.00150008
Cytoskeleton_Intermediate filaments	0.001545727
Cell adhesion_Platelet aggregation	0.002265429
Cell adhesion_Synaptic contact	0.002710427
Cell cycle_S phase	0.004038802
Cell adhesion_Integrin-mediated cell-matrix adhesion	0.004248542

Table 4.5 A large proportion of the esiRNA dataset that modulated β -catenin accumulation in the H screen are associated with mRNA processing and translation processes.

esiRNAs were analysed for enrichment in biological processes in Metacore. Processes that were significantly over-represented included translation, mRNA processes and cell adhesion. Min(pValue); Hypergeometric pValue.

4.2.2 Enrichment Analysis of the U2OS primary (UA and UB) screens

Analysis of the primary esiRNA U2OS datasets (Tables 16 - 19, Appendix B) revealed that the majority of the putative regulators of both β -catenin accumulation and nuclear translocation in both U2OS screens were similar to the 7df3 screen, with two thirds also localised to the cytoplasm. Other regulators were mainly split between localisation at the plasma membrane and nucleus (Figure 4.10)

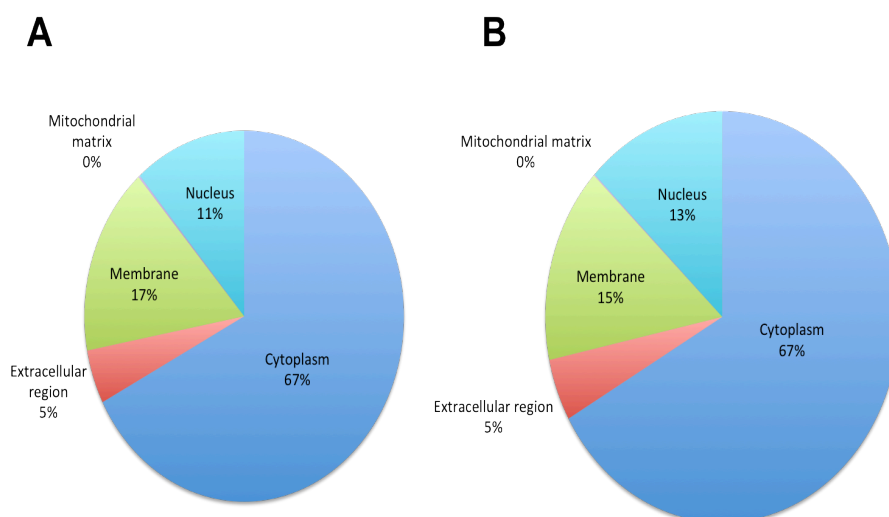


Figure 4.10 The majority of the identified genes in the primary U2OS screens are localised to the cytoplasm.

The datasets identified from the UB screen were analysed for enrichment in cellular compartments by their GO annotations in Metacore, with modulators of β -catenin localisation and β -catenin accumulation represented in (A) and (B) respectively. Of the genes linked to cellular compartments that were over-represented, 68% reside in the cytoplasm, which were similar across both data sets. Data sets from the UA screen resulted in near identical cellular component enrichment and are hence not shown.

Both U2OS screen datasets were also analysed in Genecodis for over-representation of KEGG terms to identify enrichment of specific pathways within the modulators of β -catenin accumulation and localisation. Furthermore, using their GOSlim annotations these datasets were also analysed for the enrichment of specific biological processes.

4.2.2.1 U2OS UB screen enrichment analysis

In the UB screen, pathways that were significantly over-represented in the datasets of regulators of β -catenin localisation and accumulation included Wnt, endocytosis and adhesion (Figures 4.11 and 4.12). Notch and TGF- β signalling were also over-represented in the modulators of β -catenin accumulation (Appendix B, Table 21). Crosstalk between signalling pathways will be assessed further in the summary of this section of the data analysis.

Interestingly, calcium signalling was over-represented in the esiRNAs that modulated β -catenin nuclear localisation, with components such as CAMK2A, PLCD3, PLCB4, PRKCA, ATP2A1, PDE1A and PRKCG identified (Figure 4.11). Calcium has been widely implicated as an important second messenger in non-canonical, β -catenin-independent signalling [314] with the identification of key components of the Wnt/calcium signalling components in this screen, such as CAMK2A and PKC isoforms, interesting as it hints at a potential regulatory mechanism for non-canonical Wnt signalling in β -catenin localisation. Studies have demonstrated that antagonism exists between the β -catenin-independent and β -dependent Wnt pathways, such as through the activation of nuclear factor of activated T cells (NF-AT) for example, which was demonstrated to play an essential role in mediating ventral signals in the *Xenopus* embryo through downregulating β -catenin signalling [35].

The enrichment in components of endocytosis in modulators of both β -catenin localisation and levels (Figures 4.11 and 4.12) in addition to over-representation in transport/vesicle-mediated transport processes (Tables 4.6 and 4.7) is also particularly relevant due to the role of Wnt-induced internalisation of LRP6 in regulating Wnt/ β -catenin signalling [81, 315-317]. However, the precise trafficking pathway that drives this process and how it regulates Wnt signalling is unclear, with conflicting reports regarding the role of both caveolin and clathrin-dependent endocytic pathways in activating and/or attenuating Wnt/ β -catenin signalling [82, 316]. Caveolin-1 was identified as possessing a repressive role in β -catenin stabilisation and nuclear localisation, suggesting that, in the U2OS cells at least, caveolin-mediated endocytic pathways may predominate to attenuate active signalling, contradictory to previous

reports where Wnt induced LRP6 internalisation activates the pathway [81, 318]. However, the observations in this screen are in line with a report where siRNA against caveolin-1 in EGFR over-expressing tumours resulted in increased Wnt/ β -catenin signalling, which was hypothesised to be due to decreased expression of E-cadherin following caveolin-1 depletion [317].

Comparisons of over-represented GOSlim annotations with both β -catenin nuc/cyt ratio and WC levels data sets revealed a high degree of similarity between the two, with signal transduction, cell differentiation, cell adhesion and transmembrane transport processes enriched within the modulators of β -catenin nuclear localisation and accumulation (Tables 4.6 and 4.7). Given the higher degree of overlap between these datasets compared to that observed in the H screen this is not entirely unexpected. Upon further investigation, the over-representation in transmembrane transport processes were mainly due to the identification of a surprising number of solute carrier proteins as potential regulators of β -catenin levels and localisation (Appendix B, Tables 16 and 17). While not identified in this screen, the solute carrier SLC9A3R1 (EBP50 - solute carrier family 9 (sodium/hydrogen exchanger), member 3 regulator 1) has been demonstrated to bind β -catenin in hepatocellular carcinoma cell lines and promote β -catenin-mediated TCF-transcription, but only in cells where β -catenin was already stabilised [319]. Otherwise, the role of solute carriers in β -catenin regulation is unprecedented, suggesting potential new avenues for investigation. Processes involved with mRNA processing and translation were also over-represented within the gene lists and will be discussed further in the summary of this section of the chapter (Table 4.6).

Over-representation of cell differentiation processes was observed with the identification of components from a wide range of pathways such as BMP1, FRK, NOTCH2, EFNB2, YIPF3, CTBP 1 and CTBP 2. CTBP has been demonstrated to both repress and activate Wingless nuclear targets in differing contexts in *Drosophila* [320, 321] in addition to acting as a transcriptional co-repressor in *Xenopus* [322]. How CTBP may regulate β -catenin levels rather than its transcriptional activity is unclear although it is likely to be linked to its interaction with APC, which acts as an adaptor between β -catenin and CTBP [323]. Following APC loss, CTBP1 has been

suggested to result in failed intestinal differentiation, which was demonstrated to occur in elevated cytosolic β -catenin but in the absence of detectable nuclear β -catenin [197], suggesting that it's levels may play a key role in this effect.

Number of genes per concurrent annotations

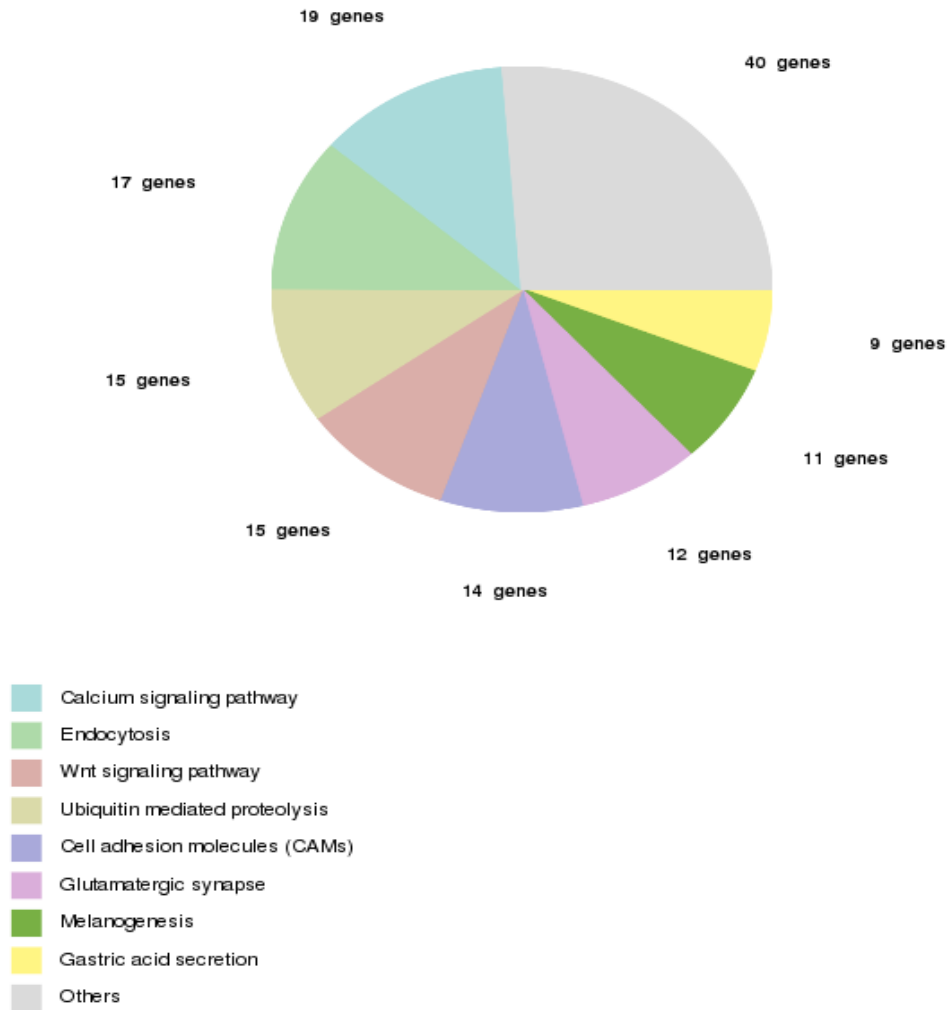


Figure 4.11 Calcium, ubiquitin and Wnt signalling pathway links were enriched within the set of esiRNAs that regulate β -catenin nuclear localisation in the UB screen.

The UB dataset that regulated β -catenin Nuc/Cyt ratio was analysed for enrichment in their occurrence in KEGG pathways using GeneCodis. The signalling pathways that were over-represented included calcium, Wnt, ubiquitin and adhesion, which had more members in the gene set than would be expected if a random set of genes were analysed. Genes not represented in the above chart were either not associated with a KEGG signalling pathway enriched relative to the genome, or had no signalling information associated with them. Associated hypergeometric p-values are provided in Appendix B, Table 20.

Number of genes per concurrent annotations

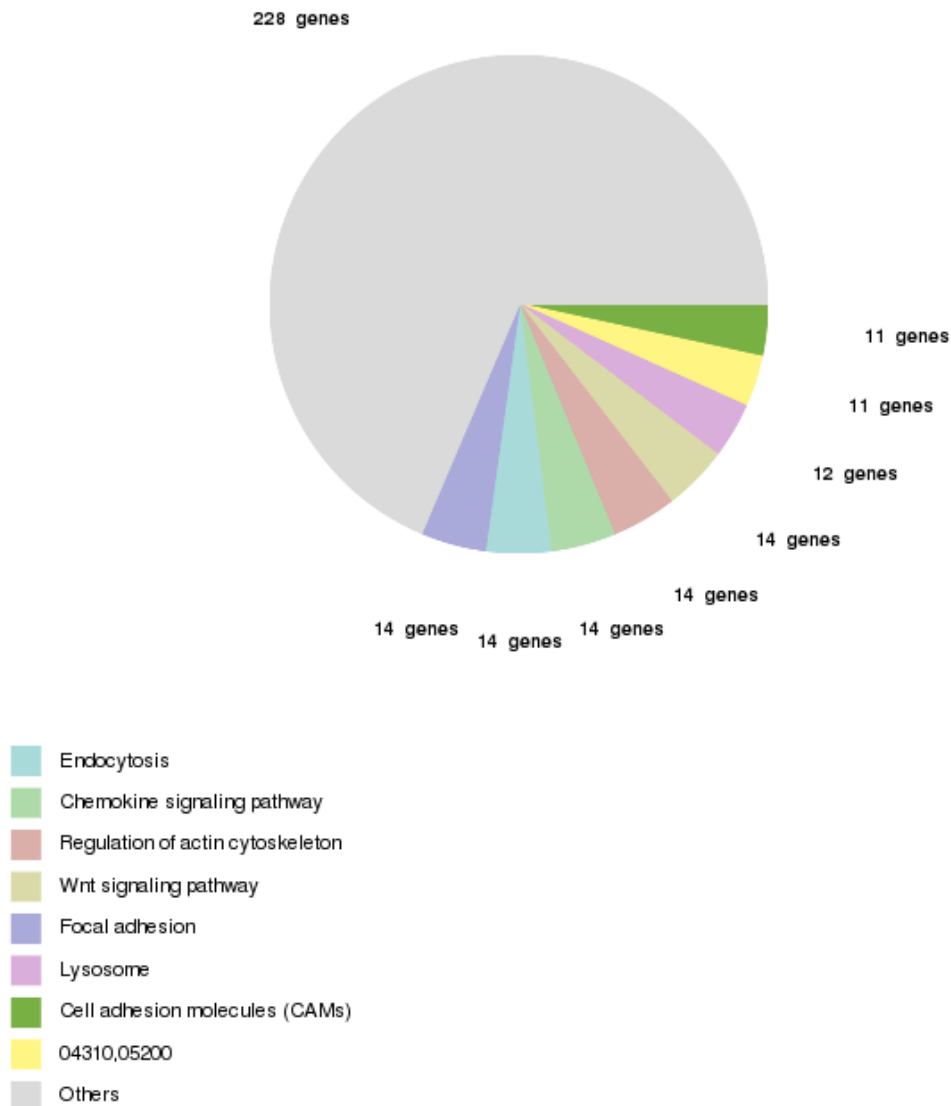


Figure 4.12 Chemokine, Wnt and adhesion/cell junction signalling pathways were enriched within the set of esiRNAs that regulate β -catenin accumulation in the UB screen.

The UB dataset that regulated β -catenin whole cell intensity was analysed for enrichment in their occurrence in KEGG pathways using Genecodis. The signalling pathways that were over-represented included chemokine, endocytosis and adhesion, which had more members in the gene set than would be expected if a random set of genes were analysed. Genes not represented in the above chart were either not associated with a KEGG signalling pathway enriched relative to the genome, or had no signalling information associated with them. Other notable pathways included Notch and TGF- β signalling. Further details and associated hypergeometric p-values are provided in Appendix B, Table 21

GOSlim annotation	min(pValue)
GO:0007165 :signal transduction (BP)	2.23E-06
GO:0030154 :cell differentiation (BP)	0.000137282
GO:0055085 :transmembrane transport (BP)	0.000185603
GO:0034641 :cellular nitrogen compound metabolic process (BP)	0.000279473
GO:0006412 :translation (BP)	0.00031567
GO:0007155 :cell adhesion (BP)	0.00124951
GO:0006810 :transport (BP)	0.001743
GO:0008219 :cell death (BP)	0.0017768
GO:0006461 :protein complex assembly (BP)	0.0055096
GO:0005975 :carbohydrate metabolic process (BP)	0.00918942
GO:0043473 :pigmentation (BP)	0.010202
GO:0016192 :vesicle-mediated transport (BP)	0.0110467
GO:0000902 :cell morphogenesis (BP)	0.0115096
GO:0006397 :mRNA processing (BP)	0.0129178

Table 4.6 A large proportion of the esiRNA dataset that modulated β -catenin nuclear localisation in the UB screen are associated with signal transduction processes and transport.

The UB screen dataset that regulated β -catenin Nuc/Cyt ratio was analysed for enrichment in biological processes using their GOSlim annotations in GeneCodis. Processes that were significantly over-represented within the gene set included translation, mRNA processes and cell adhesion. Min(pValue); Hypergeometric pValue.

Goslim annotations	min(pValue)
GO:0030154 :cell differentiation (BP)	2.49E-07
GO:0055085 :transmembrane transport (BP)	5.76E-06
GO:0007165 :signal transduction (BP)	6.88E-05
GO:0034641 :cellular nitrogen compound metabolic process (BP)	0.000299302
GO:0006412 :translation (BP)	0.00180798
GO:0007267 :cell-cell signalling (BP)	0.00258789
GO:0007155 :cell adhesion (BP)	0.00418177
GO:0006810 :transport (BP)	0.00920623

Table 4.7 A large proportion of the esiRNA dataset that modulated β -catenin accumulation in the UB screen are associated with differentiation, transport and signal transduction processes.

The UB screen dataset that regulated β -catenin whole cell intensity was analysed for enrichment in biological processes using their GOSlim annotations in GeneCodis. Processes that were significantly over-represented within the gene set included cell differentiation, transport processes and translation. Min(pValue); Hypergeometric pValue

4.2.2.2 U2OS APC (UA) screen enrichment analysis

In the UA screen, ‘pathways in cancers’ were notably over-represented in the datasets of regulators of β -catenin localisation and accumulation (Figures 4.13 and 4.14, Appendix B Tables 22 and 23). This annotation category in the KEGG database represents genes enriched in pathways aberrantly regulated in cancers. This list contains a plethora of genes ranging from Wnts, APC and β -catenin to NF- κ B, multiple FGFs, EGF, VEGF, BCL2, and STAT3, implicating a diverse range of pathways in the modulation of β -catenin upon APC downregulation. Other notable pathways, in addition to Wnt, were Insulin, MAP kinase and calcium signalling, as well as endocytosis and adhesion processes, with many also over-represented in the UB screen as discussed above.

Comparisons of over-represented GOSlim annotations within both the β -catenin localisation and stabilisation datasets revealed a high degree of similarity between the two, with signal transduction, cell differentiation and transmembrane transport processes enriched within the modulators of β -catenin nuclear localisation and accumulation (Tables 4.8 and 4.9). Processes involved with mRNA and translation were once again over-represented, with the spliceosome notably over-represented in the modulators of β -catenin accumulation. These included hnRNPA1, hnRNPA1L2, SF3A2/B1/B3 and SNRPA/B. β -catenin possesses three splice variants of varying stability therefore this may suggest the favoured production of more or less stable variants of β -catenin mRNA upon downregulation of specific splicing factors [324]. Interestingly, cell cycle and division were highly significantly enriched within the gene sets identified from the UA screen, but were not over-represented in the esiRNAs dataset from the UB screen (Compare Tables 4.8 and 4.9 with 4.6 and 4.7). These included CDK14, CDK2, CDC34, CDC23, CDCA2, GSPT2, UPF1 and CETN1. APC has been implicated in regulating cell cycle at many points with overexpression shown to lead to G1 cell cycle arrest, which is presumably related to its function in the Wnt pathway resulting in repressed transcription of cyclin D1[325]. It has also been implicated in mitosis [326, 327] and more recently in regulating G2/M transition through association with TopoisomeraseII α [328]). Disrupting cell cycle processes may indirectly affect β -catenin levels and localisation, even in the

absence of active Wnt signalling. Further experiments, such as time-lapse microscopy assays to investigate the role of downregulating the identified cell cycle components listed above on β -catenin levels and localisation, in the presence of normal and abrogated APC, may provide further insight.

Number of genes per concurrent annotations

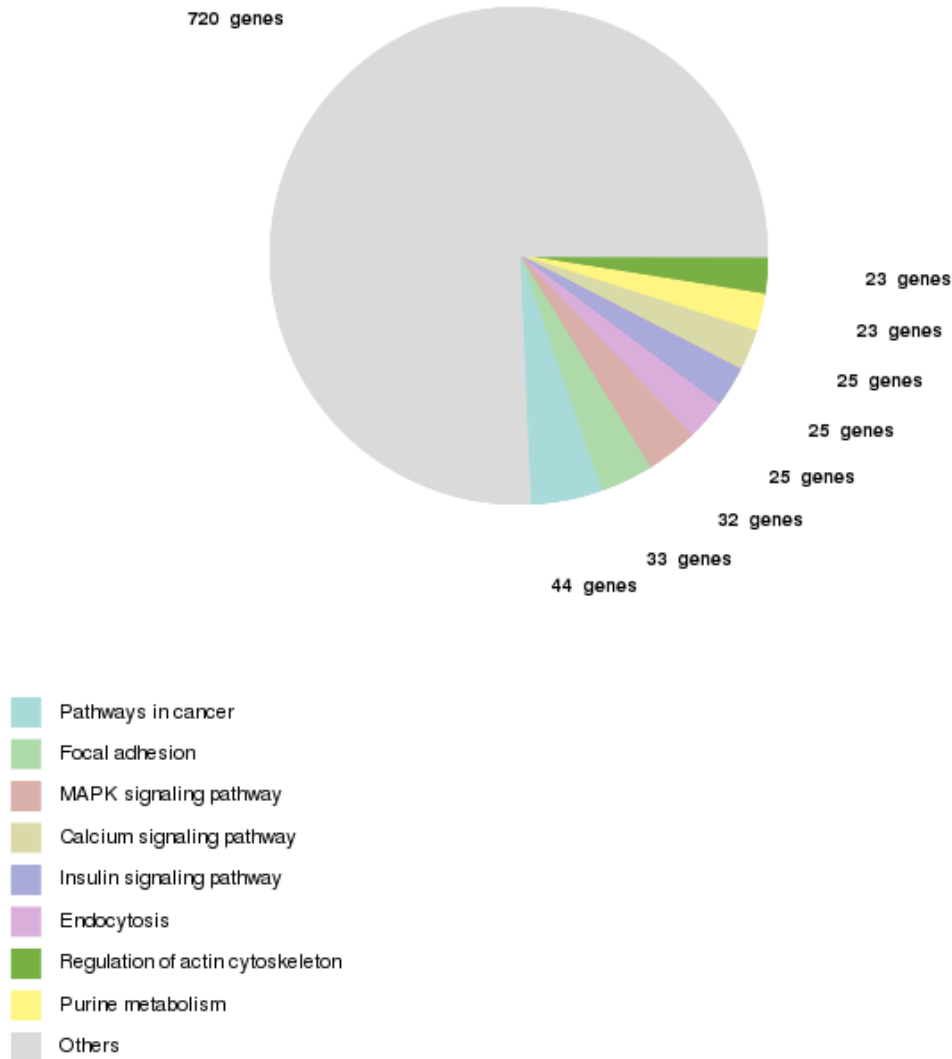


Figure 4.13 Cancer pathways were enriched within the set of esiRNAs that regulate β -catenin nuclear localisation in the UA screen.

The UA screen dataset that regulated β -catenin Nuc/Cyt ratio was analysed for enrichment in their occurrence in KEGG pathways. The pathways that were over-represented included several pathways involved in cancer (details in Appendix B table 22 and 23) with Wnt signalling not as significantly enriched compared to other signalling pathways (see Appendix B, Table 22 for further details and associated hypergeometric p-values). Genes not represented in the above chart were either not associated with a KEGG signalling pathway enriched relative to the genome, or had no signalling information associated with them.

Number of genes per concurrent annotations

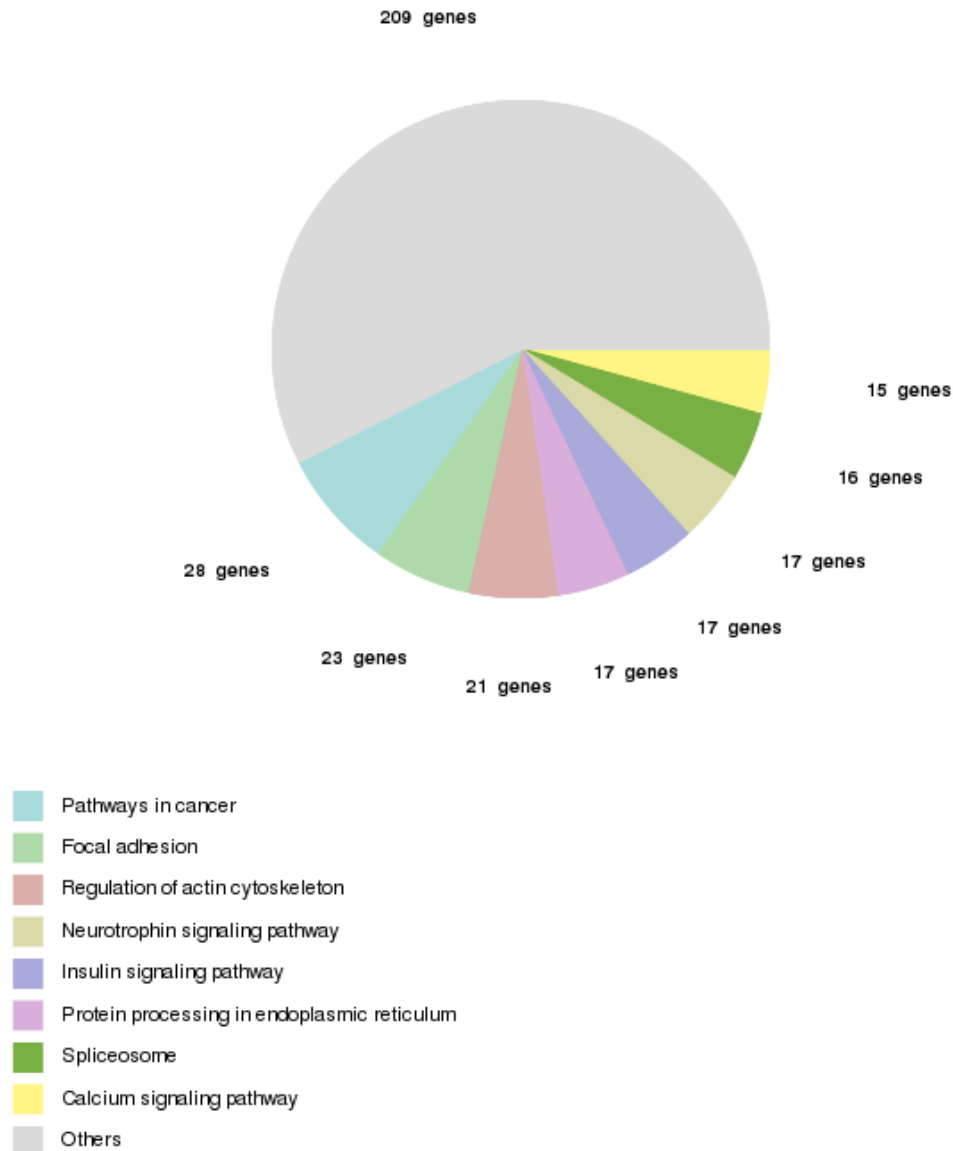


Figure 4.14 Cancer pathways were enriched within the set of esiRNAs that regulate β -catenin accumulation in the UA screen.

The UA screen dataset that regulated β -catenin whole cell intensity was analysed for enrichment in their occurrence in KEGG pathways. The pathways that were over-represented included adhesion, cytoskeletal regulation and insulin signalling, in addition to proteasomal, protein processing and spliceosome pathways (see Appendix table 24 for detailed breakdown and associated hypergeometric p-values). Wnt signalling was significantly enriched but not to the same degree as in the UB screen and when compared to other pathways such as insulin signalling (Appendix table 24) .Min(pValue); Hypergeometric pValue. Genes not represented in the above chart were either not associated with a KEGG signalling pathway enriched relative to the genome, or had no signalling information associated with them.

GOSlimAnnotations	min(pValue)
GO:0007165 :signal transduction (BP)	7.15E-17
GO:0055085 :transmembrane transport (BP)	9.87E-10
GO:0007049 :cell cycle (BP)	1.27E-09
GO:0007155 :cell adhesion (BP)	1.89E-07
GO:0051301 :cell division (BP)	1.41E-06
GO:0006810 :transport (BP)	2.84E-06
GO:0034641 :cellular nitrogen compound metabolic process (BP)	2.43E-05
GO:0005975 :carbohydrate metabolic process (BP)	2.98E-05
GO:0030154 :cell differentiation (BP)	4.83E-05
GO:0007067 :mitosis (BP)	0.000122205
GO:0006412 :translation (BP)	0.000124493
GO:0007267 :cell-cell signalling (BP)	0.000285061
GO:0006950 :response to stress (BP)	0.00219093
GO:0016192 :vesicle-mediated transport (BP)	0.0027329
GO:0008283 :cell proliferation (BP)	0.00502849
GO:0006605 :protein targeting (BP)	0.00670866
GO:0007010 :cytoskeleton organization (BP)	0.0135504

Table 4.8 A large proportion of the esiRNA dataset that modulated β -catenin nuclear localisation in the UA screen are associated with signal transduction, cell cycle and transport processes.

The UA screen dataset that regulated β -catenin Nuc/Cyt ratio was analysed for enrichment in biological processes using their GOSlim annotations. Min(pValue); Hypergeometric pValue.

GOSlim Annotations	min(pValue)
GO:0007165 :signal transduction (BP)	1.04E-10
GO:0055085 :transmembrane transport (BP)	8.36E-08
GO:0006810 :transport (BP)	6.50E-06
GO:0030154 :cell differentiation (BP)	2.20E-05
GO:0034641 :cellular nitrogen compound metabolic process (BP)	6.58E-05
GO:0007155 :cell adhesion (BP)	0.000542657
GO:0007267 :cell-cell signalling (BP)	0.00094209
GO:0006397 :mRNA processing (BP)	0.00149641
GO:0006461 :protein complex assembly (BP)	0.00161981
GO:0005975 :carbohydrate metabolic process (BP)	0.00220597
GO:0016192 :vesicle-mediated transport (BP)	0.00249899
GO:0007049 :cell cycle (BP)	0.00307428
GO:0006457 :protein folding (BP)	0.00609476
GO:0051301 :cell division (BP)	0.00674972
GO:0042592 :homeostatic process (BP)	0.00686201
GO:0006412 :translation (BP)	0.00817015
GO:0007010 :cytoskeleton organization (BP)	0.0192815

Table 4.9 A large proportion of the esiRNA dataset that modulated β -catenin accumulation in the UA screen are associated with signal transduction and cell cycle processes.

The UA screen dataset that regulated β -catenin whole cell intensity was analysed for enrichment in biological processes using their GOSlim annotations. Min(pValue); Hypergeometric pValue.

4.2.3 Overlaps and enrichment analysis summary of the 3 screens

The enrichment analysis demonstrated that the screens had identified a diverse range of potential regulators of β -catenin that are implicated in a wide range of pathways and processes. These ranged from Wnt signalling and Ubiquitin-mediated proteolysis to endocytosis and cell cycle/division. However, certain biological processes and pathways were over-represented in the regulators identified in all three screens, implying an important and conserved role for these processes in β -catenin regulation, meriting further discussion in Chapter 6. Therefore, only a brief overview of the types of genes identified within each common process/pathway will be provided below. Recurring themes in the enrichment analysis were the over-representation of components involved in:

- 1) Other signalling pathways such as TGF- β , MAP kinase and Insulin in the screens with activated Wnt signalling
- 2) Cell adhesion and cytoskeletal processes
- 3) mRNA processing and translation

4.2.3.1 Signalling crosstalk.

Many TGF- β components were identified across the 3 screening assays and include (with the screens which identified them in brackets) BMP1 (UA and UB screens) BMP2/4, (H), TGF β 1 (H) and SMAD 3 (H), SMAD9 (UA and UB) and SMAD1 (UA and UB). TGF- β signalling has been demonstrated to cross talk with many pathways, including Wnt (reviewed in [305]). For example, two of the components identified have been directly implicated in β -catenin regulation with TGF-beta1 demonstrated to induce nuclear translocation of β -catenin in mesenchymal stem cells in a Smad3-dependent manner [329]. Insulin/AKT signalling components identified in the screens included INSR (UA), PI3K3CD (UA), PIK3CB (UA,UB and H), GSK3 β (UA) IRS4 (UA), INSR (H and UA) and EIF41EB (UA). PI3-kinase signalling has been

implicated in mediating Wnt3a-induced proliferation of fibroblasts [330] in addition to AKT directly phosphorylating β -catenin to enhance its transcriptional activity [221]. A plethora of MAP3 kinases such as MAP3K1 (H), MAP3K13 (UA and UB), MAP3K6 (UA) and MAP3K4 (UA), in addition to MAP4K4 (H), MAPK3 (H) and MAP4K4 (H) were identified as putative regulators of β -catenin regulators across two different cell types. One major pathway of the MAP kinase network, relevant to Wnt in particular, is mediated by c-Jun N-terminal kinase (JNK) [331]. In addition to mediating non-canonical Wnt/PCP (or Wnt/JNK pathway), it has also been demonstrated to have a more direct role in Wnt/ β -catenin signalling by directly phosphorylating β -catenin and disrupting cell-cell junctions in keratinocytes [332] in addition to enhancing its nuclear transport, again by phosphorylation events [116].

4.2.3.2 Adhesion and cytoskeletal organisation

Cell adhesion and cytoskeletal organisation regulators were over-represented in the identified β -catenin modulators across all three screens. Putative β -catenin modulators in adhesion processes included ACTN4 (UA), TLN2 (UA), PXN (UA), LAMB3 (UA), ITGA3 (UA), ITGA8 (UB), ITGA5 (UA), CTNND1 (H), CDH2 (H, UA), EFNA4 (UB), NRXN2 (UB) and EPHA3 (UA) to name but a few. Cytoskeletal organisation is intimately linked to cell adhesion (both cell-cell and cell-matrix) and the gene lists were also enriched for RhoGTPases and their regulators such as RAC1 (UA, H), RAP1A (UA), ROCK2 (UB, H), ROCK1 (H), CDC42 (UA, H), VAV1 (H), RHOG (H), and CDC42EP2 (H). The enrichment in processes that potentially revolve around β -catenin's adhesive roles is particularly interesting, especially those involving the RhoGTPases given their activation can be mediated by JNK, which a role in Wnt/PCP signalling [333] and directly regulates β -catenin by phosphorylation [116, 332]. This may indicate a more involved role for Wnt/PCP (JNK) non-canonical signalling in β -catenin regulation than currently appreciated.

4.2.3.3 mRNA processing and translation

The over-representation of mRNA processing and translation regulators in the identified β -catenin modulators may be argued to be simply an indirect effect of

inhibiting general transcription and translation. However, validation work on a subset of hits identified from the 7df3 transcriptional screen demonstrated that no effect was observed on CMV-LacZ co-transfected in these experiments, suggesting specificity for TCF-dependent transcription rather than a general transcriptional effect (data not shown). This is likely to apply also to the CMV-driven eGFP- β -catenin in the U2OS cells. Furthermore, the fact that upregulation is observed in many of the cases suggests that this is not simply due to the blocking of the transcriptional/translation process. Lastly, a general effect on transcription/translation would be expected to kill cells and this is excluded in the esiRNA modulators that were selected for further analysis. Many pathways, such as mTor, regulate ribosomal synthesis and Axin and β -catenin have been demonstrated to bind Tor components for example, therefore prematurely disregarding ribosomal processes may well be unwise [334].

The apparent enrichment in mRNA processing is surprising, as it is often assumed, albeit presumptuously, that β -catenin synthesis regulation is independent of Wnt signalling. Components identified relating to mRNA processing included hnRNPA1 (UA,UB and H), HNRNPA1L2 (UA,UB), hnRNP H1 (UA,UAB, H), JMJD6 (UB), MAGOH (H), NHP2L1 (UA,UB H), UPF1 (UA,UB,H) and SNRPD2 (H) in addition to factors involved in RNA transport such as NUP85 (UA), NUP133 (UA), NUPL1 (UA, UB), NUP160 (UB), NUP205 (H) and NUP155 (UA, H). β -catenin mRNA stability has been demonstrated to be regulated both by Wnt and PI3-kinase though recently identified Dvl binding partners [183, 184, 335], although, for the most part, this aspect of β -catenin regulation is widely overlooked. This will be addressed further in Chapter 5, where the work will describe the study into hnRNPA1's role in regulating β -catenin.

4.3 Comparative analysis of the β -catenin esiRNA screens

Using the datasets generated in 4.1, based on the more stringent threshold criteria (Appendix B, Tables 3,4,8-11), the degree of overlaps between the primary screens were assessed to highlight esiRNAs that may have conserved roles in β -catenin regulation in multiple systems. All overlapping gene IDs in Figure 4.15 and 4.16 are

provided in Appendix B, Tables 25 and 26. Only 16 esiRNAs modulated β -catenin nuclear localisation in all three primary screens (Figure 4.15), namely; AIP, CC2D2A, CHMP7, CTNNB1, FBXO41, FBXW11, IL-18, KIAA0664L3, N4BP3, NDUFB7, PALM, RRBP1, SSX2IP, TAPBP, TIMM17B and UPF1. 31 esiRNAs overlapped in the modulators of β -catenin whole cell levels identified from the three screens (Figure 4.16), which included CTNNB1 itself, along with AXIN1, PSMD1, HNRNPA1, HNRNPH1, ANK2, HIF3A and SPEN for example.

It is well established that β -catenin is degraded through an ubiquitin-mediated pathway involving the cullin based SCF complex (SKP1, CUL1, F-box protein FBXW11 (β -TRCP)) with the substrate recognition component FBXW11 (β -TRCP), identified in all screens as a regulator of β -catenin nuclear localisation (Figure 4.15) [336, 337]. Also in the overlapping set of regulators in Figure 4.15 were FBXO41, again implicated in the E3 ubiquitin-ligase pathway, and N4BP3, a binding partner of the E3 ubiquitin ligase, NEDD-4, which mediates its localisation to vesicles within the cytoplasm [338]. In addition to β -catenin, several other Wnt regulators have been shown to be targeted for ubiquitination-mediated degradation, including Dvl [339-342], APC [343, 344] and TCF/LEF [345]. In these cases, however, much less is known about the ubiquitin ligase complexes involved [341].

SSX2IP (ADIP) is a component of adherens junctions that may be involved also in the organisation of the actin cytoskeleton [346] and could therefore present alternative forms of β -catenin regulation at junctional complexes. GJPB and ANK2 are also involved in cytoskeletal processes and were identified as potential regulators of β -catenin accumulation in all three screens (Figure 4.16). Observed in the overlapping regulators of β -catenin accumulation is SPEN homolog (or SHARP), a corepressor protein that has been implicated in the regulation of the Notch and EGF/Ras signalling pathways in *Drosophila* [347, 348] in addition to being required for Wnt-dependent signalling in the wing, eye and leg imaginal discs [349]. Furthermore, SPEN homolog was demonstrated to be a positive regulator of TCF-dependent transcription in human cancer cells, but downstream of already deregulated β -catenin levels in cancer cells [350]. Therefore, the screen results suggest an alternative mechanism is involved, potentially mediated by cross talk with EGF and Notch

signalling pathways, with the latter demonstrated to be overrepresented within the regulators of β -catenin identified (Table 4.4, Appendix B, Table 21).

EDAR (ectodysplasin A receptor), which was identified as a modulator of β -catenin levels in all screens (Figure 4.16), is a member of the TNF receptor family with key roles in ectodermal differentiation [351]. While it may mediate its influence of β -catenin via activating JNK (as mentioned earlier) [351] it has also been demonstrated to play a role alongside NF- κ B to regulate Wnt/ β -catenin activity during the maintenance of primary hair follicle placodes [352], suggesting that an assessment of the role of NF- κ B in β -catenin regulation alongside EDAR would also be insightful.

The presence of mRNA processing regulators in the overlap of modulators of β -catenin, such as hnRNPA1, hnRNPH1, and UPF1 is surprising. Indeed, hnRNP A1 knockdown resulted in one of the strongest responses in terms of elevated β -catenin levels and localisation (in the UA and UB screen) in all three screens. This particular protein and the role it may play in β -catenin regulation will be discussed in the following chapter.

CHMP7 (Charged multivesicular body protein 7) is an ESCRT (enrichment of endosomal sorting complexes required for transport) that functions in the endosomal sorting pathway [353] and was identified as a regulator of β -catenin nuclear localisation in all screens (Figure 4.15). Due to the overrepresentation of endocytosis components within the identified hits from screens UA and UB in particular (Figures 4.11, 4.12, 4.13) this may be highly relevant to the process of internalisation of LRP6 upon Wnt signalling.

Overlaps between the two cell lines were also small with 46 and 60 genes overlapping between the H screen and the UB and UA screen respectively within the regulators of β -catenin localisation (not including the central overlapping set) (Figure 4.15). Furthermore, only 30 and 36 esiRNAs were demonstrated to overlap between the cell lines for regulators of β -catenin accumulation (Figure 4.16), suggestive of cell-type specific effects. A recently published screen for regulators of TCF-dependent transcription demonstrated that the degree of overlap between hits identified in DLD-

1 and SW480 cells was also surprisingly low, despite both being APC mutant colon carcinoma cell lines [242]. Overlaps between the putative regulators of β -catenin localisation and levels identified in the UA and UB screens were far higher at 179 and 272 respectively (Figures 4.15 and 4.16). Therefore, the surprisingly low overlap between the H and UA/UB screens may be indeed a result of cell type-specificity.

In summary, the screens have identified a wide variety of components implicated in a diverse range of processes and provide sources of possible mechanistic insight into a number of areas of biology that may be involved in regulating β -catenin's functions within a cell. The subsequent section will describe the reconfirmation of a subset of 'hits' identified in each of the three screens, prior to an assessment of the relationship between β -catenin and TCF-dependent transcription.

AIP	N4BP3
CC2D2A	NDUFB7
CHMP7	PALM
CTNNB1	RRBP1
FBXO41	SSX2IP
FBXW11	TAPBP
IL18	TIMM17B
KIAA0664L3	UPF1

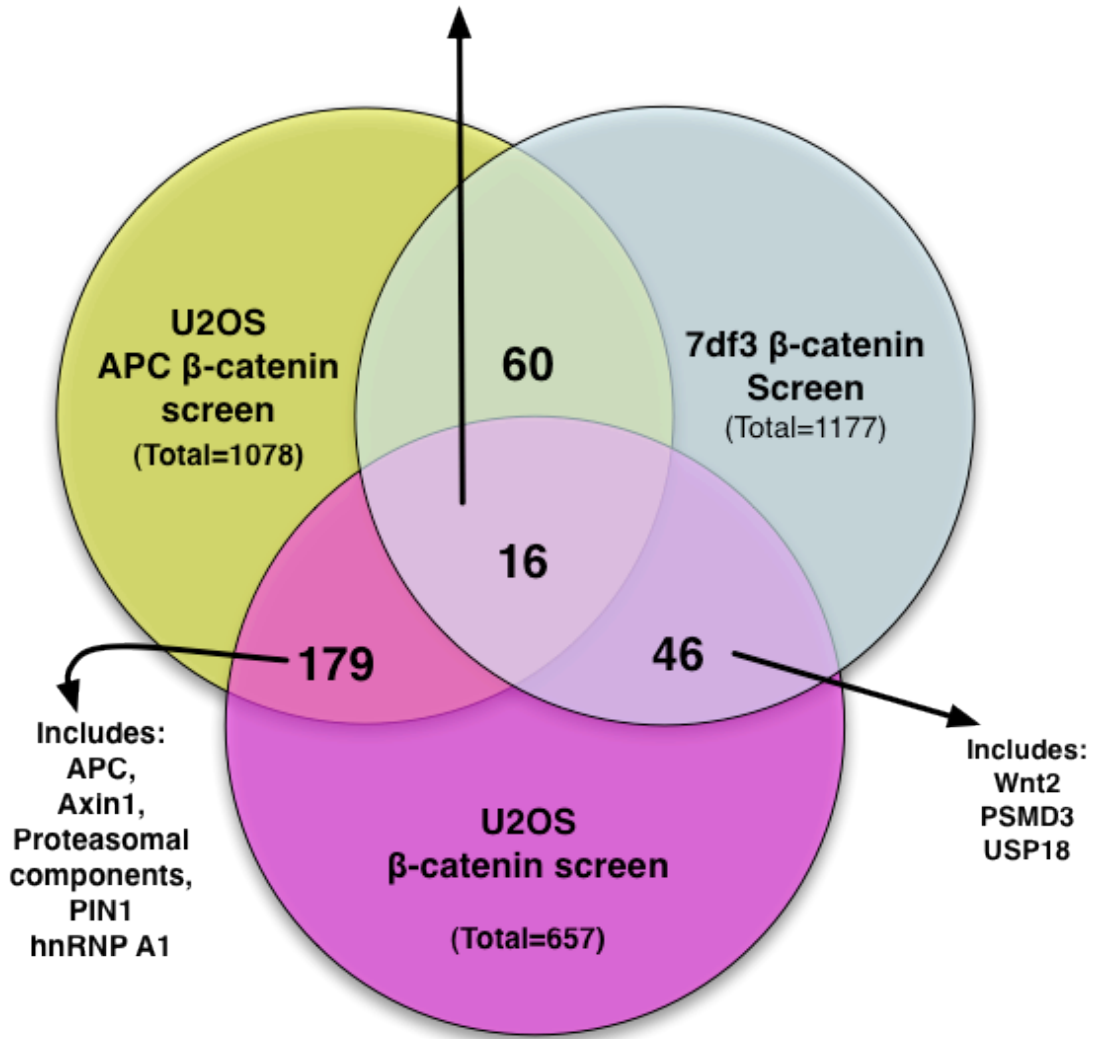


Figure 4.15. Overlapping modulators of β -catenin nuclear localisation from the three primary screens.

Raw data from the primary screen were analysed for their respective Z-scores for β -catenin Nuc/Cyt ratios. esiRNAs with Z-scores of >2 or <-1.5 in each screen that passed toxicity thresholds are indicated, in addition to the degree of overlap between screens. Known β -catenin regulators were picked up in all screens including Wnt pathway and proteasomal components. Full lists provided in Appendix B, Table 25.

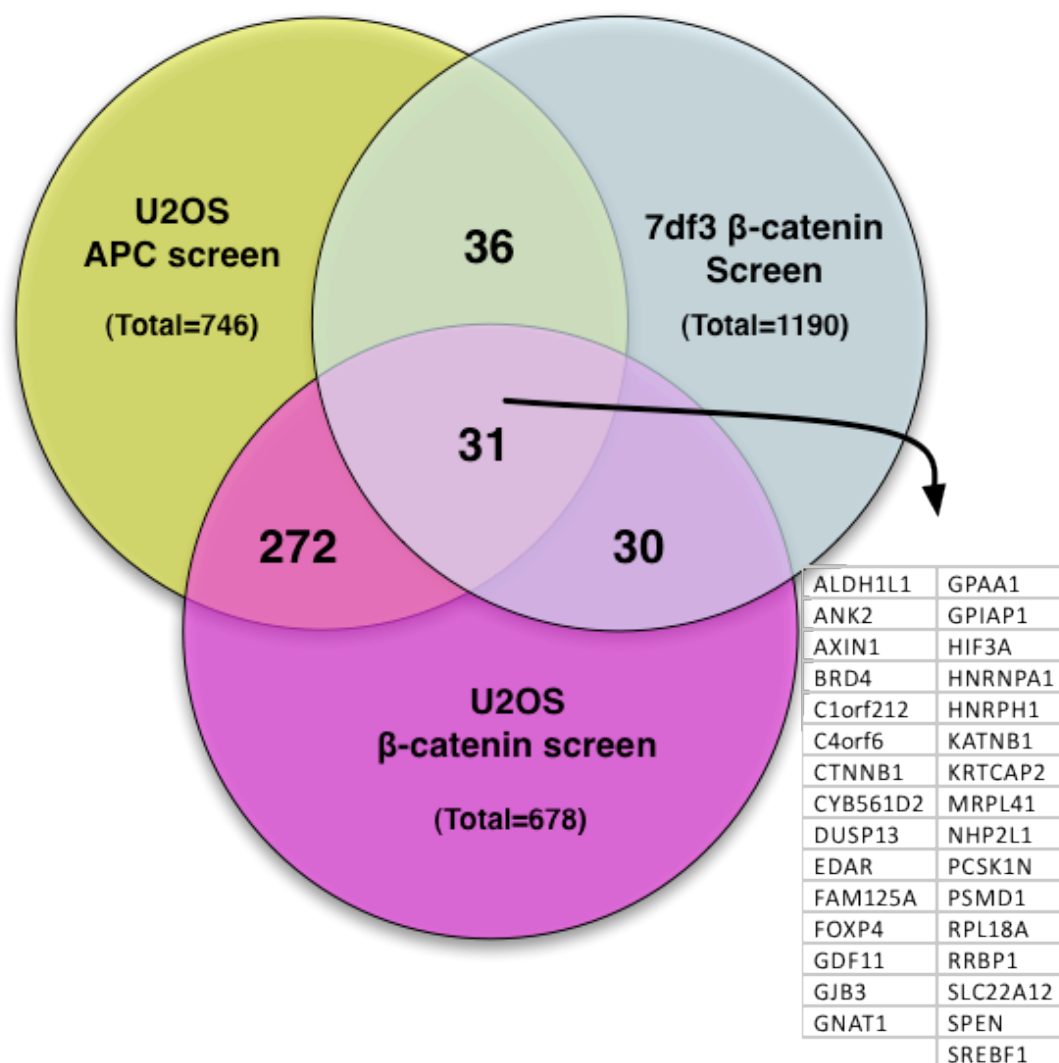


Figure 4.16. Overlapping modulators of β -catenin accumulation from the three primary screens.

Raw data from the primary screen were analysed for their respective Z-scores for β -catenin whole cell intensities. esiRNAs with Z-scores of >2 or <-1.5 in each screen that passed the cell toxicity filter are indicated, in addition to the degree of overlap between screens. Known β -catenin regulators were picked up in all screens including Wnt pathway and proteasomal components. Full lists provided in Appendix B, Table 26.

4.4 Reconfirmation assays

False positives are inherent in high-throughput experiments [248] so secondary studies, frequently utilising a non-overlapping siRNA against selected hits, are required to reconfirm the primary data. Time and resources dictated how much of the primary data that could be reconfirmed, therefore small subsets of esiRNAs from each screen were marked for revalidation through the use of new esiRNAs generated from sequences non-overlapping from those utilised in the primary library.

Approximately 225 esiRNAs were chosen for reconfirmation based on several criteria. The esiRNA lists that were generated for the inter-screen overlap assessments (Appendix B, Tables 3,4,7-10) were rank ordered by their Z-scores and were assessed for criteria such as their effects in the other primary screens, the strength of a particular assay in identifying up or down regulators of β -catenin and the performance of a particular screen as denoted by z-factor analysis of the plates. Both U2OS screens had the advantage of possessing two fields of view of the same well so esiRNAs scoring strongly positive in both fields of view were favoured above those that only scored positive in one field of view. Furthermore, the information gained from the *in silico* analysis of the data sets, such as the identification of novel pathways and processes enriched in the datasets, were also considered when selecting genes. For example, genes involved in mRNA processing and translation were particularly attractive given their surprisingly high prevalence within the identified data sets. Moreover, esiRNAs that resulted in decreased β -catenin levels and nuclear localisation in the UA esiRNA screen were also interesting given their applicability to cancers and the potential of finding novel modulators that can decrease oncogenic induced β -catenin upon knockdown/inhibition.

Of the 225 or so selected, 164 esiRNAs were successfully generated by our collaborators at the MPI in Dresden (Professor Frank Buchholz and Dr Mirko Theis) against 161 genes, with 3 (MAGOH, RBX1 and KIAA0280) possessing two esiRNAs as it wasn't possible to generate one esiRNA that didn't completely overlap with the primary sequence. Those that were not produced either failed during design or production. Details of the reconfirmatory sublibrary are provided in Appendix B

Table 27. All of the graphs from the reconfirmation assays are provided in Appendix B in the PNG folder for clarity and better resolution.

4.4.1 Reconfirmation of the selected H screen hits

All 164 secondary esiRNAs were re-assayed in the 7df3 cells with methods identical to that of the primary screen. Figures 4.17 and 4.18 display the data for β -catenin nuc/cyt ratio and β -catenin whole cell levels respectively for all 164 esiRNA. For clarity, the esiRNAs that were originally identified from the H primary screen (43 esiRNAs) are extracted with their reconfirmation data tabulated in Table 4.10.

Unfortunately, the 7df3s during the period of reconfirmation experiments were inexplicably unresponsive to β -estradiol so the effects of esiRNA were significantly attenuated compared to the primary screen. Given time these experiments would have been repeated once the source of the problem had been identified. Nevertheless, the data was still deemed to be useful in reconfirming the 'trend' of the esiRNA effects at least, even if the data lacked statistical significance. esiRNAs that increased or decreased β -catenin nuclear:cytosolic ratios and whole cell levels by 2 or 1.5 standard deviations of control means respectively were considered as reconfirming in this secondary screen. Table 4.10 display the esiRNAs that were identified in the original H screen along with their reconfirmation data and associated P-values, in addition to an indication of their reconfirmation status. 11/43 (26%) esiRNAs were considered reconfirmed and promising candidates for further validation assays before they can be considered as true regulators of β -catenin accumulation and/or nuclear localisation. A further 2 were borderline where they did have an effect on β -catenin but on a different parameter than when it was first identified e.g. MAX where it resulted in decreased β -catenin nuc/cyt ratio in the primary screen but here resulted in decreased β -catenin levels instead. Together, the reconfirmation rate for the H was 30%, which was very similar to the reconfirmation rate seen in the TCF-dependent transcriptional screen undertaken previously by Dr Seipel. Reasons for potential reconfirmation failure will be considered alongside the reconfirmation rates of the U2OS assays in the subsequent sections.

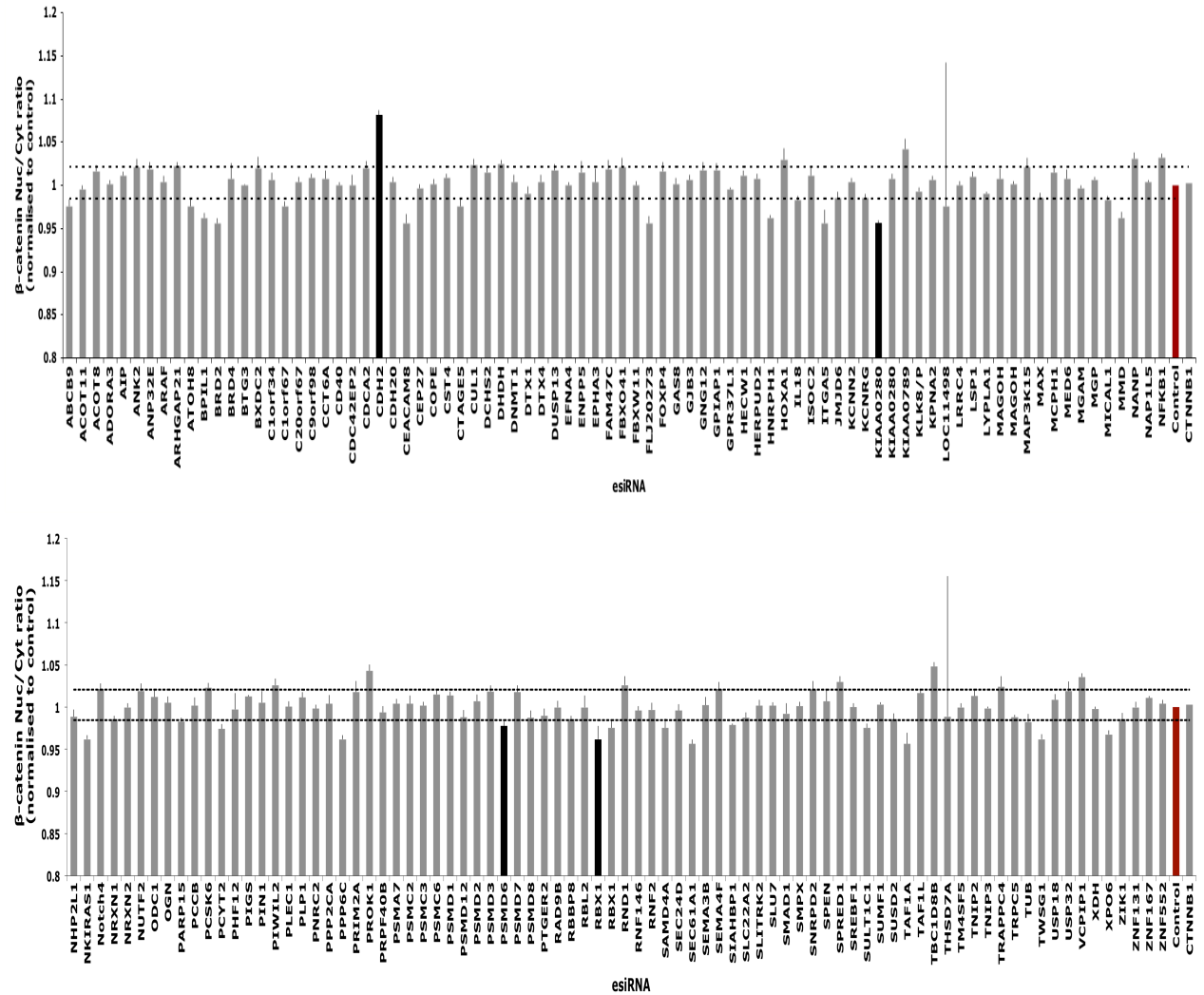


Figure 4.17 Reconfirmation of esiRNA identified in the H screen as regulators of β -catenin nuclear localisation

Secondary non-overlapping esiRNA were generated against a subset of 'hits' from all three screens and re-tested in 7df3 cells. 24hrs post transfection cells were treated with β -estradiol prior to fixation and immunostaining for β -catenin 48hrs post transfection. β -catenin nuclear to cytosolic ratios were quantified and are displayed normalised to control esiRNA. β -catenin esiRNA (CTNNB1) served as an additional control. Dotted lines represent 2 or 1.5 standard deviations above or below the mean of the esiRNA control respectively. Dark bars represent esiRNAs with p-values <0.0001 (two-tailed independent samples t-test). Mean values \pm s.e.m of two independent experiments (n=2) of triplicate wells per condition are displayed. Graphs from the reconfirmation assays are provided in Appendix B for clarity and better resolution.

esiRNA	Primary screen effect on β -catenin (All screens)	β -catenin Nuc/Cell ratio	p-value	β -catenin whole cell intensity	p-value	Reconfirmation status
ARHGAP21	HRD, HWU	1.0224	0.0027	1.0887	0.0142	+/-
BTG3	HRD	0.9994	0.8529	1.0211	0.6036	-
C9orf98	HWD	1.0088	0.1781	1.0383	0.4070	-
CDC42EP2	HWD	0.9996	0.0394	0.9996	0.0003	-
CDH2	HRU	1.0804	0.0000	0.9741	0.2432	++
CEP27	HRU	0.9962	0.5158	1.0432	0.2185	-
CUL1	HRD, HWD	1.0229	0.0387	1.2018	0.0008	-
DNMT1	HWU	1.0037	0.4071	1.0037	0.0160	-
ENPP5	HWD	1.0142	0.3742	1.0972	0.0464	-
FAM47C	HWD	1.0185	0.1390	0.9918	0.8315	-
HNRPH1	HWU,UARU,UAWU,UBRU,UBWU	0.9618	0.4656	0.9618	0.1765	-
LYPLA1	HRU	0.9899	0.0202	0.9903	0.7594	-
MAGOH	HWD	1.0068	0.6193	0.9667	0.3654	-
MAGOH	HWD	1.0017	0.7128	0.9167	0.0741	+
MAP3K15	HRD	1.0213	0.0910	1.1787	0.0439	-
MAX	HRD	0.9855	0.0606	0.9055	0.0009	+/-
MED6	HWD	1.0068	0.2728	1.0068	0.4337	-
MMD	HWU	0.9618	0.0453	0.9618	0.0563	-
NANP	HWU	1.0312	0.0033	0.9356	0.5499	-
NHP2L1	HWU, UAWU, UBRU, UBWU	0.9885	0.0323	1.0939	0.0008	+
NKIRAS1	HRU, HWU	0.9618	0.7496	0.9618	0.0044	-
ODC1	HWU	1.0120	0.0141	0.9682	0.1711	-
PPP6C	HWU	0.9618	0.5807	0.9618	0.0020	-
PSMC2	HWU	1.0037	0.0784	1.0037	0.0405	-
PSMC3	HWU	1.0017	0.0221	1.0017	0.0085	-
PSMC6	HWU	1.0151	0.0245	1.3851	0.0002	+
PSMD1	HWU, UARU, UAWU, UBRU, UBWU	1.0137	0.2031	1.3475	0.0013	+
PSMD2	HWU	1.0068	0.0050	1.0068	0.0002	-
PSMD6	HWU	0.9778	0.0000	1.2254	0.0104	+
PSMD7	HWU, UAWU (UARU)	1.0175	0.0407	1.0209	0.1631	-
RBBP8	HWU	0.9855	0.0003	0.9855	0.0374	-
RNF146	HWD	0.9960	0.5603	0.9747	0.4937	-
SAMD4A	HRD	0.9754	0.0134	0.9909	0.7161	+
SMPX	HRU	1.0009	0.9448	1.1086	0.0915	-
SNRPD2	HRU, HWU	1.0208	0.1435	0.9903	0.7540	+
SPRED1	HRU	1.0298	0.0095	1.1238	0.0023	+
SUSD2	HWU	0.9855	0.3268	0.9855	0.3778	-
TAF1L	HWU	1.0164	0.0521	0.9848	0.4830	-
TM4SF5	HRU	0.9996	0.9212	0.9624	0.1599	-
TRAPPC4	HWU	1.0241	0.1062	1.0351	0.2081	+
XPO6	HRD	0.9676	0.0015	1.0318	0.2552	+
ZNF552	HWU	1.0037	0.6980	1.0037	0.2076	-
CTAGE5	HRU	0.9754	0.7436	0.9754	0.0378	-
PPP2CA	HWU	1.0037	0.0448	1.0037	0.0114	-
Control		1.0000		1.0000		
CTNNB1		1.0027	0.5055	0.5485	0.0000	

Table 4.10 Reconfirmation of esiRNAs that modulated β -catenin accumulation and nuclear localisation in the H primary imaging screen with secondary esiRNA.

Legend overleaf

Summary of Figures 4.17 and 4.18 displaying the reconfirmation efforts of a subset of 'hits' from the primary H screen specifically. EsiRNA that resulted in β -catenin nuc/cyt ratios and whole cell intensities >2 or <-1.5 standard deviations from the controls are coloured green and pink respectively. Associated p-values are displayed (two-tailed independent samples t-test) in addition to a reference to their reconfirmation status. "-" and "+" or "++" represent negative and positive reconfirmation respectively. "-/+ " represent esiRNAs that were deemed weakly borderline reconfirmed candidates.

The esiRNAs original effects in the primary H screen in addition to any effects in both U2OS screens are indicated with the coding as follows:

H = 7DF3 Screen
UA = U2OS APC screen
UB = U2OS (library only) screen

W = whole cell β -catenin intensity
R = Ratio of nuclear to cytosolic β -catenin

D= downregulated β -catenin
U= upregulated β -catenin

e.g. HWD - 7df3 **W**hole cell β -catenin intensity **D**own
UBRU - **U**2OS **l**ibrary only screen β -catenin nuc/cyt **R**atio **U**p

4.4.2 Reconfirmation of UB screen primary hits

All 164 secondary esiRNAs were re-assayed in the eGFP- β -catenin U2OS cells with methods identical to that of the primary UB screen. Figures 4.19 and 4.20 display the data for β -catenin nuc/cyt ratio and β -catenin whole cell levels respectively for all 164 esiRNA. For clarity, the esiRNAs that were originally identified from the UB primary screen (54 esiRNAs) are extracted, with their reconfirmation data tabulated in Table 4.11. esiRNAs that increased or decreased β -catenin nuclear:cytosolic ratios and whole cell levels by 2 or 1.5 standard deviations of control means respectively were considered as reconfirming in this secondary screen. Stringent Bonferroni adjusted P-values were selected for ascertaining significance to improve the confidence that the esiRNAs had reconfirmed given the small number of controls that were able to be tested alongside the sublibrary. Table 4.11 display the esiRNAs that were identified in the original UB screen along with their reconfirmation data and associated P-values, in addition to an indication of their reconfirmation status. 38/54 esiRNAs (corresponding to 37 genes due to 2 esiRNA for KIAA0280) were considered to have reconfirmed and be promising candidates for further validation assays. This resulted in a reconfirmation rate of 70% (Table 4.11). A further 2 were borderline where they did have an effect on β -catenin but on a different parameter than when it was first identified e.g. ARAF where it resulted in increased whole cell β -catenin levels in the primary screen but resulted in increased nuc/cyt ratio in the reconfirmation assay instead. All together the reconfirmation rate for the UB screen was 74%.

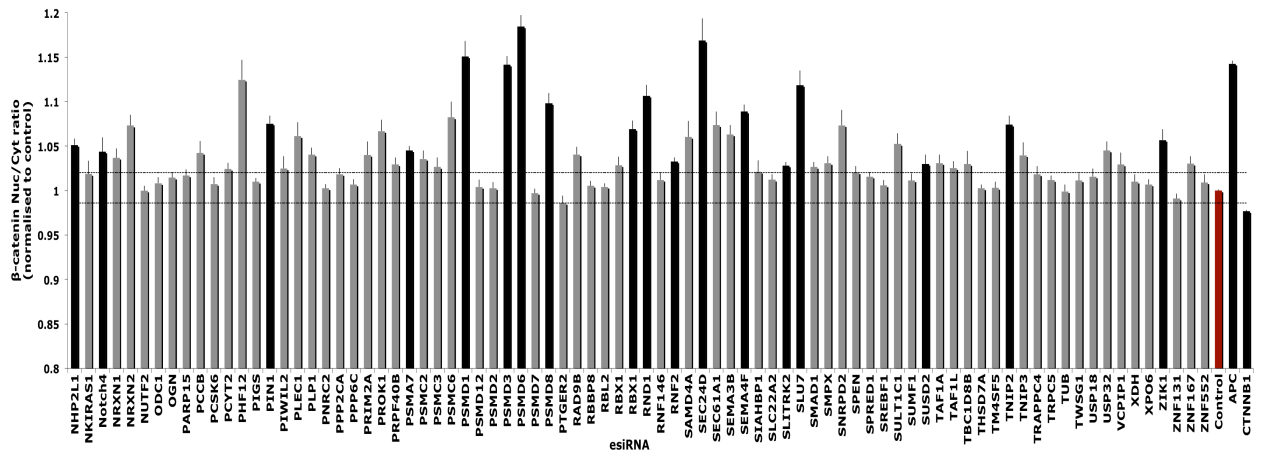
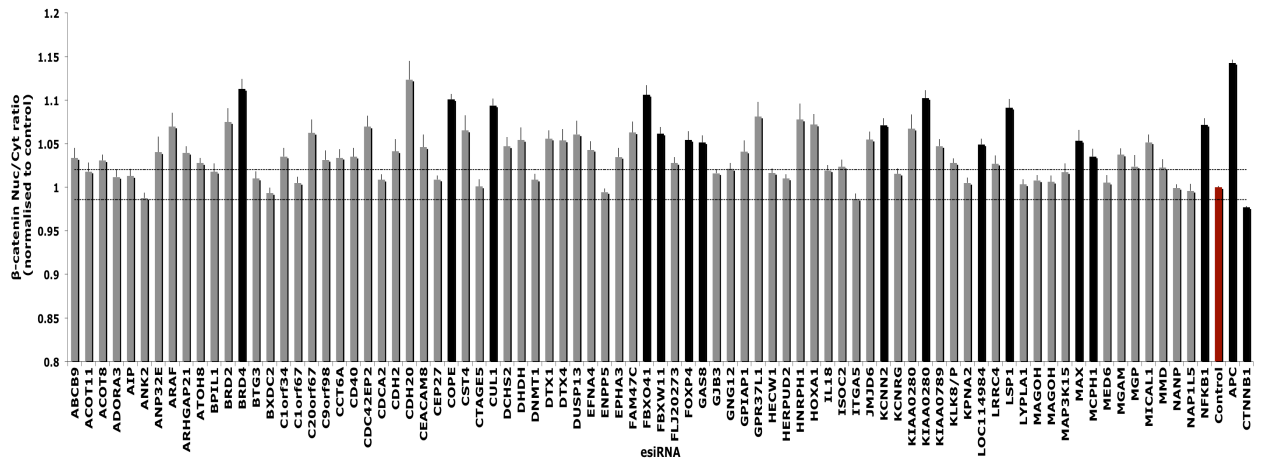


Figure 4.19 Reconfirmation of esiRNA identified in the UB screen as regulators of β -catenin nuclear localisation

Secondary non-overlapping esiRNA were generated against a subset of 'hits' from all three screens and re-tested in eGFP- β -catenin U2OS cells. 48hrs post transfection cells were fixed, DAPI stained and imaged using the IN Cell Analyzer 1000 platform. β -catenin nuclear to cytosolic ratios were quantified and are displayed normalised to control esiRNA. APC and β -catenin (CTNNB1) esiRNA served as additional controls. Dotted lines represent 2 or 1.5 standard deviations above or below the mean of the esiRNA control respectively. Dark bars represent esiRNAs with Bonferroni adjusted p-values of <0.00031 (two-tailed independent samples t-test). Mean values \pm s.e.m of three independent experiments (n=3) of triplicate wells per condition are displayed. Graphs from the reconfirmation assays are provided in Appendix B for clarity and better resolution.

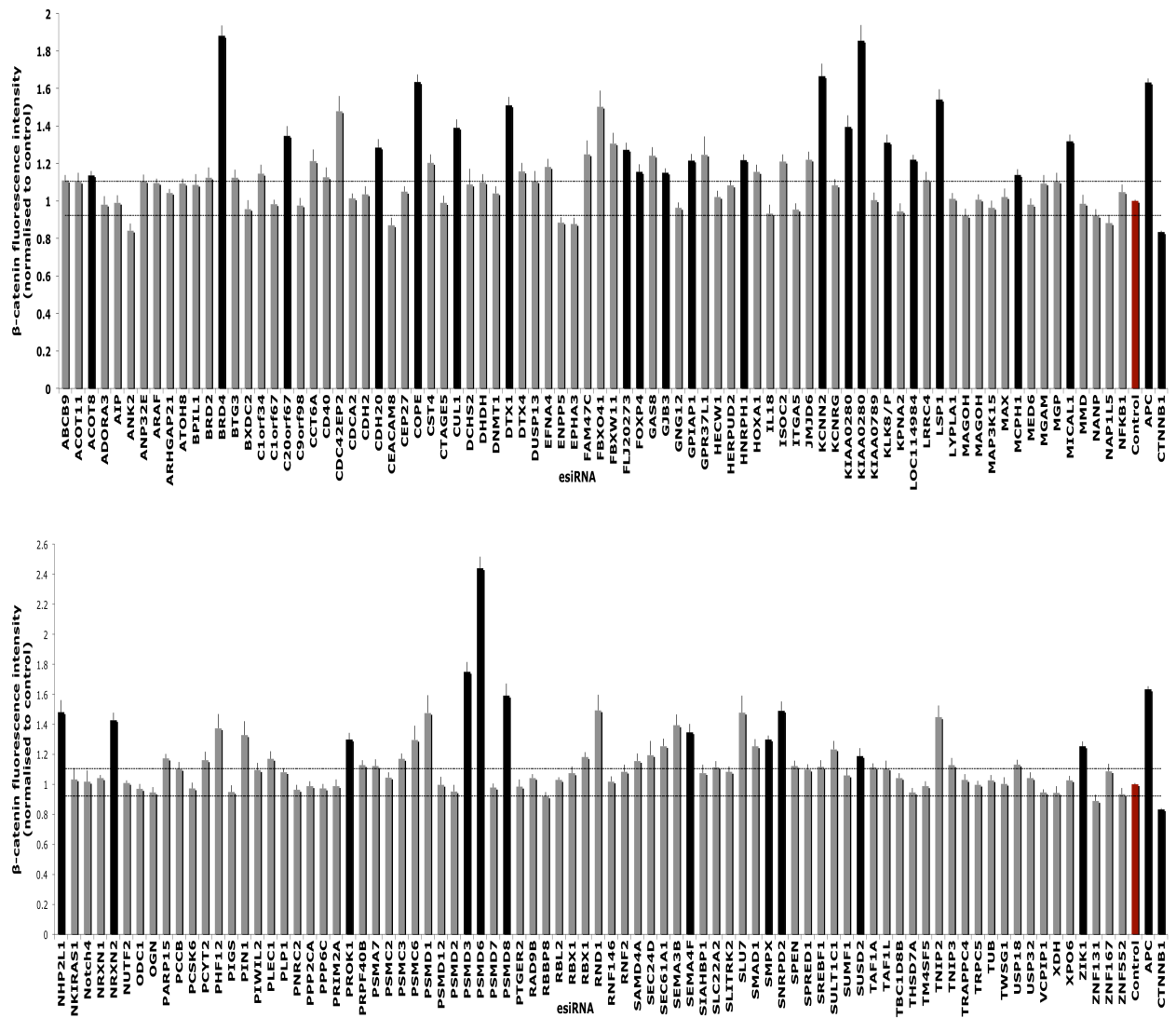


Figure 4.20 Reconfirmation of esiRNA identified in the UB screen as regulators of β -catenin accumulation.

Secondary non-overlapping esiRNA were generated against a subset of 'hits' from all three screens and re-tested in eGFP- β -catenin U2OS cells. 48hrs post transfection cells were fixed, DAPI stained and imaged using the IN Cell Analyzer 1000 platform. β -catenin whole cell levels were quantified and are displayed normalised to control esiRNA. APC and β -catenin (CTNNB1) esiRNA served as additional controls. Dotted lines represent 2 or 1.5 standard deviations above or below the mean of the esiRNA control respectively. Dark bars represent esiRNAs with Bonferroni adjusted p-values of <math><0.00031</math> (two-tailed independent samples t-test). Mean values \pm s.e.m of three independent experiments (n=3) of triplicate wells per condition are displayed. Graphs from the reconfirmation assays are provided in Appendix B for clarity and better resolution.

esiRNA	Primary screen effect on β -catenin (All screens)	β -catenin Nuc/Cell Intensity	p-value	β -catenin whole cell intensity	p-value	Reconfirmation status
AIP	UARU,UAWU,UBWU	1.013	1.61E-01	0.990	8.23E-01	-
ANK2	UARU,UAWU,UBWU	0.988	7.97E-02	0.842	3.00E-03	-
ANP32E	UBWD	1.040	5.78E-02	1.106	1.69E-02	-
ARAF	UBWU	1.070	2.35E-03	1.096	3.72E-03	+/-
BRD2	UBRU,UBWU	1.075	1.67E-03	1.125	5.00E-02	+
BXDC2	UBRD	0.993	3.04E-01	0.957	3.96E-01	-
C1orf67	UBRD	1.005	5.11E-01	0.983	5.09E-01	-
C20orf67	UBWU	1.062	3.97E-03	1.347	1.58E-04	++
CCT6A	UBWD	1.034	1.03E-02	1.211	1.12E-02	-
CD40	UAWU,UBRU,UBWU	1.035	8.64E-03	1.126	4.61E-02	+
COPE	UBWU	1.101	1.16E-07	1.633	2.15E-07	++
DCHS2	UBRU	1.047	2.50E-03	1.087	3.39E-01	+
DHDH	UBRU, UBWU	1.054	5.64E-03	1.099	6.09E-02	+
DTX1	UBRU, UBWU	1.056	3.84E-04	1.509	3.47E-06	++
EFNA4	UBWU	1.043	2.20E-03	1.180	2.86E-03	+
FBXO41	UARU,UAWU,UBRU,UBWU	1.106	1.23E-05	1.502	3.66E-04	++
FOXP4	UBRU, UBWU	1.054	3.08E-06	1.154	3.08E-06	++
GAS8	UAWU, UBRU, UBWU	1.051	1.88E-04	1.241	6.77E-04	+
GJB3	UAWU, UBWU	1.016	7.85E-03	1.151	1.29E-04	++
GPR37L1	UAWU, UBWU	1.081	1.19E-03	1.247	3.45E-02	+
HNRPH1	HWU,UARU,UAWU,UBRU,UBWU	1.078	2.73E-03	1.217	9.39E-05	++
HOXA1	UARU,UAWU,UBRU,UBWU	1.072	3.71E-04	1.154	3.94E-03	+
IL18	UBRD	1.019	1.17E-02	0.933	1.96E-01	-
ISOC2	UAWU,UBRU,UBWU	1.024	1.94E-02	1.209	5.63E-04	+
JMJD6	UBWU	1.055	3.56E-04	1.220	6.91E-04	+
KCNRG	UARU,UAWU,UBRU,UBWU	1.015	3.08E-06	1.082	3.08E-06	-
KIAA0280	UARU,UAWU,UBRU,UBWU	1.067	3.72E-03	1.394	2.23E-04	++
KIAA0280	UARU,UAWU,UBRU,UBWU	1.102	2.42E-06	1.854	7.07E-06	++
KIAA0789	UARU (UBRU)	1.047	3.28E-04	1.003	9.36E-01	+
KLK8/P	UBWU	1.028	9.23E-04	1.311	6.15E-05	++
LOC114984	UARU,UAWU,UBWU	1.049	5.68E-05	1.220	1.94E-05	++
LRRC4	UBRU, UBWU	1.027	2.25E-02	1.112	2.78E-02	+
MCPH1	UAWU,UBRU,UBWU	1.035	3.08E-06	1.138	3.08E-06	++
MGAM	UBRD	1.037	6.09E-04	1.093	7.08E-02	-
MGP	UBWU	1.024	1.07E-01	1.103	6.17E-02	+/-
MICAL1	UBRU, UBWU	1.051	3.63E-04	1.318	1.44E-05	++
NHP2L1	HWU, UAWU, UBRU, UBWU	1.051	3.08E-06	1.479	3.08E-06	++
Notch4	UAWU, UBRU, UBWU	1.044	3.08E-06	1.016	3.08E-06	++
NRXN2	UBRU	1.073	3.08E-04	1.428	2.08E-05	++
PCYT2	UBRU	1.024	7.34E-03	1.160	2.10E-02	+
PIGS	UARU, UAWU, UBRU	1.010	5.76E-02	0.949	2.78E-01	-
PRPF40B	UBWU	1.029	4.60E-03	1.127	5.73E-03	+
PSMD1	HWU, UARU, UAWU, UBRU, UBWU	1.151	2.37E-05	1.476	3.93E-03	++
PSMD8	UAWU, UBWU (UARU)	1.098	2.43E-05	1.589	8.64E-05	++
RAD9B	UBWD	1.041	1.29E-03	1.042	1.38E-01	-
RBL2	UAWD, UBWD	1.004	3.33E-01	1.028	2.02E-01	-
SEMA3B	UAWU, UBRU, UBWU	1.063	3.57E-04	1.392	5.78E-04	+
SREBF1	UBWU (UAWU)	1.006	3.95E-01	1.115	4.23E-02	+
SULT1C1	UAWU, UBRU, UBWU	1.052	2.51E-03	1.234	3.31E-03	+
TBC1D8B	UBWD	1.030	8.15E-02	1.042	2.08E-01	-
TNIP2	UBRU, UBWU	1.074	9.79E-05	1.446	4.26E-04	+
USP32	UBRU, UBWU	1.045	2.18E-03	1.041	3.32E-01	+
XDH	UBRU, UBWU	1.010	2.86E-01	0.942	2.44E-01	-
ZNF131	UARD, UAWD, UBWD	0.991	1.59E-01	0.889	3.28E-02	+
Control		1.000		1.000		
APC		1.143	1.70E-46	1.631	2.25E-36	
CTNNB1		0.977	7.18E-22	0.833	2.06E-27	

Table 4.11 Reconfirmation of esiRNAs that modulated β -catenin accumulation and nuclear localisation in the UB primary imaging screen with secondary esiRNA.

Legend overleaf

Summary of Figures 4.19 and 4.20 displaying the reconfirmation efforts of a subset of 'hits' from the primary UB screen. EsiRNA that resulted in β -catenin nuc/cyt ratios and whole cell intensities >2 or <-1.5 standard deviations from the controls are coloured green and pink respectively. Associated p-values are displayed (two-tailed independent samples t-test) in addition to a reference to their reconfirmation status. "-" and "+" or "++" represent negative and positive reconfirmation respectively. "-/+" represent esiRNAs that were deemed weakly borderline reconfirmed candidates.

The esiRNAs original effects in the primary UB screen in addition to any effects in the UA and H screens are indicated with the coding as follows:

H = 7DF3 Screen
UA = U2OS APC screen
UB = U2OS (library only) screen

W = whole cell β -catenin intensity
R = Ratio of nuclear to cytosolic β -catenin

D= downregulated β -catenin
U= upregulated β -catenin

e.g.

UBRU - **U2OS library only screen β -catenin nuc/cyt Ratio Up**
UBWD – **U2OS library only screen Whole cell β -catenin intensity Down**

4.4.3. Reconfirmation of UA primary screen hits

All 164 secondary esiRNAs were co-transfected with APC esiRNA to be re-assayed in the eGFP- β -catenin U2OS cells with methods identical to that of the primary UA screen. Figures 4.21 and 4.22 display the data for β -catenin nuc/cyt ratio and β -catenin whole cell levels respectively for all 164 esiRNA. For clarity, the esiRNAs that were originally identified from the UA primary screen (96 esiRNAs for 94 genes, 2 esiRNA for KIAA0280 and RBX1) are extracted, with their reconfirmation data tabulated in Table 4.12. esiRNAs that increased or decreased β -catenin nuclear:cytosolic ratios and whole cell levels by 2 or 1.5 standard deviations of control means respectively were considered as reconfirming in this secondary screen. Stringent Bonferroni adjusted P-values were selected for ascertaining significance to improve the confidence that the esiRNAs had reconfirmed given the small number of controls that were able to be tested alongside the sublibrary. Table 4.12 display the esiRNAs that were identified in the original UA screen along with their reconfirmation data and associated P-values in addition to an indication of their reconfirmation status. 31/96 esiRNAs (corresponding to 30 genes due to 2 esiRNA for KIAA0280) were considered having reconfirmed and promising candidates for further validation assays (Table 4.12). A further 9 were borderline where they did have an effect on β -catenin but either weren't significant or had an effect on a different parameter than when it was first identified e.g. EPHA3 where it resulted in decreased nuc/cyt ratio in the primary screen but resulted in decreased β -catenin whole cell levels in the reconfirmation assay instead. Taken together the reconfirmatory rate for this screen was 42%.

Table 4.12 Reconfirmation of esiRNAs that modulated β -catenin accumulation and nuclear localisation in the UA primary imaging screen with secondary esiRNA

esiRNA	Primary screen effect on β -catenin (All screens)	β -catenin Nuc/Cell Intensity	p-value	β -catenin whole cell intensity	p-value	Reconfirmation status
ABCB9	UAWU	1.0367	6.77E-03	1.1691	9.95E-03	+
ACOT11	UARD	0.9643	1.96E-03	0.8294	1.23E-05	++
ACOT8	UAWU	1.0102	5.04E-01	1.0620	2.69E-01	-
ADORA3	UARD	1.0337	3.93E-07	1.1121	1.37E-03	-
AIP	UARU,UAWU,UBWU	0.9485	3.65E-07	0.8098	5.32E-07	-
ANK2	UARU,UAWU,UBWU	0.9350	1.02E-06	0.6697	3.59E-07	-
ATOH8	UARU,UAWU	1.0186	1.90E-01	1.0680	1.96E-01	-
BPIL1	UAWU	0.9695	8.96E-04	0.9087	2.54E-04	-
BRD4	UARU,UAWU	1.0732	4.47E-04	1.5890	1.47E-03	+
C1orf34	UARD	1.0258	7.57E-02	1.0743	9.14E-02	-
CD40	UAWU,UBRU,UBWU	0.9854	7.09E-02	0.9277	6.29E-02	-
CDCA2	UARD	0.9559	1.02E-04	0.7427	7.47E-15	++
CDH20	UARD	1.0339	1.41E-01	1.0862	2.84E-01	-
CEACAM8	UARD, UAWD	0.9754	2.14E-01	0.6957	2.58E-04	++
CST4	UAWU	1.0583	1.74E-06	1.3477	8.56E-06	++
DTX4	UARD	0.9650	6.42E-03	0.8249	1.15E-03	+
DUSP13	UAWU	0.9674	4.30E-02	0.8307	2.80E-02	-
EPHA3	UARD	0.9813	8.71E-02	0.7125	2.13E-08	+/-
FBXO41	UARU,UAWU,UBRU,UBWU	1.0309	1.12E-01	1.0887	2.46E-02	-
FBXW11	UARU	1.0261	1.67E-02	1.0907	2.65E-03	-
FLJ20273	UARU	0.9874	8.76E-02	1.1501	1.28E-04	+/-
GAS8	UAWU,UBRU,UBWU	1.0239	2.32E-02	1.1103	7.72E-03	-
GJB3	UAWU,UBWU	0.9944	2.12E-01	1.0165	5.30E-01	-
GNG12	UAWD	0.9874	3.76E-02	0.8496	2.77E-05	++
GPIAP1	UAWU	0.9985	8.39E-01	1.0157	7.37E-01	-
GPR37L1	UAWU,UBWU	1.0219	1.18E-01	0.9683	4.90E-01	-
HECW1	UAWD	0.9560	1.17E-04	0.8160	1.92E-05	++
HERPUD2	UAWU	1.0208	3.14E-02	1.0793	1.24E-01	-
HNRPH1	HWU,UARU,UAWU,UBRU,UBWU	1.0740	1.13E-03	1.2389	1.49E-03	+
HOXA1	UARU,UAWU,UBRU,UBWU	1.0336	2.78E-03	1.0559	8.21E-02	+/-
ISOC2	UAWU,UBRU,UBWU	1.0118	4.21E-01	1.0450	2.85E-01	-
ITGA5	UARD	0.9572	2.14E-02	0.8681	2.57E-02	+
KCNN2	UAWD (UARD)	1.0019	3.08E-06	1.3225	3.08E-06	-
KCNRG	UARU,UAWU,UBRU,UBWU	1.0143	3.08E-06	1.0655	3.08E-06	-
KIAA0280	UARU,UAWU,UBRU,UBWU	1.0441	4.56E-03	1.3361	5.36E-05	++
KIAA0280	UARU,UAWU,UBRU,UBWU	1.0596	2.80E-04	1.6697	1.00E-05	++
KIAA0789	UARU (UBRU)	0.9693	3.85E-02	0.7362	1.65E-05	-
KPNA2	UARD	0.9916	1.45E-01	0.8911	2.54E-05	+/-
LOC114984	UARU,UAWU,UBWU	1.0245	9.54E-03	1.1469	1.45E-03	+
LSP1	UARU	0.9496	6.84E-01	1.3089	1.15E-01	+/-
MCPH1	UAWU,UBRU,UBWU	0.9821	3.08E-06	0.8420	3.08E-06	-
NAP1L5	UARU	0.9330	3.08E-06	0.6748	3.21E-06	-
NFKB1	UAWD	1.0290	7.96E-03	0.9071	6.10E-05	++
NHP2L1	HWU, UAWU,UBRU,UBWU	0.9985	3.08E-06	1.1191	3.08E-06	++
Notch4	UAWU,UBRU,UBWU	1.0027	3.08E-06	0.9527	3.08E-06	-
NRXN1	UARU	1.0338	5.10E-02	1.0630	1.86E-01	+
NUTF2	UARU	0.9674	1.00E-05	0.8063	1.01E-06	-
OGN	UARD, UAWD	1.0098	1.25E-01	0.9426	1.12E-02	-
PARP15	UAWD	1.0337	6.04E-03	1.2886	3.68E-05	-
PCCB	UARU	1.0044	7.08E-01	0.9811	6.35E-01	-
PCSK6	UARD	0.9230	3.36E-06	0.7001	2.63E-08	++
PHF12	UARD	1.0519	2.51E-03	1.2042	1.57E-02	-
PIGS	UARU, UAWU,UBRU	0.9818	5.68E-04	0.8917	9.25E-08	-
PIN1	UAWU	1.0251	1.61E-02	0.9793	7.99E-01	-
PIWIL2	UARD	0.9713	1.35E-02	0.8817	1.34E-02	+
PLEC1	UAWU	1.0392	8.29E-03	1.0321	3.49E-01	-
PLP1	UARD	0.9814	9.27E-02	0.8252	3.42E-05	+/-
PNRC2	UARD, UAWD	0.9964	7.46E-01	0.9190	4.77E-02	-
PRIM2A	UARD	0.9859	7.64E-03	0.8415	1.19E-04	+/-
PROK1	UAWU	1.0461	1.27E-01	1.2723	1.68E-01	+/-
PSMA7	UARU	1.0817	1.66E-02	1.0679	1.94E-01	+
PSMD1	HWU, UARU, UAWU,UBRU,UBWU	1.1396	4.30E-07	1.4514	3.99E-04	++
PSMD12	UARU, UAWU	0.9715	7.34E-04	0.8841	2.94E-04	-
PSMD3	UARU, UAWU	1.0672	1.03E-03	1.3957	1.01E-03	+

PSMD7	HWU, UAWU (UARU)	0.9506	1.00E-05	0.8122	6.20E-07	-
PSMD8	UAWU, UBWU (UARU)	1.1315	2.91E-06	1.6803	6.23E-09	++
PTGER2	UAWD	0.9535	6.55E-06	0.8507	3.99E-04	+
RBL2	UAWD, UBWD	0.8547	2.11E-01	0.8050	9.68E-02	+/-
RBX1	UAWU	0.9989	9.05E-01	0.9471	2.13E-01	-
RBX1	UAWU	1.0052	5.83E-01	0.9976	9.53E-01	-
RND1	UARD	1.0435	9.52E-05	1.3126	2.17E-04	-
RNF2	UARD	1.0629	7.27E-04	1.1304	1.15E-03	-
SEC24D	UAWD	1.0725	3.78E-03	0.9567	6.41E-01	-
SEC61A1	UARD	1.0365	4.78E-04	1.2233	2.88E-04	-
SEMA3B	UAWU, UBRU, UBWU	1.0487	8.87E-04	1.3984	3.06E-05	++
SEMA4F	UARD	1.0098	3.33E-01	0.9399	3.60E-02	-
SIAHBP1	UAWU	0.9836	4.56E-02	0.9482	1.27E-01	-
SLC22A2	UARD	0.9703	4.97E-04	0.9718	1.80E-01	+
SLITRK2	UARD, UAWD	1.0039	4.28E-01	1.0416	1.11E-01	-
SLU7	UARU, UAWU	1.0245	3.59E-02	1.0217	4.75E-01	-
SMAD1	UAWD	0.9845	9.72E-02	1.0644	7.98E-02	-
SPEN	UAWU	0.9466	5.18E-03	0.7452	9.34E-05	-
SREBF1	UBWU (UAWU)	0.9553	2.17E-04	0.9074	4.08E-03	-
SULT1C1	UAWU, UBRU, UBWU	1.0126	2.31E-01	1.0977	8.99E-02	-
SUMF1	UAWU	0.9631	1.13E-03	0.8953	1.43E-03	-
TAF1A	UARU, UAWU	0.9841	1.69E-01	0.9101	8.08E-02	-
THSD7A	UAWD	0.9808	8.95E-03	0.8633	9.27E-05	++
TNIP3	UARD, UAWU	1.0010	8.87E-01	1.0514	1.21E-01	-
TRPC5	UARD, UAWD	0.9560	7.62E-07	0.8038	1.43E-07	++
TUB	UARU	0.9460	3.38E-05	0.8369	1.02E-04	-
TWSG1	UAWD	0.9679	6.21E-05	0.8435	5.67E-09	++
USP18	UAWD	0.9917	3.12E-01	0.9643	9.99E-02	-
VCP1P1	UAWD	0.9333	9.51E-05	0.6278	7.24E-07	++
ZIK1	UARD	1.0009	3.08E-06	1.1009	3.08E-06	-
ZNF131	UARD, UAWD, UBWD	0.9625	1.56E-04	0.7980	4.76E-08	++
ZNF167	UARD	1.0307	1.81E-02	1.0400	4.50E-01	-
Control		1.0000		1.0000		
APC		1.02066	1.31E-05	1.0676	1.18E-05	
CTNNB1		0.88068	3.19E-44	0.5499	5.58E-61	

Table 4.12 Reconfirmation of esiRNAs that modulated β -catenin accumulation and nuclear localisation in the UA primary imaging screen with secondary esiRNA.

Legend overleaf

Summary of Figures 4.21 and 4.22 displaying the reconfirmation efforts of a subset of 'hits' from the primary UA screen. EsiRNA that resulted in β -catenin nuc/cyt ratios and whole cell intensities >2 or <-1.5 standard deviations from the control are coloured green and pink respectively. Associated p-values are displayed (two-tailed independent samples t-test) in addition to a reference to their reconfirmation status. "-" and "+" or "++" represent negative and positive reconfirmation respectively. "-/+" represents esiRNAs that were deemed weak/borderline reconfirmed candidates.

The esiRNAs original effects in the UA screen in addition to any effects in the U2OS (library only) and 7df3 screens are indicated with the coding as follows:

H = 7DF3 Screen

UA = U2OS APC screen

UB = U2OS (library only) screen

W = whole cell β -catenin intensity

R = Ratio of nuclear to cytosolic β -catenin

D= downregulated β -catenin

U= upregulated β -catenin

e.g. UBRU - U2OS library only screen β -catenin nuc/cyt Ratio Up

UBWD – U2OS library only screen Whole cell β -catenin intensity Down

4.4.4 Reconfirmation Summary

The esiRNAs that were considered to have reconfirmed and borderline were combined, resulting in a final list of 81 esiRNAs representing 80 genes (as both esiRNAs against KIAA0280 reconfirmed) (Table 4.13). These include esiRNAs that reconfirmed in more than one screening assay, which are highlighted in red. Therefore, overall, the reconfirmation rate in the secondary assays was approximately 49% (81/164 secondary esiRNAs tested), which was higher than that of the reconfirmation rate of the TCF-dependent luciferase screen, at 30% (Data not shown) and that of a published Wnt screen [242]. The difference in reconfirmatory rates between the 3 assays (H. UA and UB) may be a reflection of the strength of each particular assay in identifying up or down regulators of β -catenin and the number of ‘up’ and ‘down’ hits chosen for reconfirmation in each particular assay. The particularly low reconfirmation rate in the 7df3 cell line is likely to be due to the cells unresponsiveness to β -estradiol treatment at the time (i.e. activation of the Wnt pathway) with repeat assays merited once the issue is rectified. The secondary esiRNAs were required to be generated from non-overlapping sequences to that used to produce the primary library. In some cases sub optimal sequences may have had to be used to ensure this, which could have resulted in less potent esiRNAs. Therefore, low reconfirmation rates is as likely to be due to a failure in confirming true hits as the labelling of false hits.

Many of the esiRNAs that did not reconfirm in the screening assay in which they were originally identified did have an effect in one or both of the other reconfirmatory assays. While these are not included in the final reconfirmation rate a summary table displaying the effect of each secondary esiRNA in all three screens is included in Appendix B, Table 28. Given time and resources, tertiary reconfirmatory experiments would have been undertaken, such as utilising chemically synthesised siRNA against the subset above and repeating the assays in the standard (not expressing eGFP- β -catenin) U2OS cell line and staining for endogenous β -catenin to further validate the regulators identified, prior to undertaking mechanistic studies on a select few.

esiRNA	Gene name	Function/ Description	Primary screen effect on β -catenin (All screens)	Reconfirmation status
ABCB9	ATP-binding cassette sub-family B member 9	ATP-dependent peptide transporter	UAWU	+
ACOT11	acyl-CoA thioesterase 11	Catalyses the conversion of activated fatty acids to the corresponding non-esterified fatty acid and coenzyme A	UARD	++
ARAF	Proto-oncogene A-Raf	Ser/Thr protein kinase involved in the transduction of mitogenic signals from the cell membrane to the nucleus	UBWU	+/-
ARHGAP21	Rho GTPase activating protein 21	RHOA and CDC42 GAP. Downstream partner of ARF1 and required for CTNNA1 recruitment to adherens junctions	HRD, HWU	+/-
BRD2	bromodomain containing 2	Transcriptional regulator that associates with acetylated chromatin during mitosis.	UBRU,UBWU	+
BRD4	bromodomain containing 4	Plays a role in a process governing chromosomal dynamics during mitosis (By similarity).	UARU,UAWU	+
C20orf67	PDX1 C-terminal inhibiting factor 1	May play a role in transcription elongation or in coupling transcription to pre-mRNA processing	UBWU	++
CD40	CD40 molecule, TNF receptor superfamily member 5	Mediates a broad variety of immune and inflammatory responses	UAWU,UBRU,UBWU	+
CDCA2	cell division cycle associated 2	Regulator of chromosome structure during mitosis	UARD	++
CDH2	cadherin 2, type 1, N-cadherin (neuronal)	Cell adhesion protein that functions during gastrulation and is required for establishment of left-right asymmetry.	HRU	++
CEACAM8	carcinoembryonic antigen-related cell adhesion molecule 8	Single chain, GPI-anchored, highly glycosylated protein	UARD, UAWD	++
COPE	coatamer protein complex, subunit epsilon	Mediates biosynthetic protein transport from the ER, via the Golgi up to the trans Golgi network.	UBWU	++
CST4	cystatin 5	Inhibits papain and ficin, partially inhibits stem bromelain and bovine cathepsin c	UAWU	++
DCHS2	dachsous 2 (Drosophila)	Calcium-dependent cell-adhesion protein (By similarity)	UBRU	+
DHDH	dihydrodiol dehydrogenase (dimeric)	Member of dihydrodiol dehydrogenase family involved in the metabolism of xenobiotics and sugars.	UBRU, UBWU	+
DTX1	deltex homolog 1 (Drosophila)	Positive regulator of the Notch-signaling pathway in Drosophila.	UBRU, UBWU	++
DTX4	deltex homolog 4 (Drosophila)	Regulator of Notch signaling (By similarity)	UARD	+
EFNA4	ephrin-A4	Receptor protein-tyrosine kinase implicated in mediating developmental events, especially in the nervous system and in erythropoiesis.	UBWU	+
EPHA3	EPH receptor A3	Receptor for members of the ephrin-A family. EPH and EPH-related receptors have been implicated in mediating developmental events, particularly in the nervous system.	UARD	+/-
FBXO41	F-box protein 41	Substrate-recognition component of the SCF (SKP1-CUL1-F-box protein)-type E3 ubiquitin ligase complex (By similarity).	UARU,UAWU,UBRU,UBWU	+
FLJ20273	RNA binding motif protein 47	Contains three RRM (RNA Recognition motifs) domains	UARU	+/-
FOXP4	forkhead box P4	Belongs to subfamily P of the forkhead box (FOX) transcription factor family	UBRU, UBWU	++
GAS8	growth arrest-specific 8	Cytoskeletal linker which binds microtubules and probably functions in axonemal and non-axonemal dynein regulation	UAWU, UBRU, UBWU	+
GJB3	gap junction protein, beta 3, 31kDa	A component of gap junctions	UAWU, UBWU	++

GNG12	guanine nucleotide binding protein (G protein), gamma 12	G proteins are involved as a modulator or transducer in various transmembrane signaling systems. The beta and gamma chains are required for GTPase activity	UAWD	++
GPR37L1	G protein-coupled receptor 37 like 1	Orphan receptor, Expressed in the central nervous system.	UAWU, UBWU	+
HECW1	HECT, C2 and WW domain containing E3 ubiquitin protein ligase 1	E3 ubiquitin-protein ligase that mediates ubiquitination and subsequent degradation of DVL1	UAWD	++
HNRPH1	heterogeneous nuclear ribonucleoprotein H1	RNA binding protein. Mediates pre-mRNA alternative splicing regulation.	HWU, UARU, UAWU, UBRU, UBWU	+
HOXA1	homeobox A1	Sequence-specific transcription factor - part of a developmental regulatory system that provides cells with specific positional identities on the anterior-posterior axis	UARU, UAWU, UBRU, UBWU	+/-
ISOC2	isochorismatase domain containing 2	Interacts with CDKN2A	UAWU, UBRU, UBWU	+
ITGA5	integrin, alpha 5 (fibronectin receptor, alpha polypeptide)	Receptor for fibronectin and fibrinogen. Participate in cell-surface mediated signalling and adhesion.	UARD	+
JMJD6	jumonji domain containing 6	Dioxygenase - acts as a histone arginine demethylase and a lysyl-hydroxylase. May act as a RNA hydroxylase. Required for differentiation of multiple organs during embryogenesis.	UBWU	+
KIAA0280	Tongue cancer chemotherapy resistance-associated protein 1	Belongs to the FAM168 protein family	UARU, UAWU, UBRU, UBWU	++
KIAA0280	Tongue cancer chemotherapy resistance-associated protein 1	Belongs to the FAM168 protein family	UARU, UAWU, UBRU, UBWU	++
KIAA0789	WSC domain containing 2	Potential single pass membrane protein	UARU (UBRU)	+
KLK8/P	kallikrein-related peptidase 8	Serine protease, capable of degrading a number of proteins such as casein, fibrinogen, kininogen, fibronectin and collagen type IV.	UBWU	++
KPNA2	karyopherin alpha 2 (RAG cohort 1, importin alpha 1)	Functions in nuclear protein import as an adapter protein for nuclear receptor KPNB1	UARD	+/-
LOC114984	FLYWCH family member 2	Phosphoprotein	UARU, UAWU, UBWU	+
LRRC4	leucine rich repeat containing 4	Synaptic adhesion protein. Regulates the formation of excitatory synapses through the recruitment of pre-and-postsynaptic proteins.	UBRU, UBWU	+
LSP1	lymphocyte-specific protein 1	F-actin binding protein. May regulate neutrophil motility, adhesion to fibrinogen matrix proteins, and transendothelial migration.	UARU	+/-
MAGOH	mago-nashi homolog, proliferation-associated (Drosophila)	Component of a splicing-dependent multiprotein exon junction complex (EJC) deposited at splice junction on mRNAs.	HWD	+
MAX	MYC associated factor X	Transcription regulator - The MYC-MAX complex is a transcriptional activator.	HRD	+/-
MCPH1	microcephalin 1	Implicated in chromosome condensation and DNA damage induced cellular responses.	UAWU, UBRU, UBWU	++
MGP	matrix Gla protein	Associates with the organic matrix of bone and cartilage. Thought to act as an inhibitor of bone formation	UBWU	+/-
MICAL1	microtubule associated monooxygenase, calponin and LIM domain containing 1	May be a cytoskeletal regulator that connects NEDD9 to intermediate filaments	UBRU, UBWU	++
NFKB1	nuclear factor of kappa light polypeptide gene enhancer in B-cells 1	NF-kappa-B is a pleiotropic transcription factor involved in inflammation, immunity, differentiation, cell growth, tumorigenesis and apoptosis.	UAWD	++
NHP2L1	NHP2 non-histone chromosome protein 2-	Binds to the 5'-stem-loop of U4 snRNA and may play a role in the late stage of spliceosome assembly.	HWU, UAWU, UBRU, UBWU	++

	like 1 (<i>S. cerevisiae</i>)			
Notch4	Notch 4	Functions as a receptor for membrane-bound ligands Jagged1, Jagged2 and Delta1 to regulate cell-fate determination.	UAWU, UBRU, UBWU	++
NRXN1	neurexin 1	Neuronal cell surface protein that may be involved in cell recognition and cell adhesion by forming intracellular junctions through binding to neuroligins.	UARU	+
NRXN2	neurexin 2	Neuronal cell surface protein that may be involved in cell recognition and cell adhesion	UBRU	++
PCSK6	proprotein convertase subtilisin/kexin type 6	An endoprotease within the constitutive secretory pathway	UARD	++
PCYT2	phosphate cytidylyltransferase 2, ethanolamine	Enzyme that catalyzes the formation of CDP-ethanolamine from CTP and phosphoethanolamine in phospholipid synthesis.	UBRU	+
PIWIL2	piwi-like 2 (<i>Drosophila</i>)	Functions in development and maintenance of germline stem cells.	UARD	+
PLP1	proteolipid protein 1	Role in the formation or maintenance of the multilamellar structure of myelin	UARD	+/-
PRIM2A	primase, DNA, polypeptide 2	Polymerase that synthesizes small RNA primers for the Okazaki fragments made during discontinuous DNA replication	UARD	+/-
PROK1	prokineticin 1	Potently contracts gastrointestinal (GI) smooth muscle. Induces proliferation, migration and fenestration (the formation of membrane discontinuities) in capillary endothelial cells derived from endocrine glands.	UAWU	+/-
PRPF40B	PRP40 pre-mRNA processing factor 40 homolog B (<i>S. cerevisiae</i>)	May be involved in pre-mRNA splicing	UBWU	+
PSMA7	proteasome (prosome, macropain) subunit, alpha type, 7	A 20S core alpha subunit of proteasome	UARU	+
PSMC6	proteasome (prosome, macropain) 26S subunit, ATPase, 6	The 26S protease is involved in the ATP-dependent degradation of ubiquitinated proteins. The regulatory (or ATPase) complex confers ATP dependency and substrate specificity to the 26S complex	HWU	+
PSMD1	proteasome (prosome, macropain) 26S subunit, non-ATPase, 1	Acts as a regulatory subunit of the 26 proteasome which is involved in the ATP dependent degradation of ubiquitinated proteins	HWU, UARU, UAWU, UBRU, UBWU	++
PSMD3	proteasome (prosome, macropain) 26S subunit, non-ATPase, 3	Acts as a regulatory subunit of the 26 proteasome which is involved in the ATP-dependent degradation of ubiquitinated proteins	UARU, UAWU	+
PSMD6	proteasome (prosome, macropain) 26S subunit, non-ATPase, 6	Acts as a regulatory subunit of the 26S proteasome which is involved in the ATP-dependent degradation of ubiquitinated proteins	HWU	+
PSMD8	proteasome (prosome, macropain) 26S subunit, non-ATPase, 8	Acts as a regulatory subunit of the 26S proteasome which is involved in the ATP-dependent degradation of ubiquitinated proteins. Necessary for activation of the CDC28 kinase	UAWU, UBWU (UARU)	++
PTGER2	prostaglandin E receptor 2 (subtype EP2), 53kDa	Receptor for prostaglandin E2 (PGE2)	UAWD	+
RBL2	retinoblastoma-like 2 (p130)	Key regulator of entry into cell division. Binds to cyclins A and E. May act as a tumor suppressor	UAWD, UBWD	+/-
SAMD4A	sterile alpha motif domain containing 4A	Acts as a translational repressor of SRE-containing messengers	HRD	+
SEMA3B	sema domain, immunoglobulin domain (Ig), short basic domain, secreted,	Important in axonal guidance and has been shown to act as a tumor suppressor by inducing apoptosis	UAWU, UBRU, UBWU	++
SLC22A2	(semaphorin) 3B	Polyspecific organic cation transporter in the liver, kidney, intestine, and other organs. Involved in elimination of endogenous small organic cations and environmental toxins	UARD	+

SNRPD2	small nuclear ribonucleoprotein D2 polypeptide 16.5kDa	Required for pre-mRNA splicing. Required for snRNP biogenesis	HRU, HWU	+
SPRED1	sprouty-related, EVH1 domain containing 1	Tyrosine kinase substrate that inhibits growth-factor-mediated activation of MAP kinase.	HRU	+
SREBF1	sterol regulatory element binding transcription factor 1	Transcriptional activator required for lipid homeostasis. Regulates transcription of the LDL receptor gene and binds to the sterol regulatory element 1 (SRE-1)	UBWU (UAWU)	+
SULT1C1	sulfotransferase family, cytosolic, 1C, member 2	Catalyzes the sulfate conjugation of many drugs, xenobiotic compounds, hormones, and neurotransmitters.	UAWU, UBRU, UBWU	+
THSD7A	thrombospondin, type I, domain containing 7A	appears to interact with alpha(V)beta(3) integrin and paxillin to inhibit endothelial cell migration and tube formation. May be involved in cytoskeletal organization.	UAWD	++
TNIP2	TNFAIP3 interacting protein 2	Inhibits NF-kappa-B activation by blocking the interaction of RIPK1 with its downstream effector IKK β	UBRU, UBWU	+
TRAPPC4	Trafficking protein particle complex subunit 4	May play a role in vesicular transport from endoplasmic reticulum to Golgi.	HWU	+
TRPC5	transient receptor potential cation channel, subfamily C, member 5	A receptor-activated, non-selective calcium permeant cation channel	UARD, UAWD	++
TWSG1	Twisted gastrulation protein homolog 1	May be involved in dorsoventral axis formation. Antagonizes BMP signaling.	UAWD	++
USP32	ubiquitin specific peptidase 32	Thiol-dependent hydrolysis of ester, thioester, amide, peptide and isopeptide bonds formed by the C-terminal Gly of ubiquitin	UBRU, UBWU	+
VCPIP1	valosin containing protein (p97)/p47 complex interacting protein 1	Acts as a deubiquitinating enzyme. Necessary for VCP-mediated reassembly of Golgi stacks after mitosis	UAWD	++
XPO6	exportin 6 (RAN binding protein 20)	Mediates the nuclear export of actin and profilin-actin complexes in somatic cells	HRD	+
ZNF131	zinc finger protein 131	May be involved in transcriptional regulation. Plays a role during development and organogenesis as well as in the function of the adult central nervous system (By similarity)	UARD, UAWD, UBWD	++

Table 4.13 49% of selected esiRNAs from the primary screens reconfirmed with secondary non-overlapping esiRNA

Summary table of esiRNAs that reconfirmed in the assays that originally identified them (as denoted by screen codes) '+' denotes strength of reconfirmation with '+/-' representing borderline reconfirmation status. esiRNAs highlighted in red were reconfirmed in more than one assay. Screen codes as used in other reconfirmatory tables. Gene information obtained from Entrez Gene (<http://www.ncbi.nlm.nih.gov/gene>).

4.5 The relationship between β -catenin accumulation, nuclear localisation and TCF-dependent transcription.

As one of the project's objectives was to assess the relationship between β -catenin levels and localisation with TCF-dependent transcription, the correlation between the β -catenin imaging screening data and the previous screen for regulators of TCF dependant transcription (performed by Dr Seipel in the 7df3 cells) was investigated. A distinct lack of a relationship between TCF-dependent transcription and β -catenin levels and localisation on a genome wide scale was demonstrated in both the reporter 7df3 cell line and the U2OS screens (Figure 4.23).

This prompted further investigation into the effect of the 81 reconfirmed esiRNA on TCF-dependent transcription. The entire secondary sublibrary of 164 esiRNAs were assayed in 7df3 reporter cells for their effects on TCF-luciferase (Figure 4.24) with the relationship between β -catenin and TCF-dependent transcription of the **reconfirmed set of 81** secondary esiRNAs (see Table 4.13 for full list) subsequently assessed (Figure 4.25). By assessing only the 81 reconfirmed esiRNA (rather than the 164 esiRNAs in total) the effects of potential false positives on the analysis is minimised.

In the 7df3s, there appeared to be no correlation between TCF-dependent transcription and β -catenin localisation as dictated by its nuclear to cytosolic ratio (black points in Figure 4.25A) alongside a weak positive correlation with β -catenin whole cell levels (4.25B). A stronger positive correlation was observed in the two U2OS cell assays between TCF-dependent transcription and β -catenin nuclear localisation, far stronger than the weak positive correlation observed with β -catenin total levels (Figure 4.25). This is in line with the notion that nuclear accumulation of β -catenin is a better indicator of active transcriptional activity than simply increased levels [196].

Whilst preliminary, this data implies that β -catenin changes are not directly coupled to transcriptional effects, with alterations in β -catenin levels and localisation by the identified modulators either a) unrelated to Wnt signalling or b) necessary for Wnt

signalling but not sufficient, requiring the need for a second signal/modification to induce transcriptional changes. This interesting concept will be discussed in further depth within Chapter 6.

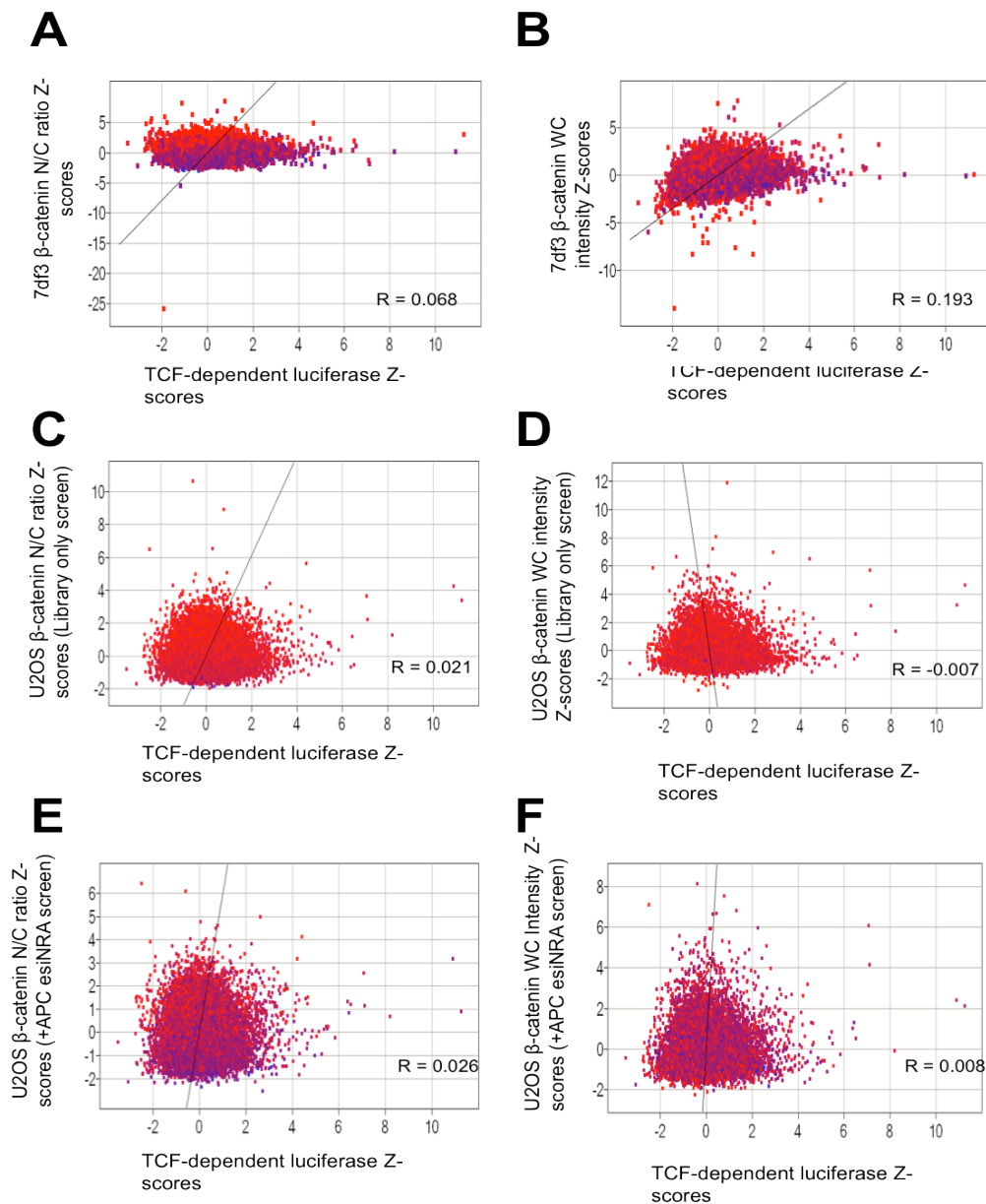


Figure 4.23 No correlation between the primary β -catenin screening data and the primary TCF-dependent transcription screen.

Z-scores of both β -catenin accumulation and localisation parameters in all three β -catenin imaging screens for all esiRNAs are plotted against their corresponding Z-scores in the previous luciferase screen for regulators of TCF-dependent transcription. Scatter plots and associated R-values show weak or no correlation between the β -catenin imaging parameters and luciferase. (A) and (B) represent the H screen data with (C)/(D) and (E)/(F) representing the UB and UA screens respectively. Lines represent orthogonal straight line fit.

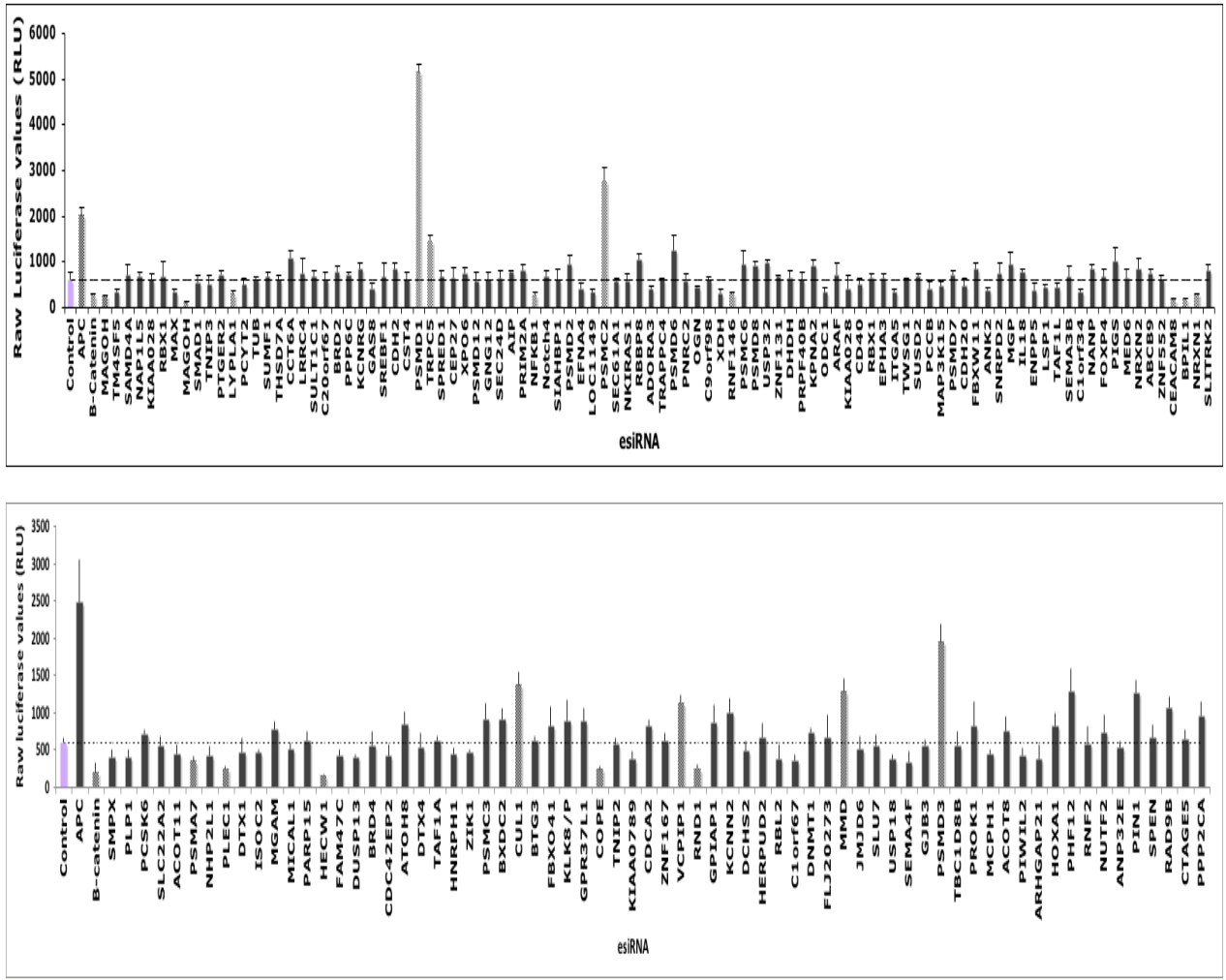


Figure 4.24 Effects of the secondary esiRNA sublibrary on TCF-dependent transcription in 7df3 reporter cells.

The secondary non-overlapping esiRNA sublibrary was reverse-transfected into 7df3 luciferase reporter cells. At 24hrs post transfection the cells were treated with β -estradiol prior to luciferase assay, 48hrs post transfection. Raw luciferase values are displayed (RLU – Relative light units) of all esiRNAs across two plates, which possessed control esiRNA, with β -catenin and APC esiRNA as additional controls. Grey bars represent esiRNAs with p-values <0.05 (two-tailed independent samples t-test). Mean values \pm s.e.m of three triplicate wells per condition displayed of a single experiment. Graphs are provided in Appendix B for clarity and better resolution.

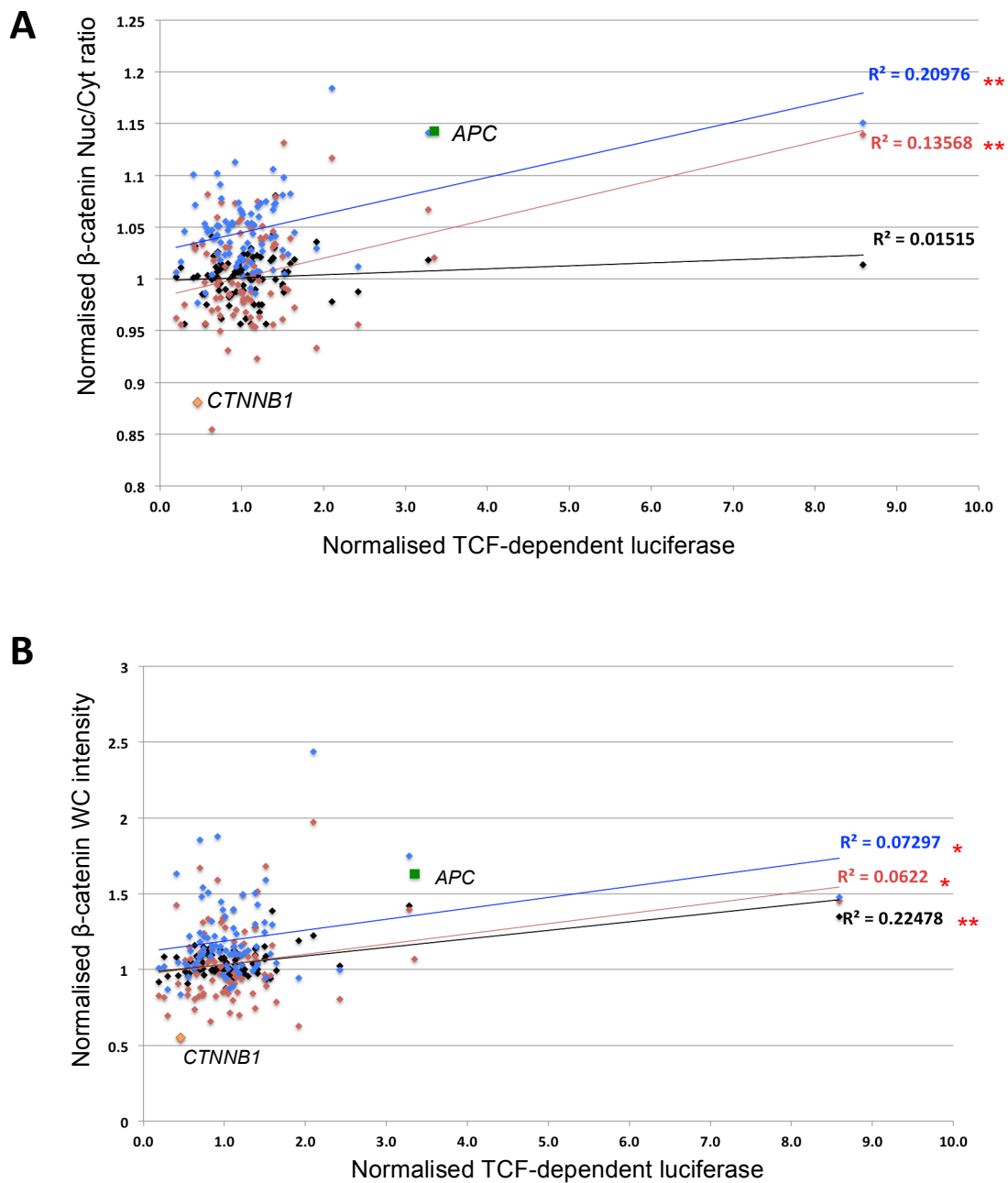


Figure 4.25 Correlation between β -catenin levels, localisation and TCF-dependent transcription in the reconfirmed set of β -catenin regulators

Scatter plot displaying the relationship between the secondary esiRNAs effect on TCF-dependent transcription and β -catenin nuclear:cytosolic ratio (A) and whole cell intensity (B) in the three screening assays. Black points represent assays in 7df3 cells, blue represents assays in the eGFP- β -catenin U2OS cell line with red indicating data from assays in the eGFP- β -catenin U2OS cell line in the presence of downregulated APC (similar to the UA screen). R2 values are displayed, in addition to lines of the appropriate colour representing orthogonal straight line fit. * $p < 0.05$, ** $p < 0.001$ (Pearson's correlation coefficient, two tailed). Mean values are of at least $n=2$ independent experiments (of triplicate wells) for the β -catenin imaging data and $n=1$ luciferase assay of esiRNAs in triplicate wells.

4.6 Comparative analysis of Wnt/ β -catenin siRNA screens in different cell lines to identify modulators of β -catenin and TCF-dependent transcription.

To define a common set of β -catenin modulators that were also implicated in regulating TCF-dependent transcription, different genome-wide RNAi screens for TCF-dependent regulators were compared with the imaging screens undertaken in this study.

Firstly, the degree of overlap between the imaging screens and the previous screen for regulators of TCF-dependant transcription in the reporter 7df3 cells (performed by Dr Seipel) was investigated. esiRNAs that possessed Z-scores of >2 and <-1.5 from the transcriptional screen (745 esiRNAs in total, Appendix B Table 29) was assessed for overlaps with the modulators identified from the H primary screen using the same z-score threshold cut offs (Appendix B, Tables 3 and 4). 70 and 111 esiRNAs from the transcriptional screen overlapped in the datasets for β -catenin nuclear localisation and whole cell levels respectively, with 27 common to all three data sets (Figure 4.26). These relatively low numbers further underlines the lack of a direct correlation between β -catenin levels and localisation with transcriptional output as implied by the genome-scale comparisons undertaken in Figure 4.23. Overlapping esiRNA IDs are provided in Appendix B, Table 30. Additionally, overlaps with both U2OS screens were investigated, which also displayed a distinct lack of common esiRNAs (Figure 4.27, Appendix B Tables 31 and 32 for UB and UA overlaps respectively). Within the U2OS screens there was a greater overlap between esiRNAs that modulated β -catenin nuclear localisation and TCF-dependent transcription compared to the set that had an effect on β -catenin whole cell levels, especially in the UA screen (Figure 4.27B). This is in line with the notion that nuclear accumulation of β -catenin is a better indicator of active transcriptional activity than simply increased levels [196]. Surprisingly, the opposite is observed with the 7df3 set where more esiRNAs overlapped with transcriptional regulators in the set that modulated β -catenin whole cell levels compared to β -catenin nuclear to cytosolic ratio (Figure 4.26). However, as mentioned earlier this particular data set possessed lower than ideal Z-factors for the

assay, which may have resulted in a greater number of false negatives, hence the smaller overlap. Overall, there was a greater degree of overlap between the β -catenin modulators identified in the H screen and the TCF-transcriptional screen within the same cell line (Figure 4.26) compared to that observed with the U2OS screen data sets (Figure 4.27). This again suggests potential cell type specific effects whereby β -catenin is regulated by different modulators in different contexts.

Known β -catenin regulatory components were observed in the overlapping modulators of β -catenin and TCF-dependent transcription such as APC (screens UB, UA), CTNNB1 itself (H, UA,UB), PSMD1 (UA,UB), PSMD12 (UA), RBX1 (UA), CUL1 (H), SIAHBP1 (UB) and RYK (UB). A plethora of ribosomal components were identified in the H and UA screen overlaps with regulators of TCF-dependent transcription (Figure 4.26 and 4.27 B) but intriguingly none were observed in the central overlap in the UB screen (Figure 4.27 A). This screen however was undertaken in the context of very low basal levels of β -catenin whereby identifying downregulators was difficult, which possibly explains the lack of ribosomal components within the modulators identified within this screen. A variety of modulators from a diverse range of biological processes were identified from the overlaps between the screens. Insights from these in terms of β -catenin regulation in the context of activated Wnt signalling and subsequent TCF-dependent transcription will be discussed upon integration with other transcriptional screens, described below.

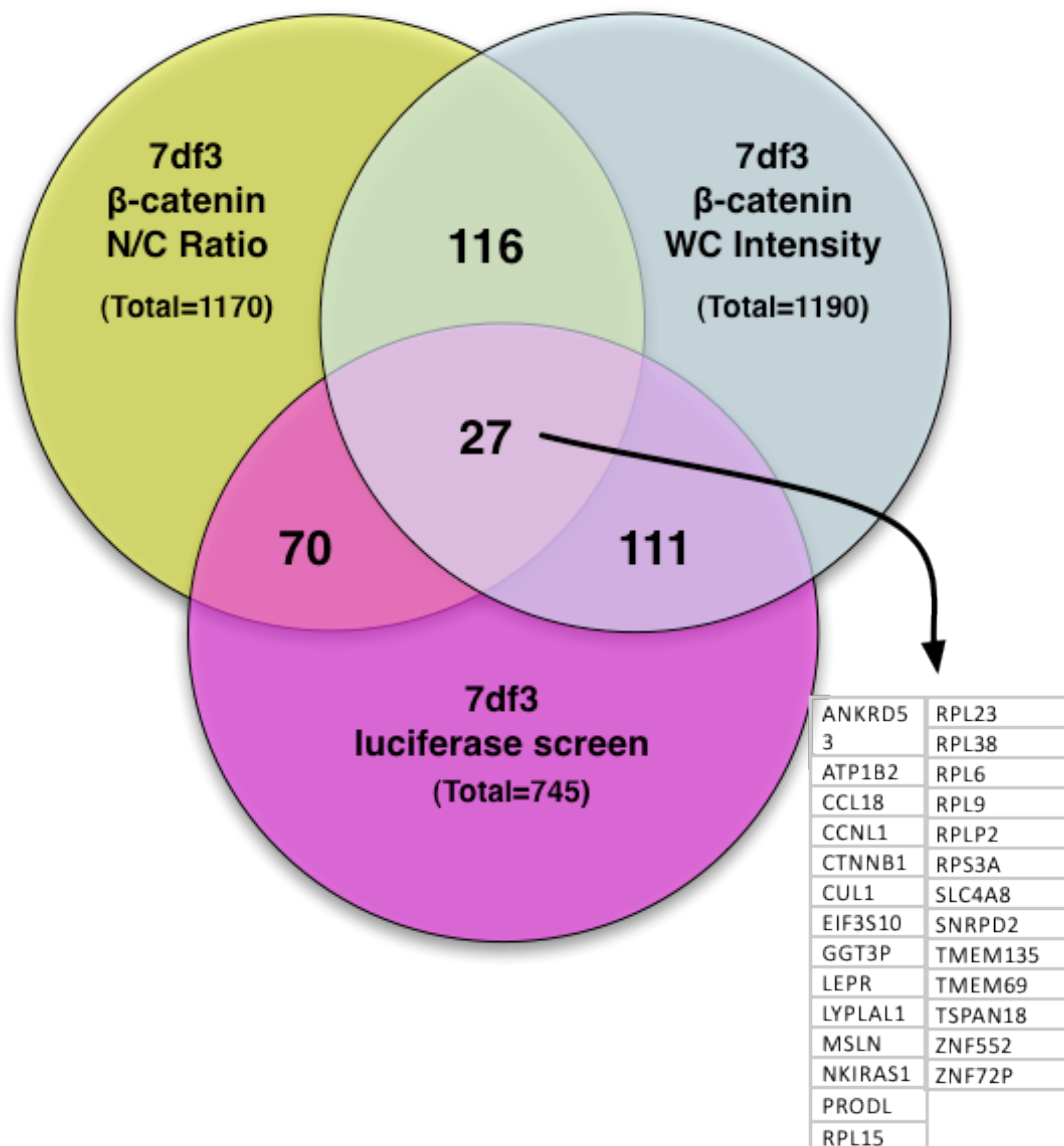


Figure 4.26. Lack of overlap between modulators of β -catenin accumulation and nuclear localisation with TCF-dependent transcription in the H screens.

esiRNAs identified from the H screen with Z-scores of >2 or <-1.5 in both β -catenin nuclear to cytosolic (N/C) ratio and whole cell (WC) intensities that passed the cell toxicity filter were cross-compared with results from a previous screen for regulators of TCF-dependent transcription in the same 7df3 cell line. Numbers of overlapping esiRNAs are indicated with the full overlaps provided in Appendix B, Table 30.

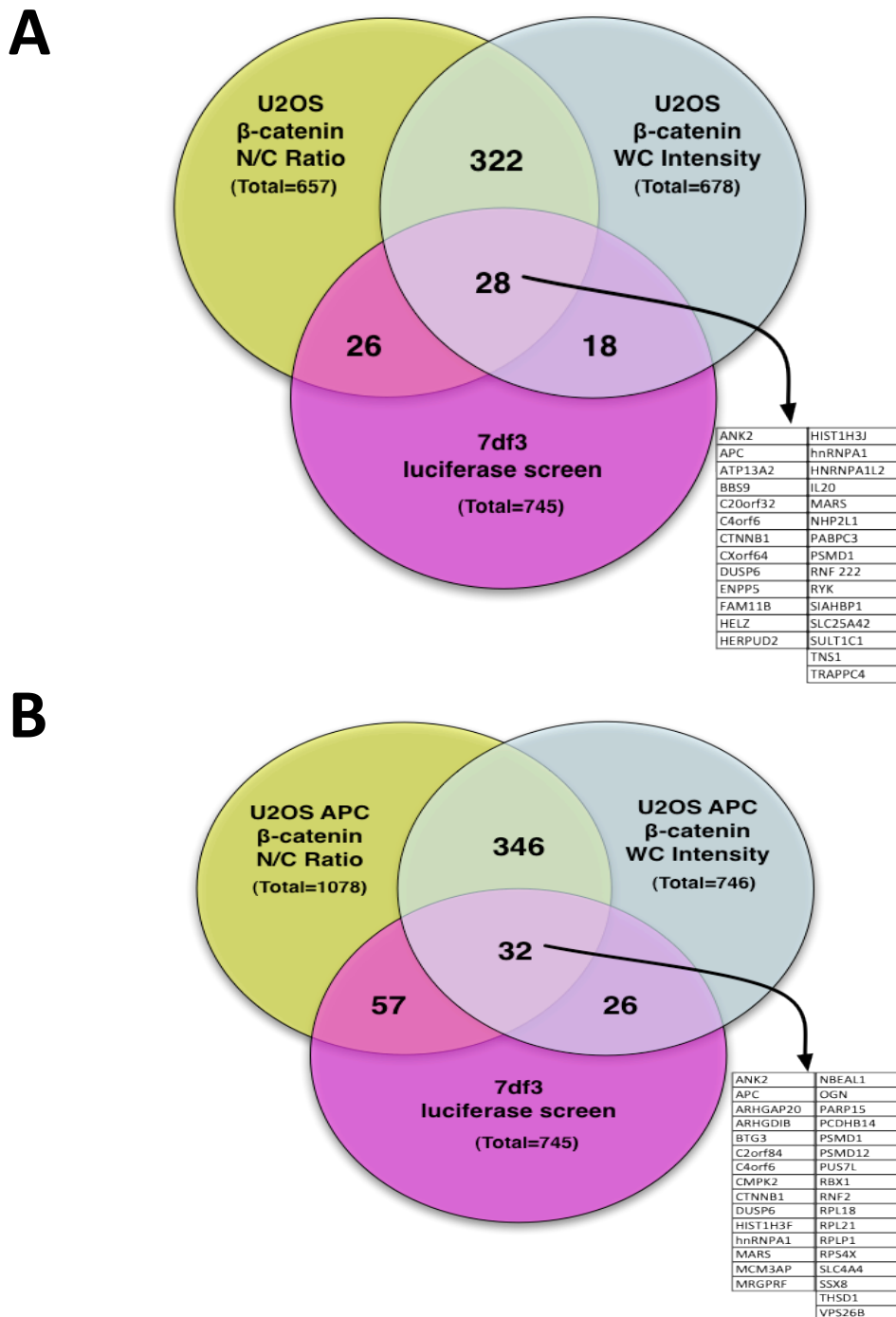


Figure 4.27. Lack of overlap between modulators of β -catenin accumulation and nuclear localisation with TCF-dependent transcription in different U2OS screens.

esiRNAs from the UB (A) and UA (B) screens with Z-scores of >2 or <-1.5 in both β -catenin nuclear to cytosolic (N/C) ratio and whole cell (WC) intensities that passed the cell toxicity filter were cross-compared with results from a previous screen for regulators of TCF-dependent transcription in the 7df3 cell line. Numbers of overlapping esiRNAs are indicated with the full overlaps provided in Appendix B, Table 31 and Table 32 for (A) and (B) respectively.

In order to extend the common set of modulators that couple β -catenin to TCF-transcriptional changes (identified in Figure 4.26 and 4.27) comparative analysis was also undertaken between the H imaging screen and two published genome-wide RNAi screens for regulators of TCF-dependent transcription.

Using the less stringent thresholds set for the previous *in silico* analysis of β -catenin modulators (Appendix B Tables 14 and 15), overlapping genes between the H screen and the TCF-transcriptional screen in the 7df3 reporter cell line were re-extracted, resulting in a larger list of 133 and 174 for β -catenin nuclear localisation and levels respectively (Figure 4.28 and 4.29, Appendix B tables 33 and 34). Additionally, overlaps with two published siRNA screens for regulators of Wnt-3a-induced TCF-dependent transcription in HeLa cervical cancer cells [267] and for endogenous levels of TCF-dependent transcription in DLD-1 colon cancer cells [242] were assessed (Figures 4.28 and 4.29, Appendix B tables 33 and 34). A smaller overlap was observed between the H imaging screen and the siRNA transcriptional screens in HeLa and DLD-1 cells than with the 7df3 transcriptional screen, indicative of cell-type and screen specificity.

In total only seven components were identified in the triple overlap set of regulators between the H screen and published siRNA transcriptional screens including β -catenin itself (CTNNB1). FBXW11 (β -TRCP) is the substrate recognition component of SCF (SKP1-CUL1-F-box protein) E3 ubiquitin-protein ligase complex, which mediates the ubiquitination of β -catenin [85]. PITX2 is a known Wnt target that mediates cellular growth response by activating Cyclin D2 [354]. Interestingly TRIM6 was identified in the regulators of β -catenin nuclear localisation and has a putative role in the recognition of cell compartments [355]. POLR2E encodes the fifth largest and most abundant subunit of RNA polymerase II, which was recently identified as a strong hit in a screen for components of the G₂-M DNA damage checkpoint [356] and is required for hepatocellular carcinoma cell proliferation [357]. This subunit was observed to bind a hepatitis virus transactivating protein, suggesting that interactions between polymerase and transcriptional activators can occur via this subunit [358]. The role of acetyl-Coenzyme A acyltransferase 1 (ACAA1), which encodes an enzyme operative in the beta-oxidation system of peroxisomes, is more

obscure, although it may provide an additional link between Wnt/ β -catenin signalling and the peroxisome proliferator-activated receptor (PPAR) pathway. CSK (c-src tyrosine kinase) has been demonstrated to form a complex with β -catenin at adherens junctions and is involved in the regulation of FYN, a kinase implicated in β -catenin phosphorylation and in controlling vertebrate gastrulation cell movements [224, 359, 360].

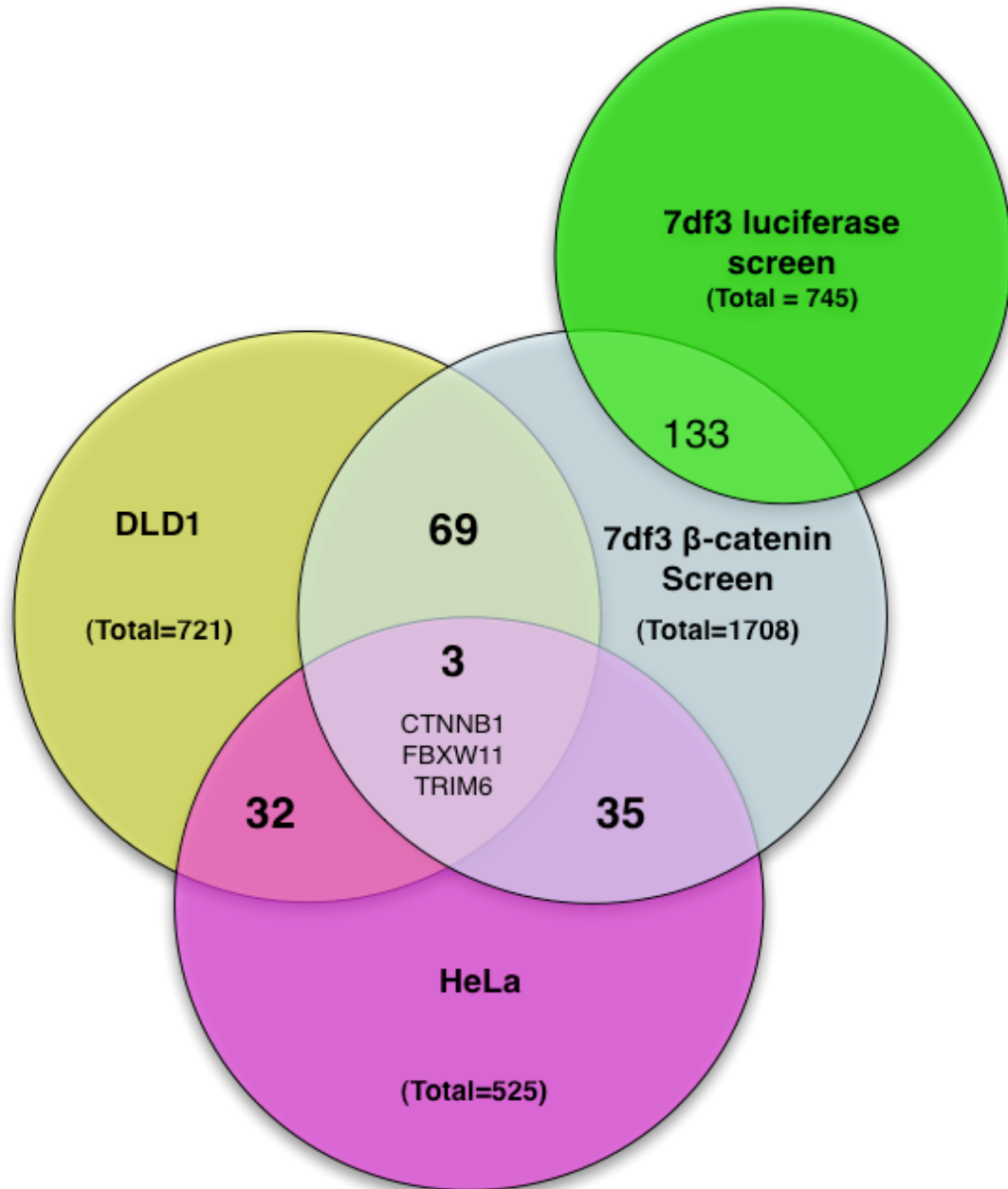


Figure 4.28. Overlapping modulators of β -catenin nuclear localisation with modulators of TCF-dependent transcription in three different cell lines

Hit comparisons in RNA interference screens for β -catenin and Wnt signalling components in different human cell lines. Primary hits of β -catenin nuclear localisation in the 7df3s compared with hits from the transcriptional screens undertaken in the 7df3 (unpublished), HeLa [267] and DLD1 [242] screens. Numbers of overlapping esiRNAs are indicated with the full overlaps provided in Appendix B, Table 33.

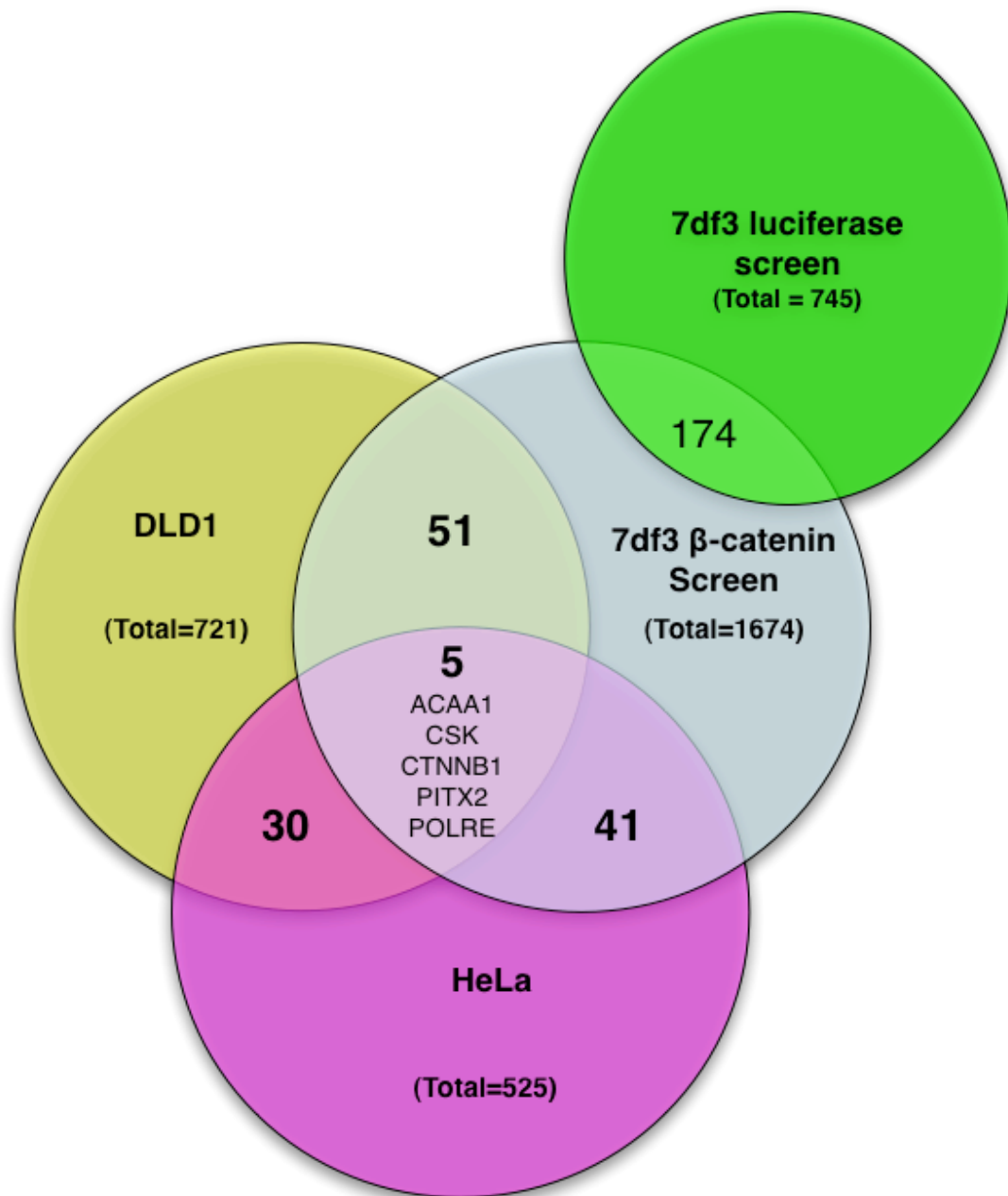


Figure 4.29. Overlapping modulators of β -catenin accumulation (whole cell levels) with modulators of TCF-dependent transcription in three different cell lines

Hit comparisons in RNA interference screens for β -catenin and Wnt signalling components in different human cell lines. Primary hits of β -catenin total levels in the 7df3s were compared with hits from the transcriptional screens undertaken in the 7df3 (unpublished), HeLa [267] and DLD1 [242] screens. Numbers of overlapping esiRNAs are indicated with the full overlaps provided in Appendix B, Table 34.

4.6.1 Integration of functional genomic data

Previous work demonstrated the utility of integrating putative Wnt modulators identified from siRNA screens with proteomic interaction networks to reveal proteins previously un-associated with the Wnt/ β -catenin pathway [242]. Moreover, integrating similar gene data sets were shown to ‘link’ siRNA regulators to other identified modulators and provide mechanistic insights gained through their associations with proteins of known function. A similar approach was applied to the modulators of β -catenin that were identified as hits in several TCF-dependent transcriptional screens identified above, in order to detect interactions that may provide insight into how β -catenin modulation couple to transcriptional changes.

The comparative analysis of various functional genomic screens undertaken above (Figure 4.28 and 4.29) resulted in a list of 511 putative β -catenin modulators that altered TCF-dependent transcription in other systems. These were combined with the esiRNAs from both U2OS screens that overlapped with the TCF-transcriptional screen in the 7df3 cell line (Figure 4.27). This resulted in a list of 698 esiRNAs. Following deletion of duplicates this resulted in a final list of 558 of identified β -catenin modulators that altered TCF-dependent transcription in various systems (Appendix B table 35).

To investigate links between the esi and siRNAs identified above, MetaCore, a knowledge database for pathway and network analysis, was used [303]. This integrated knowledge database is based on a manually curated database of human protein-protein, protein-DNA and protein compound interactions, metabolic and signalling pathways for human, mouse and rat. It allows functional relationships to be represented with genes portrayed as nodes and connections as vertices (edges). Edges represent protein-protein or protein-DNA interactions and provide specific information with regards to the nature of the regulation mediated by an interaction, such as phosphorylation, ubiquitination and transcriptional activation. The information provides a guide in which links between molecules have differing confidence levels dependent upon the number of links between molecules and the nature of the relationship. The open-source software, Cytoscape was used for

visualisation of the network generated by MetaCore [361-363] and is available for download at <http://www.cytoscape.org/download.php>.

A tab-delimited excel list of the identified 558 β -catenin modulators that altered TCF-dependent transcription in other screens (Appendix B table 35) was submitted to the MetaCore database using database default options. The protein-protein/DNA interaction network produced is displayed in Figure 4.30, in addition to being provided as a Cys file in Appendix B (Cys 1 Figure 4.30) to be opened in Cytoscape for visualisation. In the resulting interaction network, of the 558 identified 'hits' (represented as nodes) 215 possessed at least one interaction with another node in a highly connected network of 321 interactions. For clarity, only those nodes with connections are displayed with details of the nature of the interactions (i.e. edges) only visible in the associated Cys file (Legend provided in the associated Word document titled 'Appendix B legends'). The numerous interactions that were detected between the hits identified from the imaging screens (which were also identified in TCF-dependent transcriptional screens) suggest that they may constitute functional units important for the regulation of β -catenin and associated TCF-dependent transcription. 'Hubs' are highly connected nodes (genes/proteins) with β -catenin being the 'convergent' hub of this particular network i.e. the component which possesses the most interactions converging onto it to regulate its activity, such as binding by other proteins to mediate its phosphorylation for instance. This in turn aids the validation of the dataset as identified modulators of β -catenin.

In addition to the clusters of known regulators of Wnt/ β -catenin signalling, such as core Wnt components, proteasomal components and members of the ubiquitin ligase pathway, several other complexes were apparent within the network generated (Figure 4.30). The 'divergent' hub within the network (i.e. the component regulating the most other components within the network) was AP-1, a dimeric transcription factor composed of one protein of the Fos family (c-Fos, FosB, Fra-1) and one protein of the Jun family (c-Jun, JunB and JunD) [364]. Links between AP-1 and Wnt/ β -catenin signalling have previously been demonstrated, with c-Jun suggested to act as a scaffold to mediate the interaction of Dishevelled with TCF-4 and β -catenin at the promoter of Wnt target genes to regulate transcription [365]. β -catenin has been also

been co-immunoprecipitated with c-Jun and c-Fos via its armadillo repeat domain [366] with the interaction of c-Jun with TCF4 reported to be involved in colon cancer cell proliferation [367]. Interestingly, this study suggests a favoured role for junD rather than c-Jun in the regulation of Wnt/ β -catenin. Interestingly, AP-1 signalling is also reported to regulate the transcription of β -catenin, providing an additional layer of complexity in the regulation between these two pathways [364].

Cytokine signalling was also prevalent along with STAT-1, another prominent hub within the network. The JAK/STAT pathway is relevant to Wnt/ β -catenin signalling having been demonstrated to play an important role in eye disc patterning by promoting the formation of the eye field through repressing Wg [368]. Additionally, β -catenin was observed to be downregulated by a JAK2 inhibitor in leukaemia cells, which was mediated by β -Trcp [369]. The link between Wnt and JAK/STAT signalling was further highlighted by the identification of a cluster of protein-protein interactions between JAK/STAT pathway regulators and combined hits from the screen (Fig.4.30) with CHD8 (duplin) shown to repress both STAT and TCF-dependent transcription [370, 371]. SMAD3 was also well connected within the network, having been previously demonstrated to induce nuclear translocation of β -catenin in mesenchymal stem cells in response to TGF- β 1 [329] with its interactions within the network potentially providing additional insights into its precise mechanism.

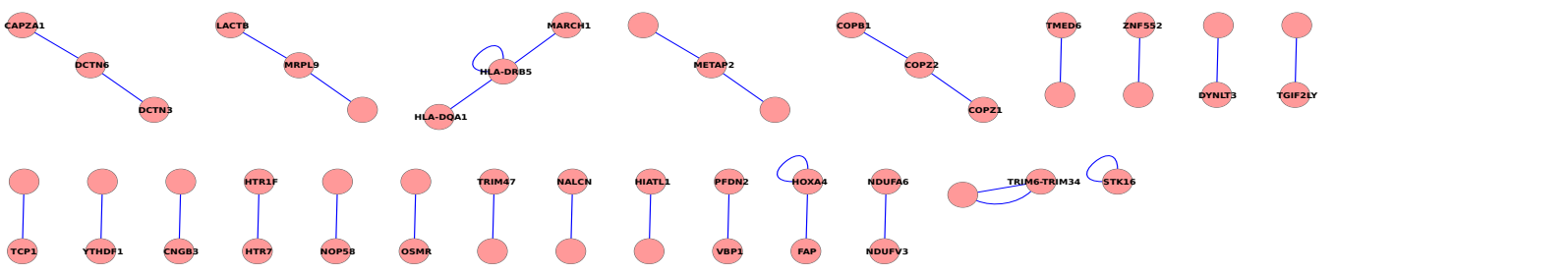
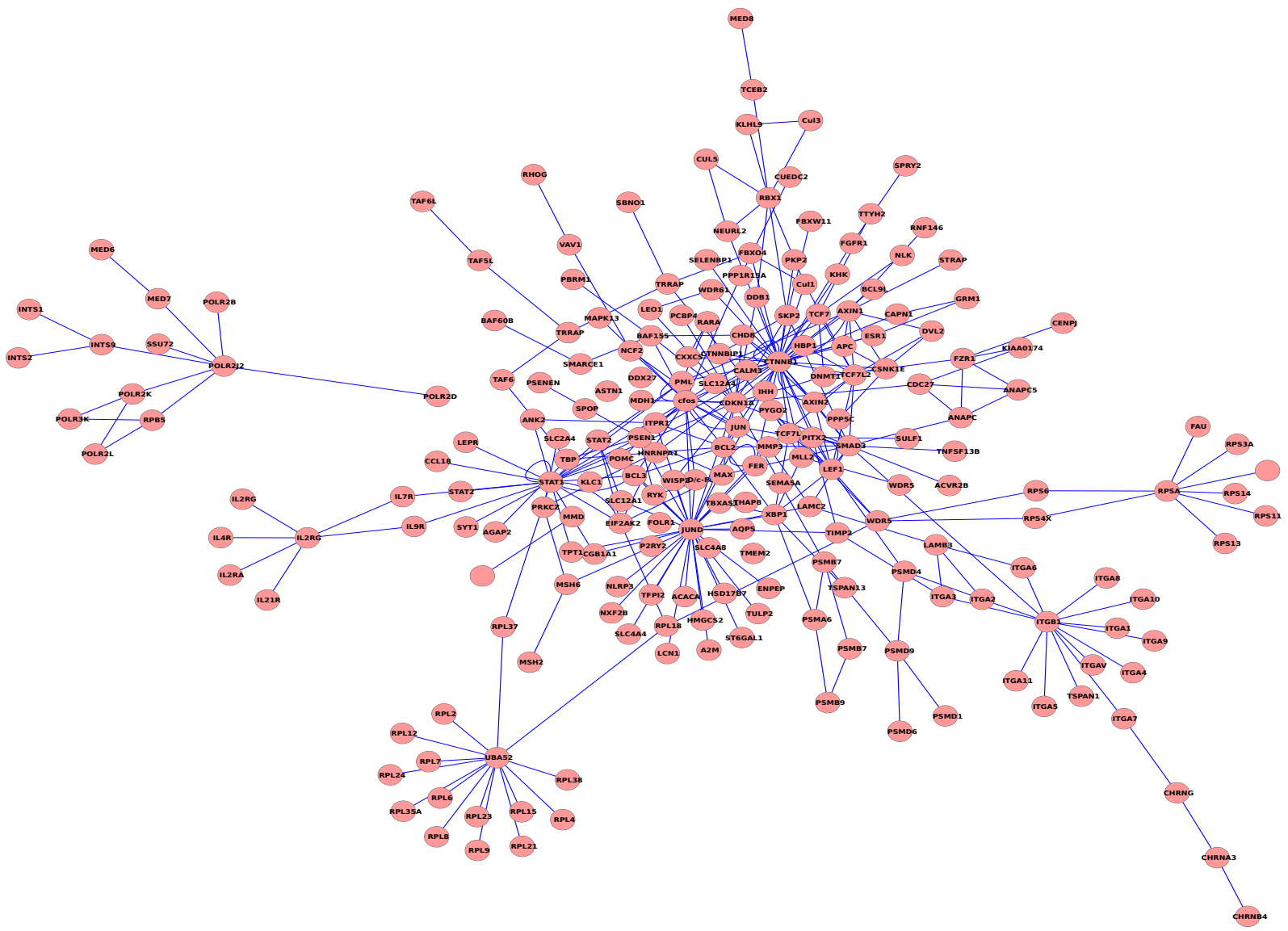
Integrin signalling was also highly associated with the identified Wnt/ β -catenin modulators (Figure 4.30). While the mechanical roles of integrins in mediating focal adhesion may be important in terms of regulating β -catenin's localisation in adherens junctions, its signalling roles may also be key. For instance, Integrin and Wnt signalling cross talk has previously been reported where the adaptor protein, Grb2, was demonstrated to bind Dvl2 and acts downstream of focal adhesion kinase (FAK) to amplify β -catenin-dependent transcription through a mechanism involving Rac1, JNK and c-jun [372]. In this study, β 1 integrin mediated signalling in response to binding to the ECM protein collagen was shown to be synergise with Wnt pathway activation [372].

Ribosomal and transcriptional complexes were also observed and while this may be a general effect, the arguments for their potential specificity in the regulation of Wnt/ β -catenin signalling has previously been presented in section 4.2.3.3. Of interest however is the role of WDR5 in linking both small and large ribosomal subunits to the core of the network, although the nature of these interactions is unspecified. WDR5 is a BMP-2 induced gene and part of the MLL1/MLL histone methyltransferase complex in addition to being involved in the expression of Runx-2, Wnt1 and Wnt3a [373]. Interestingly, WDR5 has been suggested to regulate chromatin modifications at the Twist-1 promoter leading to activation of Twist-1 expression [374]. TWIST is an EMT inducer that has, in turn, been demonstrated to regulate nuclear localisation of β -catenin and subsequent TCF-dependent transcription in breast cancer MCF7 and HeLa cells [375].

Similar network diagrams were generated from the lists of β -catenin modulators identified in all three screens that were used for the Go enrichment analysis in section 4.2 (Appendix B Cys 2-7). Nodes and edges are as described above. These networks are highly complex, with their extensive analysis beyond the scope and mathematical capabilities of the current study. However, they provide potential insights into β -catenin biology and may be of value upon considering genes in isolation. The smaller network above was generated from overlapping β -catenin modulators identified in several screens/cell lines therefore may potentially provide insights into conserved biological processes/genes involved in β -catenin regulation.

Figure 4.30 Network diagram of the β -catenin modulators identified that also regulates TCF-dependent transcription (overleaf)

Overlapping esiRNAs that were identified in the three imaging screens for modulators of β -catenin levels and localisation were integrated with the overlaps between the H screen and regulators of TCF-dependent transcription, as identified in three transcriptional RNAi screens (7df3s, Katja Seipel; HeLa cells [267] and DLD1 cells [242]) and submitted to the MetaCore database. Nodes represent genes/proteins with edges representing protein-protein/DNA interactions between nodes. Details with regards to edges are displayed in the original Cys 1 file (Appendix B) and can be visualised in Cytoscape (<http://www.cytoscape.org/download.php>).



4.7 Potential cell type specificity of the identified regulators of β -catenin

As observed in Figures 4.15 and 4.16, only 16 and 31 esiRNAs were identified as modulators of β -catenin localisation and levels in all three imaging screens respectively. Overlaps between the two cell lines were also small, with 46 and 60 genes overlapping between the H screen and the UB and UA screen respectively in the identified regulators of β -catenin localisation (not including the central overlapping set) (Figure 4.15). Furthermore, only 30 and 36 esiRNAs overlapped between the 7df3 and U2OS cells lines for regulators of β -catenin accumulation (Figure 4.16). Overlaps between the putative regulators of β -catenin localisation and levels identified in the UA and UB screens on the other hand were far higher at 179 and 272 respectively (Figures 4.15 and 4.16). Additionally, upon comparing the β -catenin imaging screen with the screen for regulators of TCF-dependent transcription in the 7df3 cells (Figures 4.26 and 4.27), the H screen displayed a far greater degree of overlap, with 208 shared esiRNAs compared to 72 and 115 in the UB and UA screens respectively. The degree of overlap when comparing the H screen with published TCF-dependent transcriptional screens in HeLa [267] and DLD1 cells[242] was also low as demonstrated in Figure 4.28 and 4.29.

Notably, even upon comparing the transcriptional screen in the 7df3s with the aforementioned published screens, the majority of the primary screen hits from each screen appeared to be specific to the respective cell line, despite the fact that comparable assay readouts were utilised (Figure 4.31). Moreover, overlaps between hits identified in DLD-1 and SW480 cells were also surprisingly low, despite both being APC mutant colon carcinoma cell lines [242]. The overlapping gene sets were selectively enriched for ‘core pathway’ components including Axin, APC, CTNNB1 and TCF, suggesting that these proteins are essential for TCF-dependent signalling in many cellular contexts (Figure 4.31). The other common components comprised the chromatin regulator ATF7IP (MCAF1) and the transcription factor PITX2. ATF7IP (MCAF1) is an MBD1-dependent transcriptional repressor [376] found to be frequently overexpressed in naturally occurring cancers where it is implicated in

immortalisation by maintenance of telomerase activity [377]. PITX2 is a known Wnt target and mediates the cellular growth response by activating the Cyclin D2 gene. NAE1 (formerly APPBP1) is able to bind and activate the ubiquitin-like protein NEDD8 and has been implicated in the downregulation of β -catenin during neuronal death in Alzheimer's disease [378]. The overlap between any two cell lines was also small, 17 to 28 genes, including more Wnt pathway 'core' components such as AXIN1, BCL9, DVL2, LEF1, PYGO2, TLE1, WNT7 (Figure 4.31, Appendix B Table 36).

Therefore, the majority of the primary screen hits from each screen appeared to be specific to the respective cell line.

Figure 3

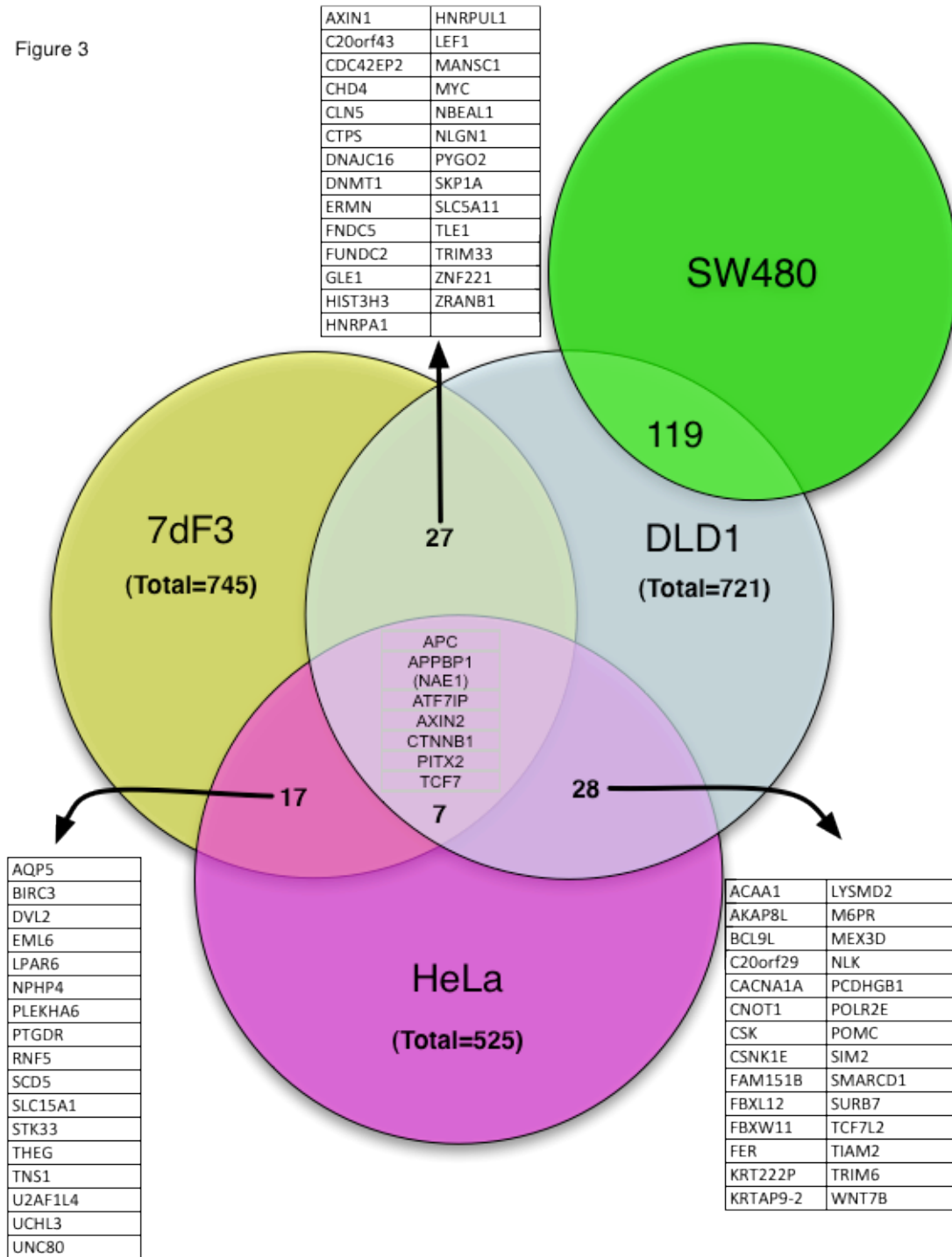


Figure 4.31 VENN Diagram of Wnt pathway components identified by RNAi screens in different human cell lines.

Hit comparison in RNA interference screens for Wnt signalling components in different human cell lines: Primary hits in the 7df3 (our data), HeLa [267] and DLD1 screen [242]. Numbers of hits in the different compartments are indicated.

4.8 Summary

The three screens developed in Chapter 3 for the identification of novel regulators of β -catenin were successfully undertaken. Hundreds of esiRNAs were identified as potential novel regulators of β -catenin levels and localisation within two cell lines of differing Wnt signalling contexts. Various *in silico* analysis methods were employed to characterise the ‘hits’ further with known Wnt and β -catenin regulators identified, providing confidence in the validity of the screens to identify both novel up- and down- regulators. In addition to Wnt signalling, other pathways and processes were over-represented in the gene sets, from MAP kinase signalling and cell cycle processes to cytoskeletal organisation, adhesion and mRNA processing and translation. 49% of the esiRNAs selected for secondary assays reconfirmed their effects from the primary screens. The screens provided genome scale insights into cellular processes linked to β -catenin and the possible mechanistic processes involved from the identified modulators.

Interestingly, a lack of a significant correlation was observed when comparing the β -catenin imaging screening data with the previous screen for regulators of TCF-dependent transcription in the 7df3 reporter cell screen. Within the reconfirmed set, there was a slight positive correlation between β -catenin nuclear localisation and TCF-dependent transcription in the U2OS cell line. This suggested that alterations in β -catenin are not necessarily directly coupled to transcriptional changes.

Comparing the β -catenin imaging screening data with several genome-wide screens for regulators of TCF-dependent transcription revealed an overlapping subset of genes that were highly connected, which strongly implicated processes such as Integrin and AP-1 signalling to the role of β -catenin in TCF-dependent transcription. Overlaps between the screen ‘hits’ were low between the different cell lines, indicative of cell-type specific effects. These interesting observations will be discussed further in Chapter 6. The subsequent chapter will discuss an investigation into hnRNP A1, an mRNA binding protein that was consistently identified as a potential repressor of β -catenin in all three imaging screens, in addition to the screen for TCF-dependent transcription.

**CHAPTER 5. HNRNP A1 - A NOVEL
REGULATOR OF β -CATENIN**

Having identified and reconfirmed a small subset of genes in Chapter 4, the next objective was to characterise a novel gene in an attempt to understand further how it may regulate β -catenin levels and/or localisation.

Heterogeneous nuclear ribonucleoprotein A1 (hnRNP A1) was chosen for further investigation as its downregulation resulted in strong β -catenin accumulation in the three primary screening assays, in addition to enhanced TCF-dependent transcription in the primary luciferase screen. HnRNP A1 had been shown to bind β -catenin by co-immunoprecipitation [379] and mass spectrometry [380]. Enrichment analysis strongly implicated mRNA processing, transport and translation in the primary screen data sets interrogated, suggestive of a significant degree of β -catenin control at the post-transcriptional level, an area often overlooked in the field. Therefore, it was deemed a promising and interesting candidate for further studies.

The current chapter describes the reconfirmation of hnRNP A1 as a repressor of Wnt/ β -catenin signalling and the investigation into its potential role in β -catenin regulation. As mentioned in the acknowledgements, James Platt and Rosalind Roberts were two undergraduate students assigned to me for their final year projects and they ably assisted at different stages of this chapter and are credited in legends where appropriate.

Reconfirmation of hnRNP A1 was undertaken separate to the subset of esiRNAs investigated in Chapter 4. Work on HUWE1, a novel Dishevelled ubiquitin ligase identified from the TCF-dependent screen, was also undertaken but will not be discussed further here as it would require the presentation of significant amounts of data from collaborating laboratories.

Before describing the specifics of the investigation into hnRNP A1, it is important to briefly provide background information on this protein and its known cellular functions.

5.1 Background

Following gene transcription by RNA polymerase II, the resulting precursor-messenger-RNAs (pre-mRNAs) are subject to a variety of regulatory post-transcriptional modifications, such as differential splicing, editing and polyadenylation. This in turn can significantly affect the proteins generated, both in terms of levels and, in the case of alternative splicing and translation, the precise protein isoform produced [381]. Furthermore, messenger RNA (mRNA) nuclear export and subcellular localisation, in addition to their stability and translation, are highly regulated to enable the correct functioning of these mature mRNAs. Such post-transcriptional regulatory events are mediated through the assembly of a large number of RNA-binding proteins (RBPs) [381, 382] and processing factors, such as non-coding RNAs (e.g. microRNAs [383]), in ribonucleotide (RNP) complexes.

5.1.1 Heterogeneous nuclear ribonucleoproteins (hnRNPs).

Heterogeneous nuclear ribonucleoproteins (hnRNPs) are a family of predominantly nuclear RNA-binding proteins that bind to nascent primary transcripts (pre-mRNA or historically called hnRNA), produced by RNA polymerase II, and package them into hnRNP particles [384]. HnRNPs are also loosely defined as proteins that bind to hnRNA (consisting of pre-mRNA and nuclear mRNA), but which are not stable components of other classes of RNP complexes such as small nuclear RNPs (snRNPs) [384, 385]. 20 different human hnRNP proteins with different RNA sequence binding preferences have been identified following the purification of hnRNP particles, which were named hnRNP A-U (Table 5.1). HnRNP complexes that co-purify with the same hnRNA are often large and highly diverse, consisting of several 'traditional' hnRNPs (described in Table 5.1), in addition to numerous other RBPs, such as splicing factors, that co-ordinate post-transcriptional regulation of gene expression [382]. These complexes are highly dynamic with some hnRNPs confined to binding mRNA only in the nucleus whilst others can accompany mRNAs to the cytoplasm [384]. Furthermore, events such as phosphorylation changes mediated by intracellular signalling pathways can alter the binding activity of specific hnRNP proteins, in addition to the availability of specific binding sequences [386, 387].

These multifunctional proteins have been demonstrated to be involved in a diverse range of molecular processes, from telomere biogenesis and DNA repair to cell signalling and gene expression regulation at both transcriptional and translational levels. As a result of these functions, which also includes proto-oncogene splicing, hnRNPs have been implicated in the development and progression of tumourigenesis [388]. The roles of different hnRNP family members are summarised in Table 5.1.

HnRNPs are modular proteins that share certain structural features, most notably RNA-binding/recognition domains called the RNA recognition motif (RRM) or RNA-binding domain (RBD), a prevalent motif in the proteome that is present in up to 1% of gene products [389-391]. The structure of these domains enables their binding to single stranded nucleic acids (including ssDNA) of variable length in both a sequence-specific and general non specific manner [392]. Other, less prevalent domains include K homology (KH) domains involved in RNA and DNA binding[393] and Arg-Gly-Gly (RGG) motifs, which are postulated to be involved in protein-protein interactions, nuclear localisation and transcriptional activation [384, 391].

**Table 5.1 (overleaf). Summary of hnRNP Functions.
Reproduced and adapted from [391] and [394]**

hnRNP	RNA-binding motifs	Proposed Functions	References
A0	2 x RRM, RGG	Splicing (By analogy)	[395]
A1	2 x RRM, RGG	Telomere maintenance Transcription DNA replication Splicing miRNA processing mRNA stability Translation regulation mRNA trafficking	[396-399] [400] [401] [402-405] [406, 407] [408] [409] [410, 411]
A2/B1	2 x RRM, RGG	Telomere maintenance Transcription Splicing mRNA stability Translation regulation mRNA trafficking mRNA packaging	[398, 412] [413, 414] [403, 415, 416] [417] [418] [419, 420] [421]
A3	2 x RRM, RGG	Telomere maintenance mRNA trafficking	[422] [423]
C1/C2	1 x RRM	Chromatin remodelling Transcription Splicing mRNA retention mRNA packaging mRNA stability Translational regulation Telomere biogenesis	[424] [425] (Martinez-Contreras et al, 2006) [382] [421, 426] [427] [428, 429] [399]
D1/D2 (AUF 1 p42, p45)	2 x RRM, RGG	Transcription mRNA stability Translation regulation	[430] [431] [432]
E1/E2 (poly (rc) binding protein 1-αCP1/2)	3 x KH	Transcription Telomere biogenesis Splicing mRNA stability Translational regulation	[433] [399] [434, 435] [436, 437] [435, 437-439]
F	3 x RRM	mRNA stability Splicing	[440] [416, 441]
G	1 x RRM, RGG	DNA repair Tumour Suppressor Transcription factor Splicing	[442] (Shin et al, 2008) [443] [444]
H/H' (DSEF-1)	3 x RRM	mRNA stability Splicing Polyadenylation	[440] [445] [446]
I (Polypyrimidine tract binding protein 1-PTB 1)	4 x RRM	Splicing mRNA stability Polyadenylation Translational regulation	[447-449] [450] [451] [452]
K (Transformation Up Regulated Nuclear Protein-TUNP)	3 x KH, RGG	Transcription Chromatin remodeling Telomere biogenesis Splicing Translational regulation mRNA stability	[453-455] [454] [399] [456, 457] [436, 458] [459]
L	4 x RRM	Transcription Splicing mRNA stability Polyadenylation mRNA export Translation Regulation	[460] [461] [462] [463] [463] [452, 464]
M	3 x RRM	Splicing Heat Shock Response	[434] [465]
P2 (TLS/FUS)	1 x RRM, RGG	Transcription Genome stability Splicing	[466] [467] [468]
Q (glycine and tyrosine-rich RNA binding protein (GRY-RBP)/R)	3 x RRM, RGG	Splicing RNA replication mRNA stability mRNA trafficking	[469] [470] [471] [472, 473]
U (Scaffold Attachment Factor A-SAF A)	1 x RGG	Chromatin organisation DNA binding RNA binding	[474, 475] [475]

5.1.2 hnRNP A1

HnRNP A1 is a highly abundant hnRNP consisting of an RGG and two RBD motifs, with the N-terminal RBD involved in mediating protein-protein interactions [394]. While mostly nucleoplasmic in distribution, a C-terminus proximal 38 amino acid domain, called the M9 motif, facilitates signal-mediated nucleo-cytoplasmic shuttling of hnRNP A1 [410, 476, 477], such as in response to stress [478] or post-translational modifications [479]. In turn, this implicated a function for hnRNP A1 in the nucleo-cytoplasmic shuttling of newly synthesised mRNAs for translation [410]. In support of this, it was revealed that hnRNP A1 could bind polyA⁺ mRNA in both the nucleus and cytoplasm [411]. Its protein binding function has also been demonstrated to mediate protein trafficking, with hnRNP A1 contributing to the control of NF- κ B-dependent transcription by binding NF- κ B inhibitor, I κ B α , to mediate its degradation [480].

In addition to mRNA and protein trafficking, hnRNP A1 plays a role in a plethora of other processes, both in the cytoplasm and nucleus (summarised in Figure 5.1). Its involvement as a splicing silencer is well established where it inhibits splicing by binding pre-mRNA at the same site as splicing factor 2 (SF2) [402]. Its inhibition of alternative splicing of a variety of genes, including CD44, c-src and PKM, has been linked to tumour development and progression [402-405, 481, 482]. More recently, hnRNP A1 has been suggested to play a role in microRNA biogenesis, by assisting Drosha in cleaving pre-miR-18a from its pre-miRNA transcript to generate microRNA 18a (miR-18a) and conversely inhibiting Drosha mediated processing of pri-let-7a-1 [406, 483, 484]. This latter role was shown to exert its effect by interfering with the ability of another RBP, K homology splicing regulatory protein (KSRP), to bind and promote let-7a biogenesis [406]. Furthermore, by recruiting telomerase to telomeric DNA, hnRNP A1 can maintain telomere length with further details regarding its role becoming increasingly elucidated in recent years [396-399]. HnRNP A1 has also been associated with stimulating cap-dependent translation alongside other RBPs [485] as well as regulating internal ribosome entry site (IRES) mediated translation [409, 486].

Additionally, hnRNP A1 has been demonstrated to regulate mRNA stability through association with AU-rich elements (ARE) in the 3'-untranslated region of target

mRNAs [487]. This role appears to be context dependent however, as it has been demonstrated to both stabilise mRNA [488] and promote its degradation [408].

5.1.2.1 hnRNP A1 and KSRP

HnRNP A1 has also been associated with regulating mRNA stability as part of a complex with KSRP; another RNA-binding protein involved in the decay of target transcripts [335, 489]. It was demonstrated that PI3K-AKT or Wnt signalling lead to stabilisation of KSRP target mRNA, which included hnRNP A1[489] and β -catenin mRNA [185]. More recently, KSRP was shown to interact with Dishevelled in a complex that mediated β -catenin mRNA degradation. Wnt stimulation was observed to induce β -catenin mRNA release and subsequent stabilisation, resulting in rapid translation and accumulation of protein levels. [183]. The role for hnRNP A1, if any, in this process has yet to be explored.

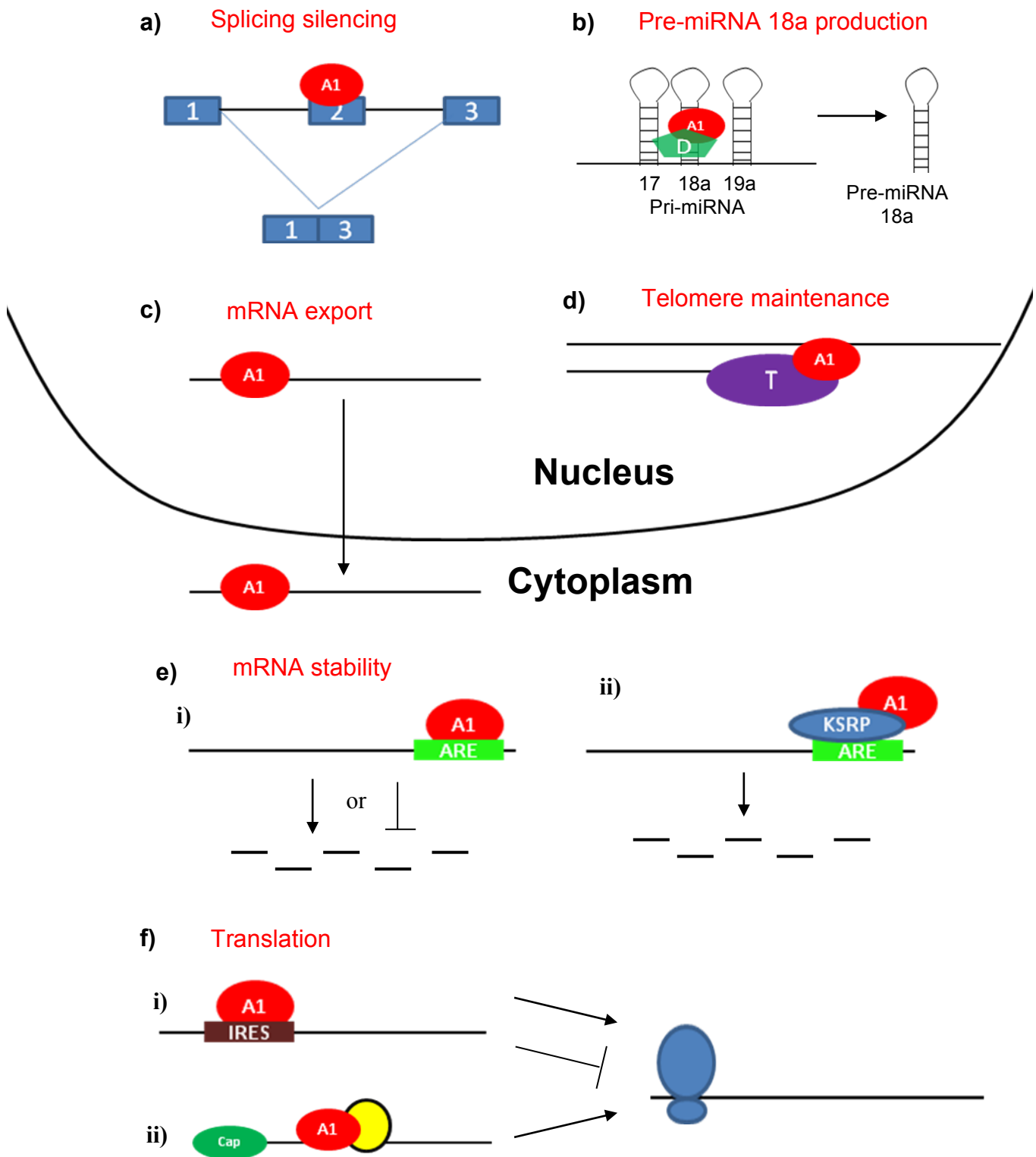


Figure 5.1. The numerous roles of hnRNP A1 (red, A1) within the cell. a) hnRNP A1 acts as a splicing silencer. **b)** hnRNP A1 aids Drosha (D) in excising pre-miRNA18a from the pri-miRNA transcript. **c)** hnRNP A1 is involved in mRNA export. **d)** hnRNP A1 aids telomerase (T) with telomere elongation. **e) i)** Through binding AU rich elements (ARE), hnRNP A1 can either promote or prevent the degradation of particular mRNAs. **ii)** hnRNP A1 also forms part of the KSRP complex, which degrades certain mRNAs. Its exact role in the complex is unknown, but it is shown here as positively regulating the activity of the complex, as proposed by our model. **f) i)** hnRNP A1 binding internal ribosome entry sites (IRES) can either promote or inhibit the translation of that mRNA. **ii)** With other general RNA binding proteins (yellow), hnRNP A1 promotes cap-mediated translation. Figure produced by Rosalind Roberts as part of her final year research project.

5.2 hnRNP A1 identified as a novel repressor of β -catenin – primary screening data.

In the primary β -catenin localisation H screen, esiRNA against hnRNP A1 resulted in increased β -catenin levels in both nuclear and cytoplasmic compartments of the cell to give a whole cell β -catenin intensity Z-score of 3.2 (Figure 5.2 A and B). However, in this particular cell line no significant change was observed in terms of β -catenin Nuclear to Cytosolic Ratio (Figure 5.2 C). Slight toxicity was observed with cell numbers reduced to 56% of the average counts from its respective plate, which was still above the filtering threshold for excluding wells on the grounds of toxicity (set at <30%) (Figure 5.2).

A similar result was obtained in the UB screen whereby hnRNP A1 esiRNA treated cells possessed striking increases in β -catenin levels and β -catenin nuclear to cytosolic ratios, as indicated by Z-scores of 5.7 and 3.6 respectively (Figures 5.3). In addition, esiRNA against its paralog, hnRNPA1-like 2, also resulted in increased β -catenin levels (Figure 5.3 B). The increase in β -catenin nuclear targeting as shown by increased Nuclear to cytosolic ratio (Figure 5.3 C) was not apparent in the 7df3 cell line (Figure 5.2 C), possibly due to the challenging morphology in these cells for accurate segmentation, as discussed previously. Cell numbers were slightly decreased in this field of view, but not detrimentally. Similarly, knockdown of hnRNP A1 further enhanced APC esiRNA induced β -catenin levels in the UA screen (Figure 5.4), with Z-scores of 2.6 and 6 observed for β -catenin nuclear:cytosolic ratio and whole cell intensities respectively. In addition, esiRNA against its paralog, hnRNPA1-like 2, also resulted in increased β -catenin levels.

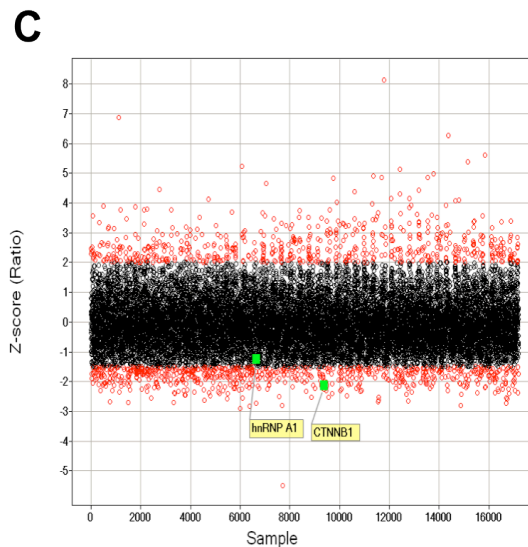
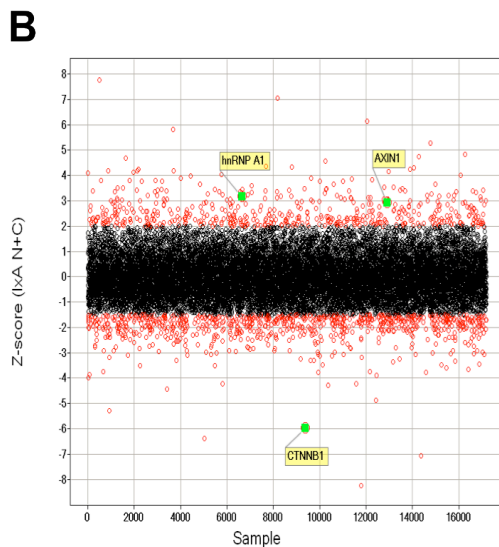
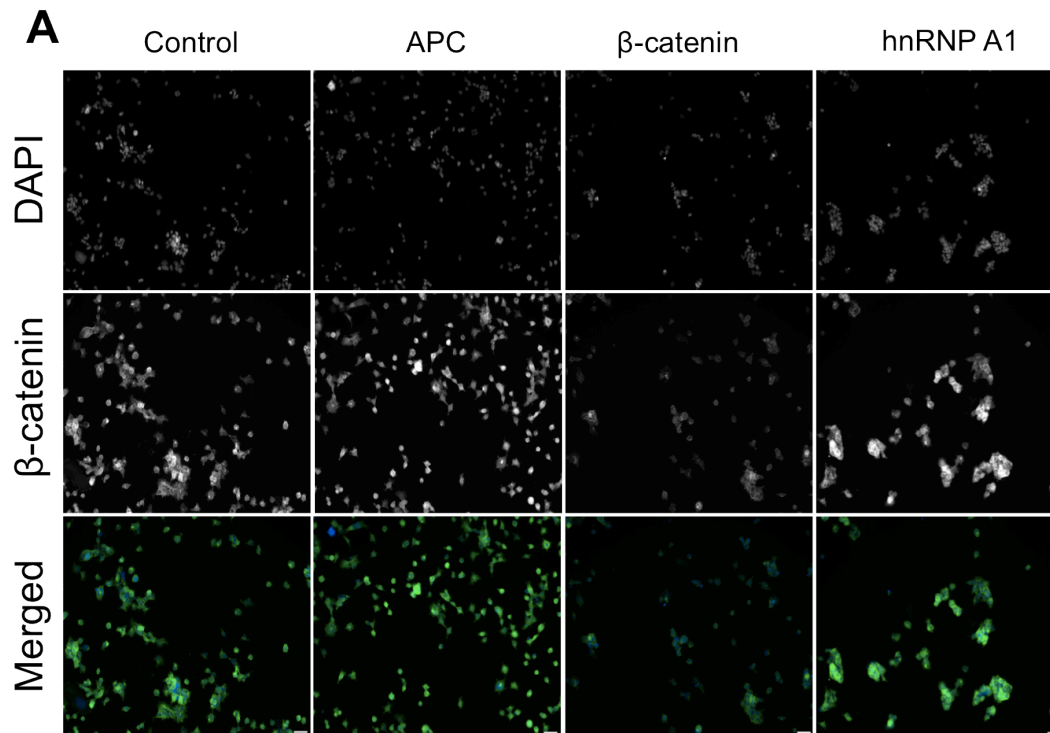


Figure 5.2 hnRNP A1 knockdown resulted in β -catenin accumulation in the H primary screen.

(A) 7df3 cells transfected with the indicated esiRNAs were fixed and immunostained for β -catenin with DAPI staining DNA. A single field of view was acquired and is displayed; bar, 50 μ m. Images were analysed for β -catenin whole cell intensity and β -catenin nuclear to cytoplasmic (Nuc/Cyt) ratio with the entire esiRNA primary screen Z-scores for both parameters plotted in (B) and (C) respectively. Each spot represents an individual esiRNA and are coloured red if passed Z-score thresholds of >2 and <-1.5 . hnRNP A1 esiRNA's Z-score in relation to the entire esiRNA library is highlighted in green along with esiRNA against known Wnt pathway components (Axin, β -catenin) in the library.

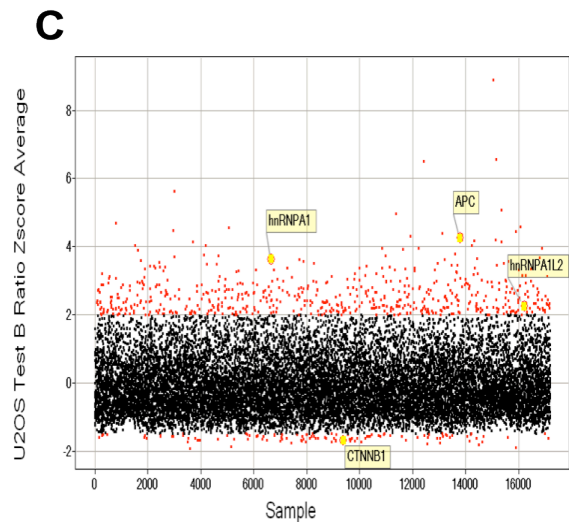
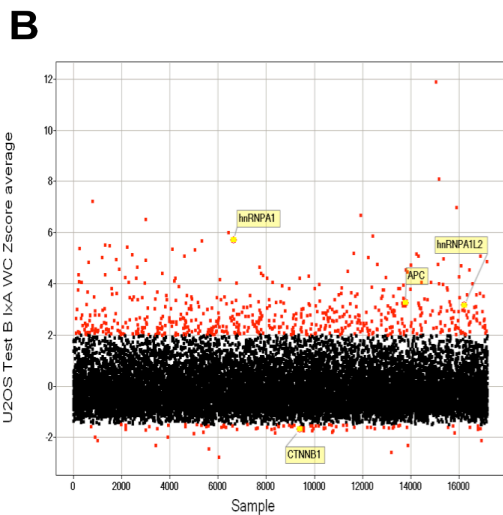
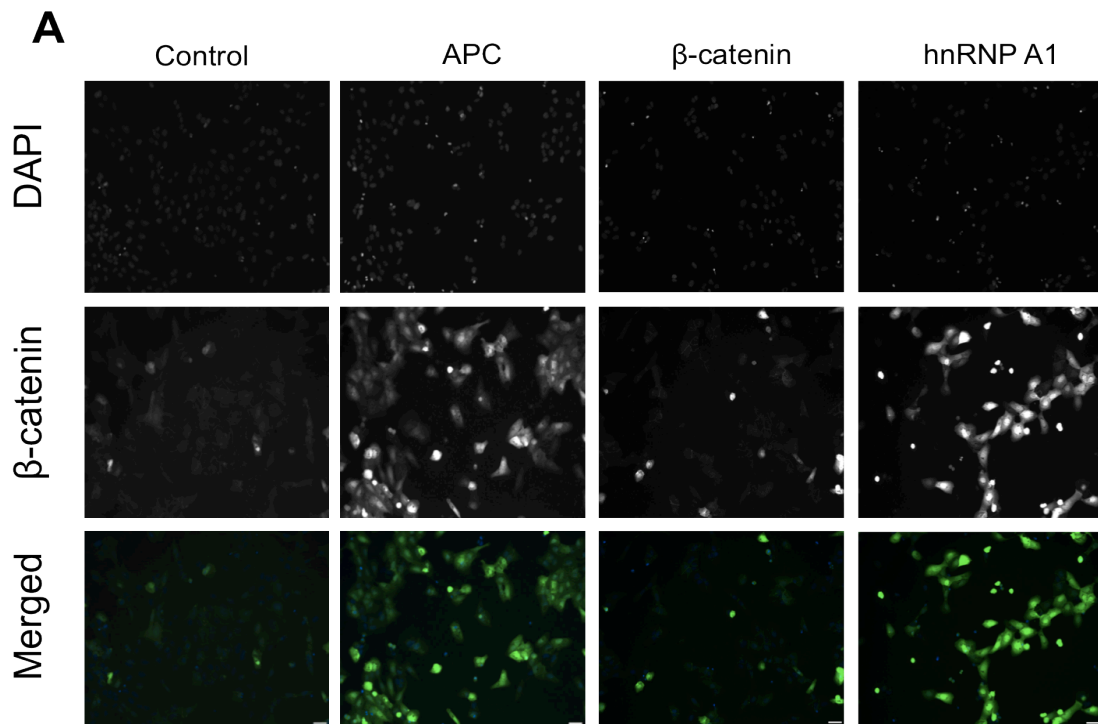


Figure 5.3 hnRNP A1 knockdown resulted in β -catenin accumulation in the UB primary screen.

(A) eGFP- β -catenin cells transfected with the indicated esiRNAs were fixed and immunostained for β -catenin with DAPI staining DNA. Two fields of view were acquired, which were in high agreement and a representative field is displayed; bar, 50 μ m. Images were analysed for β -catenin whole cell intensity and β -catenin nuclear:cytoplasmic (Nuc/Cyt) ratio with the entire esiRNA primary screen Z-scores for both parameters averaged from the two fields of view and plotted in (B) and (C) respectively. Each spot represents an individual esiRNA and are coloured red if passed Z-score thresholds of >2 and <-1.5 . Z-scores for HnRNP A1 and hnRNP A1L2 esiRNAs are highlighted in green, along with esiRNA against known Wnt pathway components (APC, β -catenin) in the library.

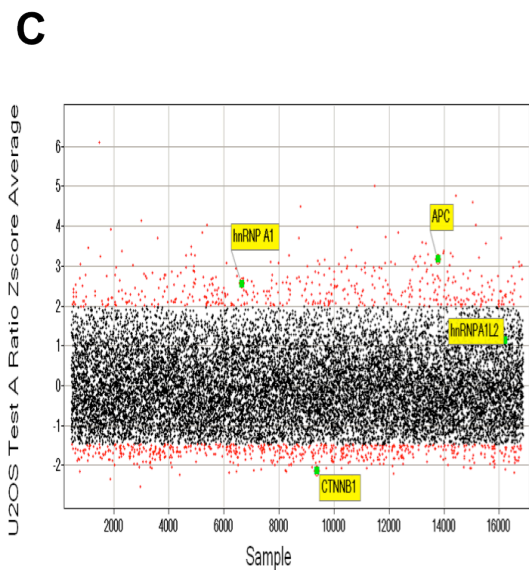
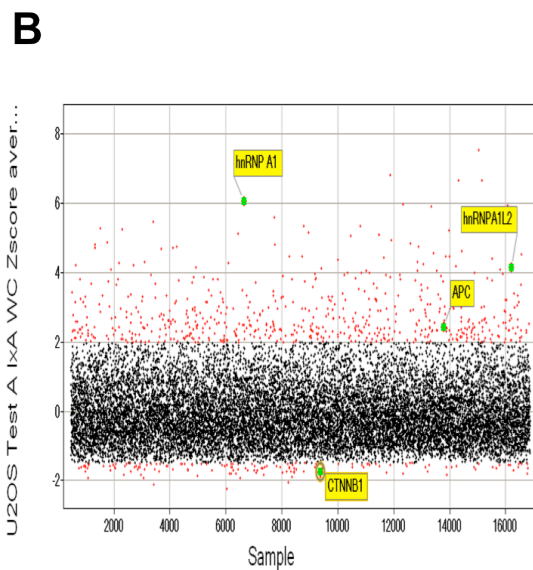
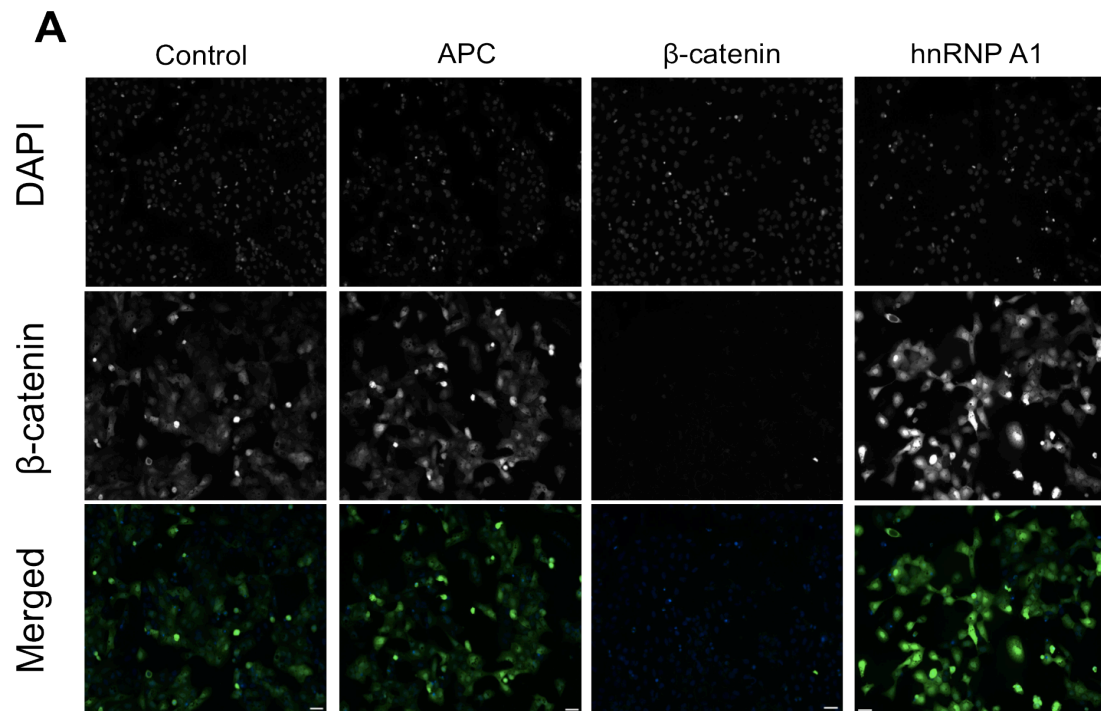


Figure 5.4 hnRNP A1 knockdown results in enhanced β -catenin accumulation in the UA primary screen.

(A) eGFP- β -catenin cells co-transfected with the indicated esiRNAs and APC esiRNA were fixed and immunostained for β -catenin with DAPI staining DNA. Two fields of view were acquired, which were in high agreement and a representative field is displayed; bar, 50 μ m. Images were analysed for β -catenin whole cell intensity and β -catenin nuclear:cytoplasmic (Nuc/Cyt) ratio with the entire esiRNA primary screen Z-scores for both parameters averaged from the two fields of view and plotted in (B) and (C) respectively. Each spot represents an individual esiRNA and are coloured red if passed Z-score thresholds of >2 and <-1.5 . Z-scores for HnRNP A1 and hnRNP A1L2 esiRNAs are highlighted in green, along with esiRNA against known Wnt pathway components (APC, β -catenin) in the library.

5.3 hnRNP A1 identified as a novel repressor of TCF-dependent transcription.

Although β -catenin has been shown to be the core effector of the Wnt pathway, many TCF-transcription factors are able to bind to the promoters of Wnt target genes and, as observed in Chapter 4, increased β -catenin levels appeared to poorly correlate with TCF-dependent transcription. However, in the case of hnRNP A1, increased β -catenin levels and nuclear localisation (as observed in the U2OS screens) following its knockdown resulted in increased TCF-dependent transcription, as demonstrated in the corresponding high-throughput luciferase screen undertaken by Dr Katja Seipel (Figure 5.5).

Furthermore, co-transfecting β -catenin esiRNA alongside hnRNP A1 esiRNA abrogated the effect of hnRNP A1 knockdown on TCF-dependent transcription, demonstrating that CTNNB1 is epistatic to hnRNP A1 and further underlying the specificity of the response to the β -catenin/Wnt signalling pathway (Appendix C, Figure 1).

The primary screening data (both experimental and *in silico*) therefore suggested that hnRNP A1 was a promising potential regulator of β -catenin in a Wnt signalling context and was hence chosen for further investigation.

5.4 Reconfirmation of hnRNP A1 as a novel repressor of β -catenin and subsequent TCF-dependent transcription.

Off target effects are an inherent issue within RNAi screening, therefore potential 'hits' must be reconfirmed in secondary and tertiary assays before proceeding to mechanistic studies.

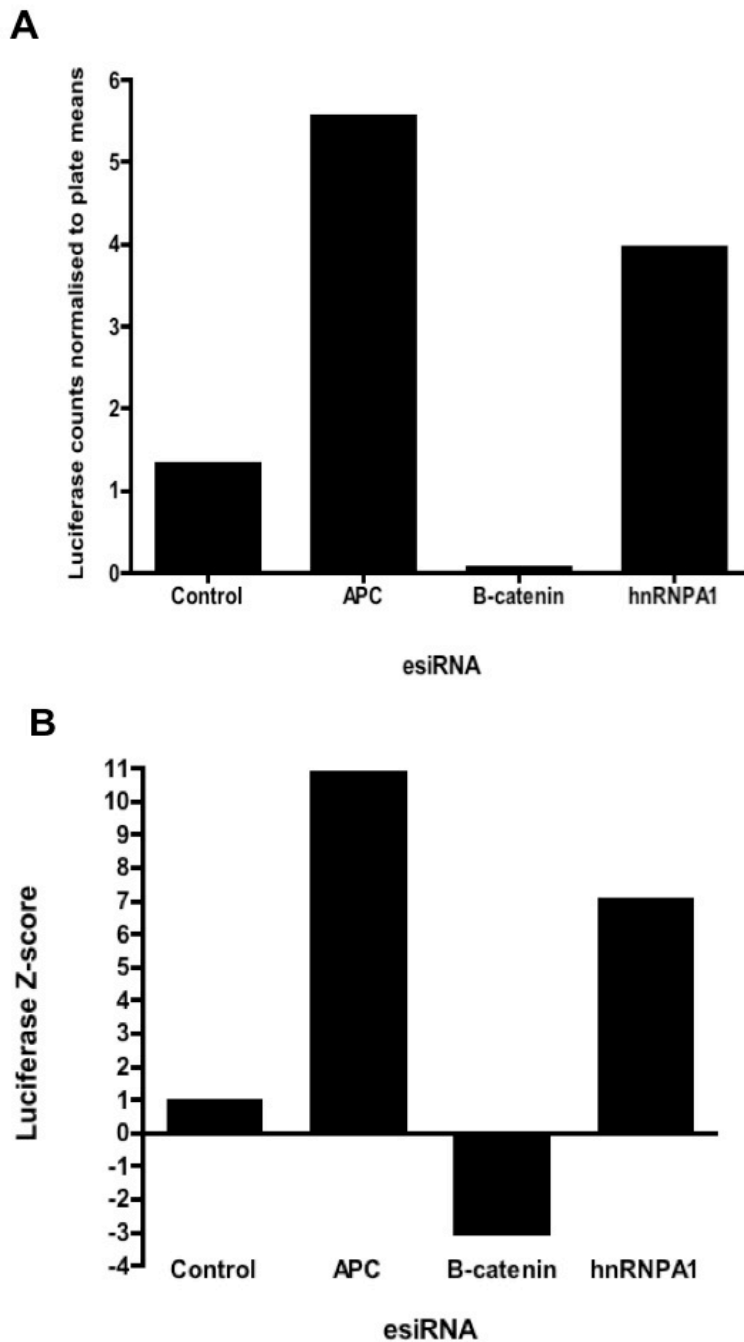


Figure 5.5 hnRNP A1 identified as a novel repressor of TCF-Dependent transcription.

Primary luciferase screen data - hnRNP A1 functions as a transcriptional repressor in β -estradiol treated 7df3 cells. HnRNP A1 esiRNA transfected cells displayed increased luciferase counts with APC and β -catenin esiRNA used as positive and negative controls respectively. Control esiRNA was used to control for non-specific esiRNA effects. A single well is displayed as fold over it's corresponding screen plate mean (A) or its corresponding Z-score (B). Data generated by Dr Seipel

5.4 Reconfirmation of hnRNP A1 as a novel repressor of β -catenin and subsequent TCF-dependent transcription.

Off target effects are an inherent issue within RNAi screening, therefore potential ‘hits’ must be reconfirmed in secondary and tertiary assays before proceeding to mechanistic studies.

5.4.1 Secondary hnRNP A1 esiRNA reagents result in β -catenin accumulation in both eGFP- β -catenin and parent U2OS cell lines.

Freshly synthesised esiRNA of the same sequence utilised in the primary library was transcribed from 7df3-based cDNA (labelled Val1) in addition to the generation of a secondary non-overlapping esiRNA against hnRNP A1 (Val2; See appendix C, table 1 for sequences). HnRNP A1 Val1 esiRNA reconfirmed the primary screen data in eGFP- β -Catenin U2OS cells with increased eGFP- β -catenin detected by fluorescence microscopy and by western blotting (Figure 5.6A and B).

HnRNP A1 esiRNA’s effect was corroborated in the standard U2OS cell line, whereby hnRNPA1 esiRNA resulted in increased endogenous β -catenin levels (Figure 5.6C), albeit more subtly (Figure 5.6 D). Despite the robustness of the activation of TCF-dependent transcription by both APC and hnRNP A1 esiRNA in the primary luciferase screen (Figure 5.5), this appears to equate to relatively small changes in β -catenin cellular levels (Figure 5.6 B and C), suggestive of highly sensitive transcriptional responses to alterations of β -catenin levels and localisation.

Western blotting was also used to verify hnRNP A1 knockdown by both of the secondary esiRNAs against hnRNP A1 (Figure 5.6 B and C), providing further confidence that the effect on β -catenin was specific. Quantitative RT-PCR was also undertaken to verify the knockdown of hnRNP A1 mRNA by the different esiRNAs, which averaged at a reduction of approximately 20-50% depending on the esiRNA utilised (example provided in Figure 5.12 C).

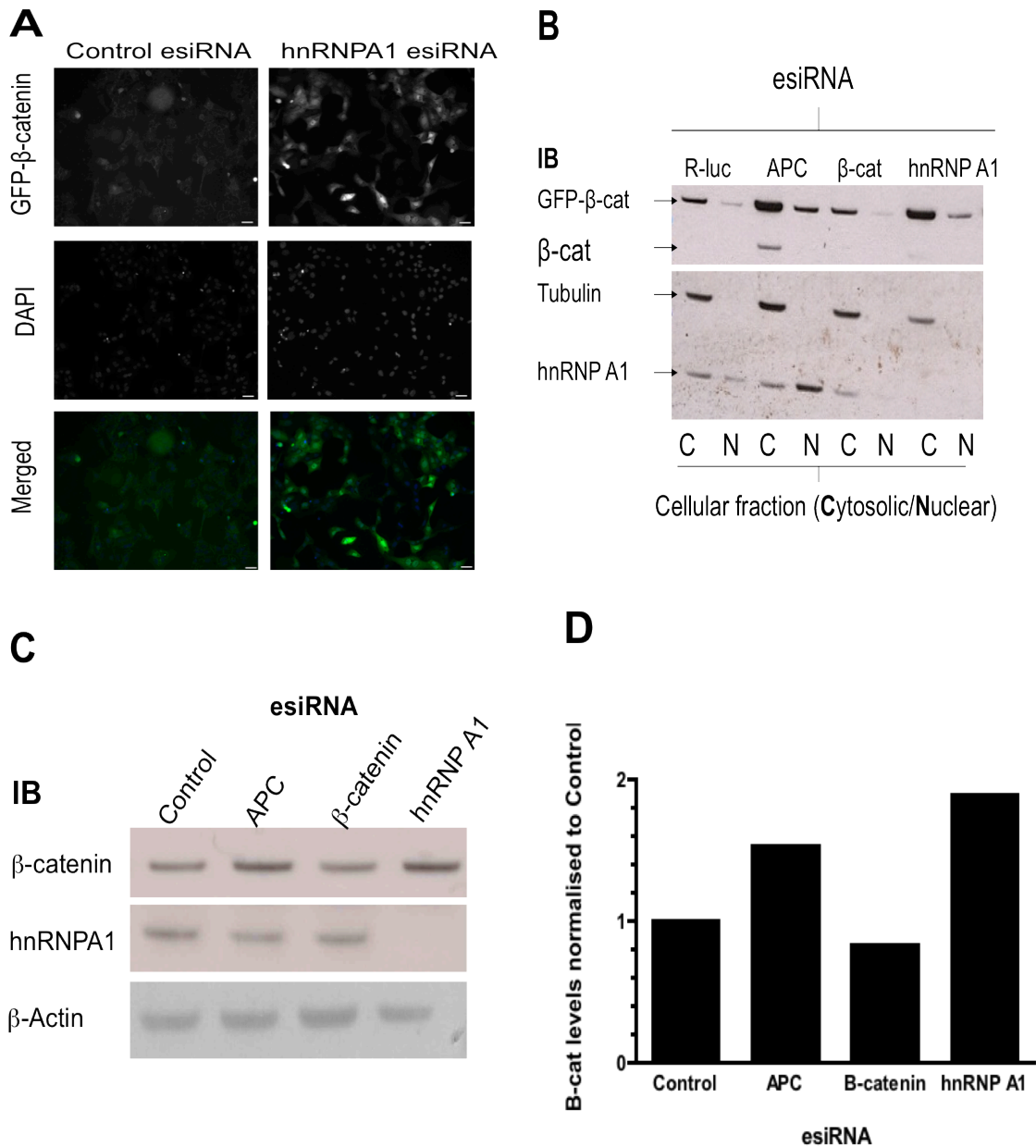


Figure 5.6 hnRNPA1 negatively regulates β-catenin – reconfirmation.

(A) hnRNPA1 depletion using a secondary esiRNA results in increased β-catenin levels. eGFP-β-catenin U2OS cells were fixed and nuclei DAPI stained 48hrs following esiRNA transfection. Representative image displayed, Bars; 50µm. (B) Crude Cytosolic and Nuclear eGFP-β-catenin U2OS extracts prepared from esiRNA transfected eGFP-β-catenin U2OS cells. Representative blot displayed. (C) Endogenous cytosolic β-catenin levels following esiRNA transfection of standard U2OS cells with secondary hnRNP A1 esiRNA, as detected by western blotting. (D) Quantification of β-catenin levels in (C) by normalising to actin loading control. Data displayed as β-catenin fold over siRNA control.

5.4.2 Rescue of hnRNP A1 depletion

Both validation esiRNAs against hnRNP A1 (Val1 and Val2) were tested in β -estradiol treated 7df3 cells along with two chemically synthesised siRNAs against the gene. The validation esiRNAs resulted in significantly increased TCF-dependent luciferase in the 7df3 cells (Figure 5.7A). Both the purchased hnRNP A1 siRNAs resulted in an increase in TCF luciferase, although this was not significant upon combining independent experiments. However, qRT-PCR analysis suggested that the knockdown efficiency of these two chemically synthesised siRNAs were not as efficient with approximately only a 30% decrease in hnRNP A1 mRNA levels observed, which may explain their comparatively weak effect (data not shown).

Expressing low levels of esiRNA-resistant mouse hnRNP A1 decreased Dvl-ER-induced TCF-dependent transcription and was able to significantly rescue the hnRNP A1 esiRNA mediated increase in TCF-luciferase when co-transfected, thus confirming the specificity of the hnRNP A1 esiRNA effect.

Overall, the data strongly suggested that hnRNP A1's apparent suppression of β -catenin/Wnt signalling was not simply due to off target effects and that it merited further investigation. The remainder of this chapter describes the various hypothesis and methods applied in an attempt to establish its mechanism further.

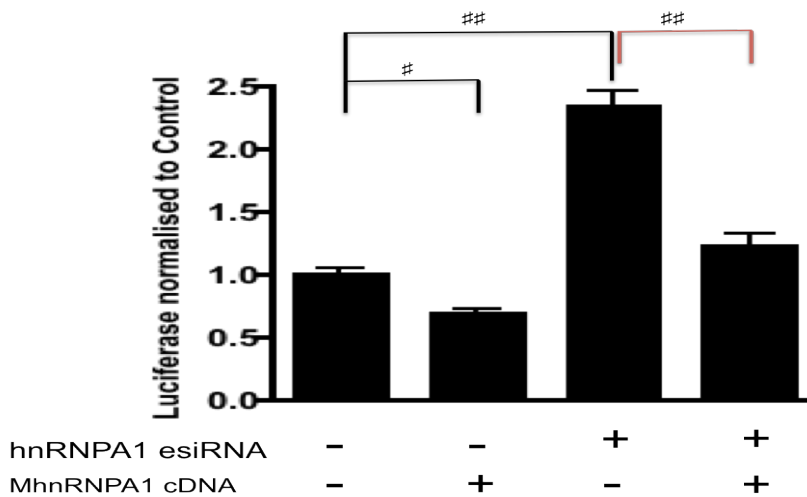
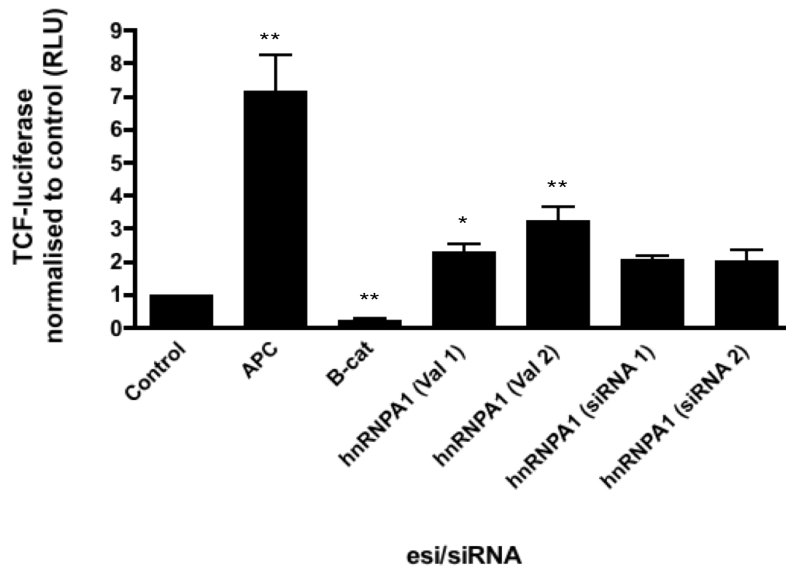


Figure 5.7 Secondary esi/siRNAs for hnRNP A1 increases TCF-dependent transcription, which can be rescued by mouse mhnRNPA1 expression.

(A) hnRNP A1 esi/siRNA transfected and β -estradiol treated 7df3 cells displayed increased luciferase counts compared to control-transfected cells, reconfirming the primary data. APC and β -catenin esiRNA were used as positive and negative controls respectively. Data represent mean RLU (relative light units) expressed as fold over control \pm s.e.m of at least two independent experiments per reagent ($n \geq 2$ of at least duplicate wells per condition). ** $p < 0.001$, * $p < 0.01$ (One-way ANOVA, Tukey's Multiple Comparison Test).

(B) Expression of low levels of esi-resistant mouse hnRNP A1 decreases TCF-dependent luciferase and rescues the effect of hnRNPA1 esiRNA in β -estradiol treated 7df3 cells. Cells were co-transfected with control or hnRNPA1 esiRNA/cDNA as indicated, induced with β -estradiol for 24hrs with luciferase assays undertaken 48hrs later. Data represent the mean \pm s.e.m. of three independent experiments ($n=3$ of multiple replicate wells per condition) normalised to control siRNA/empty vector control samples. # $p < 0.01$, ## $p < 0.001$ (Kruskal-Wallis, Dunn's multiple comparison test).

5.5 hnRNP A1 interacts with β -catenin.

Co-immunoprecipitation experiments were undertaken to investigate whether hnRNP A1 binds β -catenin in the cell lines used in the primary screening assays. No interaction was observed when using whole cell 7df3 and eGFP- β -catenin-U2OS lysates (data not shown) therefore crude nuclear and cytosolic extracts were prepared, as undertaken previously [379]. HnRNP A1 was demonstrated to bind β -catenin both in the nucleus and in the cytoplasm (Figure 5.8 A and B respectively) suggesting a potential protein shuttling role for hnRNP A1 where it may mediate the export of β -catenin into the cytoplasm for degradation, as demonstrated for I κ B α in the regulation of NF- κ B signalling [480]. Initial experiments in standard U2OS cells (therefore endogenous β -catenin only) appeared to corroborate the above observations, although given more time these would have been repeated (data not shown). Variability was observed with regards to the cellular location of this apparent binding, along with occasional issues of hnRNP A1 binding non-specifically to the bead matrix (Figure 5.8 B). While hnRNP A1 shuttles between cell compartments it is mostly localised in the nucleus, with the variability observed between experiments potentially a reflection of increased cytoplasmic distribution of hnRNP A1 in certain situations, such as cellular stress [478]. Overall, however, the co-immunoprecipitation experiments appeared to support published reports of an interaction between β -catenin and hnRNP A1 [379].

5.6 hnRNPA1 negatively regulates β -catenin levels independently of its protein turnover.

Due to the key role of β -catenin turnover in the regulation of the Wnt/ β -catenin pathway, the vast majority of research has centred on deciphering the regulation of β -catenin protein stability [185]. Therefore, assessing the role of hnRNP A1 on this aspect of β -catenin was one of the first questions tackled upon reconfirmation of the primary data.

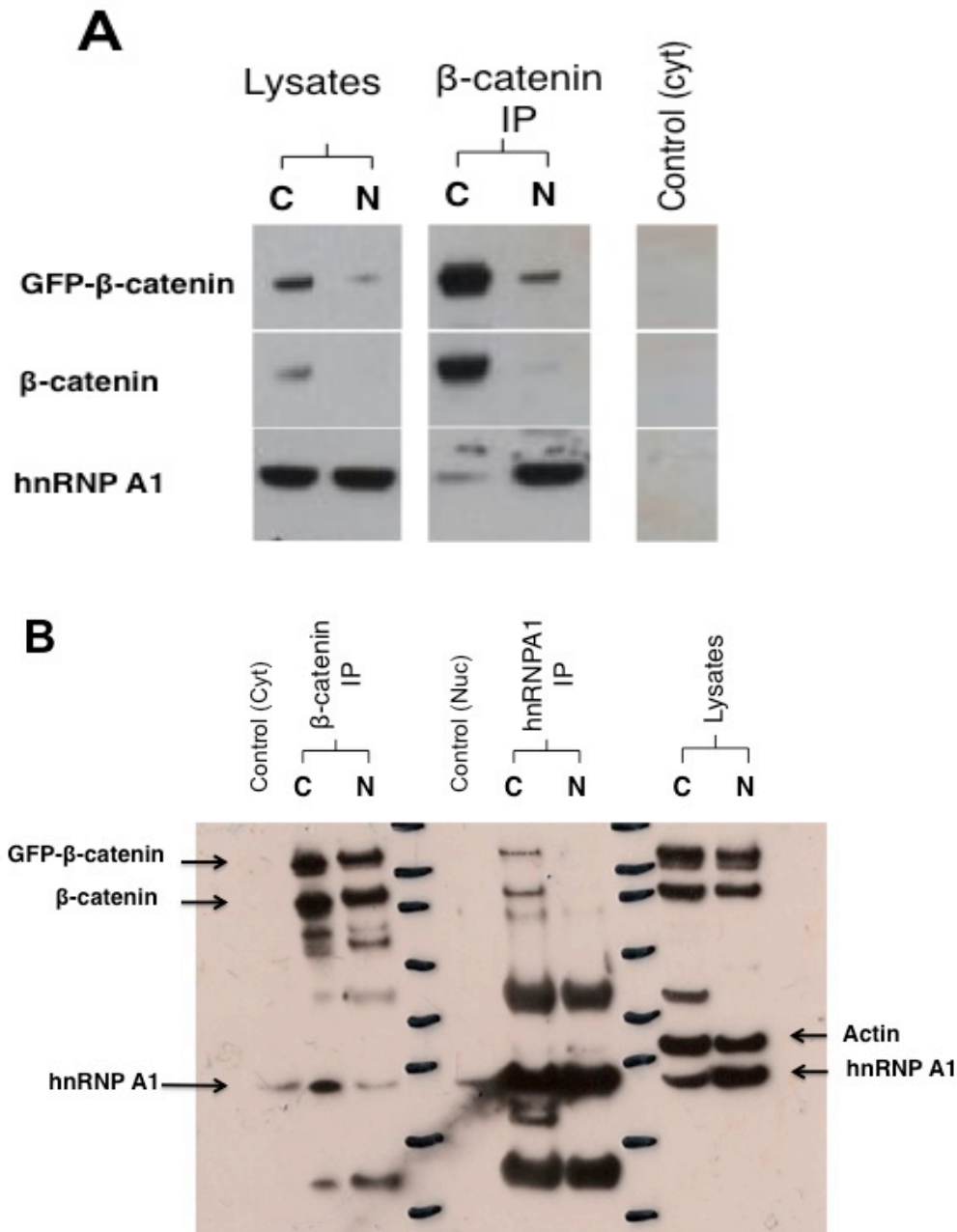


Figure 5.8 hnRNP A1 binds β -catenin

β -catenin and/or hnRNP A1 were immunoprecipitated from crude eGFP- β -Catenin U2OS nuclear (N) and cytosolic (C) lysates. Blots were subsequently probed with hnRNP A1 and β -catenin antibodies. (A) hnRNP A1 Co-IP'd with β -catenin in nuclear extracts. Produced by Rosalind Roberts as part of her final year research project. (B) Similar to (A), except that the Co-IP is displayed both ways. Controls are protein G beads alone. A degree of hnRNP A1 non-specific binding is observed in the controls (Lanes 1 and 4), although significantly less compared to samples with antibody incubation. Representative blots displayed.

Firstly, metabolic pulse-chase assays were undertaken to investigate the effect of hnRNP A1 downregulation on β -catenin protein stability. 48 hours post-esiRNA transfection, cells were incubated in 35S methionine media for an hour to label any newly synthesised protein during this period by the incorporation of radioactively labelled amino acids. Following the replacement the media with normal unlabelled media cells were harvested at varying time points, as indicated in Figure 5.9 (T_0 – harvested instantly after media replacement), and β -catenin subsequently immunoprecipitated. Therefore, proteins that were produced during the pulse would be radioactively labelled thus allowing the degradation of β -catenin to be followed over time and to observe the effects of the esiRNA upon its stabilisation.

APC esiRNA resulted in the expected stabilisation of β -catenin (i.e. its decreased degradation over time) as demonstrated by the increased levels of radiolabelled β -catenin at T_{30} and T_{45} time points in both cell types (Figure 5.9 A and B). These assays revealed that, whilst hnRNPA1 esiRNA treated cells displayed the expected increase in β -catenin levels at time zero, its degradation rate appeared far faster than APC esiRNA treated cells, suggesting that loss of hnRNPA1 did not disrupt β -catenin degradation in the same manner as loss of APC (Figure 5.9A and B). This implied that the increase in β -catenin observed at T_0 with hnRNP A1 esiRNA was due to increased synthesis of β -catenin. In the eGFP- β -Catenin U2OS cell line shorter timepoints were used based on the observation in the 7df3s that after 30minutes β -catenin in the hnRNP A1 treated sample had degraded to control levels. In the 7df3 reporter cell line the control esiRNA surprisingly does not show the expected pattern of β -catenin breakdown, which may be due, in part, to the prevalent, stable membrane bound β -catenin masking the turnover of free β -catenin. An attempt at isolating free β -catenin using a GST-E-Cadherin pull-down within these assays failed.

To support these observations, single cell time-lapse microscopy assays were undertaken in esiRNA-treated eGFP- β -catenin U2OS cells following the addition of the translational inhibitor, cycloheximide. If hnRNP A1 altered β -catenin degradation, the decay rate of eGFP- β -catenin would be expected to be delayed/slower compared to control (under circumstances where no new protein was translated). Cells were imaged every 10 minutes for approximately 15hours after cycloheximide treatment,

with eGFP- β -catenin fluorescence within individual cells quantified every hour (every 6 frames) in Image J. APC esiRNA treated cells displayed the expected increase in β -catenin stability, whilst hnRNP A1 esiRNA treated cells displayed β -catenin degradation rates similar to the control (Figure 5.9C, Movies in Appendix C). The data appeared to support the results obtained from the pulse-chase analyses. Taken together, the studies suggested that increased β -catenin levels upon hnRNP A1 ablation may be due to increased synthesis of β -catenin, rather than its decreased protein degradation, which could be attributed to increased transcription, mRNA stability or increased translation for example.

5.6.1 Dynamic regulation of β -catenin

Time-lapse microscopy was also undertaken in eGFP- β -Catenin esiRNA and Wnt3a treated cells in the absence of cycloheximide. Images were acquired every 10 minutes for approximately 29 hours with the movies provided in Appendix C. β -catenin levels was observed to cycle with a variable period time of between 5-9 hours, which was unaffected by hnRNPA1 esiRNA and Wnt3a treatment. β -catenin cycling was not observed in the presence of APC esiRNA and cycloheximide treatment (Appendix C). Moreover, levels did not appear to precisely correlate with cell cycle as previously reported [490, 491] with cells dividing in both the presence and absence of cycling detectable β -catenin. However, given time further cell numbers would have been assessed, in addition to quantification of β -catenin dynamics in synchronised cells, which would enable more accurate conclusions to be drawn. The regulation of β -catenin dynamics may reflect novel roles for its modulators with further studies warranted on this interesting observation.

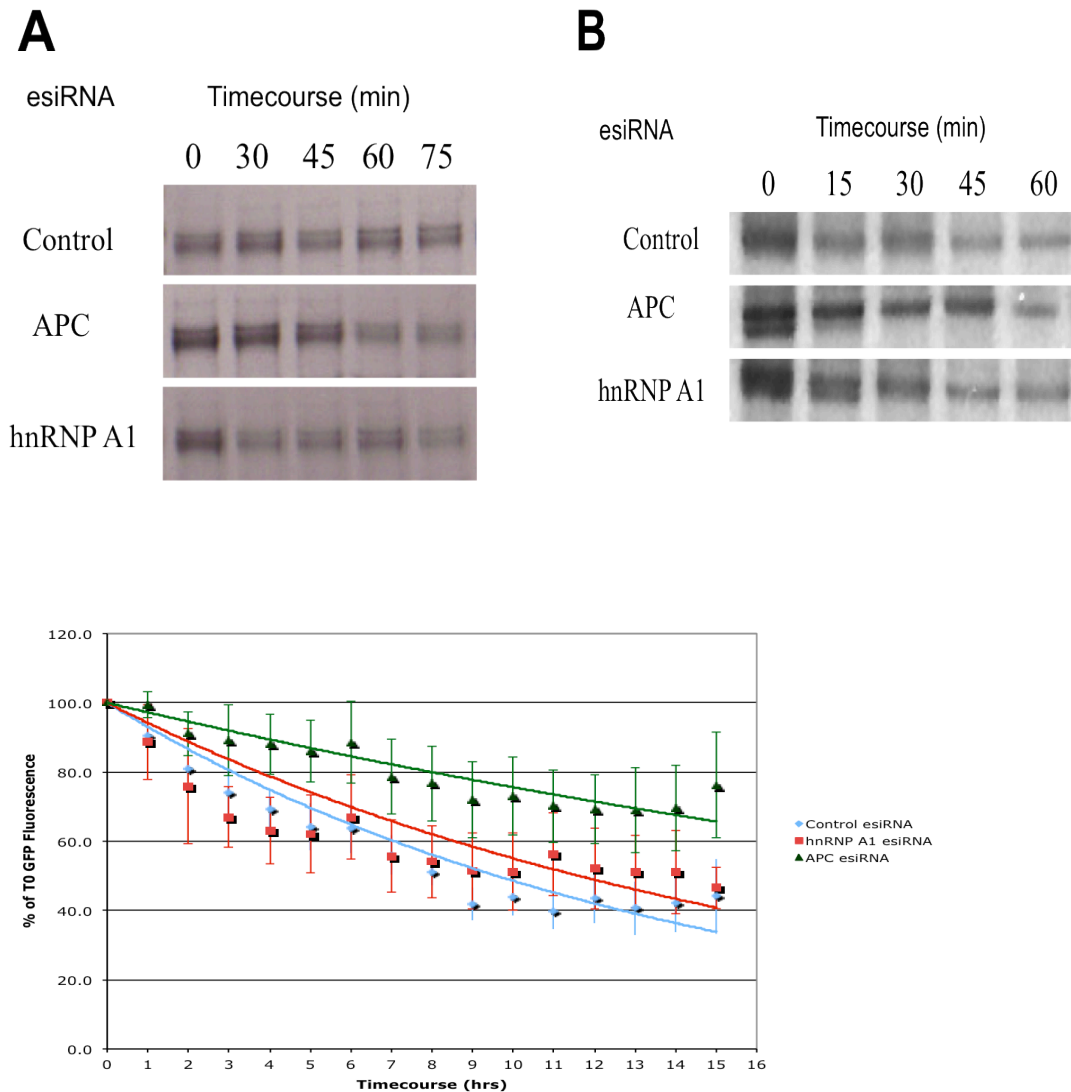


Figure 5.9 hnRNP A1 does not appear to regulate β -catenin protein stability

(A) esiRNA transfected 7df3 cells were labelled with [35 S] methionine then chased with nonradioactive medium for the indicated time points. Cells were then lysed and immunoprecipitated for β -catenin prior to western blotting analysis. Experiment in 7df3 cells undertaken by Dr Seipel and James Platt. Repeated in eGFP- β -catenin U2OS cell line (by myself) with endogenous β -catenin bands displayed (B). (C) esiRNA transfected U2OS-GFP- β -Catenin cells were treated with the translational inhibitor cycloheximide and imaged at x40 magnification for approximately 15hours. GFP fluorescence in individual cells were measured every hour using ImageJ and expressed as a percentage of Time 0 (T0) fluorescence. Points represent mean \pm SD values of between 8-11 cells per condition. Control esiRNA vs APC esiRNA $p < 0.001$ and hnRNP A1 vs APC esi RNA $p < 0.01$ (One way ANOVA, Tukey's multiple comparison test). There was no significant difference in eGFP- β -catenin degradation between control and hnRNP A1 esiRNA treated cells. Single cell data points are displayed in Appendix C, Figure 2.

5.7 hnRNPA1 negatively regulates β -catenin levels independently of its mRNA synthesis and stabilisation.

Given hnRNP A1's numerous roles in mRNA processing it was envisaged that it could be exerting its effects either pre or post-transcriptionally, by affecting β -catenin mRNA synthesis, stability or splicing for instance.

HnRNP A1 is well known as a splicing repressor, in addition to well-documented roles in regulating mRNA metabolism [405, 408, 492]. While β -catenin possesses three splice variants in the 3'UTR of differing stabilities (as indicated in the schematic in Appendix C, Figure 3) [324, 493], no evidence currently exists implicating hnRNP A1 in β -catenin splicing. The levels of each β -catenin splice variant upon hnRNP A1 knockdown in 7df3 cells were assessed by RT-PCR analysis on extracted mRNA, utilising primers for β -catenin that spanned exons 13 and 16A (Appendix C, Figure 3). A number of splice variants were uncovered and largely correlated with previous studies of β -catenin splicing ([324]. However, no effects of hnRNPA1 depletion were observed on the abundance or pattern of splicing products. As these variants exist in the 3'UTR region on β -catenin mRNA, this is not unexpected due to the absence of both 5' and 3' UTRs in the β -catenin sequence incorporated into the eGFP construct in the U2OS cells (Crude schematic provided in Appendix C, Figure 4), which suggests that the 3'UTR was not sufficient for the effects of hnRNP A1 observed with both endogenous and eGFP- β -catenin.

5.7.1 β -catenin mRNA half-life appears unaffected by hnRNP A1 downregulation

HnRNPA1 has been shown to regulate mRNA stability as part of the KSRP complex (as introduced in section 5.1.3) so its effect on β -catenin mRNA stability was assessed. To investigate the role of hnRNP A1 in regulating β -catenin mRNA stability, esiRNA transfected GFP- β -cat-U2OS cells were treated with Actinomycin D to inhibit further transcription, with RNA harvested at the indicated time points (Figure 5.10) prior to

undertaking qRT-PCR to assess β -catenin mRNA half-life. HnRNP A1 depletion appeared to have no effect on β -catenin mRNA stability, with the half-life unchanged from control conditions (Figure 5.10). β -catenin mRNA appeared to undergo rapid decay in both instances with a $t_{1/2}$ of approximately 75 minutes; similar to previous reports whereby β -catenin mRNA half-life in unstimulated Wnt conditions varied from 45 minutes [494] to 100 minutes [183], depending on cell type. GAPDH mRNA was highly stable and also did not change significantly with hnRNP A1 depletion (Figure 5.10). While the data was not entirely unexpected given the lack of 3'UTR and therefore AREs in the eGFP- β -catenin U2OS cells, the role of hnRNP A1's role in regulating mRNA stability through association with elements within the coding region, as observed with c-fos [495] and IL-2 [496] for example, should not have been discounted prior to this experiment.

5.7.1.1 hnRNP A1 and KSRP do not associate in eGFP- β -Catenin U2OS cells.

As it was hypothesised that hnRNP A1 regulated β -catenin mRNA as part of a complex with KSRP (section 5.1.3), co-immunoprecipitation assays were undertaken with eGFP- β -catenin U2OS whole cell lysates to verify the reported interaction between hnRNP A1 and KSRP [185, 489]. While both hnRNP A1 and KSRP immunoprecipitated efficiently, no interaction was detected for either (Figure 5.11A), implying that they do not interact in this particular cell line. Furthermore, hnRNP A1 mRNA stability was assessed as it was also reported to be a target of KSRP, [185, 489], with hnRNP A1 mRNA intriguingly stable in eGFP- β -catenin U2OS cells, indicating that it may not be targeted by KSRP in this particular context (Figure 5.11B).

Taken together the data suggests that, despite strong links to KSRP, hnRNP A1 appears unlikely to be mediating its effects by regulating β -catenin mRNA stability, as part of, or independently, of a ribonucleocomplex with KSRP in the cell types studied within this project.

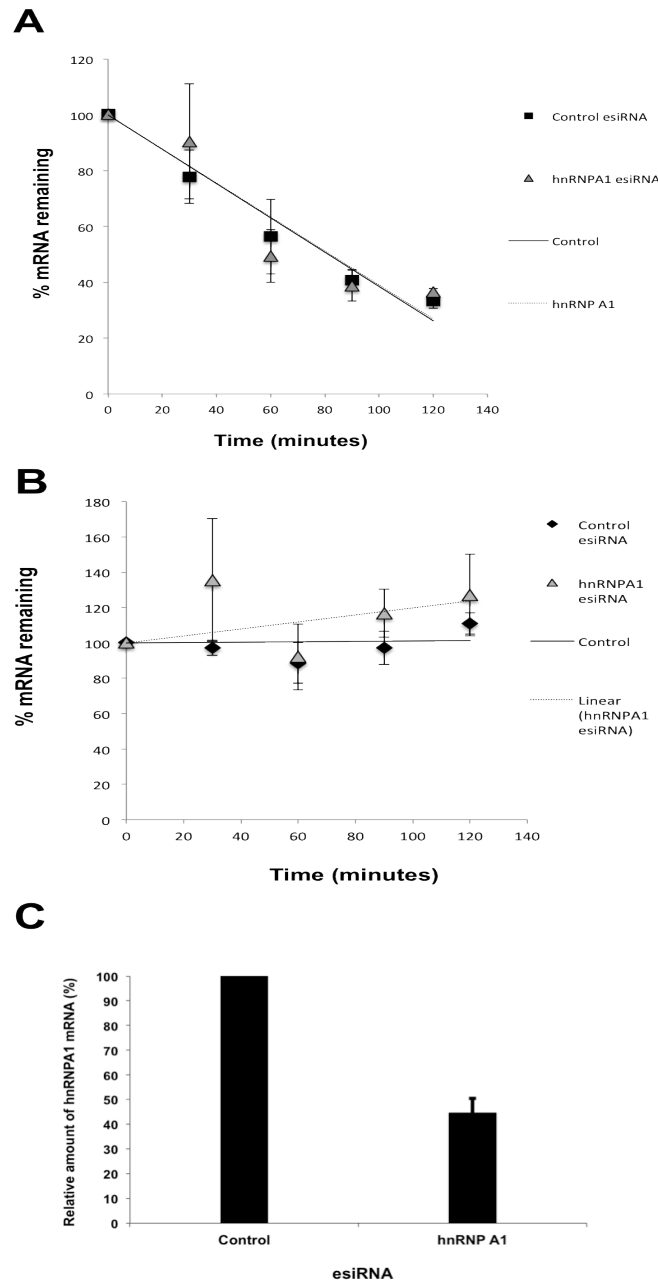


Figure 5.10 hnRNP A1 does not regulate β -catenin mRNA stability

esiRNA transfected U2OS eGFP- β -catenin cells were treated with Actinomycin D with RNA isolated at the indicated time points following treatment. Quantitative RT-PCR analysis of β -catenin (A) or GAPDH (B) mRNA levels in cells transfected with control or hnRNP A1 esiRNA. Data displayed as a percentage of the mRNA level at T0 (100%) and represents mean values \pm S.E.M from 3 independent experiments in triplicate. (C) qRT-PCR analysis of hnRNP A1 mRNA levels reveal that, in the above experiments, average knockdown by esiRNA was 56%. Data normalised to GAPDH with mean \pm S.E.M from 3 independent experiments in triplicate displayed. Rosalind Roberts contributed to the experiments and analysis as part of her final year research project.

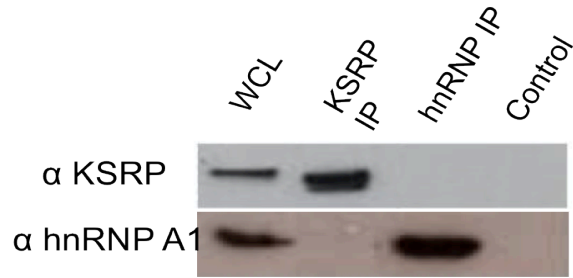
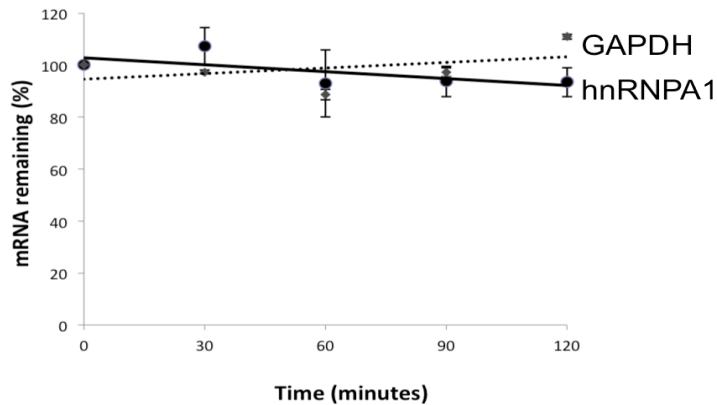
A**B**

Figure 5.11 hnRNP A1 mRNA is highly stable and does not appear to be part of the KSRP complex in eGFP-β-catenin U2OS cells.

(A) Western blot analysis of whole cell eGFP-β-Catenin U2OS cell extracts immunoprecipitated with KSRP or hnRNP A1 antibody (lanes 2 + 3, respectively). Control is protein G beads alone.

(B) Quantitative RT-PCR analysis of GAPDH or hnRNP A1 mRNA levels in control esiRNA treated cells. eGFP-β-catenin U2OS cells were treated with Actinomycin D and RNA isolated every half hour following treatment. Raw values were converted to % with $2^{(-\Delta C_T)}$ formula, with time zero values taken as 100%. The results were obtained in two independent experiments in triplicate and are shown \pm S.E.M.

Rosalind Roberts contributed to the experiments and analysis as part of her final year research project.

5.7.2 β -catenin mRNA synthesis is unaltered upon hnRNP A1 downregulation

The eGFP tagged β -catenin in the U2OS cell line is transcribed from an artificial cytomegalovirus (CMV) promoter. Therefore, it was unlikely that hnRNP A1 would be involved in regulating β -catenin mRNA synthesis as its downregulation resulted in increased β -catenin in both endogenous β -catenin in the 7df3 and parent U2OS cell lines, in addition to the eGFP- β -catenin in the U2OS cell line. However, to confirm this, β -catenin mRNA levels upon hnRNP A1 knockdown was investigated in the parent U2OS cell line by qRT-PCR.

In hnRNP A1 esiRNA transfected U2OS cells there appeared to be no increase in β -catenin mRNA levels (Figure 5.12A and B). Upon repeating in the eGFP- β -catenin U2OS cell line, a 35% increase in β -catenin mRNA was observed, which wasn't significant due to the highly variable nature of the data (Figure 5.12 C) as indicated by the large associated p-values. Therefore, the data implies that hnRNP A1 does not negatively regulate β -catenin by inhibiting its synthesis at the mRNA level.

5.7.3 hnRNP A1 may bind β -catenin mRNA.

Given recent work on a KSRP-Dishevelled complex that harboured and regulated β -catenin mRNA [183] , the ability of hnRNP A1 to also bind to its mRNA was investigated. HnRNP A1 was immunoprecipitated from standard U2OS cell lysates with RNA subsequently isolated and amplified by qRT-PCR. β -catenin transcripts were found in an abundance of over 9 fold compared to bead only control in both nuclear and cytoplasmic compartments (Figure 5.13). This was also observed in eGFP- β -catenin U2OS cells, although to a lesser degree (approximately 4 fold, data not shown). This interesting preliminary result hints at a possible role for hnRNP A1 in transporting β -catenin mRNA between compartments and potentially harbouring it in the cytoplasm ready for release and subsequent translation upon initiation of Wnt signalling. Future assays will investigate this observation further.

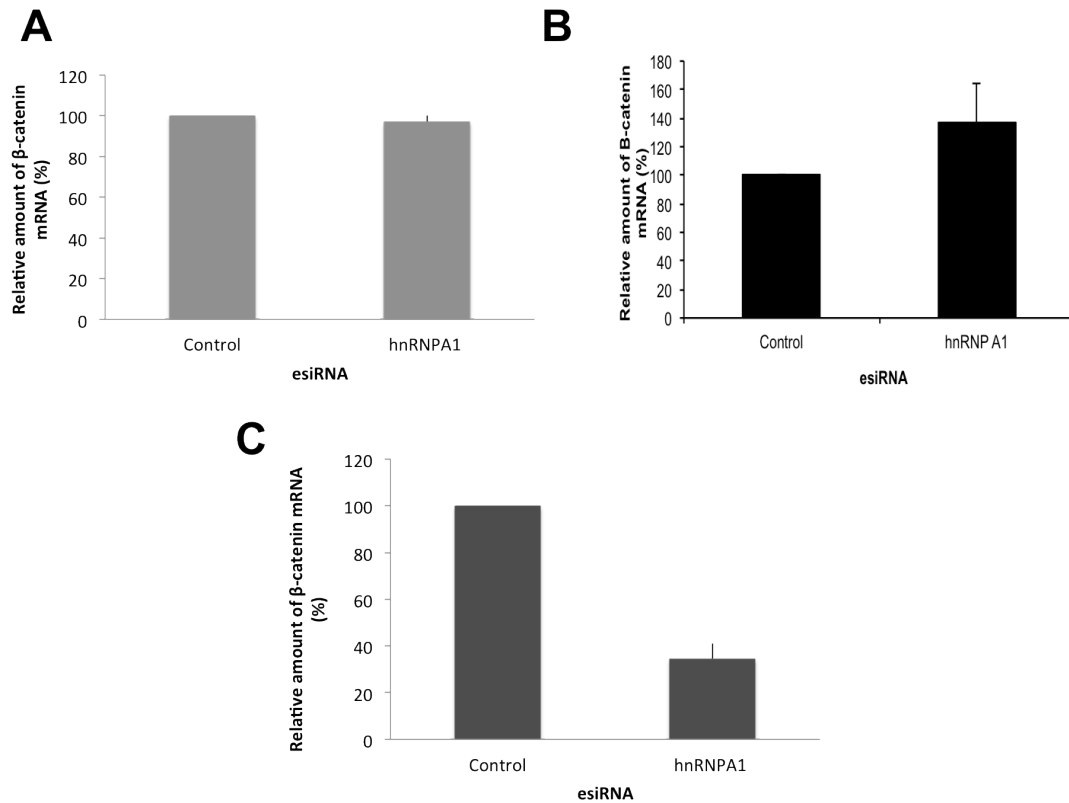


Figure 5.12 hnRNP A1 down regulation has no effect on β -catenin mRNA levels in both eGFP- β -catenin and parent U2OS cell lines.

qRT-PCR analysis of β -catenin mRNA levels in cells treated with control and hnRNP A1 esiRNA in standard U2OS cells (A) and eGFP- β -catenin U2OS cells (B) following normalisation to RPL32 and GAPDH respectively using the $2^{(-\Delta\Delta C_T)}$ formula. Mean values \pm s.e.m of triplicates from n=2 (A) or n=3 (B) independent experiments are displayed. (C) qRT-PCR analysis of hnRNP A1 mRNA levels in (A) revealed a 66% knockdown by hnRNP A1 esiRNA in the standard U2OS cell line. Data normalised to RPL32 with mean \pm S.E.M from 2 independent experiments in triplicate displayed. Rosalind Roberts contributed to the experiments and analysis in part (B) of the figure as part of her final year research project.

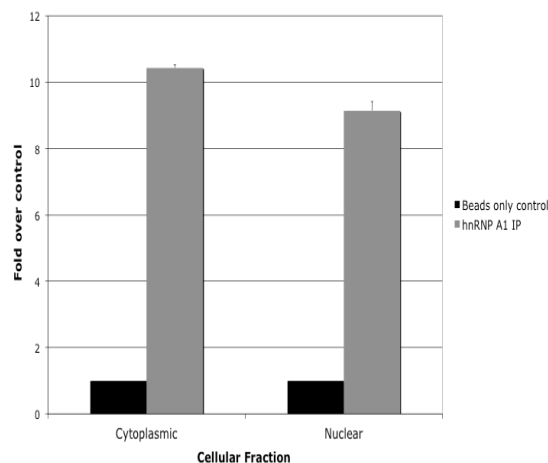


Figure 5.13 hnRNP A1 binds β -catenin mRNA

RNA immunoprecipitation assay of U2OS cell lysates with anti-hnRNP A1 antibody. RNA isolated from the immunoprecipitates were analysed by qRT-PCR with primers specific for β -catenin with bars representing relative amounts of β -catenin mRNA compared to bead only control of a single experiment in triplicate.

5.8 Summary

HnRNP A1 was identified in the three imaging screens in two different cell lines as a potential novel regulator of β -catenin and subsequent TCF-dependent transcription. The primary data was extensively reconfirmed and validated using alternative RNAi reagents in addition to rescue experiments. Whilst an interaction between hnRNP A1 and β -catenin was observed, it appeared to play no role in regulating β -catenin protein stability, with the investigation then turning to its many mRNA processing functions. HnRNP A1 knockdown did not appear to affect the stability of β -catenin mRNA, nor was hnRNPA1 a part of a KSRP complex, the strongest published link to β -catenin mRNA regulation currently available. Preliminary data indicated that hnRNP A1 was able to bind β -catenin mRNA, which in turn suggested possible roles in regulating β -catenin mRNA localisation and/or translation initiation. Further studies will be required to fully understand hnRNP A1's suppressive regulatory role in the Wnt/ β -catenin signalling pathway.

CHAPTER 6. DISCUSSION

The β -catenin/Wnt signalling pathway is a highly conserved pathway crucial to several aspects of development and disease. The aim of this study was to develop high-throughput imaging assays to identify novel regulators of β -catenin levels and nuclear localisation in the context of Wnt signalling. Three genome-wide screens were undertaken, with all identifying known β -catenin/Wnt signalling components, in addition to genes previously unassigned to this pathway. Subsets of esiRNA from each screen were selected for reconfirmation, with 81 genes being identified as promising candidates for further validation and mechanistic studies. The identity and potential insights gained from some of the identified novel Wnt regulators in β -catenin regulation will be discussed briefly alongside consideration of the two main findings of the study; the lack of correlation between β -catenin levels and localisation with TCF-dependent transcription and the identification of a novel post-transcriptional regulator of β -catenin, hnRNP A1. Firstly, the apparent cell-type specificity of the β -catenin regulators identified will be briefly discussed.

6.1 Cell type specificity of β -catenin and TCF-dependent transcription regulation.

The degree of overlap between the genes that regulated β -catenin levels and nuclear localisation in both U2OS screens was relatively high, despite the fact that β -catenin levels were at basal levels in the UB screen and at induced levels (via loss of APC) in the UA screen (Figure 4.15 and Figure 4.16). However, upon comparing the data sets obtained from different cell lines the majority of the components identified in these genome-scale screens were detected in only one cell line. This was true for both the H and UA/UB imaging screens, in addition to the comparisons between the different screens for regulators of TCF-dependent transcription (Figure 4.31). The overlap gene sets from the TCF-dependent transcriptional screens (7df3, this lab, HeLa [267], DLD-1 [242]) were selectively enriched for 'core pathway' components including Axin, APC and TCF, suggesting that these proteins are essential for TCF-dependent signalling in many cellular contexts. The overlap between any two cell lines from the transcriptional screens was rather small, 17 to 28

genes, including more Wnt pathway ‘core’ components like AXIN1, BCL9, DVL2, LEF1, PYGO2, TLE1, WNT7 (Figure 4.31).

A number of factors could contribute to this apparent specificity. Most trivially, screen-specific RNAi reagents could non-specifically alter levels of ‘core-pathway’ regulators through off-target effects. However, the use of siRNA reagents that target non-overlapping regions of target mRNAs can exclude off target effects in >70% of cases [497-499]. The number of hits validated through the use of non-overlapping siRNA reagents were broadly similar in the imaging screens, the 7df3 transcriptional screen and the DLD-1 screen [242] representing 49% (average of the three imaging screens), 33% and 39% of primary hits respectively. Importantly, the majority of genes that were validated through the use of non-overlapping siRNA reagents in the transcriptional screens were found only within one of the cell lines examined, suggesting that most regulators of TCF-dependent transcription are cell type specific. Similar cell-type specific differences were highlighted by Major et al., who showed that only 40% (119/298) of the validated regulators identified in DLD-1 colon cancer cells were shared by SW480 colon cancer cells [242]. While no large-scale comparisons can be made with the β -catenin imaging screens, comparisons between the re-confirmed esiRNAs corroborate the above, with only 9 of the 81 regulators that reconfirmed with non-overlapping esiRNA scoring positive in both cell lines (Table 4.13).

Genetic redundancy, differences in the efficacy of siRNA mediated action and the use of arbitrary ‘hit’ selection thresholds all lead to apparent ‘cell-type specificity’. However, several of these limitations are not applicable upon comparing the β -catenin imaging screens undertaken in this study, as the same esiRNA reagents, in addition to data analysis methods, were utilised. Mining of mRNA expression databases show that the majority of HEK293-specific hits identified were differentially expressed in a range of cell lines and tissues (UCSC genome browser database: [500]; data not shown), suggesting that cell-type specific effects on β -catenin levels and activity, in addition to TCF-dependent transcription, may result, at least in part, from cell-specific expression of the regulators. Similar analysis is required for the gene sets identified in the U2OS imaging screens to corroborate this further. Overall, the data implies the

presence of cell-type specific regulation of both β -catenin levels and activity, in addition to TCF-dependent transcription in response to gene downregulation.

The physiological relevance of having many potential β -catenin and TCF-dependent regulators within Wnt signalling, in addition to 'core' pathway components, is currently unclear. As will be discussed in subsequent sections, the complexity of β -catenin regulation within Wnt signalling is such that the pathway can no longer be considered a single linear entity interacting linearly with others [282, 501]. Unprecedented levels of cross-talk between the major signal transduction pathways, and indeed even between different Wnt 'pathways', were revealed in the screens undertaken within this study, which will be discussed in further detail in the subsequent section of this chapter. This, along with mounting evidence in the literature, suggests that the 'out-put' from β -catenin signalling in the Wnt pathway (i.e. activated transcription of target genes) relies heavily on additional inputs from other signalling modules, including those downstream of PI-3-kinase and upstream of c-jun [116, 372]. It has been suggested that such complexity would allow for context-dependent Wnt/ β -catenin signalling, whereby Wnt stimulation induces different gene expression patterns in different cells depending on the degree of cross-talk with other pathways and the variety of secondary inputs [282, 372].

This may explain, at least in part, the surprisingly small overlap in gene expression profiles obtained from Wnt3a stimulation of different cells [502-504]. Different levels of Wnt can result in the transcription of different target genes, suggesting that it can act as a graded morphogen in its regulation of development. For instance, different levels of β -catenin activation was observed to have different phenotypic consequences [505] with Wnt/ β -catenin regulating stemness, proliferation and differentiation in adult stem niches, such as the skin and hair follicle, in a dosage and context-dependent manner [152, 153]. Recent theoretical and functional assays suggested that fold changes in β -catenin and not absolute levels dictated the output of Wnt signalling and is a more precise reporter of Wnt stimulation in a heterogeneous cell population [205]. This signalling system may act to compensate for natural biological (both environmental and genetic) noise so that, despite large variations in basal nuclear levels of β -catenin, the actual fold change is equivalent between all cells

[205, 506]. This is corroborated in a study where fold changes in nuclear ERK2 and not its absolute levels were more reliable indicators of response to ligand stimulation [506].

Taken together, the data suggests the need to consider the Wnt/ β -catenin pathway as a larger network of interactions, with 'core' pathway components providing the backbone that connects cell-type specific regulators of β -catenin levels and localisation to a common transcriptional output [282, 501]. The overall organisation of the Wnt/ β -catenin network would differ between cells, resulting in the observed cell-specificities.

6.2 β -catenin and TCF-dependent transcription.

A widely held and extensively advocated notion within the field is that increased total levels of β -catenin correlate with increased nuclear localisation and subsequently with activation of TCF-dependent transcription [66, 91]. Genome scale correlation analysis between the primary imaging screens (H, UB and UA) and a previous screen for TCF-dependent transcription in the 7df3 reporter cell line suggested that there was no relationship between β -catenin levels, localisation and transcriptional activity (Figure 4.23). A slight positive correlation was observed between β -catenin localisation in the UA and UB screens and TCF-dependent transcription in the reconfirmed set of identified β -catenin regulators. Comparative analysis of the putative β -catenin modulators identified in the H screen with the transcriptional screen in the same cell line displayed a surprising lack of overlap (Figures 4.26), which was even smaller when comparing with published TCF-transcriptional RNAi screens in DLD-1 [242] and HeLa cells [267] (Figures 4.28 and 4.29). Comparative analysis of the primary β -catenin imaging screen data from both U2OS screens with TCF-transcriptional screen data in the 7df3s also displayed a lack of significant overlap in the identified modulators (Figure 4.27). Overall, the data challenged the prevailing model of Wnt/ β -catenin signalling and suggested that modulating β -catenin levels and localisation does not directly couple to transcriptional changes.

One could argue that a number of trivial, technical factors may contribute to these observations, as it is widely appreciated that within each individual screening approach there are inherent experimental and/or theoretical limitations, such as high false positive and negative discovery rates [248, 262, 507]. However, the imaging screens were deemed high quality as assessed by: 1) good screen associated Z-factors, 2) the identification of known Wnt/ β -catenin pathway regulators in each screen and 3) the enrichment of Wnt and ubiquitin mediated proteolysis pathways in the identified regulators of β -catenin. Cell type specificity is another potential reason as to why the modulators of β -catenin identified in the imaging screens were not picked up in comparative TCF-transcriptional screens. However, this cannot be the case in the H screen as it was undertaken, not only in the same cell line, but also utilising the same esiRNA reagents as one of the TCF-transcriptional assays compared to. Nevertheless, greater overlaps in identified ‘hits’ were observed between screens undertaken in the same cell line (Figures 4.15, 4.16, 4.26 and 4.27), indicative of the cell-type specific effects described in the previous section. In subsequent sections, the lack of correlation between β -catenin levels and localisation with transcriptional activity will be discussed in further detail, alongside examples of some of the mechanistic insights provided by the screening data obtained from this work.

6.2.1 β -catenin phosphor-isoforms and transcriptional activity

While accumulation and nuclear localisation of β -catenin is often regarded as the hallmark of Wnt activation, the observations within this study, whereby β -catenin levels and localisation did not correlate with transcriptional changes, is supported by several examples in the literature [92, 153, 186-188, 508, 509]. For example, studies have demonstrated activated Wnt signalling in the absence of detectable nuclear β -catenin, such as in colon carcinoma cells [197, 202, 510, 511] and that levels of β -catenin alone did not fully explain β -catenin/TCF-transcriptional activation [186]. In *Xenopus* embryos, β -catenin’s signalling ability was demonstrated to be dependent on its N-terminal GSK3- β phosphorylation sites (S33, S37, T41), irrespective of total levels [186]. This was corroborated in mammalian cells whereby a β -catenin Ser37 and Thr41 de-phospho specific antibody (Active β -catenin (ABC) antibody) was

utilised to demonstrate that transcriptional activity was mediated by molecular forms of β -catenin that remained unphosphorylated at these sites [187]. ABC, representing a small fraction of the total β -catenin pool, resides in membrane in unstimulated conditions [188, 219, 512], and is associated with increased cytosolic levels and transcriptional activity upon Wnt stimulation [187, 219]. More recently, phosphorylation at S45 has also been suggested to be associated with transcriptional activity, with this form increasingly membrane localised upon stimulation of transcriptional activity [219].

Other notable β -catenin phospho-isoforms that regulate its localisation and transcriptional function include a C-terminal Y654, phosphorylated by src kinase, which lowers β -catenin's affinity for E-cadherin and increases its availability for interactions with TCF proteins to activate transcription [223]. Phosphorylation at Y142 by the tyrosine kinases Fer, Fyn or Met also disrupts β -catenin's interactions with α -catenins in adherens junctions [224] and promotes its interaction with BCL9-2 to sequester it in the nucleus [124]. CSK (c-src tyrosine kinase) has been demonstrated to form a complex with β -catenin at adherens junctions and is involved in the regulation of FYN [224, 359, 360], so may also be involved in mediating β -catenin phosphorylation at Y142. Notably, CSK was observed as a modulator of β -catenin in the H imaging screen, in addition to the RNAi screens for regulators of TCF-dependent transcription in HeLa and DLD-1 cell lines, suggesting a key role in regulating β -catenin levels and transcriptional activity in different cell contexts (Figure 4.29). An assessment of the phosphorylation status of β -catenin Y142 and other tyrosines, especially Y654 mentioned above, upon CSK knockdown may provide further insight into its precise role in β -catenin regulation.

In addition to phosphorylation, other post-translational modifications appear to play a role in mediating β -catenin's levels and transcriptional activity. For example, O-GlcNAc glycosylation (O-GlcNAcylation) of β -catenin has been demonstrated to negatively regulate its levels in the nucleus and is associated with decreased transcriptional activity [115]. Furthermore, HDAC6 deacetylation of β -catenin at lysine 49 in response to EGF stimulation was observed to inhibit β -catenin phosphorylation at serine 45, resulting in its nuclear localisation and increased c-myc

gene expression [112]. Intriguingly, some forms of Wnt activation result in the induction of the export of a repressive TCF from the nucleus, suggesting that the active form of β -catenin may itself be out of the nucleus and a scaffold role for a membrane complex, which may aid signalling to a subset of target genes that are derepressed [513, 514].

Taken together, the levels and localisation of specific transcriptionally competent forms of β -catenin, especially ABC, are increasingly considered as the hallmark of β -catenin transcriptional activity, rather than simply changes to total levels, which was the form of β -catenin assayed within this study. Recently, a multiplexed assay has been developed that combines protein-protein interaction, co-immunoprecipitation and sandwich immunoassays in a single suspension bead array to allow for the quantification of different forms of one protein within the same sample [235]. This was elegantly used to quantify total β -catenin, its phosphorylation at multiple sites and the ratio of complexed and free β -catenin in HEK293s treated with Wnt3a and GSK-3 β inhibitors [235]. Future studies utilising this technique, along with more traditional isoelectric focusing assays, to investigate the novel β -catenin regulators identified within this work may be highly beneficial in ascertaining their roles in regulating the dynamics of specific β -catenin isoforms.

6.2.2 Fine tuning the Wnt signalling output

As described above, post-translational modifications, such as phosphorylation, acetylation and sumoylation can dictate β -catenin's binding partners and therefore its subcellular localisation and subsequent function within a cell [232-234]. It is becoming increasingly appreciated that the Wnt signalling pathway is neither in an 'on' or 'off' state, but rather has a range of activation levels, with β -catenin post-translational regulation, especially phosphorylation events, key to the "fine-tuning" of Wnt signalling [234]. This fine-tuning means that β -catenin and its regulatory components are subject to inputs from a myriad of factors, notably kinases, involved in diverse signalling pathways, from src kinases [224] and PKC[226] to AKT[221] and CDKs [227]. Depending on the cell and environmental contexts at the time, both

Wnt-dependent and -independent β -catenin modifications are likely to co-operate or compete in modulating its localisation and function in order to regulate the required adhesion and signalling responses [42, 235].

The precise components and pathways that mediate the balance and/or switching between β -catenin's transcriptional and non-transcriptional roles have yet to be fully established and are likely to be highly context dependent. The screening data presented here may provide further insights into the pathways/processes that may be particularly involved in switching β -catenin from a transcriptionally inactive form to a form capable of activating transcription of Wnt target genes; potential examples of these are discussed further in section 6.3.

6.2.2.1 Switching between β -catenin's roles in adhesion and activated TCF-dependent transcription.

β -catenin's role in calcium dependent adherens junctions is well established, providing a means of associating plasma membrane cadherins with other catenins, such as α -catenin, which dynamically links adherens junctions (AJs) with the actin cytoskeleton [45]. The disruption of the β -catenin/cadherin interactions, by post-translational modifications to β -catenin for example, has significant consequences for cell-cell adhesion in addition to cytoskeletal organisation, with both processes playing key roles in many disease states, such as cancer, upon their aberrant regulation [48].

An enrichment of adhesion and cytoskeletal components were identified in all the screens undertaken within the study (Chapter 4.2). Given β -catenin's well-established role in adherens junctions this is not entirely surprising, but the fact that this appears seemingly uncoupled from TCF-dependent transcription on a genome-wide scale was unexpected.

It's acknowledged that changes in β -catenin's levels and localisation may be an indirect consequence of disrupting junctional complexes, with the screens, by proxy, identifying regulators of junctional formation in cells. The utility of high content

analysis allows for the re-interrogation of images using alternative algorithms to address new questions. Therefore, re-analysing the images for the degree of cell clustering/boundaries and correlating this with β -catenin levels and localisation for example would allow for the identification of more specific regulators of cell-cell junction formation and would, in turn, provide further insights into how this may, or may not, be linked to Wnt/ β -catenin signalling.

Studies have demonstrated that β -catenin's interactions with cadherins in AJs govern its ability to interact with its Wnt signalling co-activators in the nucleus [158]. Loss of E-cadherin has been shown to result in increased β -catenin nuclear localisation and TCF-dependent transcription in various cell types [158, 515-517]. Expression of E-cadherin and N-cadherin was observed to trigger the relocalisation of β -catenin to the membrane resulting in inhibition of TCF/LEF1 mediated transcription [517, 518]. However, studies have also demonstrated that the absence of E-cadherin alone does not induce β -catenin nuclear accumulation and activate Wnt signalling, except in cases where aberrant β -catenin is already present [519, 520]. siRNA-induced downregulation of E-cadherin appeared to enhance TCF-dependent transcription in colon carcinoma cells with mutated APC (and therefore compromised β -catenin degradation), while having no effect in normal non-transformed HaCaT keratinocytes [520]. In addition, loss of E-cadherin did not enhance Wnt signalling in Rip1Tag2 mice [521] while shRNA against E-cadherin resulted in β -catenin nuclear translocation in Ras transformed mammary gland cells [522]. This indicates that Wnt-dependent gene expression may be modulated by E-cadherin regulating the availability of β -catenin, especially ABC, but that, in the absence of Wnt signalling, this has negligible impact on transcriptional activation [520]. This suggests therefore, that loss of junctional integrity, which results in release of β -catenin from the membranes, may not be sufficient for induction of transcriptional activity and requires additional signal input(s) to mediate the nuclear accumulation of a specific transcriptionally competent form of β -catenin, such as ABC. Such inputs may mediate the phosphorylation or conformational changes to β -catenin that is required for nuclear transport [116] and binding to specific interaction partners, such as BCL9-2 for example [124], to sequester it in the nucleus. Furthermore, it has been demonstrated that distinct molecular forms of β -catenin, with different binding

properties to TCF and cadherins, dictate its role in adhesion or Wnt signalling, suggesting that its role in both processes may be regulated independently [158, 206]. The non-Wnt-stimulated form of β -catenin forms a dimer with α -catenin, while Wnt induces a monomeric form selective for TCF-binding with β -catenin's C-terminus regulating the availability of the ARM repeat region for other binding partners such as cadherin [206-208].

In addition, β -catenin's ability to co-activate the transcription of Wnt target genes rely on several other factors, such as TCFs, CBP/p300 histone acetylases and mixed-lineage-leukaemia (MLL1/MLL2) histone methyltransferase complexes, and these are also highly regulated by local activation of kinases [42, 523]. For example, phosphorylation of TCF3 by CK1 enhances its binding to β -catenin, while GSK3 β mediated phosphorylation of TCF3 inhibits this interaction [524].

Taken together, this might suggest that, while disruption of β -catenin's contacts at cell junctions often results in its enhanced cellular distribution, other modifications, as discussed in the preceding section of the chapter, are required to convert β -catenin (and its co-factors) into a form capable of activating TCF-dependent transcription [158]. Therefore, some of the regulators of β -catenin levels and localisation identified in the screen might also turn out to be TCF-transcriptional regulators if combined with other activating events within the pathway, with the implication that β -catenin modulation is necessary but insufficient for activated TCF-dependent transcription in these cases. For example, SPEN homolog (or SHARP), a corepressor protein implicated in the regulation of the Notch and EGF/Ras signalling pathways in *Drosophila* and identified as regulating β -catenin levels in the three imaging screens (Figure 4.16) [347, 348], is required for Wnt-dependent signalling in the wing, eye and leg imaginal discs [349] and was demonstrated to be a positive regulator of TCF-dependent transcription downstream of mutant β -catenin [350]. Another example is the solute carrier, SLC9A3R1 (EBP50 - solute carrier family 9 (sodium/hydrogen exchanger), member 3 regulator 1), which has been demonstrated to promote β -catenin-mediated TCF-transcription, but only in cells where β -catenin was already stabilised [319]. This may even indicate that mutant β -catenin could be subject to other forms of transcriptional activity regulation, possibly by binding to proteins that

may prevent access to the nucleus for example, or by requiring secondary inputs from other signalling pathways, such as phosphorylation mediated by AKT signalling [221] and src signalling [229]. This interesting concept will be discussed in further detail in section 6.3 below, alongside examples of insights gained from the primary screening data.

6.3 Mechanistic insights from the primary screen data

The high-throughput imaging screens undertaken within this study identified a wide variety of potential regulators of β -catenin, with most appearing to be uncoupled to transcriptional regulation. Plausible explanations for this interesting finding have been extensively discussed above, with this section aiming to provide examples of insights gained from the screens that may support the ideas presented in the preceding section.

Whilst the primary ‘hits’ obtained from each of the three β -catenin screens differed greatly, recurring themes were observed:

1) β -catenin regulation by adhesion and cytoskeletal components - There were significant enrichments in genes involved in various aspects of adhesion and cytoskeletal regulation within each of the data sets obtained from the primary screens. These included: ACTN4 (UA), TLN2 (UA), PXN (UA), LAMB3 (UA), ITGA3 (UA), ITGA8 (UB), ITGA5 (UA), CTNND1 (H), CDH2 (H, UA), EFNA4 (UB), NRXN2 (UB), EPHA3 (UA), RAC1 (UA, H), RAP1A (UA), ROCK2 (UB, H), ROCK1 (H), CDC42 (UA, H), VAV1 (H), RHOG (H), and CDC42EP2 (H). (Chapter 4.2)

2) Signalling cross-talk - β -catenin regulation appears to involve various other major signalling pathways other than Wnt, such as JNK/MAP kinase, Insulin/PI3-kinase TGF- β and Notch signalling, which were all overrepresented in the identified modulators of β -catenin.

3) Transcriptional and translational regulators - a surprising number of transcriptional and translational regulators were identified from all screens, implying

that β -catenin regulation at this level may be of greater importance and more limiting than previously anticipated. mRNA processing factors included hnRNPA1 (UA, UB and H), HNRNPA1L2 (UA, UB), hnRNP H1 (UA, UB, H), JMJD6 (UB), MAGOH (H), NHP2L1 (UA, UB, H), UPF1 (UA, UB, H) and SNRPD2 (H), in addition to factors involved in RNA transport such as NUP85 (UA), NUP133 (UA), NUPL1 (UA, UB), NUP160 (UB), NUP205 (H) and NUP155 (UA, H) (Chapter 4.2).

The sheer variety of potentially interesting components and biological processes identified from the screens mean that an extensive discussion on all the findings is impossible within the space constraints of this thesis. Given the primary aim of the study was to identify β -catenin regulators in the context of Wnt signalling, the molecular processes and components identified in various combinations of the screens that may regulate both β -catenin levels/localisation and transcriptional activity (as observed through comparative analysis with published RNAi screens for regulators of TCF-dependent transcription) are particularly interesting, especially those that implicate signalling cross talk with that of Wnt/ β -catenin signal transduction. Links between Wnt/ β -catenin regulation and two specific molecular processes/pathways identified in the screens will be discussed: namely Ephrin and Integrin mediated adhesion and signalling, in addition to a brief discussion into non-canonical Wnt/Calcium signalling.

6.3.1 Ephrin-mediated signalling

Numerous Ephrin receptors and ligands were identified in the U2OS imaging screens for regulators of β -catenin levels and localisation, which included EPHA3 (UA), EPHA8 (UB), EFNA4 (UB), EFNB2 (H), with EFNA4 (UB) and EPHA3 (UA) selected for secondary assays and reconfirming their primary screen effects (Table 4.13). Ephrin receptors and associated ligands are involved with regulating tissue morphogenesis during development and in adult life [525]. Genes encoding the receptors EphB2 and EphB3 are known β -catenin/Tcf4 target genes in normal and cancerous intestinal cells [149, 173] with EphB signalling regulating the positioning of cell types along the crypt-villus axis [173, 526]. EphB has been demonstrated to

suppress progression of colorectal cancers [527] and is believed to compartmentalise the expansion of CRC cells in a manner dependent on E-cadherin mediated adhesion [526]. The identification of Ephrin Receptors of the 'A' group in β -catenin regulation is interesting and suggests a wider role of Ephrin signalling in Wnt/ β -catenin signalling than envisioned, with previous research mostly dedicated on the Ephrin receptor B group due to their tumour suppressive roles [528].

Intriguingly, increased nuclear localisation of β -catenin following ablation of various Ephrin receptors and ligands did not result in transcriptional activation, suggesting that in certain cellular contexts (such as in the 7df3 reporter cells), an additional step is required to mediate β -catenin transcriptional activity, as discussed in section 6.2 of this chapter. Potentially relevant to the regulation of β -catenin's activity by phosphorylation, is the link between Ephrin signalling and activation of c-src signalling, with the observation that clustering of Ephrin-A molecules and Ephrin-A receptors leads to the recruitment of Fyn; a kinase known to be important for the Tyr142 phosphorylation of β -catenin [224]. Significantly, c-src tyrosine kinase (CSK) is involved in FYN regulation [360] and was observed as one of the few overlapping genes between the β -catenin imaging screens and various transcriptional screens suggesting a conserved role in different contexts (Figure 4.29). Assessing β -catenin's tyrosine phosphorylation upon loss of Ephrin for example, may provide further insight into this potential link to the regulation of β -catenin activity.

Alternatively, Ephrin receptor activity also provides avenues for the stimulation of multiple Rho family GTPases, through the activation of various Rho GTPase exchange factors. For example, Ephrin-A receptor ligand binding activates the Rho exchange factors, Ephexin, VAV-2 [529] and Tiam 1 [530], leading to both RhoA and Rac1 activation. Rac1 has been implicated in Wnt induced nuclear accumulation of β -catenin by stimulating JNK2 mediated phosphorylation of β -catenin at Ser191 and Ser605, thus providing a potential link between Ephrin induced modulation of β -catenin levels and its transcriptional activity.

6.3.2 Integrin mediated signalling.

Amongst the many cell adhesion molecules identified from all screens, focal adhesion components were particularly prevalent in addition to mediators of Integrin signalling. These included ACTN4 (UA), TLN1/2 (UA), PXN (UA, UB), LAMB3 (UA), ITGA3 (UA, UB), ITGB8 (UA, UB, H), ITGAV (UA, H), ITGB1 (H), ITGB8 (UB, H) ITGA8 (UB), ITGA5 (UA, UB), ROCK2 (UB, H), PIK3R5 (UB, UA), MYLPP (UA, UB), PRKCG (UA, UB) and PIK3CB (UA) to name but a few. Integrins were also prevalent in the overlapping list of genes between the imaging screens and the comparative screens for regulators of TCF-dependent transcription (as displayed in Figure 4.30).

Integrins mediate connections between focal adhesions and the extracellular matrix (ECM) and have been demonstrated to also be important during embryonic development, tissue maintenance and repair [531]. In addition to their mechanical roles in mediating adhesion to the extracellular matrix and to other cells, integrins facilitate so called ‘outside-in signalling’, whereby extracellular chemical signals are transmitted intracellularly to regulate the cellular responses, such as differentiation, survival and migration required in relation to the cells local environment and adhesive state at a time [531]. Focal adhesion kinase (FAK) and integrin-linked kinase (ILK) are two receptor associated kinases that mediate integrin signalling [532] and while FAK knockdown had no effect in cell lines utilised in the primary screens, downregulation of ILK resulted in increased β -catenin levels in the U2OS screen. Integrin-linked kinase (ILK), interacts with the cytoplasmic domain of β -1 integrin and acts as a proximal receptor kinase regulating integrin-mediated signal transduction [532]. Interestingly, ILK has been previously demonstrated to induce β -catenin nuclear translocation, in the absence of increased overall levels [533] with its inhibition in colon carcinoma cells resulting in decreased nuclear β -catenin and transcriptional activity [534]. ILK was also reported to be stimulated upon cell attachment of cells to fibronectin and by insulin in a PI(3)-kinase-dependent manner to directly phosphorylate GSK- β , in addition to AKT, resulting in its activation [535]. Integrin mediated signalling has previously been implicated in potentiating insulin receptor phosphorylation [536] with focal adhesion kinase demonstrated to play a role

in mediating the cytoskeletal remodelling required for glucose uptake following insulin stimulation [537]. Many Insulin/AKT signalling components were identified in the screens, including PI3K3CD (UA), PIK3CB (UA, UB and H), GSK3 β (UA) IRS4 (UA), INSR (H and UA) and EIF41EB (UA), suggesting a potential role for PI3-kinase signalling in β -catenin regulation in response to changes in Integrin mediated adhesion. PI3-kinase signalling has been implicated in mediating Wnt3a-induced proliferation of fibroblasts via AKT activation [330], while EGFR stimulated AKT activation has previously been demonstrated to phosphorylate β -catenin at S552, resulting in its dissociation from cell-cell junctions and increased nuclear translocation [221]. Furthermore, Integrin and Wnt signalling cross talk has previously been reported via the adaptor protein, Grb2, which was demonstrated to bind Dvl2 and acts downstream of focal adhesion kinase (FAK) to amplify β -catenin-dependent transcription through a mechanism involving Rac1, JNK and c-jun [372]. In this study, β 1 integrin mediated signalling in response to binding to the ECM protein collagen was shown to synergise with Wnt pathway activation [372]. Rac1 and JNK have both been implicated in regulating β -catenin nuclear localisation by phosphorylation on S191 and S605, downstream of PI3-kinase [116]. The effect of ILK and integrin ITGB1 knockdown on β -catenin phosphorylation at S552, S191 and S605, in both the absence and presence of PI3-kinase inhibitors such as LY294002 and Wortmannin, may provide further insights into this link between Integrin and Insulin/PI3-kinase signalling and β -catenin regulation. Investigating whether integrin associated complexes may directly associate with or modify β -catenin may reveal further insights into this link identified from the screens, such as undertaking *in vitro* kinase experiments to assess the ability of ILK for example to phosphorylate β -catenin on the key residues implicated in its localisation. Interestingly, Paxillin, an adaptor protein that recruits components such as ILK, FAK, and CSK to focal adhesions in addition to binding to integrin cytoplasmic tails, has been reported to interact with β -catenin during Rac/Cdc42-mediated endothelial barrier-protective response to oxidized phospholipids [538]. This interaction between focal adhesions and AJ complexes via paxillin and β -catenin association was demonstrated to be critically dependent on Rac and Cdc42 activities [538]. Interestingly, in both UA and UB primary screens downregulation of Paxillin resulted in increased β -catenin levels. Taken together, the data may suggest a means of transmitting extracellular signals

from cell surface integrin-ECM interactions to the modulation of Wnt/ β -catenin driven gene expression in response to specific environmental cues and changes to the extracellular matrix. Further investigation however would be required to ascertain if integrin signalling plays a more direct role in β -catenin regulation than previous studies suggest [372, 533].

6.3.3 Non-canonical Wnt pathways in β -catenin regulation

‘Non-canonical’ Wnt pathways, such as the Wnt/Calcium and Wnt/JNK (or PCP) pathways, possess roles in cytoskeletal and adhesion processes and have been demonstrated to both activate or suppress Wnt/ β -catenin signalling [39]. Different Wnt ligands can stimulate distinct Wnt pathways through binding of different combinations of unrelated receptors, even upon recruiting shared components such as Dvl, Axin and GSK3 [29, 30].

6.3.3.1. Wnt/Calcium signalling

A wide variety of genes implicated in calcium signalling were identified from the UB and UA screens, including CAMK2A, PDE1A, PTK2B, PRKCA, PLCB4, PLCD3, PRCKG. Protein kinase C (PKC) has been demonstrated to negatively regulate Wnt/ β -catenin signalling through phosphorylating β -catenin, which resulted in its degradation [226]. In line with this, downregulation of PKC α , in addition to PKC γ , resulted in increased β -catenin nuclear localisation in the U2OS imaging screen. Calcium has been widely implicated as an important second messenger in non-canonical (β -catenin) independent signalling [314], with the identification of key components of the Wnt/calcium signalling pathway in this screen, such as CAMK2A and PKC isoforms, interesting as it hints at a more involved regulatory role for non-canonical Wnt signalling in β -catenin localisation. Studies have demonstrated that antagonism exists between the β -catenin-independent and -dependent Wnt pathways, such as through the activation of NF-AT for example, which was demonstrated to play an essential role in mediating ventral signals in the *Xenopus* embryo through downregulating β -catenin signalling [35]. NF-AT, via activated Nemo-Like Kinase

(NLK), is known to inhibit Wnt dependent transcription of target genes through the phosphorylation of TCF transcription factors [37]. The screens, however, suggests that non-canonical Wnt/Calcium signalling may play a more intimate role in regulating β -catenin levels and localisation than currently envisioned. Conversely, given β -catenin's crucial role in calcium dependent adhesion, the effect of the calcium signalling components identified on β -catenin levels and localisations may also have been as a result of aberrant adherens junction formation. Further investigations, such as the re-analysis of the primary imaging data to assess the effects of the identified components above on cell boundaries, in addition to assays involving Wnt5a/Wnt 11 stimulation of cells along with downregulation of key components may clarify this issue.

6.3.4 Transcriptional and Translation regulation of β -catenin

Significantly over-represented within the genes identified from all screens were components of transcriptional, mRNA processing and translational processes. While the plethora of ribosomal components identified may well be a general effect, for reasons stated in Chapter 4.2, such as the identification of upregulators of β -catenin and the lack of toxicity observed upon knockdown of the components that were selected for further analysis, a more involved role for Wnt/ β -catenin signalling in ribosomal processes cannot be discounted. Especially in light of β -catenin's ability to bind Tor components [334], with the mTor pathway demonstrated to be involved in ribosomal biogenesis [539].

Components identified in the screens relating to mRNA processing included hnRNPA1 (UA, UB and H), HNRNPA1L2 (UA, UB), hnRNP H1 (UA, UB, H), JMJD6 (UB), MAGOH (H), NHP2L1 (UA, UB H), UPF1 (UA, UB, H) and SNRPD2 (H), in addition to factors involved in RNA transport such as NUP85 (UA), NUP133 (UA), NUPL1 (UA, UB), NUP160 (UB), NUP205 (H) and NUP155 (UA, H). Moreover, the mRNA processing factors hnRNP H1, JMJD6, MAGOH, NHP2L1 and SNRPD2 were reconfirmed in secondary assays (Table 4.13) and merit further investigation in future studies. As described in Chapter 5, an investigation into the

role of hnRNP A1 is underway, which will be discussed in further detail in the penultimate section of this chapter. Research into β -catenin's transcriptional and post transcriptional regulation is lacking with the general assumption that these processes are not linked to active Wnt signalling. Data from the imaging screens undertaken within this study implies otherwise and may reveal further insight into unanticipated levels of control within this complex developmental pathway.

In summary, this section has focused on a few molecular processes that were identified as regulating β -catenin levels and localisation in the imaging screens undertaken within this study, in addition to regulating transcriptional activity as revealed by comparative analysis with genome wide TCF-dependent transcription. These are examples of where the work has provided further insights into the processes and signalling events that regulate β -catenin, in addition to highlighting potential novel regulators that merit further investigation in future studies. The degree of overrepresentation of components from several signalling pathways, such as Insulin/PI3-kinase, Calcium, Notch and TGF- β signalling, observed within the primary imaging data was unprecedented. This implies a high level of cross talk between β -catenin (which does not automatically mean Wnt signalling as the primary data demonstrated) and other major signal transduction pathways, which recapitulate a common theme of 'cross-pathway interactions' that is supported by independent studies of selected pathways [305, 540-543]. Unfortunately, a detailed discussion of all the pathways and processes implicated in β -catenin regulation in this study is beyond the scope of this thesis, although the work may provide the foundations for several other projects in the future.

6.4 Dynamic regulation of β -catenin

Preliminary time-lapse microscopy revealed that β -catenin levels appeared to cycle with variable periods of approximately 5-9 hours, which was still present in the presence of hnRNPA1 esiRNA, Wnt-3A but not in the presence of APC or cycloheximide (movies provided in Appendix C). β -catenin has been reported to oscillate with stages of the cell cycle, increasing in S-phase to peak at G2/M, before

decreasing as the cells enter into a new G1 phase, which was suggested as a means of protecting cells from suspension-induced apoptosis (anoikis) [308, 490, 491].

In the assays presented in Chapter 5, β -catenin levels appeared to not correlate precisely with cell division in all cells imaged, although a greater number of cells require analysis, in addition to utilising similar assay conditions as previous studies (such as synchronising the cells), prior to drawing any conclusions. These movies provide a link between the gene lists and a dynamic process that has multiple parameters, which might account for the observations in the fixed cell populations. For example, it may explain, at least in part, the lack of correlation between TCF-dependent transcription and β -catenin levels and localisation, in addition to the heterogeneous responses observed with esiRNA and Wnt3a treatment, which could be attributed to asynchronous responses of individual cells.

This cycling appeared masked upon stabilisation of β -catenin by inhibition of the destruction complex with APC esiRNA (Appendix C, movies APC 1 and 2) and is also not observed with inhibition of translation by cycloheximide treatment. Treating the cells with a transcriptional inhibitor, such as Actinomycin D, may shed further light on the process and whether it may be due to a level of control at translation initiation. Investigating select components identified in the screens (such as those identified in more than one cell line and identified in transcriptional screens) using time-lapse imaging would potentially be extremely useful in ascertaining their functions in β -catenin regulation. For example, utilising time-lapse microscopy assays to investigate the role of downregulating the identified cell cycle components on β -catenin cycling, in the presence of normal and abrogated APC, may provide clear clues as to their mechanisms of action. A more in-depth, quantitative analysis to obtain an indication of the cycling period of β -catenin in normal situations is required, which would then allow for the effects of the identified esiRNAs on β -catenin's cycling period to be observed. Not only would assays utilising life-cell imaging aid the mechanistic studies into the novel regulators of β -catenin identified, but it would also allow for a systematic analysis of the effects of gene deletion on β -catenin modification status.

The screens only display a frozen snap shot of what is a highly dynamic process, with Wnt signalling regulating the expression of specific genes required at precise points in time in response to various stimuli. There are many parameters associated with the dynamics of cycling, which may be targeted by the genes identified and be relevant to changes in β -catenin itself, from its phosphorylation status to its interaction partners. This may be particularly relevant as the assays suggest the possibility of a regulatory process for β -catenin analogous to that of the NF- κ B system, where cycling is intimately linked to the phosphorylation of the transcription factor, its nuclear dephosphorylation (and inactivation) followed by its export to allow for re-phosphorylation [544]. For example, a similar negative feedback loop may regulate β -catenin levels, whereby Axin2, for example, may be directly involved in mediating β -catenin nuclear export for its degradation as an additional role to its established function in the reformation of the β -catenin destruction complex [101, 545].

Due to time constraints, this exciting data was unfortunately not repeated. Future studies are warranted to investigate β -catenin's dynamic regulation further, alongside the many interesting potential novel regulators identified in the screens undertaken within this study.

6.5 hnRNP A1's regulation of β -catenin and TCF-dependent transcription.

HnRNP A1 was identified as a negative regulator of β -catenin in all three imaging screens, in addition to the screen for novel regulators of TCF-dependent transcription. hnRNP A1 is an RNA binding protein, primarily known for its role in pre-mRNA splicing inhibition [402] but also functions in various other mRNA processing events such as mRNA transport [410, 411], mRNA stability [546] and translation [409]. hnRNP A1 also possesses a protein binding domain, with it being implicated in the regulation of NF- κ B-dependent transcription by binding NF- κ B inhibitor, I κ B α , to mediate its degradation [480]. Therefore, hnRNP A1 may be involved in regulating β -catenin at the protein level or mRNA level (by synthesis, degradation or translational control), which will be considered in further detail in the subsections below.

6.5.1 hnRNP A1 and β -catenin protein regulation

Due to the key role of β -catenin turnover in the regulation of the Wnt/ β -catenin pathway, the vast majority of research has centred on deciphering the regulation of β -catenin protein stability [185]. Therefore, once the primary screening data had been reconfirmed, assessing the role of hnRNP A1 in this aspect of β -catenin regulation was one of the first questions addressed.

Both the pulse-chase assays and time-lapse microscopy of cycloheximide treated cells demonstrated that hnRNP A1 did not affect β -catenin protein degradation, thus implying an unanticipated level of regulation at β -catenin synthesis.

Co-immunoprecipitation assays demonstrated that hnRNP A1 was able to bind β -catenin, confirming previous reports where an interaction was shown by mass-spectrometry [380] and co-immunoprecipitation [379]. This interaction poses interesting questions with regards to hnRNP A1's role in β -catenin protein regulation. Originally, it was postulated that this interaction between β -catenin and hnRNP A1 allowed β -catenin to function in the splicing of target genes, implying a role for hnRNP A1 in regulating the activity of β -catenin rather than its levels [379]. This in turn could imply dual roles for hnRNP A1, where it could be regulating the activity of β -catenin in one part of the cell and its levels in another [379], analogous to the relationship between APC and β -catenin. In this case, APC is crucial for the regulation of β -catenin levels in the cytoplasm and has also been demonstrated to regulate its transactivating activity in the nucleus [130, 523]. Alternatively, hnRNP A1 may be involved in trafficking β -catenin from the nucleus for its degradation in the cytosol, similar to its role in the cytoplasmic shuttling of the NF- κ B inhibitor, I κ B α , to regulate NF- κ B-dependent transcription [480]. This is supported by the observation of increased nuclear localisation of β -catenin upon hnRNP A1 knockdown in the primary U2OS screens.

6.5.2 hnRNP A1 and β -catenin mRNA synthesis and stability

The protein stability assays mentioned above indicated that hnRNP A1 may be involved in regulating β -catenin post transcriptionally. hnRNP A1 has been associated with regulating mRNA stability as part of a complex with KSRP; an RNA-binding protein that mediates the degradation of β -catenin mRNA that can be inactivated by Wnt and PI3-kinase signalling [185, 489]. A more recent study extended this, whereby a KSRP-Dvl complex was demonstrated to mediate β -catenin mRNA degradation, with Wnt stimulation inducing β -catenin mRNA release and subsequent stabilisation, resulting in rapid translation and accumulation of protein levels. [183]. It was therefore hypothesised that hnRNP A1 might regulate β -catenin mRNA stability as part of a complex with KSRP.

qRT-PCR assays demonstrated that hnRNP A1 had no apparent effect on β -catenin mRNA stability, in addition to having no observed effect on its mRNA synthesis. Additionally, no association between hnRNP A1 and KSRP was observed in the U2OS cell line, contradictory to previous reports [489, 494]. However, the studies that first described an interaction between hnRNP A1 and KSRP were mainly reliant on murine α T3-1 pituitary cells [489, 494], with the more recent study, which revealed a role for a Dvl-KSRP complex in the de-stabilisation of β -catenin mRNA, utilising F9 mouse teratocarcinoma cells [183]. Therefore, cell type specific differences may explain the discrepancies between the data presented here and these reports [183, 489, 494].

Taken together the data suggests that, despite strong links to KSRP, hnRNP A1 appears unlikely to be mediating its effect by regulating β -catenin mRNA stability, as part of, or independently, of a ribonucleocomplex with KSRP in the cell types studied within this project.

6.5.3 hnRNP A1 and β -catenin mRNA transport and translation

Preliminary experiments revealed that hnRNP A1 interacted with β -catenin mRNA in the nucleus and cytoplasm of both U2OS and eGFP- β -catenin U2OS cells. Future

experiments could utilise *in vitro* UV cross-linking, affinity chromatography and electrophoretic mobility shift assays to reconfirm the data and to identify the regions of β -catenin mRNA that are required for hnRNPA1 interaction. The studies suggests that regions within the coding sequence are involved, since the eGFP- β -catenin cDNA expression construct present in the U2OS cells lacked 5' and 3' β -catenin UTR sequences. If the data unequivocally demonstrates that hnRNP A1 can bind β -catenin mRNA in both cellular compartments, its potential role in regulating mRNA localisation and translation initiation merits investigation. For instance, the levels of cytosolic and nuclear β -catenin mRNA in the presence of hnRNP A1 knockdown could be assessed using qRT-PCR and mFISH assays [547]. Luciferase reporter plasmids containing the hnRNP A1 binding region of β -catenin mRNA could be utilised to demonstrate that hnRNP A1 interaction regulates translation.

HnRNP A1 has been shown to regulate cap-mediated translation [485], in addition to both positively and negatively regulating IRES-mediated translation of specific mRNAs [409, 486, 548]. Despite the absence of an IRES in the β -catenin sequence, the frequent discovery of new roles for hnRNP A1 in diverse cellular processes [388] makes an investigation into its role in regulating β -catenin translation, using the assays mentioned above, prudent.

6.5.4 hnRNP A1 in sequestering β -catenin mRNA?

Overall levels of β -catenin mRNA were unaltered upon hnRNP A1 downregulation, suggesting that the regulation of its translation is important. Within the control of translation, many complexes have been implicated, including processing bodies (P-bodies) and stress granules (SGs). mRNA degradation and translational processes are often in competition, which in turn appears to be dependent on their localisation [549]. Both P-bodies and SGs play key roles in the localisation and spatial control of mRNAs, with observations suggesting the interaction and exchange of mRNA-protein complexes between them [550].

mRNA targeted for degradation are often concentrated with mRNA decay factors in P-bodies while translating mRNAs are distributed throughout the cytosol [551]. SGs,

on the other hand, appear to be highly dynamic and composed of mRNAs that have stalled in translation initiation, along with specific translation initiation factors (eIF4E, eIF4G, eIF4A, eIF3, and eIF2), the 40S ribosomal subunit, poly (A) binding protein (Pab1)[549, 550, 552] and Ras GTPase activating protein-binding protein 1 (G3BP1) [553]. Interestingly, G3BP1 has been demonstrated to associate with Dvl to regulate β -catenin mRNA in response to Wnt signalling [184]. In this study, G3BP1 was demonstrated to harbour β -catenin mRNA, with its methylation in response to Wnt3a treatment resulting in β -catenin mRNA dissociation and subsequent translation [184]. Interestingly, hnRNP A1 has also been shown to localise to stress granules, as described in further detail below [478].

SGs accumulate in response to heat shock, genotoxic and oxidative stresses and harbour translationally arrested mRNAs and protein components ranging from RNA helicases, translation and stability regulators to factors involved in cell signalling [550]. It is postulated that by harbouring mRNAs in an abortive translation initiation complex, SGs enable the rapid re-initiation of translation and subsequent protein production upon recovery from stress [550]. In response to various extracellular stresses, a number of signalling cascade components, such as c-jun N-terminal kinases and p38 mitogen-activated (MAP) kinase, are activated to regulate the transcriptional and post-transcriptional events that drive the functional response to the stress applied [483]. Activation of the p38 MKK (3/6)-signalling cascade has been demonstrated to result in the hyperphosphorylation and stress-induced cytoplasmic accumulation of hnRNP A1 [479], which, when bound to mRNA, can localise to SGs [478]. While β -catenin mRNA has yet to be identified in SGs, the *arm*-repeat family member and structural component of desmosomes Plakophilin (PKP) 3, has been reported to be harboured in SGs, along with FXR1, G3BP and PABPC1 [554]. Interestingly, all 3 of these RNA-binding proteins, along with PKP2, resulted in increased TCF-dependent transcription and/or β -catenin nuclear localisation upon knockdown in the primary screens (data not shown). Additionally, in many cases, stress induced phosphorylation of the translation initiation factor eIF2 alpha triggers translational silencing and intriguingly the eIF2alpha kinase, eIF2AK2 (PKR), was identified in the overlapping hits between the imaging and TCF-dependent screen (Appendix B table 35), with

network analysis in Metacore revealing that hnRNP A1 is involved in eIF2AK2 transcriptional regulation (Figure 4.30).

Taken together, the data suggests that an investigation into the presence of β -catenin mRNA in stress granules along with hnRNP A1 is merited. Of particular interest is the role of G3BP and its ability to interact with hnRNP A1 could be investigated using co-immunoprecipitation and co-localisation assays in stress-induced cells. Also of interest is the stress mediated interaction of histone deacetylase 6 (HDAC6) with G3BP and its subsequent localisation to SGs in a manner dependent on its ubiquitin binding domain [555]. HDAC6 deacetylation of β -catenin at lysine 49 in response to EGF stimulation was observed to inhibit β -catenin phosphorylation at serine 45, resulting in its nuclear localisation and increased c-myc gene expression [112]. Therefore, a study into SGs, β -catenin and hnRNP A1 appears to be warranted.

6.5.5 Alternative roles for hnRNPA1 in β -catenin regulation

More recently, hnRNP A1 has been suggested to play a role in microRNA biogenesis, with these non-coding RNAs implicated in gene expression regulation as translational inhibitors in animals [483, 484, 556]. hnRNP A1 has been implicated in the biogenesis of microRNA 18a (miR-18a) in addition to inhibiting Drosha mediated processing of pri-let-7a-1 [406, 483, 484]. This latter role was shown to exert its effect by interfering with the ability of KSRP to bind and promote let-7a biogenesis, providing another link between these two RNA-binding proteins [406]. While miR-18a has been demonstrated to inhibit oestrogen receptor- α (ER α) mRNA translation [557], in addition to targeting K-Ras [558], it has not been associated with β -catenin mRNA regulation, although further targets are yet to be identified [559]. The possibility that hnRNP A1 may regulate β -catenin through modulating the abundance of a specific endogenous microRNA is enticing, with several microRNA's identified as regulators of Wnt/ β -catenin signalling, such as miR-135a/b (reviewed in [560]).

hnRNP A1 has been demonstrated to be transcriptionally regulated by c-myc [403], an established Wnt/ β -catenin target gene [49], which in turn raises the possibility of a

negative feed mechanism in the regulation of β -catenin upon Wnt signalling activation. This would imply that hnRNP A1 expression may be upregulated by active Wnt signalling, via the induction of *myc*, and that this increased expression may lead to a decrease in β -catenin levels, in order to reset the system to normal, reminiscent of the Axin2 feedback loop [545]. Indeed, during this study it was occasionally noticed that in the presence of downregulated APC, hnRNP A1 levels appeared to increase concurrently with elevated β -catenin levels, while β -catenin knockdown lead to decreased hnRNP A1 levels (Figure 5.5 for example). This was however, not consistently reproduced. Moreover, other hnRNP proteins were observed to modulate β -catenin levels and/or TCF-dependent transcription in the primary screens, with hnRNP H1's effect on β -catenin reconfirming with non-overlapping esiRNA (Table 4.13). Therefore, the possibility of the involvement of a larger hnRNP complex in mediating the regulation of Wnt/ β -catenin signalling is raised.

To summarise, hnRNP A1 was identified as a putative repressor of Wnt/ β -catenin signalling with work conducted within this study suggesting that it plays a role in the post-transcriptional regulation of β -catenin. Future work will aim to investigate the role of hnRNP A1 in regulating β -catenin mRNA localisation and translation initiation. hnRNP A1 is implicated in a wide range of cellular processes, which in turn could suggest that it may regulate β -catenin indirectly or on multiple levels. A greater understanding of the post-transcriptional regulation of β -catenin will allow for an improved appreciation of the Wnt signalling pathway and how it must be tightly regulated on various levels.

6.6 Conclusions

Genome wide RNAi screens were successfully developed and undertaken to identify novel regulators of β -catenin in Wnt signalling. The study has provided sources of possible mechanistic insights into a number of areas of biology that may be involved in β -catenin regulation. Furthermore, it revealed an unprecedented degree of cross talk between Wnt and many other major signalling pathways, demonstrating the complexity of the regulation involved in what is a key developmental pathway.

Moreover, the data indicated a degree of cell type specificity in the regulators identified and, significantly, a lack of correlation between β -catenin levels and transcriptional activity. The standard 'textbook' model of Wnt signalling, extensively advocated in major reviews of the field, states that increased total levels of β -catenin correlates with increased nuclear localisation and subsequently with activation of transcription, despite emerging evidence to the contrary. This work demonstrates, on a genome-wide scale, that this view is simplistic and more in line with the increasing belief that distinct isoforms of β -catenin are of greater importance in mediating Wnt dependent transcription. Future studies into the effect of the reconfirmed regulators on β -catenin phosphorylation will help to link specific candidate molecules to this molecular complexity.

The recent time-lapse data that displayed β -catenin levels and localisation dynamically changing over time (Appendix C movies) bears striking resemblance to the oscillations in the nuclear translocation of NF- κ B upon activation of this pathway [544, 561]. Due to time constraints, this exciting observation was unfortunately not repeated and while it is not possible to speculate as to the significance of this data in terms of regulated gene expression by β -catenin, future studies will concentrate on characterising the dynamics and mechanism of its nuclear translocation further.

The screens identified a surprising number of genes involved in mRNA processing and translation, including hnRNP A1, which was identified in the screens as a potential negative regulator of β -catenin. Investigations into its mechanistic role implied that hnRNP A1 regulates β -catenin post transcriptionally and not through the regulation of its protein turnover. Given the key role of β -catenin protein degradation in Wnt signalling regulation, this observation, along with the enrichment of genes involved in mRNA processing and translation from the primary screens, reveal an unanticipated level of β -catenin regulation at the mRNA level. This, in turn, implies that transcriptional and translational regulation of β -catenin are more intricately involved in Wnt signalling than first assumed and that this should be taken into consideration in future studies. Further work is required to decipher hnRNP A1's precise mechanism of action, with the gene lists identified here providing a useful

entry point into the future analysis of regulators of β -catenin post-transcriptional control and how it relates to Wnt signalling.

This study has highlighted the complexity of β -catenin regulation and its role in mediating transcription of Wnt target genes, in addition to providing insights into the processes and individual components that are likely to be involved and merit further investigation in future studies. The novel regulators may provide new information on the role of β -catenin in tumour biology and provide promising targets for drug and combinatorial therapies. A greater appreciation of the regulation and interplay between β -catenin's transcriptional and non-transcriptional roles, and how this relates to development and disease, is especially important. In turn, a better understanding would aid interpretation, diagnosis and prognosis of tumours in a clinical setting

Bibliography

1. Pires-daSilva, A. and R.J. Sommer, *The evolution of signalling pathways in animal development*. Nat Rev Genet, 2003. **4**(1): p. 39-49.
2. Barolo, S. and J.W. Posakony, *Three habits of highly effective signaling pathways: principles of transcriptional control by developmental cell signaling*. Genes Dev, 2002. **16**(10): p. 1167-81.
3. Cadigan, K.M. and R. Nusse, *Wnt signalling: a common theme in animal development*. Genes Dev., 1997. **11**: p. 3286-3305.
4. Moon, R.T., et al., *The promise and perils of Wnt signaling through beta-catenin*. Science, 2002. **296**(5573): p. 1644-6.
5. Ingham, P.W. and A.P. McMahon, *Hedgehog signalling in animal development: paradigms and principles*. Genes Dev., 2001. **15**: p. 3059-3087.
6. Massague, J. and Y.G. Chen, *Controlling TGF-[beta] signalling*. Genes Dev., 2000. **14**: p. 627-644.
7. Tan, P.B. and S.K. Kim, *Signalling specificity: the RTK/RAS/MAP kinase pathway in metazoans*. Trends Genet., 1999. **15**: p. 145-149.
8. Castelli-Gair Hombria, J. and S. Brown, *The fertile field of Drosophila JAK/STAT signalling*. Curr. Biol., 2002. **12**: p. R569.
9. Mumm, J.S. and R. Kopan, *Notch signalling: from the outside in*. Dev. Biol., 2000. **228**: p. 151-165.
10. McKenna, N.J. and B.W. O'Malley, *Combinatorial control of gene expression by nuclear receptors and coregulators*. Cell, 2002. **108**: p. 465-474.
11. Perez-Moreno, M. and E. Fuchs, *Catenins: Keeping Cells from Getting Their Signals Crossed*. Developmental Cell, 2006. **11**(5): p. 601-612.
12. Stepniak, E., G.L. Radice, and V. Vasioukhin, *Adhesive and Signaling Functions of Cadherins and Catenins in Vertebrate Development*. Cold Spring Harbor Perspectives in Biology, 2009. **1**(5).
13. Nusse, R., *Wnt signaling in disease and in development*. Cell Res, 2005. **15**(1): p. 28-32.
14. Clevers, H., *Wnt/beta-catenin signaling in development and disease*. Cell, 2006. **127**(3): p. 469-80.
15. Reya, T. and H. Clevers, *Wnt signalling in stem cells and cancer*. Nature, 2005. **434**(7035): p. 843-50.
16. McMahon, A.P. and R.T. Moon, *Ectopic expression of the proto-oncogene int-1 in Xenopus embryos leads to duplication of the embryonic axis*. Cell, 1989. **58**(6): p. 1075-84.
17. Sokol, S., et al., *Injected Wnt RNA induces a complete body axis in Xenopus embryos*. Cell, 1991. **67**(4): p. 741-52.
18. Shimizu, H., et al., *Transformation by Wnt family proteins correlates with regulation of beta-catenin*. Cell Growth Differ, 1997. **8**(12): p. 1349-58.
19. Wong, G.T., B.J. Gavin, and A.P. McMahon, *Differential transformation of mammary epithelial cells by Wnt genes*. Mol Cell Biol, 1994. **14**(9): p. 6278-86.
20. Torres, M.A., et al., *Activities of the Wnt-1 class of secreted signaling factors are antagonized by the Wnt-5A class and by a dominant negative cadherin in early Xenopus development*. J Cell Biol, 1996. **133**(5): p. 1123-37.

21. Moon, R.T., et al., *Xwnt-5A: a maternal Wnt that affects morphogenetic movements after overexpression in embryos of Xenopus laevis*. Development, 1993. **119**(1): p. 97-111.
22. Wodarz, A. and R. Nusse, *Mechanisms of Wnt signaling in development*. Annu Rev Cell Dev Biol, 1998. **14**: p. 59-88.
23. Pinson, K.I., et al., *An LDL-receptor-related protein mediates Wnt signalling in mice*. Nature, 2000. **407**(6803): p. 535-8.
24. Tamai, K., et al., *LDL-receptor-related proteins in Wnt signal transduction* Nature, 2000. **407**(6803): p. 530-5.
25. Wehrli, M., et al., *arrow encodes an LDL-receptor-related protein essential for Wingless signalling* Nature, 2000. **407**(6803): p. 527-30.
26. Lu, W., et al., *Mammalian Ryk is a Wnt coreceptor required for stimulation of neurite outgrowth*. Cell, 2004. **119**(1): p. 97-108.
27. Inoue, T., et al., *C. elegans LIN-18 is a Ryk ortholog and functions in parallel to LIN-17/Frizzled in Wnt signaling*. Cell, 2004. **118**(6): p. 795-806.
28. Hikasa, H., et al., *The Xenopus receptor tyrosine kinase Xror2 modulates morphogenetic movements of the axial mesoderm and neuroectoderm via Wnt signaling*. Development, 2002. **129**(22): p. 5227-39.
29. Grumolato, L., et al., *Canonical and noncanonical Wnts use a common mechanism to activate completely unrelated coreceptors*. Genes & Development, 2010. **24**(22): p. 2517-2530.
30. Gao, C. and Y.-G. Chen, *Dishevelled: The hub of Wnt signaling*. Cellular Signalling, 2010. **22**(5): p. 717-727.
31. Fanto, M. and H. McNeill, *Planar polarity from flies to vertebrates*. J Cell Sci, 2004. **117**(Pt 4): p. 527-33.
32. Huelsken, J. and J. Behrens, *The Wnt signalling pathway*. J Cell Sci, 2002. **115**(Pt 21): p. 3977-8.
33. Veeman, M.T., J.D. Axelrod, and R.T. Moon, *A second canon. Functions and mechanisms of beta-catenin-independent Wnt signaling*. Dev Cell, 2003. **5**(3): p. 367-77.
34. De Calisto, J., et al., *Essential role of non-canonical Wnt signalling in neural crest migration*. Development, 2005. **132**(11): p. 2587-97.
35. Saneyoshi, T., et al., *The Wnt/calcium pathway activates NF-AT and promotes ventral cell fate in Xenopus embryos*. Nature, 2002. **417**(6886): p. 295-9.
36. Kuhl, M., *The WNT/calcium pathway: biochemical mediators, tools and future requirements*. Front Biosci, 2004. **9**: p. 967-74.
37. Ishitani, T., et al., *The TAK1-NLK mitogen-activated protein kinase cascade functions in the Wnt-5a/Ca(2+) pathway to antagonize Wnt/beta-catenin signaling*. Mol Cell Biol, 2003. **23**(1): p. 131-9.
38. Fradkin, L.G., J.-M. Dura, and J.N. Noordermeer, *Ryks: new partners for Wnts in the developing and regenerating nervous system*. Trends in Neurosciences, 2010. **33**(2): p. 84-92.
39. Mikels, A.J. and R. Nusse, *Purified Wnt5a protein activates or inhibits beta-catenin-TCF signaling depending on receptor context*. PLoS Biol, 2006. **4**(4): p. e115.
40. Schambony, A. and D. Wedlich, *Wnt-5A/Ror2 regulate expression of XPAPC through an alternative noncanonical signaling pathway*. Dev Cell, 2007. **12**(5): p. 779-92.
41. Coates, J.C., *Armadillo Repeat Protein: beyond the animal kingdom*. Trends Cell Biol, 2003. **13**: p. 463-471.

42. Daugherty, R.L. and C.J. Gottardi, *Phospho-regulation of Beta-catenin Adhesion and Signalling Functions*. Physiology, 2007. **22**: p. 303-309.
43. Huber, A.H., Nelson, W.J., Weis, W.I., *Three-dimensional structure of the armadillo repeat region of beta-catenin*. Cell, 1997. **90**: p. 871-882.
44. Daugherty, R.L., Gottardi, C.J., *Phospho-regulation of Beta-catenin Adhesion and Signalling Functions*. Physiology, 2007. **22**: p. 303-309.
45. Drees, F., et al., *Alpha-catenin is a molecular switch that binds E-cadherin-beta-catenin and regulates actin-filament assembly*. Cell, 2005. **123**(903-915).
46. Huber, A.H., et al., *The cadherin cytoplasmic domain is unstructured in hte absence of beta-catenin; a possible mechanism for regulating cadherin turnover*. J Biol Chem, 2001. **276**: p. 12301-12309.
47. Pierceall, W.E., et al., *Frequent alterations in E-cadherin and alpha- and beta-catenin expression in human breast cancer cell lines*. Oncogene, 1995. **11**(7): p. 1319-26.
48. Jeanes, A., C.J. Gottardi, and A.S. Yap, *Cadherins and cancer: how does cadherin dysfunction promote tumor progression?* Oncogene, 2008. **27**(55): p. 6920-9.
49. He, T.C., et al., *Identification of c-MYC as a target of the APC pathway*. Science, 1998. **281**(5382): p. 1509-12.
50. Kim, J.S., et al., *Oncogenic beta-catenin is required for bone morphogenetic protein 4 expression in human cancer cells*. Cancer Res, 2002. **62**(10): p. 2744-8.
51. Tetsu, O. and F. McCormick, *Beta-catenin regulates expression of cyclin D1 in colon carcinoma cells*. Nature, 1999. **398**(6726): p. 422-6.
52. Orford, K., et al., *Serine phosphorylation-regulated ubiquitination and degradation of beta-catenin*. J Biol Chem, 1997. **272**(40): p. 24735-8.
53. Ha, N.C., et al., *Mechanism of phosphorylation-dependent binding of APC to beta-catenin and its role in beta-catenin degradation*. Mol Cell, 2004. **15**(4): p. 511-21.
54. Rubinfeld, B., D.A. Tice, and P. Polakis, *Axin-dependent phosphorylation of the adenomatous polyposis coli protein mediated by casein kinase Iepsilon*. J Biol Chem, 2001. **276**(42): p. 39037-45.
55. Liu, C., et al., *Control of beta-catenin phosphorylation/degradation by a dual-kinase mechanism*. Cell, 2002. **108**(6): p. 837-47.
56. Liu, J., et al., *Identification of the Wnt signaling activator leucine-rich repeat in Flightless interaction protein 2 by a genome-wide functional analysis*. Proc Natl Acad Sci U S A, 2005. **102**(6): p. 1927-32.
57. Daniels, D.L. and W.I. Weis, *Beta-catenin directly displaces Groucho/TLE repressors from Tcf/Lef in Wnt-mediated transcription activation*. Nat Struct Mol Biol, 2005. **12**(4): p. 364-71.
58. Moon, R.T., et al., *WNT and beta-catenin signalling: diseases and therapies*. Nat Rev Genet, 2004. **5**(9): p. 691-701.
59. Cliffe, A., F. Hamada, and M. Bienz, *A Role of Dishevelled in Relocating Axin to the Plasma Membrane during Wingless Signaling*. Curr Biol, 2003. **13**(11): p. 960-6.
60. Mao, J., et al., *Low-density lipoprotein receptor-related protein-5 binds to Axin and regulates the canonical Wnt signaling pathway*. Mol Cell, 2001. **7**(4): p. 801-9.
61. Cong, F., et al., *Requirement for a nuclear function of beta-catenin in Wnt signaling*. Mol Cell Biol, 2003. **23**(23): p. 8462-70.

62. Rulifson, E.J., C.H. Wu, and R. Nusse, *Pathway specificity by the bifunctional receptor frizzled is determined by affinity for wingless*. Mol Cell, 2000. **6**(1): p. 117-26.
63. Hsieh, J.C., et al., *Biochemical characterization of Wnt-frizzled interactions using a soluble, biologically active vertebrate Wnt protein*. Proc Natl Acad Sci U S A, 1999. **96**(7): p. 3546-51.
64. Lin, X. and N. Perrimon, *Dally cooperates with Drosophila Frizzled 2 to transduce Wingless signalling*. Nature, 1999. **400**(6741): p. 281-4.
65. Perrimon, N. and M. Bernfield, *Specificities of heparan sulphate proteoglycans in developmental processes*. Nature, 2000. **404**(6779): p. 725-8.
66. MacDonald, B.T., K. Tamai, and X. He, *Wnt/ \leq -Catenin Signaling: Components, Mechanisms, and Diseases*. Developmental Cell, 2009. **17**(1): p. 9-26.
67. Mao, B., et al., *LDL-receptor-related protein 6 is a receptor for Dickkopf proteins*. Nature, 2001. **411**(6835): p. 321-5.
68. Semenov, M.V., et al., *Head inducer Dickkopf-1 is a ligand for Wnt coreceptor LRP6*. Curr Biol, 2001. **11**(12): p. 951-61.
69. Mao, B., et al., *Kremen proteins are Dickkopf receptors that regulate Wnt/beta-catenin signalling*. Nature, 2002. **417**(6889): p. 664-7.
70. Bafico, A., et al., *Interaction of frizzled related protein (FRP) with Wnt ligands and the frizzled receptor suggests alternative mechanisms for FRP inhibition of Wnt signaling*. J Biol Chem, 1999. **274**(23): p. 16180-7.
71. Tamai, K., et al., *A mechanism for Wnt coreceptor activation*. Mol Cell, 2004. **13**(1): p. 149-56.
72. Swiatek, W., et al., *Negative regulation of LRP6 function by casein kinase I epsilon phosphorylation*. J Biol Chem, 2006. **281**(18): p. 12233-41.
73. Davidson, G., et al., *Casein kinase I gamma couples Wnt receptor activation to cytoplasmic signal transduction*. Nature, 2005. **438**(7069): p. 867-72.
74. Piao, S., et al., *Direct inhibition of GSK3beta by the phosphorylated cytoplasmic domain of LRP6 in Wnt/beta-catenin signaling*. PLoS ONE, 2008. **3**(12): p. e4046.
75. Cselenyi, C.S., et al., *LRP6 transduces a canonical Wnt signal independently of Axin degradation by inhibiting GSK3's phosphorylation of beta-catenin*. Proceedings of the National Academy of Sciences of the United States of America, 2008. **105**(23): p. 8032-7.
76. Schwarz-Romond, T., et al., *The DIX domain of Dishevelled confers Wnt signaling by dynamic polymerization*. Nat Struct Mol Biol, 2007. **14**(6): p. 484-92.
77. Schwarz-Romond, T., C. Metcalfe, and M. Bienz, *Dynamic recruitment of axin by Dishevelled protein assemblies*. J Cell Sci, 2007. **120**(Pt 14): p. 2402-12.
78. Pan, W., et al., *Wnt3a-mediated formation of phosphatidylinositol 4,5-bisphosphate regulates LRP6 phosphorylation*. Science (New York, N.Y., 2008. **321**(5894): p. 1350-3.
79. Tanneberger, K., et al., *Amer1/WTX couples Wnt-induced formation of PtdIns(4,5)P2 to LRP6 phosphorylation*. EMBO J, 2011. **30**(8): p. 1433-1443.
80. Niehrs, C. and J. Shen, *Regulation of Lrp6 phosphorylation*. Cellular and Molecular Life Sciences, 2010. **67**(15): p. 2551-2562.

81. Yamamoto, H., H. Komekado, and A. Kikuchi, *Caveolin is necessary for Wnt-3a-dependent internalization of LRP6 and accumulation of beta-catenin*. *Dev Cell*, 2006. **11**(2): p. 213-23.
82. Gagliardi, M., E. Piddini, and J.-P. Vincent, *Endocytosis: A Positive or a Negative Influence on Wnt Signalling?* *Traffic*, 2008. **9**(1): p. 1-9.
83. <http://www.stanford.edu/~rnusse/pathways/cell2.html>.
84. Amit, S., et al., *Axin-mediated CKI phosphorylation of beta-catenin at Ser 45: a molecular switch for the Wnt pathway*. *Genes Dev*, 2002. **16**(9): p. 1066-76.
85. Hart, M., et al., *The F-box protein beta-TrCP associates with phosphorylated beta-catenin and regulates its activity in the cell*. *Curr Biol*, 1999. **9**(4): p. 207-10.
86. Kimelman, D. and W. Xu, *beta-catenin destruction complex: insights and questions from a structural perspective*. *Oncogene*, 2006. **25**(57): p. 7482-91.
87. Su, Y., et al., *APC is essential for targeting phosphorylated beta-catenin to the SCFbeta-TrCP ubiquitin ligase*. *Mol Cell*, 2008. **32**(5): p. 652-61.
88. Xing, Y., et al., *Crystal structure of a beta-catenin/axin complex suggests a mechanism for the beta-catenin destruction complex*. *Genes Dev*, 2003. **17**(22): p. 2753-64.
89. Zeng, X., et al., *A dual-kinase mechanism for Wnt co-receptor phosphorylation and activation*. *Nature*, 2005. **438**(7069): p. 873-7.
90. Liu, X., J.S. Rubin, and A.R. Kimmel, *Rapid, Wnt-Induced Changes in GSK3beta Associations that Regulate beta-Catenin Stabilization Are Mediated by Galpha Proteins*. *Curr Biol*, 2005. **15**(22): p. 1989-97.
91. Logan, C.Y. and R. Nusse, *The Wnt signaling pathway in development and disease*. *Annu Rev Cell Dev Biol*, 2004. **20**: p. 781-810.
92. Tolwinski, N.S., et al., *Wg/Wnt Signal Can Be Transmitted through Arrow/LRP5,6 and Axin Independently of Zw3/Gsk3beta Activity*. *Dev Cell*, 2003. **4**(3): p. 407-18.
93. Lee, E., et al., *The Roles of APC and Axin Derived from Experimental and Theoretical Analysis of the Wnt Pathway*. *PLoS Biol*, 2003. **1**(1): p. E10.
94. Quimby, B.B. and A.H. Corbett, *Nuclear transport mechanisms*. *Cell.Mol.Life Sci*, 2001. **58**: p. 1766-1773.
95. Pemberton, L.F. and B.M. Paschal, *Mechanisms of Receptor Mediated Nuclear Import and Nuclear Export*. *Traffic*, 2005. **6**: p. 187-198.
96. Fagotto, F., U. Gluck, and B.M. Gumbiner, *Nuclear localisation signal-independent and importin/karyopherin-independent nuclear import of -catenin*. *Curr. Biol*, 1998. **8**: p. 181-190.
97. Suh, E.K. and B.M. Gumbiner, *Translocation of beta-catenin into the nucleus independent of interactions with FG-rich nucleoporins*. *Exp. Cell. Res*, 2003. **290**: p. 447-456.
98. Neufeld KL, et al., *Adenomatous polyposis coli protein contains two nuclear export signals and shuttles between the nucleus and cytoplasm*. *Proc Natl Acad Sci U S A*, 2000. **97**(22): p. 12085-90.
99. Henderson, B.R., *Nuclear-cytoplasmic shuttling of APC regulates beta-catenin subcellular localization and turnover*. *Nat Cell Biol*, 2000. **2**(9): p. 653-660.
100. Neufeld, K.L., et al., *APC-mediated downregulation of beta-catenin activity involves nuclear sequestration and nuclear export*. *EMBO Reports*, 2000. **1**: p. 519-523.

101. Cong, F. and H. Varmus, *Nuclear-cytoplasmic shuttling of Axin regulates subcellular localization of β -catenin*. Proc Natl Acad Sci U S A, 2004. **101**(9): p. 2882-2887.
102. Tolwinski, N.S. and E. Wieschaus, *Armadillo nuclear import is regulated by cytoplasmic anchor Axin and nuclear anchor dTCF/Pan*. Development, 2001. **128**(11): p. 2107-17.
103. Hendriksen, J., et al., *RanBP3 enhances nuclear export of active (beta)-catenin independently of CRM1*. J Cell Biol, 2005. **171**(5): p. 785-97.
104. Thompson, M.D., M.J. Dar, and S.P.S. Monga, *Pegylated interferon alpha targets Wnt signaling by inducing nuclear export of β -catenin*. Journal of hepatology, 2011. **54**(3): p. 506-512.
105. Yokoya, F., et al., *Beta-catenin can be transported into the nucleus in a Ran-unassisted manner*. Mol. Biol. Cell, 1999. **10**: p. 1119-1131
106. Yoneda, Y., A. Kametaka, and T. Sekimoto, *How many pathways are available for nuclear protein import in cells*. Acta Histochem Cytochem, 2002. **35**(6): p. 435-440.
107. Eleftheriou, A., M. Yoshida, and B.R. Henderson, *Nuclear export of human β -catenin can occur independent of CRM1 and APC tumour suppressor*. J Biol Chem, 2001. **276**: p. 25883-25888.
108. Townsley, F.M., A. Cliffe, and M. Bienz, *Pygopus and Legless target Armadillo/ β -catenin to the nucleus to enable its transcriptional co-activator function*. Nat Cell Biol, 2004. **6**: p. 626-633.
109. Krieghoff, E., J. Behrens, and B. Mayr, *Nucleo-cytoplasmic distribution of β -catenin is regulated by retention*. J. Cell.Sci, 2006. **119**: p. 1453-1463.
110. Jamieson, C., M. Sharma, and B.R. Henderson, *Regulation of β -Catenin Nuclear Dynamics by GSK-3 β Involves a LEF-1 Positive Feedback Loop*. Traffic, 2011. **12**(8): p. 983-999.
111. Stadeli, R., R. Hoffmans, and K. Basler, *Transcription under the Control of Nuclear Arm/ β -Catenin*. Current Biology, 2006. **16**(10): p. R378-R385.
112. Li, Y., et al., *HDAC6 is required for epidermal growth factor-induced β -catenin nuclear localization*. The Journal of biological chemistry, 2008. **283**(19): p. 12686-90.
113. Thyssen, G., et al., *LZTS2 is a novel β -catenin-interacting protein and regulates the nuclear export of β -catenin*. Mol. Cell Biol, 2006. **26**(23): p. 8857-8867.
114. Li, F.-Q., et al., *Chibby cooperates with 14-3-3 to regulate β -catenin subcellular distribution and signalling activity*. J. Cell Biol, 2008. **181**(7): p. 1141-1154.
115. Sayat, R., et al., *OGlcNAc-glycosylation of β -catenin regulates its nuclear localization and transcriptional activity*. Exp Cell Res, 2008: p. In Press.
116. Wu, X., et al., *Rac1 activation controls nuclear localization of β -catenin during canonical Wnt signaling*. Cell, 2008. **133**(2): p. 340-53.
117. Behrens, J., et al., *Functional interaction of β -catenin with the transcription factor LEF-1*. Nature, 1996. **382**(6592): p. 638-42.
118. Brunner, E., et al., *pangolin encodes a Lef-1 homologue that acts downstream of Armadillo to transduce the Wingless signal in Drosophila*. Nature, 1997. **385**(6619): p. 829-33.
119. van de Wetering, M., et al., *Armadillo coactivates transcription driven by the product of the Drosophila segment polarity gene dTCF*. Cell, 1997. **88**(6): p. 789-99.

120. Hoppler, S. and C.L. Kavanagh, *Wnt signalling: variety at the core*. J. Cell Science, 2007. **120**(Pt 3): p. 385-93.
121. Blauwkamp, T.A., M.V. Chang, and K.M. Cadigan, *Novel TCF-binding sites specify transcriptional repression by Wnt signalling*. Embo J, 2008. **27**(10): p. 1436-46.
122. Stadeli, R. and K. Basler, *Dissecting nuclear Wingless signalling: recruitment of the transcriptional co-activator Pygopus by a chain of adaptor proteins*. Mech Dev, 2005. **122**(11): p. 1171-82.
123. Mosimann, C., G. Hausmann, and K. Basler, *Parafibromin/Hyrax activates Wnt/Wg target gene transcription by direct association with beta-catenin/Armadillo*. Cell, 2006. **125**(2): p. 327-41.
124. Brembeck, F.H., et al., *Essential role of BCL9-2 in the switch between beta-catenin's adhesive and transcriptional functions*. Genes Dev, 2004. **18**(18): p. 2225-30.
125. Townsley, F.M., B. Thompson, and M. Bienz, *Pygopus residues required for its binding to Legless are critical for transcription and development*. J Biol Chem, 2004. **279**(7): p. 5177-83.
126. Fiedler, M., et al., *Decoding of methylated histone H3 tail by the Pygo-BCL9 Wnt signaling complex*. Mol Cell, 2008. **30**(4): p. 507-18.
127. Takemaru, K.I. and R.T. Moon, *The transcriptional coactivator CBP interacts with beta-catenin to activate gene expression*. J Cell Biol, 2000. **149**(2): p. 249-54.
128. Waltzer, L. and M. Bienz, *Drosophila CBP represses the transcription factor TCF to antagonize Wingless signalling*. Nature, 1998. **395**(6701): p. 521-5.
129. Li, J., et al., *CBP/p300 are bimodal regulators of Wnt signaling*. Embo J, 2007. **26**(9): p. 2284-94.
130. Sierra, J., et al., *The APC tumor suppressor counteracts beta-catenin activation and H3K4 methylation at Wnt target genes*. Genes Dev, 2006. **20**(5): p. 586-600.
131. Ishitani, T., et al., *The TAK1-NLK-MAPK-related pathway antagonizes signalling between beta-catenin and transcription factor TCF*. Nature, 1999. **399**(6738): p. 798-802.
132. Sachdev, S., et al., *PIASy, a nuclear matrix-associated SUMO E3 ligase, represses LEF1 activity by sequestration into nuclear bodies*. Genes & Development, 2001. **15**(23): p. 3088-3103.
133. Herman, M.A., et al., *The C. elegans gene lin-44, which controls the polarity of certain asymmetric cell divisions, encodes a Wnt protein and acts cell nonautonomously*. Cell, 1995. **83**(1): p. 101-10.
134. Bejsovec, A. and A. Martinez Arias, *Roles of wingless in patterning the larval epidermis of Drosophila*. Development, 1991. **113**(2): p. 471-85.
135. Popperl, H., et al., *Misexpression of Cwnt8C in the mouse induces an ectopic embryonic axis and causes a truncation of the anterior neuroectoderm*. Development, 1997. **124**(15): p. 2997-3005.
136. Rijsewijk, F., et al., *The Drosophila homolog of the mouse mammary oncogene int-1 is identical to the segment polarity gene wingless*. Cell, 1987. **50**(4): p. 649-57.
137. Tao, Q., et al., *Maternal wnt11 activates the canonical wnt signaling pathway required for axis formation in Xenopus embryos*. Cell, 2005. **120**(6): p. 857-71.

138. Dominguez, I., K. Itoh, and S.Y. Sokol, *Role of glycogen synthase kinase 3 beta as a negative regulator of dorsoventral axis formation in Xenopus embryos*. Proc. Natl. Acad. Sci. U. S. A., 1995. **92**(18): p. 8498-502.
139. Guger, K.A. and B.M. Gumbiner, *beta-Catenin has Wnt-like activity and mimics the Nieuwkoop signaling center in Xenopus dorsal-ventral patterning*. Dev. Biol, 1995. **172**(1): p. 115-25.
140. He, X., et al., *Glycogen synthase kinase-3 and dorsoventral patterning in Xenopus embryos*. Nature, 1995. **374**: p. 617-622.
141. Kinzler, K.W., et al., *Identification of FAP locus genes from chromosome 5q21*. Science, 1991. **253**(5020): p. 661-5.
142. Nakamura, Y., et al., *Mutations of the adenomatous polyposis coli gene in familial polyposis coli patients and sporadic colorectal tumors*. Princess Takamatsu Symp, 1991. **22**: p. 285-92.
143. Rubinfeld, B., et al., *Association of the APC gene product with β -catenin*. Science, 1993. **262**: p. 1731-1733.
144. Lee, H.Y., et al., *Instructive role of Wnt/beta-catenin in sensory fate specification in neural crest stem cells*. Science, 2004. **303**(5660): p. 1020-3.
145. Torres, M.A. and W.J. Nelson, *Colocalization and redistribution of dishevelled and actin during Wnt-induced mesenchymal morphogenesis*. J Cell Biol, 2000. **149**(7): p. 1433-42.
146. Burstyn-Cohen, T., et al., *Canonical Wnt activity regulates trunk neural crest delamination linking BMP/noggin signaling with G1/S transition*. Development, 2004. **131**(21): p. 5327-39.
147. Rulifson, I.C., et al., *Wnt signaling regulates pancreatic beta cell proliferation*. Proc Natl Acad Sci U S A, 2007. **104**(15): p. 6247-52.
148. Nusse, R., *Wnt signaling and stem cell control*. Cell Res, 2008. **18**(5): p. 523-7.
149. van de Wetering, M., et al., *The beta-Catenin/TCF-4 Complex Imposes a Crypt Progenitor Phenotype on Colorectal Cancer Cells*. Cell, 2002. **111**(2): p. 241-50.
150. Reya T, Duncan A W, Ailles L, Domen J, Scherer D, Willert K, Hintz L, Nusse R, Weissman I, *A role for Wnt signalling in self renewal of haematopoietic stem cells*. Nature, 2003. **423**: p. 409-414.
151. Woodward, W.A., et al., *On mammary stem cells*. Journal of Cell Science, 2005. **118**(16): p. 3585-3594.
152. Lowry, W.E., et al., *Defining the impact of beta-catenin/Tcf transactivation on epithelial stem cells*. Genes Dev, 2005. **19**(13): p. 1596-611.
153. Fodde, R. and T. Brabletz, *Wnt/ β -catenin signaling in cancer stemness and malignant behavior*. Current Opinion in Cell Biology, 2007. **19**(2): p. 150-158.
154. Stark, K., et al., *Epithelial transformation of metanephric mesenchyme in the developing kidney regulated by Wnt-4*. Nature, 1994. **372**: p. 679-682.
155. Ikeya, M., et al., *Wnt signalling required for expansion of neural crest and CNS progenitors*. Nature, 1997. **389**(6654): p. 966-70.
156. Polakis, P., *The many ways of Wnt in cancer*. Curr Opin Genet Dev, 2007. **17**(1): p. 45-51.
157. Li, Y., et al., *Evidence that transgenes encoding components of the Wnt signaling pathway preferentially induce mammary cancers from progenitor cells*. Proc Natl Acad Sci U S A, 2003. **100**(26): p. 15853-8.

158. Heuberger, J. and W. Birchmeier, *Interplay of Cadherin-Mediated Cell Adhesion and Canonical Wnt Signaling*. Cold Spring Harbor Perspectives in Biology, 2010. **2**(2).
159. Rubinfeld, B., et al., *Stabilization of beta-catenin by genetic defects in melanoma cell lines*. Science, 1997. **275**(5307): p. 1790-2.
160. Pasca di Magliano, M., et al., *Common activation of canonical Wnt signaling in pancreatic adenocarcinoma*. PLoS ONE, 2007. **2**(11): p. e1155.
161. Uematsu, K., et al., *Wnt pathway activation in mesothelioma: evidence of Dishevelled overexpression and transcriptional activity of beta-catenin*. Cancer Res, 2003. **63**(15): p. 4547-51.
162. Uematsu, K., et al., *Activation of the Wnt pathway in non small cell lung cancer: evidence of dishevelled overexpression*. Oncogene, 2003. **22**(46): p. 7218-21.
163. Oshima, H., et al., *Carcinogenesis in mouse stomach by simultaneous activation of the Wnt signaling and prostaglandin E2 pathway*. Gastroenterology, 2006. **131**(4): p. 1086-95.
164. Bhatia, N. and V.S. Spiegelman, *Activation of Wnt/beta-catenin/Tcf signaling in mouse skin carcinogenesis*. Mol Carcinog, 2005. **42**(4): p. 213-21.
165. Aguilera, O., et al., *Epigenetic inactivation of the Wnt antagonist DICKKOPF-1 (DKK-1) gene in human colorectal cancer*. Oncogene, 2006. **25**(29): p. 4116-21.
166. Suzuki, H., et al., *Frequent epigenetic inactivation of Wnt antagonist genes in breast cancer*. Br J Cancer, 2008. **98**(6): p. 1147-56.
167. Fukui, T., et al., *Transcriptional silencing of secreted frizzled related protein 1 (SFRP 1) by promoter hypermethylation in non-small-cell lung cancer*. Oncogene, 2005. **24**(41): p. 6323-7.
168. Polakis, *Wnt signaling and cancer*. Genes and Development, 2000. **14**: p. 1837-1851.
169. Pinto, D. and H. Clevers, *Wnt control of stem cells and differentiation in the intestinal epithelium*. Exp Cell Res, 2005. **306**(2): p. 357-63.
170. Pinto, D. and H. Clevers, *Wnt, stem cells and cancer in the intestine*. Biol Cell, 2005. **97**(3): p. 185-96.
171. Hall, P.A., et al., *Regulation of cell number in the mammalian gastrointestinal tract: the importance of apoptosis*. J Cell Sci, 1994. **107 (Pt 12)**: p. 3569-77.
172. Gregorieff, A. and H. Clevers, *Wnt signaling in the intestinal epithelium: from endoderm to cancer*. Genes & Development, 2005. **19**(8): p. 877-890.
173. Battle, E., J.T. Henderson, and H. Beghtel, *[beta]-catenin and TCF mediate cell positioning in the intestinal epithelium by controlling the expression of EphB/ephrinB*. Cell, 2002. **111**: p. 251-263.
174. Korinek, V., et al., *Depletion of epithelial stem-cell compartments in the small intestine of mice lacking Tcf-4*. Nat Genet, 1998. **19**(4): p. 379-83.
175. Kim, K.-A., et al., *Mitogenic Influence of Human R-Spondin1 on the Intestinal Epithelium*. Science, 2005. **309**(5738): p. 1256-1259.
176. Sansom, O.J., et al., *Loss of Apc in vivo immediately perturbs Wnt signaling, differentiation, and migration*. Genes Dev, 2004. **18**(12): p. 1385-90.
177. Barker, N., et al., *Identification of stem cells in small intestine and colon by marker gene Lgr5*. Nature, 2007. **449**(7165): p. 1003-7.
178. Barker, N., et al., *Crypt stem cells as the cells-of-origin of intestinal cancer*. Nature, 2009. **457**(7229): p. 608-611.

179. Sparks, A.B., et al., *Mutational analysis of the APC/beta-catenin/Tcf pathway in colorectal cancer*. *Cancer Res*, 1998. **58**(6): p. 1130-4.
180. Fodde, R., R. Smits, and H. Clevers, *APC, signal transduction and genetic instability in colorectal cancer*. *Nature reviews*, 2001. **1**(1): p. 55-67.
181. Shibata, H., et al., *Rapid colorectal adenoma formation initiated by conditional targeting of the Apc gene*. *Science*, 1997. **278**(5335): p. 120-3.
182. Sansom, O.J., et al., *Myc deletion rescues Apc deficiency in the small intestine*. *Nature*, 2007. **446**(7136): p. 676-9.
183. Bikkavilli, R.K. and C.C. Malbon, *Dishevelled-KSRP complex regulates Wnt signaling through post-transcriptional stabilization of beta-catenin mRNA*. *Journal of Cell Science*, 2010. **123**(Pt 8): p. 1352-62.
184. Bikkavilli, R.K. and C.C. Malbon, *Arginine methylation of G3BP1 in response to Wnt3a regulates β -catenin mRNA*. *Journal of Cell Science*, 2011. **124**(13): p. 2310-2320.
185. Gherzi, R., et al., *The RNA-Binding Protein KSRP Promotes Decay of β -Catenin mRNA and Is Inactivated by PI3K-AKT Signaling*. *PLoS Biology*, 2007. **5**(1): p. e5.
186. Guger, K.A. and B.M. Gumbiner, *A mode of regulation of beta-catenin signaling activity in Xenopus embryos independent of its levels*. *Dev Biol*, 2000. **223**(2): p. 441-8.
187. Staal, F.J., et al., *Wnt signals are transmitted through N-terminally dephosphorylated beta-catenin*. *EMBO Rep*, 2002. **3**(1): p. 63-8.
188. Hendriksen, J., et al., *Plasma membrane recruitment of dephosphorylated β -catenin upon activation of the Wnt pathway*. *Journal of Cell Science*, 2008. **121**(11): p. 1793-1802.
189. Tolwinski, N.S. and E. Wieschaus, *A Nuclear Function for Armadillo/beta-Catenin*. *PLoS Biol*, 2004. **2**(4): p. E95.
190. Somorjai, I.M.L. and A. Martinez-Arias, *Wingless Signalling Alters the Levels, Subcellular Distribution and Dynamics of Armadillo and E-Cadherin in Third Instar Larval Wing Imaginal Discs*. *PloS one*, 2008. **3**(8): p. e2893.
191. Chan, T.A., et al., *Targeted inactivation of CTNNB1 reveals unexpected effects of beta-catenin mutation*. *Proc Natl Acad Sci U S A*, 2002. **99**(12): p. 8265-70.
192. Munoz-Descalzo, S., et al., *Modulation of the ligand-independent traffic of Notch by Axin and Apc contributes to the activation of Armadillo in Drosophila*. *Development*, 2011. **138**(8): p. 1501-1506.
193. Hayward, P., et al., *Notch modulates Wnt signalling by associating with Armadillo/ β -catenin and regulating its transcriptional activity*. *Development*, 2005. **132**(8): p. 1819-30.
194. Kwon, C., et al., *Notch post-translationally regulates β -catenin protein in stem and progenitor cells*. *Nat Cell Biol*, 2011. **advance online publication**.
195. Labbe, E., A. Letamendia, and L. Attisano, *Association of Smads with lymphoid enhancer binding factor 1/T cell-specific factor mediates cooperative signaling by the transforming growth factor-beta and wnt pathways*. *Proc Natl Acad Sci U S A*, 2000. **97**(15): p. 8358-63.
196. Fodde, R. and I. Tomlinson, *Nuclear beta-catenin expression and Wnt signalling: in defence of the dogma*. *The Journal of pathology*, 2010. **221**(3): p. 239-41.
197. Phelps, R.A., et al., *A two-step model for colon adenoma initiation and progression caused by APC loss*. *Cell*, 2009. **137**(4): p. 623-34.

198. Gavert, N., Ben-Ze'ev, A., *B-catenin signaling in biological control and cancer*. J. Cell. Biochem, 2007. **102**: p. 820-828.
199. Shtutman, M., et al., *The cyclin D1 gene is a target of the beta-catenin/LEF-1 pathway*. Proc Natl Acad Sci U S A, 1999. **96**(10): p. 5522-7.
200. Kinzler, K.W. and B. Vogelstein, *Lessons from hereditary colorectal cancer*. Cell, 1996. **87**: p. 159-170.
201. Brabletz, T., et al., *Nuclear overexpression of the oncoprotein beta-catenin in colorectal cancer is localized predominantly at the invasion front*. Pathol Res Pract, 1998. **194**(10): p. 701-704.
202. Anderson, C.B., K.L. Neufeld, and R.L. White, *Subcellular distribution of Wnt pathway proteins in normal and neoplastic colon*. Proceedings of the National Academy of Sciences of the United States of America, 2002. **99**(13): p. 8683-8.
203. Gaspar, C. and R. Fodde, *APC dosage effects in tumorigenesis and stem cell differentiation*. Int. J. Dev. Biol., 2004. **48**: p. 377-386.
204. Bafico, A., et al., *An autocrine mechanism for constitutive Wnt pathway activation in human cancer cells*. Cancer Cell, 2004. **6**(5): p. 497-506.
205. Goentoro, L. and M.W. Kirschner, *Evidence that fold-change, and not absolute level, of beta-catenin dictates Wnt signaling*. Molecular cell, 2009. **36**(5): p. 872-84.
206. Gottardi, C.J. and B.M. Gumbiner, *Distinct molecular forms of [beta]-catenin are targeted to adhesive or transcriptional complexes*. J. Cell Biol., 2004. **167**: p. 339-349.
207. Choi, H.J., A.H. Huber, and W.I. Weis, *Thermodynamics of beta -catenin-ligand interactions. The roles of the N- and C-terminal tails in modulating binding affinity*. J Biol Chem, 2005.
208. Castano, J., I. Raurell, and J.A. Piedra, *[beta]-Catenin N- and C-terminal tails modulate the coordinated binding of adherens junction proteins to [beta]-catenin*. J Biol Chem, 2002. **277**: p. 31541-31550.
209. Kielman, M.F., et al., *Apc modulates embryonic stem-cell differentiation by controlling the dosage of beta-catenin signaling*. Nat Genet, 2002. **32**(4): p. 594-605.
210. Ying, Q.-L., et al., *The ground state of embryonic stem cell self-renewal*. Nature, 2008. **453**(7194): p. 519-523.
211. Doble, B.W., et al., *Functional redundancy of GSK-3[agr] and GSK-3[bgr] in Wnt/[bgr]-catenin signaling shown by using an allelic series of embryonic stem cell lines*. Dev. Cell, 2007. **12**: p. 957-971.
212. Ogawa, K., et al., *Synergistic action of Wnt and LIF in maintaining pluripotency of mouse ES cells*. Biochem. Biophys. Res. Commun., 2006. **343**: p. 159-166.
213. Yi, F., et al., *Opposing effects of Tcf3 and Tcf1 control Wnt stimulation of embryonic stem cell self-renewal*. Nat Cell Biol, 2011. **13**(7): p. 762-770.
214. Lyashenko, N., et al., *Differential requirement for the dual functions of [beta]-catenin in embryonic stem cell self-renewal and germ layer formation*. Nat Cell Biol, 2011. **13**(7): p. 753-761.
215. Kelly, K.F., et al., *beta-Catenin Enhances Oct-4 Activity and Reinforces Pluripotency through a TCF-Independent Mechanism*. Cell stem cell, 2011. **8**(2): p. 214-227.

216. Wray, J., et al., *Inhibition of glycogen synthase kinase-3 alleviates Tcf3 repression of the pluripotency network and increases embryonic stem cell resistance to differentiation*. Nat Cell Biol, 2011. **13**(7): p. 838-845.
217. Bahmanyar, S., et al., *beta-Catenin is a Nek2 substrate involved in centrosome separation*. Genes & Development, 2008. **22**(1): p. 91-105.
218. Maher, M.T., et al., *Activity of the $\text{E}\leq$ -catenin phosphodestruction complex at cell-cell contacts is enhanced by cadherin-based adhesion*. The Journal of Cell Biology, 2009. **186**(2): p. 219-228.
219. Maher, M.T., et al., *$\text{E}\leq$ -Catenin Phosphorylated at Serine 45 Is Spatially Uncoupled from $\text{E}\leq$ -Catenin Phosphorylated in the GSK3 Domain: Implications for Signaling*. PloS one, 2010. **5**(4): p. e10184.
220. Thorne, M.E. and C.J. Gottardi, *Terminating Wnt signals: a novel nuclear export mechanism targets activated $\{\beta\}$ -catenin*. J Cell Biol, 2005. **171**(5): p. 761-3.
221. Fang, D., et al., *Phosphorylation of beta-catenin by AKT promotes beta-catenin transcriptional activity*. The Journal of biological chemistry, 2007. **282**(15): p. 11221-9.
222. Taurin, S., et al., *Phosphorylation of $\text{E}\leq$ -catenin by PKA promotes ATP-induced proliferation of vascular smooth muscle cells*. American Journal of Physiology - Cell Physiology, 2008. **294**(5): p. C1169-C1174.
223. Roura, S., et al., *Regulation of E-cadherin/catenin association by tyrosine phosphorylation*. J. Biol. Chem., 1999. **274**: p. 36734-36740.
224. Piedra, J., *p120 catenin-associated Fer and Fyn tyrosine kinases regulate $[\beta]$ -catenin Tyr-142 phosphorylation and $[\beta]$ -catenin- $[\alpha]$ -catenin interaction*. Mol. Cell Biol., 2003. **23**: p. 2287-2297.
225. Rhee, J., et al., *Cables links Robo-bound Abl kinase to N-cadherin-bound $[\beta]$ -catenin to mediate Slit-induced modulation of adhesion and transcription*. Nat Cell Biol, 2007. **9**(8): p. 883-892.
226. Gwak, J., et al., *Protein-kinase-C-mediated $\text{E}\leq$ -catenin phosphorylation negatively regulates the Wnt/ $\text{E}\leq$ -catenin pathway*. Journal of Cell Science, 2006. **119**(22): p. 4702-4709.
227. Park, C.S., et al., *Modulation of beta-catenin phosphorylation/degradation by cyclin-dependent kinase 2*. The Journal of biological chemistry, 2004. **279**(19): p. 19592-9.
228. Aberle, H., et al., *beta-catenin is a target for the ubiquitin-proteasome pathway*. EMBO J., 1997. **16**(13): p. 3797-3804.
229. Piedra, J., S. Miravet, and J. Castano, *p120 Catenin-associated Fer and Fyn tyrosine kinases regulate $[\beta]$ -catenin Tyr-142 phosphorylation and $[\beta]$ -catenin- $[\alpha]$ -catenin interaction*. Mol Cell Biol, 2003. **23**: p. 2287-2297.
230. Du, C., et al., *Protein Kinase D1, $\text{E}\leq$ Mediated Phosphorylation and Subcellular Localization of $\text{E}\leq$ -Catenin*. Cancer Research, 2009. **69**(3): p. 1117-1124.
231. Park, C.S., et al., *Modulation of $\text{E}\leq$ -catenin by cyclin-dependent kinase 6 in Wnt-stimulated cells*. European Journal of Cell Biology, 2007. **86**(2): p. 111-123.
232. Kikuchi, A., S. Kishida, and H. Yamamoto, *Regulation of Wnt signaling by protein-protein interaction and post-translational modifications*. Exp Mol Med, 2006. **38**(1): p. 1-10.
233. Harris, T.J.C. and M. Peifer, *Decisions, decisions: β -catenin chooses between adhesion and transcription*. Trends in Cell Biology, 2005. **15**(5): p. 234-237.

234. Verheyen, E.M. and C.J. Gottardi, *Regulation of Wnt/ β -catenin signaling by protein kinases*. Developmental Dynamics, 2010. **239**(1): p. 34-44.
235. Luckert, K., et al., *Snapshots of Protein Dynamics and Post-translational Modifications In One Experiment, β -Catenin and Its Functions*. Molecular & Cellular Proteomics, 2011. **10**(5).
236. Aigner, A., *Gene silencing through RNA interference (RNAi) in vivo: strategies based on the direct application of siRNAs*. J. Biotech, 2006. **124**: p. 12-25.
237. Yang, D., et al., *Short RNA duplexes produced by hydrolysis with Escherichia coli RNase III mediate effective RNA interference in mammalian cells*. Proc Natl Acad Sci U S A, 2002. **99**(15): p. 9942-9947.
238. Buchholz, F., et al., *Enzymatically prepared RNAi libraries*. Nature methods, 2006. **3**(9): p. 696-700.
239. Kittler, R., et al., *Production of endoribonuclease-prepared short interfering RNAs for gene silencing in mammalian cells*. Nat Methods, 2005. **2**(10): p. 779-84.
240. Kittler, R., et al., *An endoribonuclease-prepared siRNA screen in human cells identifies genes essential for cell division*. Nature, 2004. **432**(7020): p. 1036-40.
241. Krausz, E., *High-content siRNA screening* Mol. BioSyst, 2007(3): p. 232-240.
242. Major, M.B., et al., *New regulators of Wnt/beta-catenin signaling revealed by integrative molecular screening*. Sci Signal, 2008. **1**(45): p. 1-12.
243. Foley, E. and P.H. O'Farrell, *Functional Dissection of an Innate Immune Response by a Genome-Wide RNAi Screen*. PLoS Biol, 2004. **2**(8): p. E203.
244. Ashrafi, K., et al., *Genome-wide RNAi analysis of Caenorhabditis elegans fat regulatory genes*. Nature, 2003. **421**(6920): p. 268-72.
245. Echeverri, C.J. and N. Perrimon, *High-throughput RNAi screening in cultured cells: a user's guide*. Nature reviews. Genetics, 2006. **7**(5): p. 373-84.
246. Zanella, F., J.B. Lorens, and W. Link, *High content screening: seeing is believing*. Trends in biotechnology, 2010. **28**(5): p. 237-45.
247. Armknecht, S., et al., *High-throughput RNA interference screens in Drosophila tissue culture cells*. Methods Enzymol, 2005. **392**: p. 55-73.
248. Echeverri, C.J., et al., *Minimizing the risk of reporting false positives in large-scale RNAi screens*. Nat Methods, 2006. **3**(10): p. 777-9.
249. Zock, J.M., *Applications of High Content Screening in Life Science Research*. Combinatorial Chemistry & High Throughput Screening, 2009. **12**(9): p. 870-876.
250. Rines, D.R., et al., *Whole genome functional analysis identifies novel components required for mitotic spindle integrity in human cells*. Genome Biol, 2008. **9**(2): p. R44.
251. Pelkmans, L., et al., *Genome-wide analysis of human kinases in clathrin- and caveolae/raft-mediated endocytosis*. Nature, 2005. **436**(7047): p. 78-86.
252. Xu, Y., Y. Shi, and S. Ding, *A chemical approach to stem-cell biology and regenerative medicine*. Nature, 2008. **453**(7193): p. 338-344.
253. Chen, S., *Self-renewal of embryonic stem cells by a small molecule*. Proc. Natl Acad. Sci. USA, 2006. **103**: p. 17266-17271.
254. Evensen, L., et al., *Mural Cell Associated VEGF Is Required for Organotypic Vessel Formation*. PloS one, 2009. **4**(6): p. e5798.

255. Gasparri, F. and A. Galvani, *Image-based high-content reporter assays: limitations and advantages*. Drug Discovery Today: Technologies, 2010. **7**(1): p. e21-e30.
256. Nickischer, D., et al., *Development and Implementation of Three Mitogen-Activated Protein Kinase (MAPK) Signaling Pathway Imaging Assays to Provide MAPK Module Selectivity Profiling for Kinase Inhibitors: MK2, EGFP Translocation, c-Jun, and ERK Activation*, in *Methods in Enzymology*, I. James, Editor 2006, Academic Press. p. 389-418.
257. Au, Q., et al., *Identification of Inhibitors of HSF1 Functional Activity by High-Content Target-Based Screening*. Journal of Biomolecular Screening, 2009. **14**(10): p. 1165-1175.
258. Lundholt, B.K., et al., *A Simple Cell-Based HTS Assay System to Screen for Inhibitors of p53-Hdm2 Protein-Protein Interactions*. ASSAY and Drug Development Technologies, 2006. **4**(6): p. 679-688.
259. Duan, Z., et al., *SD-1029 Inhibits Signal Transducer and Activator of Transcription 3 Nuclear Translocation*. Clinical Cancer Research, 2006. **12**(22): p. 6844-6852.
260. Ding, G.J.F., et al., *Characterization and Quantitation of NF- κ B Nuclear Translocation Induced by Interleukin-1 and Tumor Necrosis Factor- α* . Journal of Biological Chemistry, 1998. **273**(44): p. 28897-28905.
261. Link, W., et al., *Chemical Interrogation of FOXO3a Nuclear Translocation Identifies Potent and Selective Inhibitors of Phosphoinositide 3-Kinases*. Journal of Biological Chemistry, 2009. **284**(41): p. 28392-28400.
262. Miller, B.W., et al., *Application of an integrated physical and functional screening approach to identify inhibitors of the Wnt pathway*. Molecular systems biology, 2009. **5**: p. 315.
263. Luo, W., et al., *Protein phosphatase 1 regulates assembly and function of the beta-catenin degradation complex*. The Embo Journal, 2007. **26**(6): p. 1511-21.
264. Gonsalves, F.C., et al., *Feature Article: From the Cover: An RNAi-based chemical genetic screen identifies three small-molecule inhibitors of the Wnt/wingless signaling pathway*. Proceedings of the National Academy of Sciences, 2011. **108**(15): p. 5954-5963.
265. Cruciat, C.-M., et al., *Requirement of Prorenin Receptor and Vacuolar H⁺-ATPase-Mediated Acidification for Wnt Signaling*. Science, 2010. **327**(5964): p. 459-463.
266. James, R.G., et al., *Bruton's Tyrosine Kinase Revealed as a Negative Regulator of Wnt- β -Catenin Signaling*. Sci. Signal., 2009. **2**(72): p. ra25-.
267. Tang, W., et al., *A genome-wide RNAi screen for Wnt/beta-catenin pathway components identifies unexpected roles for TCF transcription factors in cancer*. Proceedings of the National Academy of Sciences of the United States of America, 2008. **105**(28): p. 9697-702.
268. Dasgupta, R., et al., *Functional Genomic Analysis of the Wnt-Wingless Signaling Pathway*. Science, 2005. **308**: p. 826-832.
269. Korinek V, Barker N, Moerer P, van Donselaar E, Huls G, Peters P J, Clevers H, *Depletion of epithelial stem cell compartments in the small intestine of mice lacking Tcf-4*. Nature Genetics, 1998. **19**: p. 379-383.
270. Ciani, L., et al., *A divergent canonical WNT-signaling pathway regulates microtubule dynamics: Dishevelled signals locally to stabilize microtubules*. J Cell Biol, 2004. **164**(2): p. 243-53.

271. Ewan, K., et al., *A useful approach to identify novel small-molecule inhibitors of Wnt-dependent transcription*. *Cancer research*, 2010. **70**(14): p. 5963-73.
272. Haney, S.A., et al., *High-content screening moves to the front of the line*. *Drug discovery today*, 2006. **11**(19-20): p. 889-94.
273. Borchert, K.M., et al., *High-Content Screening Assay for Activators of the Wnt/Fzd Pathway in Primary Human Cells*. *ASSAY and Drug Development Technologies*, 2005. **3**(2): p. 133-141.
274. Borchert, K.M., et al., *Screening for Activators of the Wingless Type/Frizzled Pathway by Automated Fluorescent Microscopy*, in *Methods in Enzymology*, I. James, Editor 2006, Academic Press. p. 140-150.
275. Verkaar, F., et al., *Discovery of Novel Small Molecule Activators of b-Catenin Signaling*. *PloS one*, 2011. **6**(4): p. 1-7
276. Verkaar, F., et al., *CE₂-Galactosidase enzyme fragment complementation for the measurement of Wnt/CE₂-catenin signaling*. *The FASEB Journal*, 2010. **24**(4): p. 1205-1217.
277. Unterreiner, V., et al., *Comparison of Variability and Sensitivity between Nuclear Translocation and Luciferase Reporter Gene Assays*. *Journal of Biomolecular Screening*, 2009. **14**(1): p. 59-65.
278. Barrios-Rodiles, M., et al., *High-Throughput Mapping of a Dynamic Signaling Network in Mammalian Cells*. *Science*, 2005. **307**(5715): p. 1621-1625.
279. Varelas, X., et al., *TAZ controls Smad nucleocytoplasmic shuttling and regulates human embryonic stem-cell self-renewal*. *Nat Cell Biol*, 2008. **10**(7): p. 837-848.
280. Xu, L., et al., *Msk is required for nuclear import of TGF- β /BMP-activated Smads*. *The Journal of Cell Biology*, 2007. **178**(6): p. 981-94.
281. Levy, L., et al., *Arkadia Activates Smad3/Smad4-Dependent Transcription by Triggering Signal-Induced SnoN Degradation*. *Mol. Cell. Biol.*, 2007. **27**(17): p. 6068-6083.
282. van Amerongen, R. and R. Nusse, *Towards an integrated view of Wnt signaling in development*. *Development*, 2009. **136**(19): p. 3205-14.
283. Smalley, M.J., et al., *Dishevelled (Dvl-2) activates canonical Wnt signalling in the absence of cytoplasmic puncta*. *J Cell Sci*, 2005. **118**(Pt 22): p. 5279-89.
284. Samuels, M.L., et al., *Conditional transformation of cells and rapid activation of the mitogen-activated protein kinase cascade by an estradiol-dependent human raf-1 protein kinase*. *Mol Cell Biol*, 1993. **13**(10): p. 6241-52.
285. McKendry, R., et al., *LEF-1/TCF proteins mediate wnt-inducible transcription from the Xenopus nodal-related 3 promoter*. *Dev Biol*, 1997. **192**(2): p. 420-31.
286. Korinek, V., et al., *Constitutive transcriptional activation by a β -catenin-Tcf complex in APC-/- colon carcinoma*. *Science*, 1997. **275**: p. 1784-1787.
287. Zhang, J.-H., T.D.Y. Chung, and K.R. Oldenburg, *A simple statistical parameter for use in evaluation and validation of high throughput screening assays*. *J. Biomol. Screening*, 1999. **4**(2): p. 67-73.
288. Zhang, J.H., *A Simple Statistical Parameter for Use in Evaluation and Validation of High Throughput Screening Assays*. *Journal of Biomolecular Screening*, 1999. **4**(2): p. 67-73.
289. Birmingham, A., et al., *Statistical methods for analysis of high-throughput RNA interference screens*. *Nat Meth*, 2009. **6**(8): p. 569-575.

290. Livak, K.J. and T.D. Schmittgen, *Analysis of Relative Gene Expression Data Using Real-Time Quantitative PCR and the 2- $\Delta\Delta C_T$ Method*. *Methods*, 2001. **25**(4): p. 402-408.
291. Boutros, M. and J. Ahringer, *The art and design of genetic screens: RNA interference*. *Nature reviews. Genetics*, 2008. **9**(7): p. 554 - 566.
292. Zhang, X.D., *A pair of new statistical parameters for quality control in RNA interference high-throughput screening assays*. *Genomics*, 2007. **89**(4): p. 552-561.
293. Zhang, X.D., *Novel Analytic Criteria and Effective Plate Designs for Quality Control in Genome-Scale RNAi Screens*. *Journal of Biomolecular Screening*, 2008. **13**(5): p. 363-377.
294. Ziauddin, J. and D.M. Sabatini, *Microarrays of cells expressing defined cDNAs*. *Nature*, 2001. **411**(6833): p. 107-110.
295. Silva, J.M., *RNA interference microarrays: High-throughput loss-of-function genetics in mammalian cells*. *PNAS*, 2004. **101**: p. 6548-6552.
296. Neumann, B., *High-throughput RNAi screening by time-lapse imaging of live human cells*. *Nature methods*, 2006. **3**: p. 385-390.
297. Dietrich, C., et al., *Subcellular localisation of beta-catenin is regulated by cell density*. *Biochem. Biophys. Res. Comm*, 2002. **292**: p. 195-199.
298. Marchesini, N., J.A. Jones, and Y.A. Hannun, *Confluence induced threonine41/serine45 phospho-[beta]-catenin dephosphorylation via ceramide-mediated activation of PP1c[gamma]*. *Biochimica et Biophysica Acta (BBA) - Molecular and Cell Biology of Lipids*, 2007. **1771**(12): p. 1418-1428.
299. Malo, N., et al., *Statistical practice in high-throughput screening data analysis*. *Nat Biotech*, 2006. **24**(2): p. 167-175.
300. Markowitz, F., *How to Understand the Cell by Breaking It: Network Analysis of Gene Perturbation Screens*. *PLoS Comput Biol*, 2010. **6**(2): p. e1000655.
301. Carmona-Saez, P., et al., *GENECODIS: a web-based tool for finding significant concurrent annotations in gene lists*. *Genome Biol*, 2007. **8**(1): p. R3.
302. Kanehisa, M., et al., *KEGG for linking genomes to life and the environment*. *Nucleic Acids Res*, 2008. **36**(Database issue): p. D480-4.
303. <http://www.genego.com/metacore.php>.
304. Gadue, P., et al., *Wnt and TGF- β signaling are required for the induction of an in vitro model of primitive streak formation using embryonic stem cells*. *Proceedings of the National Academy of Sciences*, 2006. **103**(45): p. 16806-16811.
305. Guo, X. and X.F. Wang, *Signaling cross-talk between TGF-beta/BMP and other pathways*. *Cell Res*, 2009. **19**(1): p. 71-88.
306. Matsuda, Y., et al., *WNT signaling enhances breast cancer cell motility and blockade of the WNT pathway by sFRP1 suppresses MDA-MB-231 xenograft growth*. *Breast Cancer Research*, 2009. **11**(3): p. R32.
307. Davidson, G. and C. Niehrs, *Emerging links between CDK cell cycle regulators and Wnt signaling*. *Trends in Cell Biology*, 2010. **20**(8): p. 453-460.
308. Davidson, G., et al., *Cell Cycle Control of Wnt Receptor Activation*. *Developmental Cell*, 2009. **17**(6): p. 788-799.

309. Brembeck, F.H., M. Rosario, and W. Birchmeier, *Balancing cell adhesion and Wnt signaling, the key role of beta-catenin*. *Curr. Opin. Gen. Dev*, 2006. **16**(1): p. 51-9.
310. Murata-Kamiya, N., et al., *Helicobacter pylori CagA interacts with E-cadherin and deregulates the [beta]-catenin signal that promotes intestinal transdifferentiation in gastric epithelial cells*. *Oncogene*, 2007. **26**(32): p. 4617-4626.
311. Cheng, X.-X., et al., *Frequent loss of membranous E-cadherin in gastric cancers: A cross-talk with Wnt in determining the fate of β -catenin*. *Clinical and Experimental Metastasis*, 2005. **22**(1): p. 85-93.
312. Sokolova, O., P.M. Bozko, and M. Naumann, *Helicobacter pylori Suppresses Glycogen Synthase Kinase 3 β to Promote β -Catenin Activity*. *Journal of Biological Chemistry*, 2008. **283**(43): p. 29367-29374.
313. Gnad, T., et al., *Helicobacter pylori-induced activation of beta-catenin involves low density lipoprotein receptor-related protein 6 and Dishevelled*. *Molecular Cancer*, 2010. **9**(1): p. 31.
314. Kohn, A.D. and R.T. Moon, *Wnt and calcium signaling: [beta]-catenin-independent pathways*. *Cell Calcium*, 2005. **38**: p. 439-446.
315. Blitzer, J.T. and R. Nusse, *A critical role for endocytosis in Wnt signaling*. *BMC Cell Biol*, 2006. **7**: p. 28.
316. Kikuchi, A. and H. Yamamoto, *Regulation of Wnt signalling by receptor-mediated endocytosis*. *Journal of biochemistry*, 2007. **141**(4): p. 443-51.
317. Lu, Z., et al., *Downregulation of caveolin-1 function by EGF leads to the loss of E-cadherin, increased transcriptional activity of beta-catenin, and enhanced tumor cell invasion*. *Cancer Cell*, 2003. **4**(6): p. 499-515.
318. Yamamoto, H., et al., *Wnt3a and Dkk1 regulate distinct internalization pathways of LRP6 to tune the activation of beta-catenin signaling*. *Dev Cell*, 2008. **15**(1): p. 37-48.
319. Shibata, T., et al., *EBP50, a β -catenin-associating protein, enhances Wnt signaling and is over-expressed in hepatocellular carcinoma*. *Hepatology*, 2003. **38**(1): p. 178-186.
320. Bhambhani, C., et al., *The oligomeric state of CtBP determines its role as a transcriptional co-activator and co-repressor of Wingless targets*. *EMBO J*, 2011. **30**(10): p. 2031-2043.
321. Fang, M., et al., *C-terminal-binding protein directly activates and represses Wnt transcriptional targets in Drosophila*. *The Embo Journal*, 2006. **25**(12): p. 2735-45.
322. Brannon, M., et al., *XCTBP is a XTcf-3 co-repressor with roles throughout Xenopus development*. *Development*, 1999. **126**(14): p. 3159-70.
323. Hamada, F. and M. Bienz, *The APC Tumor Suppressor Binds to C-Terminal Binding Protein to Divert Nuclear β -Catenin from TCF*. *Developmental Cell*, 2004. **7**(5): p. 677-685.
324. Thiele, A., et al., *AU-rich elements and alternative splicing in the beta-catenin 3'UTR can influence the human beta-catenin mRNA stability*. *Exp Cell Res*, 2006. **312**(12): p. 2367-78.
325. Heinen, C.D., et al., *The APC tumor suppressor controls entry into S-phase through its ability to regulate the cyclin D/RB pathway*. *Gastroenterology*, 2002. **123**(3): p. 751-63.
326. Fodde, R., et al., *Mutations in the APC tumour suppressor gene cause chromosomal instability*. *Nat Cell Biol*, 2001. **3**(4): p. 433-8.

327. Kaplan, K.B., et al., *A role for the Adenomatous Polyposis Coli protein in chromosome segregation*. Nat Cell Biol, 2001. **3**(4): p. 429-32.
328. Wang, Y., et al., *Interaction between Tumor Suppressor Adenomatous Polyposis Coli and Topoisomerase II α : Implication for the G2/M Transition*. Molecular Biology of the Cell, 2008. **19**(10): p. 4076-4085.
329. Jian, H., et al., *Smad3-dependent nuclear translocation of beta-catenin is required for TGF-beta1-induced proliferation of bone marrow-derived adult human mesenchymal stem cells*. Genes Dev, 2006. **20**(6): p. 666-74.
330. Kim, S.-E., W.-J. Lee, and K.-Y. Choi, *The PI3 kinase-Akt pathway mediates Wnt3a-induced proliferation*. Cellular Signalling, 2007. **19**(3): p. 511-518.
331. Davis, R.J., *Signal transduction by the JNK group of MAP kinases* Cell, 2000. **103**(2): p. 239-52.
332. Lee, M.-H., et al., *JNK phosphorylates β -catenin and regulates adherens junctions*. The FASEB Journal, 2009. **23**(11): p. 3874-3883.
333. Yamanaka, H., et al., *JNK functions in the non-canonical Wnt pathway to regulate convergent extension movements in vertebrates*. EMBO Rep., 2002. **3**(1): p. 69-75.
334. Mak, B.C., et al., *Aberrant beta-catenin signaling in tuberous sclerosis*. American J. Path, 2005. **167**(1): p. 107 - 117.
335. Gherzi, R., et al., *A KH Domain RNA Binding Protein, KSRP, Promotes ARE-Directed mRNA Turnover by Recruiting the Degradation Machinery*. Molecular cell, 2004. **14**(5): p. 571-583.
336. Cardozo, T. and M. Pagano, *The SCF ubiquitin ligase: insights into a molecular machine*. Nat Rev Mol Cell Biol, 2004. **5**(9): p. 739-51.
337. Latres, E., D.S. Chiaur, and M. Pagano, *The human F box protein beta-Trcp associates with the Cull1/Skp1 complex and regulates the stability of beta-catenin*. Oncogene, 1999. **18**(4): p. 849-54.
338. Murillas, R., et al., *Identification of Developmentally Expressed Proteins That Functionally Interact with Nedd4 Ubiquitin Ligase*. Journal of Biological Chemistry, 2002. **277**(4): p. 2897-2907.
339. Chan, D.W., et al., *Prickle-1 negatively regulates Wnt/beta-catenin pathway by promoting Dishevelled ubiquitination/degradation in liver cancer*. Gastroenterology, 2006. **131**(4): p. 1218-27.
340. Wharton, K.A., Jr., *Runnin' with the Dvl: proteins that associate with Dsh/Dvl and their significance to Wnt signal transduction*. Dev Biol, 2003. **253**(1): p. 1-17.
341. Wharton, K.A., Jr., et al., *Vertebrate proteins related to Drosophila Naked Cuticle bind Dishevelled and antagonize Wnt signaling*. Dev Biol, 2001. **234**(1): p. 93-106.
342. Tauriello, D.V., et al., *Loss of the tumor suppressor CYLD enhances Wnt/beta-catenin signaling through K63-linked ubiquitination of Dvl*. Molecular cell, 2010. **37**(5): p. 607-19.
343. Choi, J., et al., *Adenomatous Polyposis Coli Is Down-regulated by the Ubiquitin-Proteasome Pathway in a Process Facilitated by Axin*. J Biol Chem, 2004. **279**(47): p. 49188-98.
344. Choi, J., et al., *APC is down-regulated by the ubiquitin-proteasome pathway in a process facilitated by Axin*. J Biol Chem, 2004.
345. Yamada, M., et al., *NARF, an NLK-associated ring finger protein regulates the ubiquitylation and degradation of TCF/LEF*. J Biol Chem, 2006.

346. Asada, M., et al., *ADIP, a Novel Afadin- and C^{\pm} -Actinin-Binding Protein Localized at Cell-Cell Adherens Junctions*. Journal of Biological Chemistry, 2003. **278**(6): p. 4103-4111.
347. Kuang, B., et al., *split ends encodes large nuclear proteins that regulate neuronal cell fate and axon extension in the Drosophila embryo*. Development, 2000. **127**(7): p. 1517-1529.
348. Chen, F. and I. Rebay, *split ends, a new component of the Drosophila EGF receptor pathway, regulates development of midline glial cells*. Current biology : CB, 2000. **10**(15): p. 943-S2.
349. Lin, H.V., et al., *Splits ends is a tissue/promoter specific regulator of Wingless signaling*. Development, 2003. **130**(14): p. 3125-3135.
350. Feng, Y., et al., *Drosophila split ends homologue SHARP functions as a positive regulator of Wnt/beta-catenin/T-cell factor signaling in neoplastic transformation*. Cancer Research, 2007. **67**(2): p. 482-91.
351. Kumar, A., et al., *The Ectodermal Dysplasia Receptor Activates the Nuclear Factor- κ B, JNK, and Cell Death Pathways and Binds to Ectodysplasin A*. Journal of Biological Chemistry, 2001. **276**(4): p. 2668-2677.
352. Zhang, Y., et al., *Reciprocal Requirements for EDA/EDAR/NF- κ B and Wnt/ β -Catenin Signaling Pathways in Hair Follicle Induction*. Developmental Cell, 2009. **17**(1): p. 49-61.
353. Horii, M., et al., *CHMP7, a novel ESCRT-III-related protein, associates with CHMP4b and functions in the endosomal sorting pathway*. The Biochemical journal, 2006. **400**(1): p. 23-32.
354. Kioussi, C., et al., *Identification of a Wnt/Dvl/beta-Catenin --> Pitx2 Pathway Mediating Cell-Type-Specific Proliferation during Development*. Cell, 2002. **111**(5): p. 673-85.
355. Reymond, A., et al., *The tripartite motif family identifies cell compartments*. EMBO J, 2001. **20**(9): p. 2140-2151.
356. Kondo, S. and N. Perrimon, *A Genome-Wide RNAi Screen Identifies Core Components of the G2-M DNA Damage Checkpoint*. Sci. Signal., 2011. **4**(154): p. rs1-.
357. Yang, H., et al., *RPB5-mediating Protein Is Required for the Proliferation of Hepatocellular Carcinoma Cells*. Journal of Biological Chemistry, 2011. **286**(13): p. 11865-11874.
358. Le, T.T.T., et al., *Mutational Analysis of Human RNA Polymerase II Subunit 5 (RPB5): The Residues Critical for Interactions with TFIIF Subunit RAP30 and Hepatitis B Virus X Protein*. Journal of biochemistry, 2005. **138**(3): p. 215-224.
359. Lee, N.P.Y. and C.Y. Cheng, *Protein kinases and adherens junction dynamics in the seminiferous epithelium of the rat testis*. Journal of Cellular Physiology, 2005. **202**(2): p. 344-360.
360. Jopling, C. and J.d. Hertog, *Essential role for Csk upstream of Fyn and Yes in zebrafish gastrulation*. Mechanisms of Development, 2007. **124**(2): p. 129-136.
361. Smoot, M.E., et al., *Cytoscape 2.8: new features for data integration and network visualization*. Bioinformatics, 2011. **27**(3): p. 431-432.
362. Cline, M.S., et al., *Integration of biological networks and gene expression data using Cytoscape*. Nat. Protocols, 2007. **2**(10): p. 2366-2382.

363. Shannon, P., et al., *Cytoscape: A Software Environment for Integrated Models of Biomolecular Interaction Networks*. Genome Research, 2003. **13**(11): p. 2498 - 2504.
364. Eferl, R. and E.F. Wagner, *AP-1: a double-edged sword in tumorigenesis*. Nat Rev Cancer, 2003. **3**(11): p. 859-868.
365. Gan, X.-q., et al., *Nuclear Dvl, c-Jun, β -catenin, and TCF form a complex leading to stabilization of β -catenin, Δ TCF interaction*. The Journal of Cell Biology, 2008. **180**(6): p. 1087-1100.
366. Toualbi, K., et al., *Physical and functional cooperation between AP-1 and β -catenin for the regulation of TCF-dependent genes*. Oncogene, 2006. **26**(24): p. 3492-3502.
367. Nateri, A.S., B. Spencer-Dene, and A. Behrens, *Interaction of phosphorylated c-Jun with TCF4 regulates intestinal cancer development*. Nature, 2005. **437**(7056): p. 281-5.
368. Ekas, L.A., et al., *JAK/STAT signaling promotes regional specification by negatively regulating wingless expression in Drosophila*. Development, 2006. **133**(23): p. 4721-4729.
369. Liu, Y.-C., et al., *Blockade of JAK2 activity suppressed accumulation of β -catenin in leukemic cells*. Journal of Cellular Biochemistry, 2010. **111**(2): p. 402-411.
370. Rui, H.L., et al., *SUMO-1 modification of the carboxyl-terminal KVEKVD of Axin is required for JNK activation, but has no effect on Wnt signaling*. J Biol Chem, 2002.
371. Yamashina, K., et al., *Suppression of STAT3 activity by Duplin, which is a negative regulator of the Wnt signal*. Journal of biochemistry, 2006. **139**(2): p. 305-14.
372. Crampton, S.P., et al., *Integration of the β -Catenin-Dependent Wnt Pathway with Integrin Signaling through the Adaptor Molecule Grb2*. PloS one, 2009. **4**(11): p. e7841.
373. Zhu, E.D., M.B. Demay, and F. Gori, *Wdr5 Is Essential for Osteoblast Differentiation*. Journal of Biological Chemistry, 2008. **283**(12): p. 7361-7367.
374. Gori, F., E.D. Zhu, and M.B. Demay, *Perichondrial expression of Wdr5 regulates chondrocyte proliferation and differentiation*. Dev Biol, 2009. **329**(1): p. 36-43.
375. Li, J. and B. Zhou, *Activation of beta-catenin and Akt pathways by Twist are critical for the maintenance of EMT associated cancer stem cell-like characters*. BMC Cancer, 2011. **11**(1): p. 49.
376. Fujita, N., et al., *MCAF mediates MBD1-dependent transcriptional repression*. Mol Cell Biol, 2003. **23**(8): p. 2834-43.
377. Liu, L., et al., *MCAF/AM is involved in Sp1-mediated maintenance of cancer-associated telomerase activity*. The Journal of biological chemistry, 2009. **284**(8): p. 5165-74.
378. Chen, Y.Z., *APP induces neuronal apoptosis through APP-BP1-mediated downregulation of beta-catenin*. Apoptosis, 2004. **9**(4): p. 415-22.
379. Sato, S., et al., *beta-catenin interacts with the FUS proto-oncogene product and regulates pre-mRNA splicing*. Gastroenterology, 2005. **129**(4): p. 1225-36.
380. Tian, Q., et al., *Proteomic analysis identifies that 14-3-3zeta interacts with beta-catenin and facilitates its activation by Akt*. Proceedings of the National

- Academy of Sciences of the United States of America, 2004. **101**(43): p. 15370-5.
381. Glisovic, T., et al., *RNA-binding proteins and post-transcriptional gene regulation*. FEBS J, 2008. **582**(14): p. 1977-1986.
 382. Dreyfuss, G., V.N. Kim, and N. Kataoka, *Messenger-RNA-binding proteins and the messages they carry*. Nat Rev Mol Cell Biol, 2002. **3**(3): p. 195-205.
 383. Valencia-Sanchez, M.A., et al., *Control of translation and mRNA degradation by miRNAs and siRNAs*. Genes & Development, 2006. **20**(5): p. 515-24.
 384. Dreyfuss, G., et al., *hnRNP proteins and the biogenesis of mRNA*. Annu. Rev. Biochem, 1993. **62**: p. 289-321.
 385. Moore, M.J., *From birth to death: the complex lives of eukaryotic mRNAs*. Science, 2005. **309**(5740): p. 1514-8.
 386. Stone, J.R. and T. Collins, *Rapid Phosphorylation of Heterogeneous Nuclear Ribonucleoprotein C1/C2 in Response to Physiologic Levels of Hydrogen Peroxide in Human Endothelial Cells*. Journal of Biological Chemistry, 2002. **277**(18): p. 15621-15628.
 387. Municio, M.M., et al., *Identification of Heterogeneous Ribonucleoprotein A1 as a Novel Substrate for Protein Kinase C*. Journal of Biological Chemistry, 1995. **270**(26): p. 15884-15891.
 388. Carpenter, B., et al., *The roles of heterogeneous nuclear ribonucleoproteins in tumour development and progression*. Biochimica et Biophysica Acta (BBA) - Reviews on Cancer, 2006. **1765**(2): p. 85-100.
 389. Hoffman, D.W., et al., *RNA-binding domain of the A protein component of the U1 small nuclear ribonucleoprotein analyzed by NMR spectroscopy is structurally similar to ribosomal proteins*. Proc Natl Acad Sci U S A, 1991. **88**(1826055): p. 2495-2499.
 390. Lunde, B.M., C. Moore, and G. Varani, *RNA-binding proteins: modular design for efficient function*. Nat Rev Mol Cell Biol, 2007. **8**(17473849): p. 479-490.
 391. Han, S.P., Y.H. Tang, and R. Smith, *Functional diversity of the hnRNPs: past, present and perspectives*. Biochem J, 2010. **430**(3): p. 379-392.
 392. Maris, C., C. Dominguez, and F.d.r.H.T. Allain, *The RNA recognition motif, a plastic RNA-binding platform to regulate post-transcriptional gene expression*. FEBS Journal, 2005. **272**(9): p. 2118-2131.
 393. Iwanaga, K., et al., *Heterogeneous nuclear ribonucleoprotein B1 protein impairs DNA repair mediated through the inhibition of DNA-dependent protein kinase activity*. Biochemical and Biophysical Research Communications, 2005. **333**(3): p. 888-895.
 394. Krecic, A. and M. Swanson, *hnRNP complexes: composition, structure, and function*. Curr Opin Cell Biol, 1999. **11**: p. 363-371.
 395. Myer, V.E. and J.A. Steitz, *Isolation and characterization of a novel, low abundance hnRNP protein: A0*. Rna, 1995. **1**(2): p. 171-182.
 396. LaBranche, H., et al., *Telomere elongation by hnRNP A1 and a derivative that interacts with telomeric repeats and telomerase*. Nat Genet, 1998. **19**(2): p. 199-202.
 397. Zhang, Q.-S., et al., *hnRNP A1 associates with telomere ends and stimulates telomerase activity*. Rna, 2006. **12**(16603717): p. 1116-1128.
 398. Flynn, R.L., et al., *TERRA and hnRNPA1 orchestrate an RPA-to-POT1 switch on telomeric single-stranded DNA*. Nature, 2011. **advance online publication**.

399. Ford, L.P., W.E. Wright, and J.W. Shay, *A model for heterogeneous nuclear ribonucleoproteins in telomere and telomerase regulation*. *Oncogene*, 2002. **21**(11850782): p. 580-583.
400. Campillos, M., et al., *Specific interaction of heterogeneous nuclear ribonucleoprotein A1 with the -219T allelic form modulates APOE promoter activity*. *Nucleic Acids Res*, 2003. **31**(12799433): p. 3063-3070.
401. Chai, Q., et al., *Interaction and Stimulation of Human FEN-1 Nuclease Activities by Heterogeneous Nuclear Ribonucleoprotein A1 in CE±-Segment Processing during Okazaki Fragment Maturation*. *Biochemistry*, 2003. **42**(51): p. 15045-15052.
402. Mayeda, A. and A.R. Krainer, *Regulation of alternative pre-mRNA splicing by hnRNP A1 and splicing factor SF2*. *Cell*, 1992. **68**(1531115): p. 365-375.
403. David, C.J., et al., *HnRNP proteins controlled by c-Myc deregulate pyruvate kinase mRNA splicing in cancer*. *Nature*, 2010. **463**(20010808): p. 364-368.
404. Choi, Y.D., et al., *Heterogeneous nuclear ribonucleoproteins: role in RNA splicing*. *Science*, 1986. **231**(3952495): p. 1534-1539.
405. Dery, K.J., et al., *Mechanistic Control of Carcinoembryonic Antigen-related Cell Adhesion Molecule-1 (CEACAM1) Splice Isoforms by the Heterogeneous Nuclear Ribonuclear Proteins hnRNP L, hnRNP A1, and hnRNP M*. *The Journal of biological chemistry*, 2011. **286**(18): p. 16039-51.
406. Michlewski, G. and J.F. Caceres, *Antagonistic role of hnRNP A1 and KSRP in the regulation of let-7a biogenesis*. *Nature structural & molecular biology*, 2010. **17**(8): p. 1011-8.
407. Guil, S. and J.F. Caceres, *The multifunctional RNA-binding protein hnRNP A1 is required for processing of miR-18a*. *Nat Struct Mol Biol*, 2007. **14**(17558416): p. 591-596.
408. Zhao, T.T., et al., *hnRNP A1 regulates UV-induced NF-kappaB signalling through destabilization of cIAP1 mRNA*. *Cell Death Differ*, 2009. **16**(18846111): p. 244-252.
409. Cammas, A., et al., *Cytoplasmic relocation of heterogeneous nuclear ribonucleoprotein A1 controls translation initiation of specific mRNAs*. *Molecular Biology of the Cell*, 2007. **18**(12): p. 5048-59.
410. Izaurralde, E., et al., *A Role for the M9 Transport Signal of hnRNP A1 in mRNA Nuclear Export*. *The Journal of Cell Biology*, 1997. **137**(1): p. 27-35.
411. Mili, S., et al., *Distinct RNP Complexes of Shuttling hnRNP Proteins with Pre-mRNA and mRNA: Candidate Intermediates in Formation and Export of mRNA*. *Molecular and Cellular Biology*, 2001. **21**(21): p. 7307-7319.
412. Moran-Jones, K., et al., *hnRNP A2, a potential ssDNA/RNA molecular adapter at the telomere*. *Nucleic Acids Res*, 2005. **33**(15659580): p. 486-496.
413. Gao, C., et al., *S-Nitrosylation of Heterogeneous Nuclear Ribonucleoprotein A/B Regulates Osteopontin Transcription in Endotoxin-stimulated Murine Macrophages*. *Journal of Biological Chemistry*, 2004. **279**(12): p. 11236-11243.
414. Guha, M., et al., *Heterogeneous nuclear ribonucleoprotein A2 is a common transcriptional coactivator in the nuclear transcription response to mitochondrial respiratory stress*. *Mol Biol Cell*, 2009. **20**(19641020): p. 4107-4119.
415. Moran-Jones, K., et al., *hnRNP A2 regulates alternative mRNA splicing of TP53INP2 to control invasive cell migration*. *Cancer Res*, 2009. **69**(19934309): p. 9219-9227.

416. Martinez-Contreras, R., et al., *Intronic Binding Sites for hnRNP A/B and hnRNP F/H Proteins Stimulate Pre-mRNA Splicing*. PLoS Biol, 2006. **4**(2): p. e21.
417. Fahling, M., et al., *Heterogeneous nuclear ribonucleoprotein-A2/B1 modulate collagen prolyl 4-hydroxylase, alpha (I) mRNA stability*. J Biol Chem, 2006. **281**(16464861): p. 9279-9286.
418. Hamilton, B.J., et al., *hnRNP A2 and hnRNP L bind the 3'UTR of glucose transporter 1 mRNA and exist as a complex in vivo*. Biochem Biophys Res Commun, 1999. **261**(10441480): p. 646-651.
419. Shan, J., et al., *A Molecular Mechanism for mRNA Trafficking in Neuronal Dendrites*. The Journal of Neuroscience, 2003. **23**(26): p. 8859-8866.
420. Muslimov, I.A., et al., *Spatial code recognition in neuronal RNA targeting: Role of RNA, hnRNP A2 interactions*. The Journal of Cell Biology, 2011.
421. Huang, M., et al., *The C-protein tetramer binds 230 to 240 nucleotides of pre-mRNA and nucleates the assembly of 40S heterogeneous nuclear ribonucleoprotein particles*. Mol Cell Biol, 1994. **14**(8264621): p. 518-533.
422. Tanaka, E., et al., *HnRNP A3 binds to and protects mammalian telomeric repeats in vitro*. Biochem Biophys Res Commun, 2007. **358**(17502110): p. 608-614.
423. Ma, A.S.W., et al., *Heterogeneous nuclear ribonucleoprotein A3, a novel RNA trafficking response element-binding protein*. J Biol Chem, 2002. **277**(11886857): p. 18010-18020.
424. Mahajan, M.C., et al., *Heterogeneous nuclear ribonucleoprotein C1/C2, MeCP1, and SWI/SNF form a chromatin remodeling complex at the beta-globin locus control region*. Proc Natl Acad Sci U S A, 2005. **102**(16217013): p. 15012-15017.
425. Chen, H., M. Hewison, and J.S. Adams, *Functional Characterization of Heterogeneous Nuclear Ribonuclear Protein C1/C2 in Vitamin D Resistance*. Journal of Biological Chemistry, 2006. **281**(51): p. 39114-39120.
426. Shahied, L., et al., *An antiparallel four-helix bundle orients the high-affinity RNA binding sites in hnRNP C: a mechanism for RNA chaperonin activity*. J Mol Biol, 2001. **305**(11162094): p. 817-828.
427. Rajagopalan, L.E., et al., *hnRNP C increases amyloid precursor protein (APP) production by stabilizing APP mRNA*. Nucleic Acids Research, 1998. **26**(14): p. 3418-3423.
428. Kim, J.H., et al., *Heterogeneous Nuclear Ribonucleoprotein C Modulates Translation of c-myc mRNA in a Cell Cycle Phase-Dependent Manner*. Mol. Cell. Biol., 2003. **23**(2): p. 708-720.
429. Schepens, B., et al., *A role for hnRNP C1/C2 and Unr in internal initiation of translation during mitosis*. EMBO J, 2007. **26**(17159903): p. 158-169.
430. Tolnay, M., L.A. Vereshchagina, and G.C. Tsokos, *Heterogeneous nuclear ribonucleoprotein D0B is a sequence-specific DNA-binding protein*. The Biochemical journal, 1999. **338 (Pt 2)**(10024518): p. 417-425.
431. Pautz, A., et al., *Similar regulation of human inducible nitric-oxide synthase expression by different isoforms of the RNA-binding protein AUF1*. J Biol Chem, 2009. **284**(19074427): p. 2755-2766.
432. Paek, K.Y., et al., *RNA-binding protein hnRNP D modulates internal ribosome entry site-dependent translation of hepatitis C virus RNA*. J Virol, 2008. **82**(18842733): p. 12082-12093.

433. Choi, H.S., et al., *Poly(C)-binding proteins as transcriptional regulators of gene expression*. *Biochem Biophys Res Commun*, 2009. **380**(19284986): p. 431-436.
434. Martinez-Contreras, R., et al., *hnRNP proteins and splicing control*. *Adv Exp Med Biol*, 2007. **623**(18380344): p. 123-147.
435. Meng, Q., et al., *Signaling-dependent and coordinated regulation of transcription, splicing, and translation resides in a single coregulator, PCBP1*. *Proc Natl Acad Sci U S A*, 2007. **104**(17389360): p. 5866-5871.
436. Ostareck-Lederer, A., D.H. Ostareck, and M.W. Hentze, *Cytoplasmic regulatory functions of the KH-domain proteins hnRNPs K and E1/E2*. *Trends Biochem Sci*, 1998. **23**(9852755): p. 409-411.
437. Perrotti, D., et al., *BCR-ABL suppresses C/EBPalpha expression through inhibitory action of hnRNP E2*. *Nat Genet*, 2002. **30**(11753385): p. 48-58.
438. Kosturko, L.D., et al., *Heterogeneous nuclear ribonucleoprotein (hnRNP) E1 binds to hnRNP A2 and inhibits translation of A2 response element mRNAs*. *Mol Biol Cell*, 2006. **17**(16775011): p. 3521-3533.
439. Pickering, B.M., et al., *Bag-1 internal ribosome entry segment activity is promoted by structural changes mediated by poly(rC) binding protein 1 and recruitment of polypyrimidine tract binding protein 1*. *Mol Cell Biol*, 2004. **24**(15169918): p. 5595-5605.
440. Alkan, S.A., K. Martincic, and C. Milcarek, *The hnRNPs F and H2 bind to similar sequences to influence gene expression*. *The Biochemical journal*, 2006. **393**(16171461): p. 361-371.
441. Dominguez, C. and F.H.T. Allain, *NMR structure of the three quasi RNA recognition motifs (qRRMs) of human hnRNP F and interaction studies with Bcl-x G-tract RNA: a novel mode of RNA recognition*. *Nucleic Acids Res*, 2006. **34**(16885237): p. 3634-3645.
442. Shin, K.-H., M.K. Kang, and N.-H. Park, *Heterogeneous nuclear ribonucleoprotein G, nitric oxide, and oral carcinogenesis*. *Nitric Oxide*, 2008. **19**(18474262): p. 125-132.
443. Shin, K.-H., et al., *Heterogeneous nuclear ribonucleoprotein G shows tumor suppressive effect against oral squamous cell carcinoma cells*. *Clin Cancer Res*, 2006. **12**(16707624): p. 3222-3228.
444. Hofmann, Y. and B. Wirth, *hnRNP-G promotes exon 7 inclusion of survival motor neuron (SMN) via direct interaction with Htra2-CE1*. *Human Molecular Genetics*, 2002. **11**(17): p. 2037-2049.
445. Chou, M.Y., et al., *hnRNP H is a component of a splicing enhancer complex that activates a c-src alternative exon in neuronal cells*. *Mol Cell Biol*, 1999. **19**(9858532): p. 69-77.
446. Bagga, P.S., G.K. Arhin, and J. Wilusz, *DSEF-1 is a member of the hnRNP H family of RNA-binding proteins and stimulates pre-mRNA cleavage and polyadenylation in vitro*. *Nucleic Acids Research*, 1998. **26**(23): p. 5343-5350.
447. Sharma, S., et al., *Polypyrimidine tract binding protein controls the transition from exon definition to an intron defined spliceosome*. *Nat Struct Mol Biol*, 2008. **15**(18193060): p. 183-191.
448. Lamichhane, R., et al., *RNA looping by PTB: Evidence using FRET and NMR spectroscopy for a role in splicing repression*. *Proc Natl Acad Sci U S A*, 2010. **107**(20160105): p. 4105-4110.

449. Xue, Y., et al., *Genome-wide analysis of PTB-RNA interactions reveals a strategy used by the general splicing repressor to modulate exon inclusion or skipping*. Mol Cell, 2009. **36**(20064465): p. 996-991006.
450. Knoch, K.-P., et al., *Polypyrimidine tract-binding protein promotes insulin secretory granule biogenesis*. Nat Cell Biol, 2004. **6**(15039777): p. 207-214.
451. Lou, H., et al., *Polypyrimidine Tract-Binding Protein Positively Regulates Inclusion of an Alternative 3'-Terminal Exon*. Mol. Cell. Biol., 1999. **19**(1): p. 78-85.
452. Majumder, M., et al., *The hnRNA-Binding Proteins hnRNP L and PTB Are Required for Efficient Translation of the Cat-1 Arginine/Lysine Transporter mRNA during Amino Acid Starvation*. Mol. Cell. Biol., 2009. **29**(10): p. 2899-2912.
453. Stains, J.P., et al., *Heterogeneous nuclear ribonucleoprotein K represses transcription from a cytosine/thymidine-rich element in the osteocalcin promoter*. The Biochemical journal, 2005. **385**(15361071): p. 613-623.
454. Bomsztyk, K., O. Denisenko, and J. Ostrowski, *hnRNP K: one protein multiple processes*. Bioessays, 2004. **26**(15170860): p. 629-638.
455. Lynch, M., et al., *hnRNP K binds a core polypyrimidine element in the eukaryotic translation initiation factor 4E (eIF4E) promoter, and its regulation of eIF4E contributes to neoplastic transformation*. Mol Cell Biol, 2005. **25**(16024782): p. 6436-6453.
456. Expert-Bezancou, A., J.P. Le Caer, and J. Marie, *Heterogeneous nuclear ribonucleoprotein (hnRNP) K is a component of an intronic splicing enhancer complex that activates the splicing of the alternative exon 6A from chicken beta-tropomyosin pre-mRNA*. J Biol Chem, 2002. **277**(11867641): p. 16614-16623.
457. Revil, T., et al., *Heterogeneous nuclear ribonucleoprotein K represses the production of pro-apoptotic Bcl-xS splice isoform*. J Biol Chem, 2009. **284**(19520842): p. 21458-21467.
458. Habelhah, H., et al., *ERK phosphorylation drives cytoplasmic accumulation of hnRNP-K and inhibition of mRNA translation*. Nat Cell Biol, 2001. **3**(11231586): p. 325-330.
459. Fukuda, T., et al., *hnRNP K interacts with RNA binding motif protein 42 and functions in the maintenance of cellular ATP level during stress conditions*. Genes Cells, 2009. **14**(19170760): p. 113-128.
460. Kuninger, D.T., et al., *Human AP-endonuclease 1 and hnRNP-L interact with a nCaRE-like repressor element in the AP-endonuclease 1 promoter*. Nucleic Acids Res, 2002. **30**(11809897): p. 823-829.
461. Motta-Mena, L.B., F. Heyd, and K.W. Lynch, *Context-dependent regulatory mechanism of the splicing factor hnRNP L*. Mol Cell, 2010. **37**(20122404): p. 223-234.
462. Hui, J., G. Reither, and A. Bindereif, *Novel functional role of CA repeats and hnRNP L in RNA stability*. Rna, 2003. **9**(8): p. 931-936.
463. Guang, S., A.M. Felthouser, and J.E. Mertz, *Binding of hnRNP L to the Pre-mRNA Processing Enhancer of the Herpes Simplex Virus Thymidine Kinase Gene Enhances both Polyadenylation and Nucleocytoplasmic Export of Intronless mRNAs*. Mol. Cell. Biol., 2005. **25**(15): p. 6303-6313.
464. Hwang, B., et al., *hnRNP L is required for the translation mediated by HCV IRES*. Biochemical and Biophysical Research Communications, 2009. **378**(3): p. 584-588.

465. Gattoni, R., et al., *The human hnRNP-M proteins: structure and relation with early heat shock-induced splicing arrest and chromosome mapping*. Nucleic Acids Res, 1996. **24**(8692693): p. 2535-2542.
466. Perrotti, D., et al., *TLS/FUS, a pro-oncogene involved in multiple chromosomal translocations, is a novel regulator of BCR/ABL-mediated leukemogenesis*. Embo J, 1998. **17**(15): p. 4442-55.
467. Hicks, G.G., et al., *Fus deficiency in mice results in defective B-lymphocyte development and activation, high levels of chromosomal instability and perinatal death*. Nature genetics, 2000. **24**(2): p. 175-9.
468. Yang, L., L.J. Embree, and D.D. Hickstein, *TLS-ERG leukemia fusion protein inhibits RNA splicing mediated by serine-arginine proteins*. Mol Cell Biol, 2000. **20**(10779324): p. 3345-3354.
469. Chen, H.-H., et al., *The RNA binding protein hnRNP Q modulates the utilization of exon 7 in the survival motor neuron 2 (SMN2) gene*. Mol Cell Biol, 2008. **28**(18794368): p. 6929-6938.
470. Liu, H.M., et al., *SYNCRIP (synaptotagmin-binding, cytoplasmic RNA-interacting protein) is a host factor involved in hepatitis C virus RNA replication*. Virology, 2009. **386**(19232660): p. 249-256.
471. Grosset, C., et al., *A Mechanism for Translationally Coupled mRNA Turnover: Interaction between the Poly(A) Tail and a c-fos RNA Coding Determinant via a Protein Complex*. Cell, 2000. **103**(1): p. 29-40.
472. Bannai, H., et al., *An RNA-interacting Protein, SYNCRIP (Heterogeneous Nuclear Ribonuclear Protein Q1/NSAPI) Is a Component of mRNA Granule Transported with Inositol 1,4,5-Trisphosphate Receptor Type 1 mRNA in Neuronal Dendrites*. Journal of Biological Chemistry, 2004. **279**(51): p. 53427-53434.
473. Rossoll, W., et al., *Specific interaction of Smn, the spinal muscular atrophy determining gene product, with hnRNP-R and gry-rbp/hnRNP-Q: a role for Smn in RNA processing in motor axons?* Hum Mol Genet, 2002. **11**(11773003): p. 93-9105.
474. Fackelmayer, F.O. and A. Richter, *Purification of two isoforms of hnRNP-U and characterization of their nucleic acid binding activity*. Biochemistry, 1994. **33**(8068679): p. 10416-10422.
475. Kim, M.K. and V.M. Nikodem, *hnRNP U Inhibits Carboxy-Terminal Domain Phosphorylation by TFIIH and Represses RNA Polymerase II Elongation*. Mol. Cell. Biol., 1999. **19**(10): p. 6833-6844.
476. Siomi, H. and G. Dreyfuss, *A Nuclear Localization Domain in the hnRNP A1 Protein*. Journal of Cell Biology, 1995. **129**(3): p. 551-560.
477. Michael, W.M., et al., *Signal sequences that target nuclear import and nuclear export of pre-mRNA-binding proteins*. Cold Spring Harb Symp Quant Biol, 1995. **60**: p. 663-8.
478. Guil, S., J.C. Long, and J.F. Caceres, *hnRNP A1 relocation to the stress granules reflects a role in the stress response*. Molecular and cellular biology, 2006. **26**(15): p. 5744-58.
479. van der Houven van Oordt, W., et al., *The MKK(3/6)-p38-signaling cascade alters the subcellular distribution of hnRNP A1 and modulates alternative splicing regulation*. J Cell Biol, 2000. **149**(2): p. 307-316.
480. Hay, D.C., et al., *Interaction between hnRNPA1 and I κ B α Is Required for Maximal Activation of NF- κ B-Dependent Transcription*. Mol. Cell. Biol., 2001. **21**(10): p. 3482-3490.

481. Matter, N., et al., *Heterogeneous ribonucleoprotein A1 is part of an exon-specific splice-silencing complex controlled by oncogenic signaling pathways*. J Biol Chem, 2000. **275**(10958793): p. 35353-35360.
482. Rooke, N., et al., *Roles for SR proteins and hnRNP A1 in the regulation of c-src exon NI*. Mol Cell Biol, 2003. **23**(12612063): p. 1874-1884.
483. Guil, S. and J.F. Cáceres, *The multifunctional RNA-binding protein hnRNP A1 is required for processing of miR-18a*. Nat Struct Mol Biol, 2007. **14**(7): p. 591-596.
484. Michlewski, G., S. Guil, and J. Cáceres, *Stimulation of pri-miR-18a Processing by hnRNP A1*. Advances in Experimental Medicine and Biology, 2011. **700**: p. 28-35.
485. Svitkin, Y.V., et al., *General RNA binding proteins render translation cap dependent*. EMBO J, 1996. **15**(24): p. 7147-7155.
486. Bonnal, S., et al., *Heterogeneous Nuclear Ribonucleoprotein A1 Is a Novel Internal Ribosome Entry Site trans-Acting Factor That Modulates Alternative Initiation of Translation of the Fibroblast Growth Factor 2 mRNA*. Journal of Biological Chemistry, 2005. **280**(6): p. 4144-4153.
487. Hamilton, B.J., et al., *Association of Heterogeneous Nuclear Ribonucleoprotein A1 and C Proteins with Reiterated AUUUA Sequences*. J. Biol. Chem, 1993. **268**(12): p. 8881-8887.
488. Henics, T., et al., *Enhanced Stability of Interleukin-2 mRNA in MIA 144 Cells*. J Biol Chem, 1994. **269**(7): p. 5377-5383.
489. Ruggiero, T., et al., *Identification of a set of KSRP target transcripts upregulated by PI3K-AKT signaling*. BMC Mol Biol, 2007. **8**: p. 28.
490. Orford, K., C.C. Orford, and S.W. Byers, *Exogenous expression of beta-catenin regulates contact inhibition, anchorage-independent growth, anoikis, and radiation-induced cell cycle arrest*. J Cell Biol, 1999. **146**(4): p. 855-68.
491. Olmeda, D., et al., *Beta-catenin regulation during the cell cycle: implications in G2/M and apoptosis*. Molecular Biology of the Cell, 2003. **14**(7): p. 2844-60.
492. Mayeda, A., D.M. Helfman, and A.R. Krainer, *Modulation of Exon Skipping and Inclusion by Heterogeneous Nuclear Ribonucleoprotein A1 and Pre-mRNA Splicing Factor SF2/ASF*. Molecular and Cellular Biology, 1993. **13**(5): p. 2993-3001.
493. Roth, M.J., et al., *beta-Catenin splice variants and downstream targets as markers for neoplastic progression of esophageal cancer*. Genes Chromosomes Cancer, 2005. **44**(4): p. 423-8.
494. Gherzi, R., et al., *The RNA-binding protein KSRP promotes decay of beta-catenin mRNA and is inactivated by PI3K-AKT signaling*. PLoS Biol, 2006. **5**(1): p. e5.
495. Shyu, A.B., M.E. Greenberg, and J.G. Belasco, *The c-fos transcript is targeted for rapid decay by two distinct mRNA degradation pathways*. Genes & Development, 1989. **3**(1): p. 60-72.
496. Ragheb, J.A., M. Deen, and R.H. Schwartz, *CD28-Mediated Regulation of mRNA Stability Requires Sequences Within the Coding Region of the IL-2 mRNA*. The Journal of Immunology, 1999. **163**(1): p. 120-129.
497. Jackson, A.L. and P.S. Linsley, *Noise amidst the silence: off-target effects of siRNAs?* Trends Genet, 2004. **20**(11): p. 521-4.
498. Ma, Y., et al., *Prevalence of off-target effects in Drosophila RNA interference screens*. Nature, 2006.

499. DasGupta, R., et al., *A case study of the reproducibility of transcriptional reporter cell-based RNAi screens in Drosophila*. *Genome biology*, 2007. **8**(9): p. R203.
500. Karolchik, D., et al., *The UCSC Genome Browser Database: 2008 update*. *Nucleic Acids Res*, 2008. **36**(Database issue): p. D773-9.
501. Kestler, H.A. and M. Kuhl, *From individual Wnt pathways towards a Wnt signalling network*. *Philosophical transactions of the Royal Society of London. Series B, Biological sciences*, 2008. **363**(1495): p. 1333-47.
502. Jackson, A., et al., *Gene array analysis of Wnt-regulated genes in C3H10T1/2 cells*. *Bone*, 2005. **36**(4): p. 585-598.
503. Staal, F.J.T., et al., *Wnt Target Genes Identified by DNA Microarrays in Immature CD34+ Thymocytes Regulate Proliferation and Cell Adhesion*. *The Journal of Immunology*, 2004. **172**(2): p. 1099-1108.
504. Vlad, A., et al., *The first five years of the Wnt targetome*. *Cellular Signalling*, 2008. **20**(5): p. 795-802.
505. Silva-Vargas, V., et al., *Beta-catenin and Hedgehog signal strength can specify number and location of hair follicles in adult epidermis without recruitment of bulge stem cells*. *Dev Cell*, 2005. **9**(1): p. 121-31.
506. Cohen-Saidon, C., et al., *Dynamics and Variability of ERK2 Response to EGF in Individual Living Cells*. *Molecular cell*, 2009. **36**(5): p. 885-893.
507. Moffat, J. and D.M. Sabatini, *Building mammalian signalling pathways with RNAi screens*. *Nat Rev Mol Cell Biol*, 2006. **7**(3): p. 177-187.
508. Lawrence, N., et al., *dTcf antagonises Wingless signalling during the development and patterning of the wing in Drosophila*. *Int. J. Dev. Biol.*, 2000. **44**: p. 749-756.
509. Fagotto, F., K. Guger, and B.M. Gumbiner, *Induction of the primary dorsalizing center in Xenopus by the Wnt/GSK/ β -catenin signaling pathway, but not by Vg1, Activin or Noggin*. *Development*, 1997. **124**: p. 453-460.
510. Brabletz, T., et al., *Variable β -catenin expression in colorectal cancers indicates tumor progression driven by the tumor environment*. *Proceedings of the National Academy of Sciences*, 2001. **98**(18): p. 10356-10361.
511. Janssen, K.Ä., et al., *APC and Oncogenic KRAS Are Synergistic in Enhancing Wnt Signaling in Intestinal Tumor Formation and Progression*. *Gastroenterology*, 2006. **131**(4): p. 1096-1109.
512. Maher, M.T., et al., *Issues associated with assessing nuclear localization of N-terminally unphosphorylated β -catenin with monoclonal antibody 8E7*. *Biology direct*, 2009. **4**(1): p. 5.
513. Blauwkamp, T.A., M.V. Chang, and K.M. Cadigan, *Novel TCF-binding sites specify transcriptional repression by Wnt signalling*. *The Embo Journal*, 2008. **27**(10): p. 1436-46.
514. Yang, X.-D., et al., *Distinct and mutually inhibitory binding by two divergent β -catenins coordinates TCF levels and activity in C. elegans*. *Development*, 2011. **138**(19): p. 4255-4265.
515. Eger, A., et al., *Epithelial mesenchymal transition by c-Fos estrogen receptor activation involves nuclear translocation of beta-catenin and upregulation of beta-catenin/lymphoid enhancer binding factor-1 transcriptional activity*. *J Cell Biol*, 2000. **148**(1): p. 173-88.
516. Orsulic, S., et al., *E-cadherin binding prevents b-catenin nuclear localization and b-catenin/LEF-1-mediated transactivation*. *J Cell Sci*, 1999. **112**: p. 1237-1245.

517. Gottardi, C.J., E. Wong, and B.M. Gumbiner, *E-cadherin suppresses cellular transformation by inhibiting beta- catenin signaling in an adhesion-independent manner*. J Cell Biol, 2001. **153**(5): p. 1049-60.
518. Sadot, E., et al., *Inhibition of beta-catenin-mediated transactivation by cadherin derivatives*. Proc Natl Acad Sci U S A, 1998. **95**(26): p. 15339-44.
519. van de Wetering, M., et al., *Mutant E-cadherin breast cancer cells do not display constitutive Wnt signaling*. Cancer Res, 2001. **61**(1): p. 278-84.
520. Kuphal, F. and J.r. Behrens, *E-cadherin modulates Wnt-dependent transcription in colorectal cancer cells but does not alter Wnt-independent gene expression in fibroblasts*. Experimental Cell Research, 2006. **312**(4): p. 457-467.
521. Herzig, M., et al., *Tumor progression induced by the loss of E-cadherin independent of [beta]-catenin//Tcf-mediated Wnt signaling*. Oncogene, 2006. **26**(16): p. 2290-2298.
522. Onder, T.T., et al., *Loss of E-Cadherin Promotes Metastasis via Multiple Downstream Transcriptional Pathways*. Cancer Research, 2008. **68**(10): p. 3645-3654.
523. Willert, K. and K.A. Jones, *Wnt signaling: is the party in the nucleus?* Genes & Development, 2006. **20**(11): p. 1394-1404.
524. Lee, E., A. Salic, and M.W. Kirschner, *Physiological regulation of [beta]-catenin stability by Tcf3 and CK1epsilon*. J Cell Biol, 2001. **154**(5): p. 983-93.
525. Arvanitis, D. and A. Davy, *Eph/ephrin signaling: networks*. Genes & Development, 2008. **22**(4): p. 416-429.
526. Cortina, C., et al., *EphB-ephrin-B interactions suppress colorectal cancer progression by compartmentalizing tumor cells*. Nat Genet, 2007. **39**(11): p. 1376-1383.
527. Batlle, E., et al., *EphB receptor activity suppresses colorectal cancer progression*. Nature, 2005. **435**(7045): p. 1126-30.
528. Clevers, H. and E. Batlle, *EphB/EphrinB receptors and Wnt signaling in colorectal cancer*. Cancer Res, 2006. **66**: p. 2-5.
529. Cowan, C.W., et al., *Vav Family GEFs Link Activated Ephs to Endocytosis and Axon Guidance*. Neuron, 2005. **46**(2): p. 205-217.
530. Tanaka, M., et al., *Tiam1 mediates neurite outgrowth induced by ephrin-B1 and EphA2*. EMBO J, 2004. **23**(5): p. 1075-1088.
531. Harburger, D.S. and D.A. Calderwood, *Integrin signalling at a glance*. Journal of Cell Science, 2009. **122**(2): p. 159-163.
532. Hehlhans, S., M. Haase, and N. Cordes, *Signalling via integrins: Implications for cell survival and anticancer strategies*. Biochimica et Biophysica Acta (BBA) - Reviews on Cancer, 2007. **1775**(1): p. 163-180.
533. Delcommenne, M., et al., *Phosphoinositide-3-OH kinase-dependent regulation of glycogen synthase kinase 3 and protein kinase B/AKT by the integrin-linked kinase* Proc Natl Acad Sci U S A, 1998. **95**(19): p. 11211-6.
534. Tan, C., et al., *Inhibition of integrin linked kinase (ILK) suppresses b-catenin-Lef/Tcf-dependent transcription and expression of the E-cadherin repressor, snail, in APC7/7 human colon carcinoma cells*. Oncogene, 2001. **20**: p. 133-140.
535. Novak, A., et al., *Cell adhesion and the integrin-linked kinase regulate the LEF-1 and beta-catenin signaling pathways*. Proc Natl Acad Sci U S A, 1998. **95**(8): p. 4374-9.

536. El Annabi, S., N. Gautier, and V.r. Baron, *Focal adhesion kinase and Src mediate integrin regulation of insulin receptor phosphorylation*. FEBS Letters, 2001. **507**(3): p. 247-252.
537. Huang, D., et al., *Reduced Expression of Focal Adhesion Kinase Disrupts Insulin Action in Skeletal Muscle Cells*. Endocrinology, 2006. **147**(7): p. 3333-3343.
538. Birukova, A.A., et al., *Paxillin- β -catenin interactions are involved in Rac/Cdc42-mediated endothelial barrier-protective response to oxidized phospholipids*. American Journal of Physiology - Lung Cellular and Molecular Physiology, 2007. **293**(1): p. L199-L211.
539. Mayer, C. and I. Grummt, *Ribosome biogenesis and cell growth: mTOR coordinates transcription by all three classes of nuclear RNA polymerases*. Oncogene, 2000. **25**(48): p. 6384-6391.
540. Yun, M.S., et al., *Both ERK and Wnt/beta-catenin pathways are involved in Wnt3a-induced proliferation*. J Cell Sci, 2005. **118**(Pt 2): p. 313-22.
541. Zhang, J., et al., *Bone morphogenetic protein signaling inhibits hair follicle anagen induction by restricting epithelial stem/progenitor cell activation and expansion*. Stem Cells, 2006. **24**(12): p. 2826-39.
542. Winkel, A., et al., *Wnt-ligand-dependent interaction of TAK1 (TGF-beta-activated kinase-1) with the receptor tyrosine kinase Ror2 modulates canonical Wnt-signalling*. Cell Signal, 2008. **20**(11): p. 2134-44.
543. Weston, C.R. and R.J. Davis, *Signal transduction: signaling specificity- a complex affair*. Science, 2001. **292**(5526): p. 2439-40.
544. Nelson, D.E., et al., *Oscillations in NF- κ B Signaling Control the Dynamics of Gene Expression*. Science, 2004. **306**(5696): p. 704-708.
545. Leung, J.Y., et al., *Activation of AXIN2 expression by beta-catenin-T cell factor. A feedback repressor pathway regulating Wnt signaling*. J Biol Chem, 2002. **277**(24): p. 21657-65.
546. Zhao, T.T., et al., *hnRNP A1 regulates UV-induced NF- κ B signalling through destabilization of cIAP1 mRNA*. Cell Death and Differentiation, 2009. **16**: p. 244-252.
547. Levsky, J.M. and R.H. Singer, *Fluorescence in situ hybridization: past, present and future*. Journal of Cell Science, 2003. **116**(14): p. 2833-2838.
548. Jo, O.D., et al., *Heterogeneous Nuclear Ribonucleoprotein A1 Regulates Cyclin D1 and c-myc Internal Ribosome Entry Site Function through Akt Signaling*. Journal of Biological Chemistry, 2008. **283**(34): p. 23274-23287.
549. Balagopal, V. and R. Parker, *Polysomes, P bodies and stress granules: states and fates of eukaryotic mRNAs*. Current Opinion in Cell Biology, 2009. **21**(3): p. 403-408.
550. Buchan, J.R. and R. Parker, *Eukaryotic Stress Granules: The Ins and Outs of Translation*. Molecular cell, 2009. **36**(6): p. 932-941.
551. Teixeira, D., et al., *Processing bodies require RNA for assembly and contain nontranslating mRNAs*. Rna, 2005. **11**(4): p. 371-382.
552. Anderson, P. and N. Kedersha, *Stress granules: the Tao of RNA triage*. Trends in Biochemical Sciences, 2008. **33**(3): p. 141-150.
553. Tourrière, H., et al., *The RasGAP-associated endoribonuclease G3BP assembles stress granules*. The Journal of Cell Biology, 2003. **160**(6): p. 823-831.
554. Hofmann, I., et al., *Identification of the Junctional Plaque Protein Plakophilin 3 in Cytoplasmic Particles Containing RNA-binding Proteins and the*

- Recruitment of Plakophilins 1 and 3 to Stress Granules*. Molecular Biology of the Cell, 2006. **17**(3): p. 1388-1398.
555. Kwon, S., Y. Zhang, and P. Matthias, *The deacetylase HDAC6 is a novel critical component of stress granules involved in the stress response*. Genes & Development, 2007. **21**(24): p. 3381-3394.
556. Williams, A., *Functional aspects of animal microRNAs*. Cellular and Molecular Life Sciences, 2008. **65**(4): p. 545-562.
557. Liu, W.Ä., et al., *MicroRNA-18a Prevents Estrogen Receptor-CE± Expression, Promoting Proliferation of Hepatocellular Carcinoma Cells*. Gastroenterology, 2009. **136**(2): p. 683-693.
558. Tsang, W.P. and T.T. Kwok, *The miR-18a* microRNA functions as a potential tumor suppressor by targeting on K-Ras*. Carcinogenesis, 2009. **30**(6): p. 953-959.
559. Nielsen, A.F., P.J.F. Leuschner, and J. Martinez, *Not miR-ly a splicing factor: hnRNP A1 succumbs to microRNA temptation*. Nat Struct Mol Biol, 2007. **14**(7): p. 572-573.
560. Huang, K., et al., *MicroRNA roles in beta-catenin pathway*. Molecular Cancer, 2010. **9**(1): p. 252.
561. Ashall, L., et al., *Pulsatile Stimulation Determines Timing and Specificity of NF-CE ∫ B-Dependent Transcription*. Science, 2009. **324**(5924): p. 242-246.

Appendices

All appendices can be found on the provided DVD.

Appendix A – Chapter 3

- 1) Data sheet of the eGFP- β -catenin cell line – crude plasmid map provided by BioImage (Thermo Scientific).
- 2) Figure 1. APC downregulation enhances nuclear β -catenin localisation in 7df3 cells – shift in population effects.

Appendix B – Chapter 4

Tables folder:

- T1 - esiRNA Primary library details
- T2 - Raw and normalised H screen data
- T3 – H screen primary hits Ratio stringent selection
- T4 – H screen primary hits Whole cell stringent selection
- T5 – H screen primary hits Ratio and WC overlap
- T6 – Raw and normalised UB screen data
- T7 – Raw and normalised UA screen data
- T8 – UB screen primary hits Ratio stringent selection
- T9 – UB screen primary hits Whole cell stringent selection
- T10 – UA screen primary hits Ratio stringent selection
- T11 – UA screen primary hits Whole cell stringent selection
- T12 – UB screen primary hits Ratio and WC overlap
- T13 – UA screen primary hits Ratio and WC overlap
- T14 – H screen primary hits Ratio for *in silico*
- T15 – H screen primary hits Whole cell for *in silico*
- T16 – UB screen primary hits Ratio for *in silico*
- T17 – UB screen primary hits Whole cell for *in silico*
- T18 – UA screen primary hits Ratio for *in silico*

T19 – UA screen primary hits Whole cell for *in silico*
T20 – UB Ratio KEGG enrichment P values
T21 – UB WC KEGG enrichment P values
T22 – UA Ratio KEGG enrichment P values
T23 – UA Ratio KEGG enrichment Cancer pathways P values
T24 – UA WC KEGG enrichment P values
T25 – Overlaps in Figure 4.15
T26 – Overlaps in Figure 4.16
T27 - Secondary esiRNA list and original screen identified
T28 - Secondary esiRNA reconfirmation summary
T29 – Ensembl IDs of primary hits from TCF-dependent luciferase screen
T30 - Overlaps in Figure 4.26
T31 - Overlaps in Figure 4.27 (A) UB screen
T32 - Overlaps in Figure 4.27 (B) UA screen
T33 - Overlaps in Figure 4.28
T34 - Overlaps in Figure 4.29
T35 - Overlaps in Figure 4.27-4.29 for network analysis
T36 – Overlaps in figure 4.31

PNG folder

PNGs from reconfirmation assays at higher resolutions than can be printed due to size of the graphs.

Figure 4.17 Part 1
Figure 4.17 Part 2
Figure 4.18 Part 1
Figure 4.18 Part 2
Figure 4.19 Part 1
Figure 4.19 Part 2
Figure 4.20 Part 1
Figure 4.20 Part 2
Figure 4.21 Part 1
Figure 4.21 Part 2
Figure 4.22 Part 1
Figure 4.22 Part 2
Figure 4.24 Part 1
Figure 4.24 Part 2

Cytoscape Folder

Cys 1 Figure 4.30

Cys 2 H screen β -catenin nuc/cyt modulators network

Cys 3 H screen β -catenin WC modulators network

Cys 4 UB screen β -catenin nuc/cyt modulators network

Cys 5 UB screen β -catenin WC modulators network

Cys 6 UA screen β -catenin nuc/cyt modulators network

Cys 7 UA screen β -catenin WC modulators network

Appendix C – Chapter 5

Figure 1. β -catenin is epistatic to hnRNP A1

Table 1. Sequences used to make hnRNP A1 esiRNA (.xls file)

Figure 2. hnRNPA1 knockdown has no affect on eGFP- β -catenin decay rates in eGFP- β -catenin U2OS cells

Figure 3. hnRNP A1 downregulation appears to have no effect on β -catenin splicing.

Figure 4. Crude linear schematic of β -catenin in the eGFP-construct in U2OS cells

Movies

Cycloheximide Movies folder

Three movies per esiRNA treatment (1 frame every 10minutes for approximately 15hours)

R-luc CHX 1-3, APC CHX 1-3, hnRNP A1 CHX 1-3

β -Cat dynamics (No CHX treatment) folder

Two movies per esiRNA treatment (1 frame every 10minutes for approximately 29 hours)

R-luc 1-2, APC 1-2, hnRNPA1 1-2

Two movies Wnt3a treatment, 1 Movie DMSO treatment (1 frame every 10minutes for approximately 29 hours)

Wnt3a 1-2, DMSO 1